The deglaciation of the Americas during the Last Glacial Termination

David Palacios, Chris Stokes, Fred Phillips, John Clague, Jesús Alcalá-Reygosa, Nuria Andrés, Isandra Angel, Pierre-Henri Blard, Jason Briner, Brenda Hall, et al.

The Deglaciation of the Americas during the Last Glacial Termination

David Palacios[(1)], Chris R. Stokes[(2)], Fred M. Phillips[(3)], John J. Clague[(4)], Jesus Alcalá-Reygosa[(5)], Nuria Andres[(1)], Isandra Angel[(6)], Pierre-Henri Blard[(7.a,b)], Jason P. Briner[(8)], Brenda L. Hall[(9)], Dennis Dahms[(10)], Andrew S. Hein[(11)], Vincent Jomelli[(12)], Bryan G. Mark[(13)], Mateo A. Martini[(14.a,b,c)], Patricio Moreno[(15)], Jon Riedel[(16)], Esteban Sagredo[(17)], Nathan D. Stansell[(18)], Lorenzo Vazquez-Selem[(19)], Mathias Vuille[(20)], Dylan J. Ward[(21)].

(1) Department of Geography, Complutense University, 28040 Madrid, Spain.

(2) Department of Geography, Durham University, Durham, DH1 3LE, UK

3) Earth & Environmental Science Department, New Mexico Institute of Mining & Technology, 801 Leroy Place, Socorro NM 87801, USA.

(4) Department of Earth Sciences, Simon Fraser University, 8888 University Dr., Burnaby, Brtish Columbia V5A 1S6, Canada.

(5) Facultad de Filosofía y Letras, Universidad Nacional Autónoma de México, Ciudad Universitaria, 04510 Ciudad de México, México.

(6) Departamento de Ciencias de la Tierra, Universidad Simón Bolívar, 89000, Caracas 1081-A, Venezuela.

(7.a) Centre de Recherches Pétrographiques et Géochimiques (CRPG), UMR 7358, CNRS - Université de Lorraine, 15 rue Notre Dame des Pauvres, 54500 Vandoeuvre-lès-Nancy, France. (7.b) Laboratoire de Glaciologie, DGES-IGEOS, Université Libre de Bruxelles, 1050 Bruxelles, Belgium.

(8) Department of Geology, University at Buffalo, Buffalo, NY 14260, USA

(9) Department of Earth Sciences and the Climate Change Institute, University of Maine, Orono, ME 04469, USA

(10) Department of Geography, University of Northern Iowa, Cedar Falls, IA 50614-0406

(11) School of GeoSciences, University of Edinburgh, Drummond Street, Edinburgh, EH8 9XP, UK.

(12) Université Paris 1 Panthéon-Sorbonne, CNRS Laboratoire de Géographie Physique, 92195 Meudon, France.

(13) Byrd Polar and Climate Research Center, Ohio State University, 108 Scott Hall 1090 Carmack Rd., Columbus, OH 43210 USA

(14.a) Millennium Nucleus Paleoclimate. Universidad de Chile, Las Palmeras 3425, Ñuñoa, Chile. (14.b) Instituto de Geografía, Pontificia Universidad Católica de Chile, Avenida Vicuña Mackenna 4860, 7820436 Macul, Chile. (14.c) Centro de Investigaciones en Ciencias de la Tierra (CONICET-Facultad de Ciencias Exactas, Físicas y Naturales, UNC), Vélez Sársfled 1611, X5016GCA, Córdoba, Argentina.

(15) Millennium Nucleus Paleoclimate, Center for Climate Research and Resilience, Institute of Ecology and Biodiversity, and Department of Ecological Sciences, Universidad de Chile, Las Palmeras 3425, Ñuñoa, Santiago, Chile

(16) North Cascades National Park, U.S. National Park Service, SedroWoolley, WA, USA

(17) Millennium Nucleus Paleoclimate and Instituto de Geografía Pontificia Universidad Católica de Chile, Santiago, Chile

(18) Geology and Environmental Geosciences, Northern Illinois University, DeKalb, Illinois, IL 60115, USA

(19) Instituto de Geografía, Universidad Nacional Autónoma de México, Ciudad Unversitaria, 04510 Ciudad de México, México.

(20) Department of Atmospheric and Environmental Sciences, University at Albany, State University of New York (SUNY), Albany, NY 12222, USA

(21) Department of Geology, University of Cincinnati, Cincinnati, OH 45224, USA

Abstract

This paper reviews current understanding of deglaciation in North, Central and South America from the Last Glacial Maximum to the beginning of the Holocene. Together with paleoclimatic and paleoceanographic data, we compare and contrast the pace of deglaciation and the response of glaciers to major climate events. During the Global Last Glacial Maximum (GLGM, 26.5-19 ka), average temperatures decreased 4º to 8ºC in the Americas, but precipitation varied strongly throughout this large region. Many glaciers in North and Central America achieved their maximum extent during the GLGM, whereas others advanced even farther during the subsequent Heinrich Stadial 1 (HS-1). Glaciers in the Andes also expanded during the GLGM, but that advance was not the largest, except on Tierra del Fuego. HS-1 (17.5-14.6 ka) was a time of general glacier thickening and advance throughout most of North and Central America, and in the tropical Andes; however, glaciers in the temperate and subpolar Andes thinned and retreated during this period. During the Bølling-Allerød interstadial (B-A, 14.6-12.9 ka), glaciers retreated throughout North and Central America and, in some cases, completely disappeared. Many glaciers advanced during the Antarctic Cold Reversal (ACR, 14.6-12.9 ka) in the tropical

Andes and Patagonia. There were small advances of glaciers in North America, Central America and in northern South America (Venezuela) during the Younger Dryas (12.9-11.7 ka), but glaciers in central and southern South America retreated during this period, except on the Altiplano where advances were driven by an increase in precipitation. Taken together, we suggest that there was a climate compensation effect, or 'seesaw', between the hemispheres, which affected not only marine currents and atmospheric circulation, but also the behavior of glaciers. This seesaw is consistent with the opposing behavior of many glaciers in the Northern and Southern Hemispheres.

Key Words: Deglaciation, Termination-I, Americas, Late Pleistocene, Glacial Chronology

1. Introduction

This paper focuses on the evolution of glaciation in the Americas during the Last Glacial Termination. The American continents extend 15,000 km from 70ºN to 55ºS and are characterized on their Pacific margins by mountain ranges that are continuous over this distance and, in most cases, now have glaciers or had them during the last glacial period of the Pleistocene. Knowledge of the activity of these glaciers has increased enormously in recent years (Palacios, 2017). This knowledge provides us an opportunity to study how American glaciers behaved during the Last Glacial Termination in the context of the asynchronous climatic setting of the two hemispheres. The largely north-south orientation and nearly continuous extent of mountain ranges in the Americas provide a unique opportunity to understand synoptic latitudinal variations in global paleoclimate.

The Last Glacial Termination is generally considered to span the time period between the Global Last Glacial Maximum (GLGM) and the beginning of the current interglacial period, the Holocene (Cheng et al., 2009; Denton et al., 2010). It has also been referred to as Termination I, given that it is the last in a series of similar transitions between Pleistocene glacials and interglacials (Emiliani, 1955; Broecker and van Donk, 1970; Cheng et al., 2009; Deaney et al., 2017).

The motivation for this review paper is that there have been few attempts to summarize, synthesize, and compare evidence for late Pleistocene glacier activity across the entire extent of the Americas. Our objective is to review current understanding of the evolution of glaciers in both North and South America throughout the Last Glacial Termination and

discuss whether the contrasts between the hemispheres implied by paleoclimatic and paleooceanographic models are reflected in the behavior of the glaciers. Given the continuous nature of the processes involved in the planet's recent glacial history, parsing deglaciation into periods requires simplification of the climatic mechanisms. Different and opposite changes may occur at different latitudes, with variable response times. In the present article, we have however selected deglaciation phases in accordance with the current state of knowledge and with scientific tradition.

Section 2 introduces the study regions and then summarizes how each of the regions has responded to major climatic changes caused by the different forcings that drove deglaciation. Section 3 presents the methods that we have used in this work to select study areas, represent graphically the glacial evolution of each area, and compare glacial chronologies and paleoclimatic aspects of areas. Section 4 reviews the spatial and temporal variability of the GLGM in the Americas. The next sections review the behaviors of these glaciers during deglaciation, notably the Heinrich 1 Stadial (HS-1) (Section 5), the Bølling-Allerød (B-A) interstadial and the Antarctic Cold Reversal (Section 6), and the Younger Dryas (YD) (Section 7). These sections are followed by a discussion (Section 8) in which we: 1) consider uncertainties in numeric ages obtained on glacial landforms (Section 8.1); 2) summarize knowledge of climate evolution during the Last Glacial Termination based on research on marine sediments and polar ice cores (Section 8.2); 3) compare our results with the climatic evolution summarized in Section 8.2; and 4) compare our results with published research on glacier activity on other continents during the Last Glacial Termination (Sections 8.3 to 8.5).

2. Study Areas

Our review proceeds from north to south (Figs. 1 and 2). The study begins with the Laurentide Ice Sheet (LIS) (Fig. 1), which contributed most to sea-level rise during the Last Glacial Termination (Lambeck et al., 2014) and was capable of greatly disrupting the coupled ocean-atmosphere system during deglaciation (Broccoli and Manabe, 1987a; Heinrich, 1988; Clark, 1994; Barber et al., 1999; Hemming, 2004). We summarize the most recent syntheses about LIS deglaciation (Dyke, 2004; Stokes 2017), enabling comparisons with deglaciation in the American mountains. Alaska is traversed by high mountains and was only partially glaciated during the GLGM. We examine this region as an unusual example of mountain glaciation at northern high latitudes (Briner et al., 2017).

We next describe the Cordilleran Ice Sheet (CIS) in southwestern Canada and adjacent United States, from roughly 48°N to 52°N, which removed or buried much of the preceding alpine glacial record (Clague, 2017), and the North Cascades in Washington State from 47°N to 49°N, which provide an excellent record of the early part of the Last Glacial Termination (Porter, 1976; Porter et al., 1983; Riedel et al., 2010; Riedel, 2017). The climate of these areas is strongly influenced by the location of the northern westerlies.

There was widespread alpine glaciation in the central sector of western North America: to the west in the Sierra Nevada Mountains in California; to the east in the Rocky Mountain/Yellowstone region, and in between the numerous mountain ranges of the Basin and Range Province (Fig. 1). Glaciation in the western U.S. has been the subject of numerous recent studies (Licciardi et al., 2001, 2004; Munroe et al., 2006; Licciardi and Pierce, 2008; Refsnider et al., 2008; Thackray, 2008; Laabs et al., 2009; Young et al., 2011; Shakun et al., 2015b; Leonard et al., 2017a, 2017b; Licciardi and Pierce, 2018; Dahms et al., 2018, 2019). In the interior, we mainly focus on the greater Yellowstone glacial system and adjacent mountain ranges around 44-45°N where new glacial syntheses are available (Larsen et al., 2016; Licciardi and Pierce, 2018; Pierce et al., 2018; Dahms et al., 2018, 2919); and the Rocky Mountains of Colorado at 37-41°N, for which there are also some recent contributions (Ward et al., 2009; Young et al., 2011; Leonard et al., 2017a, 2017b; Brugger et al., 2019). The Sierra Nevada, from 36° to 38°N, is one of the most-studied mountain ranges in North America, and numerous syntheses have been written on its glacial history (Gillespie and Zehfuss, 2004; Gillespie and Clark, 2011; Phillips, 2016, 2017).

Southward, the combined effects of lower elevation and higher ELA result in the limited presence of glacial landforms in the southern United States and northern Mexico. However, in central Mexico, at about 19ºN, the high volcanoes (>5000 m above sea level, asl) of the Trans-Mexican Volcanic Belt were glaciated (Fig. 1). Elevations decrease again in southern Mexico, and there are two mountain ranges in Central America (>3800 m asl) that hosted glaciers during the Late Pleistocene: Sierra Altos Cuchumatanes in Guatemala and the Cordillera de Talamanca in Costa Rica. There are some recent syntheses of the glacial history of central Mexico (Vázquez-Selem and Heine, 2011; Vázquez-Selem and Lachniet, 2017) and the Central American glaciated ranges (Lachniet and Selzer, 2002; Roy and Lachniet, 2010; Cunningham et al., 2019; Potter et al., 2019).

Lachniet and Vázquez-Selem (2005) and Vázquez-Selem and Lachniet (2017) recently summarized the history of Quaternary glaciation for this entire region.

In South America (Fig. 2), the crest and high valleys of the Andes from the north at 11ºN to the south at 55ºS (a distance of over 7200 km) were glaciated during the last glacial cycle. The northern Andes are located between latitudes 11ºN and 4ºS, and include ranges in Venezuela, Colombia, and Ecuador. The Venezuelan Andes consist of two main ranges oriented northeast to southwest between 7ºN and 10º N, named Sierra de Perijá and the Mérida Andes; the latter contains abundant glacial landforms and extant glaciers. Numerous dating studies have been performed on glacial landforms in that region (e.g. Schubert, 1974; Bezada, 1989; Mahaney et al., 2000; Dirszowsky et al., 2005; Wesnousky et al., 2012; Angel et al., 2013, 2016, 2017; Carcaillet et al., 2013; Guzmán, 2013; Angel, 2016;). The Colombian Andes consist of three parallel ranges extending from 1ºN to 11ºN: the Cordillera Occidental (western), Cordillera Central and Cordillera Oriental (eastern). Studies have been carried out in the Cordillera Central and Cordillera Oriental involving radiocarbon dating of paleosols and glaciofluvial and glacial sediments, and more recently surface exposure ^{10}Be dating (Thouret et al., 1996; Clapperton, 2000; Helmens, 2004, 2011; Jomelli et al., 2014). The Ecuadorian Andes extend from 1ºN to 4ºS and include the Eastern and Western Cordilleras. Glaciation studies in these ranges have relied mainly on radiocarbon dating of glaciolacustrine and till sediments (Clapperton et al., 1997a; Rodbell et al., 2002; La Frenierre et al., 2011).

The central Andes extend the length of Peru, western Bolivia and northern Chile, and comprise two parallel ranges in which the highest areas have glacial landforms and extant glaciers (Fig. 2). Databases have been compiled to inform paleoclimate modeling and to compare glacier activity in Peru and Bolivia (e.g. Mark et al., 2005). Cosmogenic nuclide exposure dating methods have improved knowledge of Late Pleistocene glacial evolution, but there are significant challenges in interpreting the data (Smith et al., 2005, 2008; Zech et al., 2008; Glasser et al., 2009; Licciardi et al., 2009; Rodbell et al., 2009; Smith and Rodbell, 2010; Blard et al., 2013; Jomelli et al., 2011, 2014; Bromley et al., 2016; Martin et al., 2018). Several other studies in this region focus on the time of deglaciation (He et al., 2013; Shakun et al., 2015b; Stansell et al., 2015, 2017). A recent synthesis of Late Pleistocene glacial evolution has been published for the entire region (Mark et al., 2017), and this review has since been complemented by additional paleoglacier chronologies (Ward et al., 2017; Martin et al., 2018)

In southern Peru (Fig. 2), western Bolivia and northern Chile, the western Andean range marks the west edge of the Altiplano and Puna Plateau, a closed basin that contains the great lakes of Titicaca (3806 m asl), Poopó (3685 m asl), and Salar de Uyuni (3653 m asl). Here, typical elevations are 4000-5000 m asl; the basin is surrounded by the Western and the Eastern Andes, where large volcanoes reach elevations greater than 6000 m asl. In the north of this area, precipitation is delivered mainly by the South American monsoon in the summer months, but to the south, this gives way to extratropical systems related to the southern westerly winds in austral winter. This transition region, between 18°S and 30°S, is an area of persistent aridity known as the Arid Diagonal (De Martonne, 1934).

The western cordillera of the Andes in northern Chile crosses the Arid Diagonal between 18ºS and 27ºS (Fig. 2). Between Nevado Sajama (18.1ºS) and Cerro Tapado (30.2ºS), there are few modern glaciers because of limited precipitation (Casassa et al., 2007), but glacial deposits can be mapped as far south as ~24ºS on the north side of the Arid Diagonal and as far north as 27ºS on the south side (Jenny et al., 1996). A few small rock glaciers and permanent snowfields exist on very high peaks throughout the Arid Diagonal, where ELAs reach >6000 m asl (Ward et al., 2017).

Moving farther south to the northern part of the Argentine Andes between 22ºS and 36ºS (Fig. 2), there are two different atmospheric circulation patterns, which again are separated by the Arid Diagonal. The Arid Diagonal crosses this section of the Andes between 25ºS and 27ºS. Most of the precipitation north of the Arid Diagonal falls during the South American summer monsoon season. South of the Arid Diagonal precipitation falls mainly during the austral winter months and is related to southerly sourced westerly winds. The locations where most precipitation is related to the South American summer monsoon are Tres Lagunas (Zech et al., 2009), Nevado de Chañi (Martini et al., 2017a), Sierra de Quilmes (Zech et al., 2017), and Sierra de Aconquija (D'Arcy et al., 2019). The locations where most precipitation is related to the southern westerlies are: the Ansilta range (Terrizzano et al., 2017), Cordon del Plata (Moreiras et al., 2017) and Las Leñas valley (Zech et al., 2017). Reviews of the glacial chronology of the entire region were carried out by Zech et al. (2017) and more recently by D'Arcy et al. (2019).

From 36ºS to the southernmost tip of South America, the Patagonian Andes are a complex mountainous region with numerous present-day glaciers and two large ice fields (Campo de Hielo Patagónico Norte and Sur) (Fig. 2). Mapping of major moraine systems throughout Patagonia and early geochronological work have provided a broad framework

that underpins our knowledge of the glacial history of this region (e.g., Caldenius, 1932; Feruglio, 1950; Flint and Fidalgo, 1964, 1969; Mercer, 1969, 1976). During the GLGM, there was a large ice sheet, the Patagonian Ice Sheet (PIS), that extended 2000 km along the crest of the range, from 38°S to 55°S. With the exception of northern Patagonia, the western outlet glaciers of the Patagonian Ice Sheet terminated in the Pacific Ocean, whereas eastern outlets terminated on land. The deglaciation chronology and pattern of land-terminating outlets of the PIS have been the subject of much research (Denton et al., 1999a; Glasser et al., 2004, 2008; Kaplan et al., 2008; Moreno et al., 2009; Rabassa and Coronato, 2009; Rodbell et al., 2009; Hein et al., 2010; Harrison and Glasser, 2011; Boex et al., 2013; Mendelova et al., 2017).

The southern tip of South America, from the Strait of Magellan to Cape Horn, comprises hundreds of islands (Fig. 2). The largest island, Isla Grande de Tierra del Fuego, is dominated on its west side by the Cordillera Darwin, a mountain range with peaks over 2000 m asl. This range is currently covered by large glaciers, some of which reach the sea. The climate of Tierra del Fuego is strongly affected by the southern westerlies, and precipitation declines rapidly from the Pacific to the Atlantic coast. Hall et al. (2017a) and Hall et al. (2019) published recent syntheses of the glacial history of Tierra del Fuego during Last Glacial Termination and the Holocene, respectively.

3. Methods

3.1 Selection of studies in each area

It is impossible to include all available information on the deglaciation of the Americas in detail in a single review paper. However, this does not preclude us from carrying out a comparative analysis of the Late Glacial history of the two continents based on recent advances in knowledge that we seek to provide here. With this objective in mind, we selected regions where studies of Late Glacial history are most advanced and geographically representative. For each selected region, we review recent publications that are key to understanding the glacial history from the Last Glacial Maximum to the beginning of the Holocene, including the most up-to-date review papers or syntheses from specific regions.

3.2 Graphical expression of glacier extent for each interval

The figures in this paper illustrate generalised glacier extent for each of the intervals discussed below (Figs. 3, 4, 5, 6, and 7). A common metric is required to compare glacier advances and extent across the vast area of the Americas. Many researchers consider the Equilibrium Line Altitude (ELA) to be the best measure of climate-driven changes in glacier extent (Rea, 2009), although it may introduce errors in paleoclimatic reconstructions in active tectonic mountain ranges (Mitchell and Humphries, 2015) and is perhaps less helpful for large continental ice sheets. We are unable to use ELA in our review for three reasons. First, many studies do not report ELAs for glacial events. Second, the ELAs reported in the papers we surveyed were calculated using different methods and thus may not be comparable between regions. Third, reported ELAs are generally local values and may not be representative of regional climate. For example, an ELA reconstructed for a heavily shaded glacier in a north-facing cirque in the Northern Hemisphere will yield a much lower value than one reconstructed for an exposed glacier on the south side of the same mountain. To be quantitatively useful, both of these must be normalized to the climatic ELA – the zero-mass-balance elevation of a horizontal unshaded surface. To evaluate the climatic ELA, one must model the mass balance of the glacier using a digital elevation representation of the basin. Modeling the physical mass balance of a large number of glaciers spanning the entire Americas is beyond the scope of this paper.

We therefore use a simple, easy-to-compute metric that is based on observational data – the relative extent of a glacier (Et), expressed as a perce1642) ntage and quantified as follows:

$$E_t(\%) = \frac{Z_t - Z_P}{Z_{LLGM} - Z_P}$$

where Z_t is the elevation of the glacier terminus during the period in question, Z_P is the elevation at the end of the Little Ice Age, prior to the anthropogenic period, and Z_{LLGM} is the terminal elevation at the Local Last Glacial Maximum (LLGM). For areas that have no historic glaciers, we use the highest elevation in the catchment as a default value for Z_P. In the figures, we have grouped E_t values for each climate region in 20% intervals. Some ice masses, notably the Laurentide and Patagonian ice sheets, did not uniformly descend downslope from high-elevation accumulation areas, but rather expanded from higher elevation accumulation across vast expanses of relatively flat terrain. For these areas, we used the terminal position (in kilometers) relative to the late Holocene, or final, position as a metric of relative extent.

3.3 ELA depression in the Americas

In the text and tables, we refer to the approximate decrease in ELA for each period with respect to the current ELA. We acknowledge that glacier extents can be affected by hypsometry, but in this broad review paper and, as noted above, we are not in a position to perform original mass-balance modeling of a large number of glaciers spanning the entire Americas, which itself could be the subject of a large research project. ELA depression data included in our tables are based on cited peer-reviewed papers. The values should be considered approximations, but are useful for comparing how glaciers in each region responded to climate during each of the periods we discuss and for testing hypotheses of the large-scale driving mechanisms.

3.4 Dating glacial landforms

Our work compares chronological data obtained over recent decades through cosmogenic nuclide, surface-exposure dating methods. New scaling models and reference production rates have considerably changed the interpretation and chronological framing of many glacial landforms in recent years (e.g. Kaplan et al., 2011; Blard et al., 2013 a,b; Kelly et al., 2015; Martin et al., 2015, 2017; Borchers et al., 2016; Marrero et al., 2016, Philips et al., 2016). However, the degree of uncertainty in the production rates of most terrestrial cosmogenic isotopes, especially those that do not derive from quartz, can be greater than the amount of time separating many of the phases of deglaciation (Marrero et al., 2016), making it difficult to relate a glacier landform to a particular short period in the past.

Nevertheless, we account for these differences by identifying scaling factors explicitly or providing citations to relevant publications that allow the reader to be informed.

Other possible problems may compromise the validity of cosmogenic nuclide exposure ages. Exposure ages can be misleading if the dated glacial landforms are found to have had previous exposure to radiation or have been eroded out of till subsequent to glacier retreat (Blard et al., 2014; Briner et al., 2016; Çiner et al., 2017). Many of the dated glacial landforms discussed in this review are boulders on the crests of moraines, and their apparent ages must be interpreted in the context of advances or stillstands of glacier fronts. Care must be taken when interpreting these ages (Kirkbride and Winkler, 2012) because, once constructed, a moraine may not stabilize for a long time (Putkonen et al., 2008; Heyman et al., 2011). Moreover, weathering and exhumation since stabilization commonly remove grains from the surfaces of boulders, leading to ages that are younger than those of the moraines on which they lie (Briner et al., 2005; Hein, 2009; Heyman et al., 2011; Oliva and Ruiz-Fernández, 2015). Frequently, glacier fronts are limited in their advance by previously formed moraines and, in such cases, the glacier may deposit new boulders on old moraines. This process can be repeated several times and form a single moraine ridge that is the product of multiple advances (Osborn, 1986; Winkler and Matthews, 2010; Schimmelpfennig et al., 2014). The elevation of sample sites, which have changed frequently through the time on account of glacio-isostatic adjustments, is essential in calculating cosmogenic ages. Morever, the pattern of these changes is very difficult to know, which also introduces uncertainty in cosmogenic ages (Jones et al., 2019). Snow can reduce the exposure of surfaces to cosmogenic radiation and, in most cases, it is difficult to judge the impact of variations in snow cover over the thousands of years that a surface was exposed (Schildgen et al., 2005). Finally, in some cases, glaciers can advance or retreat independently of climatic forcing (Quincey et al., 2011; Ó Cofaigh et al., 2019).

These potential problems may not necessarily be solved by collecting and analyzing a larger number of samples from the same glacial landform. If altered boulders or boulders with prior radiation exposure are sampled, the statistic only increases the error (Palacios, 2017). Placing the results of cosmogenic nuclide exposure dating within a suitable geomorphological context is far more important than the statistics themselves. This context provides grounds for discarding impossible results and preferentially weighting others. For this reason, this review has relied not only on surface exposure ages and the

most recent production rates, but also on radiocarbon ages and regional geomorphological contexts that strengthen age interpretations and indicate the degree to which they might be in error.

3.5 Possible errors and uncertainties in ages reported in this review

The studies on which this review is based have been conducted over many decades, during a period when dating methods and standards have markedly changed. Although our focus is on recent literature, which is based on current knowledge, we include pertinent older studies that report ages calculated using earlier protocols. Given the many hundred studies and tens of thousand ages involved, reconciliation of chronological differences resulting from different methods would constitute a major research project and one that is far beyond the scope of this review. To that end, we therefore caution readers that the patterns we draw from the literature are a starting point for more detailed comparisons between specific study areas; we encourage readers to thoroughly evaluate and, if necessary, recompute ages reported in the literature for such purposes.

However, as shown below, ages cited in this paper are still comparable, because systematic uncertainties resulting from different methods and production rates are lower than 5% for most of the ages that we discuss here. Most of the ages cited in the text have been calculated using the ^{10}Be isotope and are derived from rocks containing quartz. Some ages cited in the text have been calculated using ^{36}Cl and ^{3}He in rocks without quartz, commonly volcanic rocks. Recent literature has shown that the ages derived from these three isotopes are comparable, albeit with different uncertainties (Phillips, 2016, 2017; Barth et al., 2019).

Balco and Schaefer (2006), Thompson et al. (2017), Corbett et al., (2019), and Barth et al. (2019) have recently recalculated ^{36}Cl ages cited in the Laurentide sections of this paper and have concluded that they differ little from previously published ages. All ^{10}Be ages from Alaska have been calculated using similar production rates: the Arctic value of Young et al. (2013) or the NENA value of Balco et al. (2009). Menounos et al. (2017) report ^{10}Be ages for the area of the Cordilleran Ice Sheet that are consistent with both previously and subsequently published ages from this region. Recently, ^{10}Be ages for the Rocky Mountains/Yellowstone region have been calculated or recalculated by Shakun et al. (2015a), Dahms et al. (2018), Licciardi and Pierce (2018), and Pierce et al. (2018), and shown to be internally consistent and consistent with the other ages in North America. Sierra Nevada ^{36}Cl and ^{10}Be ages are taken from Phillips (2016) and Phillips (2017) and

are based on CRONUS-Earth production rates (Borchers et al., 2016, Marrero et al., 2016a, Phillips et al., 2016). Whole-rock cosmogenic ^{36}Cl ages on moraine boulders and glacially polished rock surfaces in Mexico and Central America are based on calculations and recalculations using CRONUScalc (Marrero et al., 2016a, 2016b). Ages from Mexico reported by Vázquez-Selem and Lachniet (2017) and Central America reported by Potter et al. (2019) and Cunningham et al. (2019) are based on different scaling models, but the age differences are less than 2.5%. In conclusion, all cosmogenic ages from North and Central America cited in the text have been calculated or recalculated in the past three years, and possible differences are likely less than 5%.

Turning to South America, the Late Glacial chronology in the northern Andes is mainly based on radiocarbon and ^{10}Be cosmogenic ages. Many ^{10}Be ages were recomputed using the Cosmic Ray Exposure Program (CREp, http://crep.crpg.cnrs-nancy.fr/#/) (Martin et al., 2017) and the synthetic High Andes ^{10}Be production rate reported by Martin et al. (2015). Jomelli et al. (2014) notably homogenized and recalculated 477 published ^{10}Be and ^{3}He surface exposure ages from the Peruvian and Bolivian Andes, spanning the past 15,000 years. Aftter the publication of the paper by Jomelli et al. (2014), Martin et al. (2015) proposed a new empirical ^{10}Be production rate for the Tropical Andes that is similar, within uncertainties, to those proposed by Blard et al. (2013a) and Kelly et al. (2015). Jomelli et al (2017) and Martin et al (2018) adopted this new production rate and reported recalculated new ages, which we follow in this paper. A recent review by Mark et al. (2017) provides additional information on the Late Glacial chronology of the Peruvian and Bolivian Andes. Alcalá-Reygosa et al. (2017) report ^{36}Cl ages from volcanic areas in the Peruvian Andes, which they calculated using the spreadsheet developed by Schimmelpfennig (2009) and Schimmelpfennig et al. (2009). Bromley et al. (2011) provide ^{3}He ages for the same area. The ^{36}Cl, ^{3}He, and radiocarbon ages from the Peruvian Andes are consistent with one another (Blard et al. 2013a, 2013b; Bromley et al., 2019). ^{10}Be ages from northern Chile were calculated or recalculated by Ward et al. (2015, 2017) based on a protocol similar to that used in the Peruvian and Bolivian Andes. ^{36}Cl ages from northern Chile (Ward et al., 2017) were calculated using CRONUS-Earth production rates and the LSDn routine in CRONUScalc (Marerro et al., 2016b). Recently, D'arcy et al. (2019) recalculated all the ^{10}Be ages from the Central Andes of Argentina using local High Andes production rates (Kelly et al., 2015; Martin et al., 2015, 2017). Ages from Patagonia and Tierra del Fuego were recalculated by the CRONUS-Earth

online exposure age calculators (v. 2.2) (Balco et al., 2008), using the time-dependent Lal/Stone scaling model and the "Patagonian" production rate of Kaplan et al. (2011). As in North and Central America, the South American cosmogenic ages differ slightly between some regions, but the errors do not exceed 5% and thus do not change the overall conclusions of the paper.

We have converted ^{14}C ages from all the regions to calendar year ages using CALIB 7.1.

4. The Manifestation of the Global Last Glacial Maximum (26.5-19 ka) in the Americas and the Start of the Last Glacial Termination

4.1 The Global Last Glacial Maximum

The first period analyzed covers the time between 26.5 ka and 19 ka, when most of the northern ice sheets and many mountain glaciers reached their maximum extent in the last glacial cycle (Clark et al., 2009). This period coincides with the time of minimum sea level and is characterized by a quasi-equilibrium between the cryosphere and climate (Clark et al., 2009). Following standard usage (Clark et al., 2009; Hughes et al., 2013), we have called this period the 'Global Last Glacial Maximum' (GLGM). Clark et al. (2009) note that many ice masses, especially mountain glaciers, achieved their maximum extents prior to or after this period, and that the term 'Local Last Glacial Maximum' (LLGM) should be used to describe local maxima in particular regions. They further proposed 20-19 ka for the beginning of deglaciation, which was the time when most of the northern ice sheets began to retreat, sea level and temperatures started to increase, followed by an increase in the concentration of CO_2 in the atmosphere. Hughes et al. (2013), in an exhaustive review of the chronology of the LLGM throughout the world, show that not only did many mountain glaciers achieve their maximum extents before the GLGM, but some northern ice sheets did as well. They acknowledge, however, the fundamental role that the Laurentide Ice Sheet played in deglaciation, where the LLGM broadly coincides with the GLGM.

4.2 Laurentide Ice Sheet

The extent of glaciation during the LGM is summarized in Figure 3. The large extent of the LIS was the result of planetary cooling, but its very existence also had an effect on the evolution of mountain glaciers. The GLGM broadly coincides with the maximum size of the Laurentide Ice Sheet (LIS) (Dyke et al., 2002; Clark et al., 2009; Stokes, 2017). Despite the difficulty of precisely dating the maximum extent of the ice sheet, it is widely

accepted that different sectors of the LIS reached their local maxima at different times during the broad interval of the GLGM. For example, it has been suggested (Dyke et al., 2002) that the northwestern, northeastern and southern margins likely attained their maximum positions relatively early (~28-27 ka), whereas the southwestern and northernmost limits were probably reached slightly later (~25-24 ka). More recently, others have suggested that the northwestern margin, in the vicinity of the Mackenzie River delta, may have reached its maximum position at less than 20 ka (Murton et al., 2007; Kennedy et al., 2010; Lacelle et al., 2013) and possibly as late as 17-15 ka (Murton et al., 2015). If correct, this relatively late advance to a LLGM ice extent may have been aided by eustatic sea-level rise and the opening of the Arctic Ocean along the Beaufort Sea coastline, which provided a source of moisture and increased precipitation in the region (Lacelle et al., 2013).

Irrespective of the regional asynchronicity in the time of the local glacial maximum, it is likely that the LIS existed at its near-maximum extent for several thousand years, which would indicate that its mass balance was in equilibrium with the climate for a prolonged period of time (Dyke et al., 2002). Indeed, initial deglaciation is thought to have been slow prior to 17 ka (Dyke et al., 2002), and, as noted above, glaciers in some regions may have been advancing (e.g. in the far northwest). Possible exceptions to the generally slow recession include the major lobes of the southern margin of the ice sheet and the marine-based southeastern margin around the Atlantic Provinces. More rapid retreat of these margins was likely caused by ice-stream drawdown (Shaw et al., 2006, 2018; Margold et al., 2018) and, in the southeast, by eustatic sea-level rise (Dyke, 2004). In contrast, retreat of the land-based southern margin is thought to have been driven mainly by orbital forcing (Clark et al., 2009; Gregoire et al., 2015). Based on 22 ^{10}Be surface exposure ages on boulders on GLGM moraines in Wisconsin, Ullman et al. (2015a) dated the initial retreat of the ice sheet to as early as 23±0.6 ka, which coincided with a small increase in boreal summer insolation. ^{10}Be ages on samples 10-15 km up-ice from these moraines indicate a marked acceleration in retreat after ca. 20.5 ka that coincided with increased insolation prior to any increase in atmospheric carbon dioxide. This lends support to the notion that orbital forcing was the primary trigger for deglaciation of the LIS (see also Gregoire et al., 2015 and Heath et al., 2018).

Although increased insolation is thought to have triggered the initial retreat of the southern margin of the ice sheet (Ullman et al., 2015a), it is interesting to note that the

overall net surface mass balance likely remained positive for much of the early part of deglaciation (Ullman et al., 2015b). However, the ice sheet was clearly shrinking, which implies that the primary mechanism of mass loss was dynamic discharge/calving from major marine-based ice streams (Margold et al., 2015, 2018; Ullman et al., 2015b; Robel and Tziperman, 2016; Stokes et al., 2016). Indeed, ~25% of the ice sheet's perimeter was occupied by streaming ice at the global LGM, compared to ~10% at 11 ka (Stokes et al., 2016). Only when summer temperatures increased by 6-7˚C relative to the LGM did the overall net surface mass balance turn increasingly negative (Ullman et al., 2015b). Numerical modelling suggests that this occurred soon after ~11.5 ka and resulted in the rapid retreat of the land-based southern and western margins of the LIS (Ullman et al., 2015b). The rapid retreat of these terrestrial margins contrasts with the generally slow retreat of the northern and eastern marine-based margins and resulted in a highly asymmetric pattern of retreat towards the major dispersal centers in the east (Dyke and Prest, 1987; Margold et al., 2018).

4.3 Alaska

Alaska is located at latitudes similar to the northern LIS, but was covered largely by mountain glaciers during the GLGM. Thus, it is of interest to understand its glacial evolution as a first link between the large ice sheet and mountain glaciers. The best available evidence from Alaska suggests that glaciers expanded during Marine Isotope Stage (MIS) 2 (the Late Wisconsinan glaciation in local terminology), in step with the GLGM. Although maximum ages constraining the advance phase are sparse, constraints on LGM culmination date to ~21 ka in several regions spanning the state, including the Ahklun Mountains (Kaufman et al., 2003), the Alaska Range (Tulenko et al., 2018), the Brooks Range and Arctic Alaska (Pendleton et al., 2015). The best available maximum age for the LGM glacier advance in Alaska – ~24 ka – is arguably from the Ahklun Mountains (Kaufman et al., 2003, 2012). Deglaciation in Alaska commenced as early as ~21 ka. Recognizing that cosmogenic nuclide exposure ages of moraine boulders represent the culmination of an advance, mean exposure ages of LGM terminal moraine boulders (~21 ka) mark the transition from maximum glacier conditions to ice retreat and terminal moraine stabilization. Moraines up-valley of terminal moraines were formed in the Ahklun Mountains (Manley et al., 2001), and marine sediments were deposited within LGM extents in Cooke Inlet (Reger et al., 2007) as early as ~20 ka. In the Alaska Range, the first moraines up-valley of the LGM terminal moraines were deposited ~20 ka

(Tulenko et al., 2018). In at least one or two valleys in the Brooks Range that are accurately dated, glaciers receded well up-valley between ~21 ka and ~17 ka (Pendleton et al., 2015).

Climate conditions in Alaska during the GLGM are not well known, but several lines of evidence indicate that conditions were much more arid than today (e.g. Finkenbinder et al., 2014; Dorfman et al., 2015). Data on temperature changes during the LGM are scarce. Some paleoecological evidence exists from the Brooks Range suggesting summer temperatures 2-4°C colder than the present (Kurek et al., 2009), and pollen data from across Beringia suggest summer temperatures were ~4°C lower (Viau et al., 2008). On the other hand, climate modeling indicates rather warm conditions in Alaska during the LGM, associated with persistent shifts in atmospheric circulation related to Laurentide and Cordilleran ice sheet size (Otto-Bliesner et al., 2006; Löfverström and Liakka, 2016; Liakka and Löfverström, 2018).

The largest gaps in knowledge regarding the timing of the LGM and initial deglaciation in Alaska are related to the spatial pattern of glacier change across the state and complex climate forcing. High-resolution chronologies from moraine sequences from single valleys are scarce. Furthermore, few quantitative paleoclimate data exist, and the existing records of glaciation and snowline depression have yet to be reconciled with climate modeling results that show relatively warm LGM conditions.

4.4 Cordilleran Ice Sheet and North Cascades

Glaciers in western Canada were expanding into lowland areas on the flanks of the Coast and Rocky Mountains during the GLGM, contributing to development of the CIS (Clague, 2017). The CIS was not fully formed at the GLGM; large areas of southern British Columbia remained ice-free several thousand years later. Alpine glaciers in the southern Coast Mountains advanced into lowlands near Vancouver, British Columbia, after 25.8 ka during the Coquitlam stade in local terminology (Hicock and Armstrong, 1981; Hicock and Lian, 1995; Lian et al., 2001). To the south, alpine glaciers in the North Cascades achieved their maximum MIS 2 extents between 25.3 ka and 20.9 ka, about the same time as the GLGM (Kaufman et al., 2004; Riedel et al., 2010). The alpine advances at these sites ended with the Port Moody interstade sometime after 21.4 ka, when glaciers in the southern Coast Mountains and the North Cascades retreated (Hicock et al., 1982, 1999; Hicock and Lian, 1995; Riedel et al., 2010) (Fig. 8).

Regional pollen and macrofossil data and glacier reconstructions indicate that the climate that led to the alpine glacial advance in the North Cascades was the coldest and driest period in MIS 2 (Barnosky et al., 1987; Thackray, 2001; Riedel et al., 2010). Glacier ELAs fell by 750-1000 m from west to east across the range in response to a reduction in mean annual surface air temperature of ~8˚C and a significant reduction in precipitation (Porter et al., 1983; Bartlein et al., 1998, 2011; Liu et al., 2009). The primary reasons for the relatively arid climate were likely the lower sea surface temperatures in the Pacific Ocean, the greater distance to the coastline and large-scale changes in the atmosphere caused by formation of continental ice sheets (Hicock et al., 1999; Grigg and Whitlock, 2002; Thackray, 2008). Paleoclimatic simulations produced by global climate models suggest that three large-scale controls on climate have been especially important in the Pacific Northwest during Late Glacial time (Broccoli and Manabe, 1987a, 1987b; COHMAP Members, 1988; Bartlein et al., 1998; Whitlock et al., 2000). First, the Laurentide Ice Sheet (LIS) influenced both temperature and atmospheric circulation. Second, variations in the seasonal distribution of insolation as a result of the Earth's orbital variations affected temperature, effective precipitation and atmospheric circulation. Third, changes in atmospheric concentrations of CO_2 and other greenhouse gases affected temperatures on centennial and millennial timescales (Sowers and Bender, 1995).

4.5 Rocky Mountains/Yellowstone region

The Rocky Mountains allow us to link glacier behavior from the LIS to the north and the CIS to the northwest with lower latitudes, where only small glaciers formed during the period of maximum glacial expansion (Figs. 8, 9, 10, 11, 12, and 13). Recent ages from Colorado confirm that a number of valley glaciers reached their LLGM extent ~21-20 ka (Brugger et al., 2019) at roughly the same time as the GLGM (known locally as the Pinedale Glaciation), while in other valleys glaciers continued to advance, re-advance or remain in the same position for several thousand years until ~17 ka (see Brugger et al., 2019, and references therein).

In the Greater Yellowstone region, glaciers of the Beartooth Uplift and High Absaroka Range appear to have reached their maximum extents ~20 ka (Licciardi and Pierce, 2018). A similar pattern is evident on the eastern slope of the Teton Range, where the oldest moraines date to 19.4±1.7 ka (Pierce et al., 2018). Differences in the ages of LLGM limits in valleys surrounding the Yellowstone Plateau are likely due to local topographic factors

at the margins of the Yellowstone Ice Cap rather than general climate forcing (Young et al., 2011; Leonard et al., 2017a, 2017b; Pierce et al., 2018; Laabs et al., in preparation).

Ages of ~23-21 ka from terminal moraines of four valley glaciers in the Wind River Range, about 150 km southeast of Yellowstone Park, show that the LLGM also generally coincides with the GLGM (Phillips et al., 1997; Shakun et al., 2015a; Dahms et al., 2018). Deglaciation seems to have been swift here; ice appears to have receded to 2.6 km behind its terminus in the Middle Popo Agie valley by ~19 ka and 13 km upvalley from its terminus in the adjacent North Fork valley by ~18-17 ka. Glaciers in both valleys apparently receded 19 km and 27 km to their respective cirque riegels by 17-16 ka (Dahms et al., 2018). The glacier in the Pine Creek valley receded nearly 30 km from its terminus at Fremont Lake by 14-13 ka (Shakun et al., 2015a).

Many glaciers in the Rocky Mountains of Colorado reached their maximum extents during the GLGM, with the outermost moraines abandoned ~22-20 ka (Ward et al., 2009; Dühnforth and Anderson, 2011; Young et al., 2011; Schweinsberg et al., 2016; Leonard 2017a, 2017b; Brugger et al., 2019). In some cases, extensive deglaciation followed shortly after 20 ka (Ward et al., 2009), but elsewhere glaciers remained at, or had re-advanced to, near their maximum extents as late as 17-16 ka (Briner, 2009; Young et al., 2011; Leonard et al., 2017a, 2017b), well after the end of the GLGM. In some instances, these 17-16 ka moraines are the outermost moraines of the last glaciation.

The near complete absence of modern glaciers in the Colorado Rocky Mountains makes it difficult to estimate ELA depressions at the GLGM, although in the San Juan Mountains of southwestern Colorado it appears that they were lowered by at least 900 m (Ward et al., 2009). Recent numerical modeling of paleo-glaciers in several Colorado ranges indicates a rather modest GLGM temperature depression of 4.5º-6.0ºC compared to present-day temperatures, assuming no change in precipitation (Dühnforth and Anderson, 2011; Leonard et al., 2017a, 2017b). In contrast, work in the Mosquito Range suggests a temperature depression of 7.5º-8.1ºC (Brugger et al., 2019). Earlier work, using different paleo-glaciological approaches, indicates somewhat greater GLGM temperature depressions in the Colorado Rocky Mountains (Leonard, 1989, 2007; Brugger and Goldstein, 1999; Brugger, 2006, 2010; Refsnider et al., 2008). Global and regional climate models suggest that precipitation in the northern Rocky Mountains was significantly reduced compared to the present. In contrast, the southernmost Rocky Mountains in New Mexico were wetter at the GLGM than at present, and the central

Rocky Mountains of Colorado and Wyoming experienced close to modern precipitation (Oster et al., 2015).

4.6 Sierra Nevada

Few moraines from the early GLGM period in the Sierra Nevada have been directly dated, perhaps because such moraines were less extensive than those built during the local maximum and were thus obliterated by the later advances (Phillips et al., 2009). However, there is abundant evidence of a cooling climate during the early GLGM from nearby lacustrine records. For example, cores collected from Owens Lake, just east of the range (Smith and Bischoff, 1997), record a rise in juniper pollen, which is considered an indicator of cold temperature, between 30 ka and 25 ka, reaching a maximum between 25 ka and 20 ka (Woolfenden, 2003). In the same cores, total organic carbon, which decreases as input of glacial rock flour increases, falls from about 4% to near zero between 30 ka and 25 ka (Benson, 1998a, b). Similar patterns are observed in sediments from Mono Lake (Benson, 1998a, b), which also received direct discharge from glaciated valleys in the Sierra Nevada. The inference from lacustrine records that glaciation reached near-maximum extent at about 25 ka is confirmed by a fortuitously preserved terminal moraine in the valley of Bishop Creek, located at about 95% of the maximum LGM extent and dated to 26.5±1.7 ka (Phillips et al., 2009) (Fig. 14).

Cosmogenic and radiocarbon data for GLGM glaciation in the Sierra Nevada have recently been compiled and updated by Phillips (2016, 2017). Both ^{10}Be and ^{36}Cl surface-exposure dating yields ages ranging from 21 ka to 18 ka for the GLGM moraines (Tioga 3 in local terminology). Radiocarbon ages are slightly younger (19-18 ka), but this is because they are on organic matter accumulated in depressions behind the Tioga 3 terminal moraines and thus date to the earliest stages of retreat. The spacing of recessional moraines indicates that retreat was at first slow, but then accelerated (Phillips, 2017).

In summary, glaciers advanced in the Sierra Nevada steadily after about 30 ka, achieving positions slightly short of their maximum extents by 26 ka. They then were relatively stable for the next 5 ka, but advanced slightly between 22 ka and 21 ka to their all-time maximum limits of the last glacial cycle. Minor retreat from this maximum position began at 19 ka and accelerated rapidly after 18.0 ka to 17.5 ka. Plummer (2002) attempted to quantify both temperature and precipitation variations in the Sierra Nevada region during the GLGM by simultaneously solving water and energy balance equations for glaciers and closed-basin lakes. He concluded that precipitation during the peak LGM-maximum

period (21-18 ka) was about 140% of historical levels and temperature was 5-6°C colder than today.

4.7 Mexico and Central America

The highest mountains in Mexico and Central America were glacier covered during the GLGM. There the LLGM overlaps part of the GLGM. In central Mexico, ^{36}Cl exposure ages of moraines from the maximum advance are between 21 ka and 19 ka. Moraines were deposited as late as 15-14 ka in the mountains near the Pacific (Tancítaro, 3840 m asl) and Gulf of Mexico (Cofre de Perote, 4230 m asl), but minor recession occurred around 17 ka in the interior (Iztaccíhuatl, 5286 m asl) (Vázquez-Selem and Heine, 2011). Boulders on recessional moraines built inside the moraines from the local maximum have yielded exposure ages between ~14.5 ka and >13 ka, and exposure ages on glacial polish associated with recession range from 15 ka to 14 ka (Vázquez-Selem and Lachniet, 2017). In Cerro Chirripó (3819 m asl), Costa Rica, the local maximum is ~25 ka to 23 ka based on ^{36}Cl ages (Potter et al., 2019), whereas ^{10}Be exposure ages of lateral and recessional moraines are between ca. 18.3 ka and ~16.9 ka (Cunningham et al., 2019). They are thus younger than recessional moraines on mountains in central Mexico at a similar elevation (e.g. Tancítaro, 3840 m asl). No ages exist for the glaciated Altos Cuchumatanes (3837 m asl) of Guatemala, although a maximum around the time of the GLGM is probable based on data from central Mexico and Costa Rica (Roy and Lachniet, 2010).

ELAs in the region during the LLGM were depressed 1000-1500 m compared to modern values (equivalent to 6-9°C of cooling), which is consistent with ELA depression around the world during the GLGM (Lachniet and Vázquez-Selem, 2005).

4.8 Northern Andes

A widespread advance in the Northern Andes during the GLGM is not clear, and the limited chronological data available preclude robust interpretations. In the Venezuelan Andes, temperatures during the GLGM have been estimated to be around 8°C cooler than present, according to palynological analysis and a paleo-ELA reconstruction (Schubert and Rinaldi, 1987; Stansell et al., 2007). Some outermost moraines have been dated to around 21 ka in the Sierra Nevada based on ^{10}Be ages (modified ages from Angel, 2016; updated ages from Carcaillet et al., 2013). The Las Tapias terminal moraine at 3100 m asl in the Sierra Santo Domingo, northeastern Sierra Nevada, yielded ages of 18.2±1.0 ka

(n=3) (Angel, 2016), and a glacier advance in the Cordillera de Trujillo has been dated to around 17 ka (Bezada, 1989; Angel, 2016) (Fig. 15).

Climate in the Colombian Andes during the GLGM was cold and dry (van Geel and van der Hammen, 1973; Thouret et al., 1996). In this region, there are only a few ages from scattered valleys and it is difficult to evaluate glacier extent during the GLGM. However, in Páramo Peña Negra, close to Bogota, two moraine complexes between 3000 m and 3550 m asl were built between ~28 ka and 16 ka (Helmens, 1988). Paleo-ELAs were on average 1300 m lower than modern, likely driven by 6–8°C colder temperatures (Mark and Helmens, 2005). A till ('drift 3') on the western slopes of the Sierra Nevada del Cocuy may date to the GLGM. The onset of sedimentation in Laguna Ciega, which is located on this till at 2900 m asl has been radiocarbon-dated to ca. 27.0-24.5 ka BP (van der Hammen et al., 1981).

The glacial chronology of the Ecuadorian Andes is poorly constrained and does not allow clear conclusions to be drawn about glacier extent. There are some indications of possible advances around the time of the GLGM, such as in the Rucu Pichincha and the Papallacta valley (Heine and Heine, 1996) and in Cajas National Park (Hansen et al., 2003). Brunschön and Behling (2009) suggest that climate was cold and wet during the GLGM in the southern Ecuadorian Andes based on a pollen record and the upper timberline position in Podocarpus National Park.

4.9 Peruvian and Bolivian Andes

Evidence for the extent and chronology of past glacier advances in Peru and Bolivia at the GLGM comes from moraine chronologies and lake sediment records that provide a suite of ages before and after 21 ka (Clayton and Clapperton, 1997; Blard et al., 2013). The time of the local maximum glacier expansion, based on the average cosmogenic ages of moraine groups, is ~25 ka, but there are large uncertainties (up to 7 ka), making the exact time of the LLGM uncertain. It also remains uncertain whether LLGM moraines were constructed during a long still-stand or a re-advance that erased the previous maximum limit (Mark et al., 2017). A close examination of site records reveals that, although the LLGM was close to the GLGM, there was, in some places, a larger local maximum extension of glaciers before the GLGM (Farber et al., 2005; Smith et al., 2005; Rodbell et al., 2008). In the southern part of the Altiplano, maximum glacier extents of the last glaciation are probably as old as 60 ka (e.g. Blard et al., 2014) (Figs. 16 and 17). Lakes Titicaca and Junin, which are outside glacial moraines, have provided sediment

records that indicate deglaciation was underway by 22-19.5 ka (Seltzer et al., 2000, 2002; Baker et al., 2001a, 2001b; Rodbell et al., 2008). On the Coropuna volcano, located in southern Peru, ^{3}He ages indicate that the LLGM happened ~25 ka and deglaciation began at ~19 ka (Bromley et al., 2009).

Temperatures decreased ~6° C during the GLGM in the Peruvian and Bolivian Andes (Mark et al., 2005), and precipitation was slightly higher than today, as indicated by the Sajsi paleo-lake cycle (Seltzer et al., 2002; Blard et al., 2011, 2013). Therefore, a temperature increase was probably the main driver of deglaciation between 19 ka and 17 ka. However, precipitation variations likely played an important role in some regions where a late deglaciation is reported, such as in the vicinity of the paleo-lake Tauca, on the central Altiplano (Martin et al., 2018).

4.10 Southern Bolivia and Northern Chile

Glacier extent at the GLGM in the western cordillera of the Andes, adjacent to the Arid Diagonal, is unclear. Glacial deposits and landforms north of the Arid Diagonal that have been investigated include those at Cerro Uturuncu (Blard et al., 2014), El Tatio and Sairecabur (Ward et al., 2017), and Cerro La Torta and the Chajnantor Plateau (Ward et al., 2015). Deposits in the subtropics south of the Arid Diagonal include those in Valle de Encierro (Zech et al., 2006) and Cordón de Doña Rosa (Zech et al., 2007). At most sites north of the Arid Diagonal, a set of degraded moraines lies 2-5 km outside one or two sets of closely nested, sharper-crested moraines, which in turn are outside smaller younger up-valley moraines (Jenny et al., 1996). A few ^{10}Be and ^{36}Cl ages suggest that the outer degraded moraines date to MIS 6 (191-130 ka; Ward et al., 2015). Greater precision is not possible with available data, but this interval corresponds to the age of a broad bajada along the Salar de Atacama based on ^{36}Cl ages on terrace surfaces and a depth profile (Cesta and Ward, 2016).

A set of more prominent moraines inside these degraded moraines marks the maximum expansion of glaciers after MIS 6 (Ward et al., 2017). Widely scattered ^{10}Be and ^{36}Cl ages, ranging from about 90 to 20 ka (45-35 ka modal age), have been obtained from boulders on these moraines both north and south of the Arid Diagonal (Ward et al., 2017) (Fig. 18). Eight boulders on the sharp crest of the LLGM moraine at El Tatio yielded six ^{36}Cl ages between 41 ka and 19.8 ka, with outliers at 82 and 57 ka. At Cerro La Torta, one LLGM moraine boulder yielded a ^{10}Be age of 24.7±1.8 ka and glaciated bedrock just

inside the LLGM limit returned a ^{10}Be exposure age of 31±2.4 ka. Similar ages have been obtained from the terminal moraines at Cerro Uturuncu, south of paleolake Tauca on the Bolivian Altiplano, with 8 of 12 ^{3}He ages between 46 and 33 ka (Blard et al., 2014). Similarly, a single boulder on the outer terminal moraine in Encierro Valley yielded a ^{10}Be age of 35±2 ka (Zech et al., 2006), and 9 of 13 ^{10}Be samples from the outermost moraines, drift, and outwash at Cordón de Doña Rosa returned ages ranging from 49 to 36 ka (Zech et al., 2007).

If the local LGM moraines date to 49-35 ka, they were built at about the same time as the Incahuasi highstand, during which a deep lake formed in the Pozuelos Basin in Argentina (McGlue et al., 2013), and during a period when glaciers in the subtropical Argentine Andes expanded (see Section 4.11).

Exposure ages on bedrock inside the prominent LLGM moraines (Blard et al., 2014; Ward et al., 2015) indicate that deglaciation was underway by 20-17 ka. Assuming these ages are valid, deglaciation of the western cordillera in northern Chile may have preceded that of the Altiplano.

The scatter in cosmogenic ages on moraines in this region may be due to differences in dating methods. ^{36}Cl production is environmentally sensitive, and production rates are less certain than those for ^{10}Be. However, ^{10}Be ages on the same features also exhibit scatter (Ward et al., 2015). For example, the LLGM moraines bordering the former 200 km^2 ice cap on the Chajnantor Plateau (4500-5500 m asl) have yielded both ^{10}Be and ^{36}Cl ages ranging from 141 to 43 ka. However, ^{10}Be and ^{36}Cl exposure ages on glaciated bedrock beneath the most prominent moraines are younger and less scattered (30-18 ka), and one boulder on a small moraine ~1 km inboard of the LLGM margin yielded an age of 26.7±2.8 ka, similar to the bedrock ages (Ward et al., 2017). Additionally, the youngest bedrock exposure ages (20-18 ka) are from downvalley sites, near the terminal moraines, whereas ages higher on the plateau are older (30-26 ka) (Ward et al., 2015). This pattern cannot be explained by retreat of the glacier margin; rather it suggests that the LLGM moraines contain a significant component of older reworked material with cosmogenic inheritance. It is also consistent with the lesser, but still considerable, scatter seen in the ages on LLGM valley glacier moraines in the region.

Reliable estimates of temperature and precipitation in northern Chile during the GLGM will require more precise dating of the glacial deposits there. Kull and Grosjean (2000) performed glacier-climate modeling to reconstruct precipitation associated with construction of the major sharp-crested moraine at the El Tatio site. They assumed a regional temperature depression of ~3.5ºC, consistent with that at ca. 17 ka, and concluded that an additional 1000 mm/yr of precipitation over modern would be required to generate a glacier of the appropriate size. If instead the sharp-crested El Tatio moraines date to the GLGM, as suggested by Ward et al. (2017), temperatures were likely 5-7 C lower than today and less precipitation would be required. For example, assuming a 5.7 C temperature depression typical of the GLGM in this area, Kull et al. (2002) estimated that a 580±150 mm/yr increase over modern precipitation would be required to explain the LLGM deposits at a different western cordillera site (Encierro Valley).

4.11 Central Andes of Argentina

The maximum expansion of glaciers in the Argentine Andes occurred before the GLGM, between 50-40 ka and before 100 ka (Zech et al., 2009, 2017; Martini et al., 2017a; Luna et al., 2018; D'Arcy et al., 2019). However, there was a generalized glacier expansion during the GLGM between 22º and 35º S (Fig. 19). North of the Arid Diagonal, the LLGM is dated to 25-20 ka based on an average of 10 ^{10}Be ages on both sides of Nevado de Chañi (Martini et al., 2017a). The advance on the east side of Nevado de Chañi was less pronounced than that on the west side. Glaciers advanced between ~22 ka and ~19 ka in the Laguna Grande valley and at ~20 ka in the Peña Negra valley, both in the Tres Lagunas area (Zech et al., 2009, 2017). M2 moraines in the Sierra de Aconquija were built at ~22 ka (D'Arcy et al., 2019). There are no moraines firmly dated to the GLGM in the Sierra de Quilmes (Zech et al., 2017), but pronounced undated lateral moraines in the Nevado del Chuscha valley might be of that age. Based on the geomorphology and chronology of the moraine sequence in the same valley, Zech et al. (2017) concluded that these lateral moraines must have been deposited between 44 ka and 18 ka.

There is no consensus about precipitation levels in the subtropical Andes north of the Arid Diagonal during the GLGM. Available evidence from the nearby arid Altiplano suggests climate was only moderately wetter than present (Baker et al., 2001a, 2001b; Placzek et al., 2006). Speleothem records from the western Amazon, the Peruvian Andes, the Pantanal and southeastern Brazil all indicate wetter conditions during the GLGM

(Cruz et al., 2005; Wang et al., 2007; Kanner et al., 2012; Cheng et al., 2013; Novello et al., 2017) due to an intensification of the South American summer monsoon.

The glacial chronology south of the Arid Diagonal is poorly constrained. Moraines coincident with the GLGM have been found in the Ansilta range and Las Leñas valley. Lateral moraines in the Ansilta range have been dated to 28-19 ka based on four ^{10}Be ages, and a prominent lateral moraine in Las Leñas valley was built between 22 ka and 20 ka (Terrizano et al., 2017). Other possible evidence of GLGM glacial activity comes from the Cordon del Plata range, where one boulder on the Agostura I moraine was dated to 19 ka (Moreiras et al., 2017). Two ^{10}Be ages (31 ka and 23 ka) on a moraine close to Nahuel Huapi lake, near Bariloche in northern Patagonia, suggest a GLGM age (Zech et al., 2017). An end moraine in the Rucachoroi valley yielded two ^{10}Be ages and Zech et al. (2017) assigned an age to an end moraine in the Rucachoroi valley to 21 ka based on two ^{10}Be ages. South of the Arid Diagonal, there is evidence of wetter conditions during the GLGM compared to today (Kaiser et al., 2008; Moreno et al., 2018).

4.12 Patagonia

The time of the LLGM of the Patagonian Ice Sheet (PIS) is, unsurprisingly, variable, given the broad latitudinal range of the Patagonian Andes (38°–55°S). In most cases, Patagonian glaciers achieved their maximum extents earlier than the GLGM, during MIS 3 (Darvill et al., 2015; Garcia et al., 2018). Detailed stratigraphic and chronologic data exist in the Chilean Lake District (41°S) on the northwest side of the former ice sheet (Denton et al., 1999a; Moreno et al., 2015, 2018). Here, multiple radiocarbon-based chronologies bracket the time of local major expansions of piedmont lobes at ~33.6, ~30.8, ~26.9, ~26 and 17.8 ka (Denton et al., 1999a; Moreno et al., 2015). There is a significant gap in glacial chronologies for the area between 41° and 46°S, except for the Cisnes valley (44°S) where moraines dating to the end of the GLGM (^{10}Be mean age ~20 ka) are inside more distal moraines that are assumed to date to earlier phases of the last glacial cycle (de Porras et al., 2014; Garcia et al., 2019). However, the more distal moraines are undated, consequently it remains unclear whether or not the pattern of more extensive MIS 3 advances persists southward in central Patagonia. Farther south, additional studies have been done in the area currently occupied by the cross-border lakes of Lago General Carrera/Buenos Aires (46.5°S) and Lago Cochrane/Pueyrredón (47.5°S). In the former area, ages of ~26 ka have been obtained for the local maximum extent of the PIS (Kaplan et al., 2004, 2011; Douglass et al., 2006), coincident with the GLGM.

However, earlier glacial activity, at 34-31 ka, is suggested by Optically stimulated Luminescence (OSL) ages on buried sediments (Smedley et al., 2016). In the latter area (Lago Cochrane/Pueyrredón), the LLGM has been dated at ~29 ka, and possibly ~35 ka, with moraines of the GLGM located immediately up-ice (Hein, 2009, 2010, 2017).

Exposure dating in southern Patagonia indicates that the LLGM was far more extensive than subsequent GLGM advances. For example, the Bahía Inútil–San Sebastián ice lobe (53°S) expanded 100 km farther at ~45 ka and ~30 ka (Darvill et al., 2015a) than later advances during the GLGM at ~20 ka (McCulloch et al., 2005a; Kaplan et al., 2008). The pattern is repeated farther north where the Torres del Paine and Última Esperanza ice lobes (51°S) reached their local maximum extents at ~48 ka, with subsequent advances dated to 39.2 ka and 34 ka, and a far less extensive GLGM advance at 21.5 ka (Sagredo et al., 2011; García et al., 2018). Single exposure ages from the San Martín valley (49°S) tentatively suggest local maximum glacier expansion at ~39 ka, with a less extensive GLGM advance at ~24 ka (Glasser et al., 2011).

Considered together, the chronologies demonstrate that the LLGM in Patagonia occurred at different times, but largely during MIS 3. Presently, there is no satisfactory mechanism to adequately explain the timing of this local glacial maximum, although possible explanations include regional insolation and coupled ocean-atmosphere interactions, including the influence of the southern westerly winds, sea surface temperatures, Southern Ocean stratification and Antarctic sea ice extent (Darvill et al., 2015a, 2016; Moreno et al., 2015; García et al., 2018). Compared to the LLGM, the onset of deglaciation is more closely coupled throughout Patagonia and centered at 17.8 ka with some local variation, which is concurrent with warming of the mid to high latitudes in the Southern Hemisphere (Kaplan et al., 2004, 2007; McCulloch et al., 2005a; Douglass et al., 2006; Hein et al., 2010, 2017; Sagredo et al., 2011; Murray et al., 2012; García et al., 2014, 2019; Henríquez et al., 2015; Moreno et al., 2015, 2018, 2019; Bendle et al., 2017; Mendelova et al., 2017; Vilanova et al., 2019).

4.13 Tierra del Fuego

Caldenius (1932) constructed the first map of the Darwin ice field at the LLGM. The map has not been greatly modified since that time, and the exact position of the ice limits around large parts of the Cordillera Darwin are poorly constrained. Former ice extent is best understood where glaciers flowing northeastward from the mountains contributed to

extensive lobes in the Straits of Magellan and Bahía Inútil (Clapperton et al., 1995; Rabassa et al., 2000; Bentley et al., 2005; McCulloch et al., 2005a; Coronato et al., 2009; Darvill et al., 2014) (Fig. 20). Surface exposure ages of glacial landforms in Tierra del Fuego suggest that these lobes achieved their maximum extents by ~25 ka and remained there until ~18 ka (McCulloch et al., 2005b; Kaplan et al., 2008; Evenson et al., 2009). However, several belts of ice-marginal landforms occur outside these moraines (Caldenius, 1932; Clapperton et al., 1995; McCulloch et al., 2005a; Evenson et al., 2009), and existing exposure age data have yielded conflicting results. Some of these outer moraines have been assigned pre-GLGM ages, but an analysis of weathering of erratic boulders suggests that most, if not all, of them may date to the last glaciation (Darvill et al., 2015b). On the southern flank of the Cordillera Darwin, outlet glaciers formed an ice stream in Beagle Channel that terminated near the Atlantic Ocean (Caldenius, 1932; Rabassa et al., 2000, 2011; Coronato et al., 2004, 2009), but remains undated. Moreover, there is no convincing evidence on the Pacific Coast for the position of the GLGM ice-sheet margin, and reconstructions range from extensive ice on the continental shelf (Caldenius, 1932) to ice terminating close to the present-day shoreline (Coronato et al., 2009). Given the uncertainty in GLGM positions around most of the margin, the time of the onset of glacier recession is difficult to pinpoint. However, on both the north and south sides of the range, radiocarbon ages from bog sediments, as well as a limited number of exposure ages from erratics, indicate that glaciers had receded to the interior of the mountains by ~17 ka (Heusser, 1989; Hall et al., 2013; Menounos et al., 2013) (Fig. 20).

4.14 Synthesis

Based on current understanding, glaciers in North and Central America during the GLGM (Table 1 and Fig. 3) appear to have fluctuated near-synchronously and likely responded to the same climate drivers. In many sectors, glaciers achieved their LLGM extents around 26-21 ka. In some cases, glacier fronts remained stable from that time until shortly after 21 ka, when deglaciation began. This was the case for most of the LIS and for glaciers in Alaska, the North Cascades, several valleys in the Rocky Mountain/Yellowstone region, the Sierra Nevada, Central Mexico, and the Cordillera de Talamanca in Costa Rica.

Key climate forcing common to all these regions is the decrease in temperature during the GLGM. Based on a decrease in ELAs of approximately 900 m, temperatures decreased by approximately 7-8°C across much of the North American continent.

However, there are some differences. For example, the ELA depression in Alaska was less than 500 m, and the corresponding summer temperature depression was likewise less than in the western US. The pattern of precipitation during the GLGM apparently was even less uniform. Evidence shows a trend towards aridity during the GLGM in the North Cascades close to the ice sheet and the northern Rocky Mountains, and increased precipitation to the south in the Sierra Nevada, Basin and Range Province and southern Rocky Mountains.

We note that the behavior of glaciers during the GLGM in North and Central America was also asynchronous. Several glaciers advanced to their maximum positions several thousand years after the GLGM, at about the time of the HS-1 period. This is the case for some sectors of the LIS and CIS, some ranges in southern Alaska, some areas close to Yellowstone, the Colorado Rocky Mountains, mountains of central Mexico near the oceans, and some valleys of the Cordillera de Talamanca in Costa Rica. Differences in glacier activity within the same region could be due to local differences in precipitation stemming from orographic effects, for example in some areas of the Yellowstone region, or between oceanic and interior mountains in Mexico. Whether or not the relationship between precipitation and the glacial local maximum is generally applicable for the entire continent is a subject for future research.

The relative consistency in glacier behavior across North and Central America is not observed in South America. The lack of synchronicity in glacier growth in the Andes might possibly be due to the relative scarcity of data in the region or, alternatively, to its large latitudinal range and complex geography, which lead to large differences in precipitation. The most arid regions of the southern tropical Andes (southern Bolivia, northern Chile and Argentina) show the largest temporal variability in the time of the LLGM, probably due to strong precipitation control. In any case, the maximum local expansion of the glaciers in most areas in the Andes does not coincide with the GLGM. One of the few exceptions is in Tierra del Fuego, where glaciers may have reached their maximum extents between ~25 ka and ~18 ka. Even there, however, future work may show that moraines down-ice of this limit may also date to the last glaciation. In the rest of the Andean Cordillera, moraines were built during the GLGM, but the maximum advance apparently happened up to several thousands of years earlier; in southern Patagonia the LLGM may have occurred during MIS 3 as few other southern high latitude regions such as Kerguelen (Jomelli., et 2018). We also note that the moraines that

coincide with the GLGM are not necessarily the largest, as is commonly the case in North America where glacier fronts remained in the same position for an extended period of time.

Glaciers in the central part of the Altiplano, in the vicinity of paleo-lake Tauca, remained close to their LLGM positions until the end of H-1 (Martin et al., 2018). Elevated precipitation during H-1 apparently sustained glaciers until the end of that period. In summary, throughout the Andes, the GLGM seem to be marked by an expansion of glaciers, but that advance was not the largest everywhere. Across the Andes, this period coincided with a clear drop in temperature of ~3-8°C based on ELA depressions. Those values are consistent with temperature reductions inferred from ELA depressions in North America. Some local indicators, for example the Sajsi paleo-lake on the Altiplano show that the GLGM was characterized by slightly higher precipitation than today (Placzek et al., 2006).

5. The Impact of Heinrich-1 Stadial (HS-1) (17.5-14.6 ka) on American Glaciers

5.1 Heinrich-1 Stadial

The second period analyzed is the Heinrich 1 Stadial (HS-1), which is called the 'Oldest Dryas' in Scandinavia. The term HS-1 comes from records of marine sediments that show the massive discharge of icebergs into the North Atlantic during this period (Heinrich, 1988), mainly from the Hudson Bay/Strait region, the main drainage route for the LIS (Hemming, 2004). The use of the term as a chronological unit has been criticized (Andrews and Voelker, 2018) from a sedimentological point of view. The term Oldest Dryas, although widely used, has also been criticized because it is not clearly delimited chronologically (Rasmussen et al., 2014). In this paper, we follow the paleoclimate and paleoglaciological criteria of Denton et al. (2006), who delimit HS-1 between the Heinrich 1 "event" (17.5 ka) and the beginning of the Bølling-Allerød interstadial (14.6 ka). They refer to this period as the 'Mystery Interval' due to the fact that, although CO_2 concentrations in the atmosphere increased during this time, temperature dropped sharply in the Northern Hemisphere and in the tropics. In our study, we opt for the term HS-1 for the same time period, following the standard differentiation between "event" and "stadial" (Rasmussen et al., 2014; Heath et al., 2018).

HS-1 is a climate event that interrupted deglaciation. In the North Atlantic region, temperatures fell drastically in winter, sea ice expanded, and the ocean cooled (Barker et al., 2010). Atlantic Meridional Overturning Circulation (AMOC) was sharply reduced or even collapsed (McManus et al., 2004; Böhm et al., 2015), and many mountain glaciers advanced in Europe (Gschnitz stadial in the Alps; Ivy-Ochs, 2015), at least at the beginning of HS-1. Although the European ice sheets decreased in size during this period (Toucanne et al., 2015), it is clear that climate during HS-1 varied. There were periods with hot summers that caused massive glacier melting (Thornalley et al., 2010; Williams et al., 2012). The Asian monsoon disappeared (Wang et al., 2008), the South American monsoon intensified (Stríkis et al., 2015, 2018), and the Southern Hemisphere westerlies were displaced polewards (Denton et al., 2010). Temperatures in Antarctica increased, along with atmospheric CO_2 concentrations (Monnin et al., 2001; Ahn et al., 2012), due to Southern Ocean ventilation (Barker et al., 2009). HS-1 is the period that best demonstrates the close relationships among AMOC, atmospheric CO_2 and temperatures in Antarctica (Deaney et al., 2017).

5.2 Laurentide Ice Sheet

The extent of glaciers and ice sheets during HS-1 is summarized in Figure 4. Although explanations of Heinrich events have tended to focus on the Hudson Strait ice stream, it is clear that there are sedimentological differences both within and between individual Heinrich 'layers,' including variable source areas (Andrews et al., 1998, 2012; Piper and Skene, 1998; Hemming, 2004; Tripsanas and Piper, 2008; Rashid et al., 2012; Roger et al., 2013; Andrews and Voelker, 2018). Thus, it is likely that other ice streams along the eastern margin of the LIS, and possibly even farther afield at its northern margin (Stokes et al., 2005), may have contributed, at least in part, to some Heinrich-like events (Andrews et al., 1998, 2012; Piper and Skene, 1998). However, the extent to which these events were correlative is unclear, as are the wider impacts of Heinrich events on the dynamics of the LIS. For example, readvances or stillstands elsewhere in the Americas have been linked to HS-1, and yet evidence from the LIS is comparatively scarce.

Clark (1994) was one of the first to propose a link between Heinrich events in the Hudson Strait and the advance of ice margins/lobes resting on soft deformable sediments along the southern margin of the ice sheet. Mooers and Lehr (1997) also noted the possibility that the advance and rapid retreat of lobes in the western Lake Superior region may have been correlative with Heinrich events 2 and 1, but this idea has since received relatively

little attention and there is little clear evidence for major re-advances of the LIS during or soon after HS-1 (Heath et al., 2018). Rather, the most likely impact of HS-1 was to lower the ice surface over Hudson Bay and drive changes in the location of ice dispersal centers, with subsequent effects on ice-flow patterns (Margold et al., 2018). For example, Dyke et al. (2002) suggest that the drawdown of ice during HS-1 was likely sufficient to displace the Labrador ice divide some 900 km eastward from the coast of Hudson Bay and cause a major flow reorganization (see also Veillette et al., 1999). There is also evidence that parts of the ice sheet thinned rapidly in coastal Maine during the latter part of HS-1 (Hall et al., 2017b; Koester et al., 2017).

There is also clear evidence from several regions that the ice sheet retreated during HS-1, punctuated by brief readvances or stillstands. For example, recalculated ^{10}Be data (Balco and Schaefer, 2006), coupled with the New England varve chronology (Ridge et al., 2004), indicate retreat of the ice margin in the northeastern United States. ^{36}Cl exposure ages from the Adirondack Moutains (Barth et al., 2019) suggest that the ice sheet may have begun to thin around 19.9±0.5 ka. Thinning continued throughout HS-1 and accelerated between 15.5±0.4 ka and 14.3±0.4 ka (see also Section 5.2). Rapid ice sheet thinning has also been inferred in coastal Maine during the latter part of HS-1 (Hall et al, 2017b; Koester et al., 2017).

5.3 Alaska

Although detailed moraine chronologies needed to fully explain glacier change in Alaska during HS-1 do not exist, there is patchy information on ice extent at that time. In most locations where recessional moraines have been dated, some stillstands or re-advances have been inferred during HS-1. In the Brooks Range, a prominent recessional moraine has been dated to ~17 ka (Pendleton et al., 2015), and the Elmendorf Moraine in south-central Alaska dates to ~16.5 ka (Kopczynski et al., 2017). Given the number of recessional moraines in most valleys, for example throughout the Alaska Range, the Ahklun Mountains, and the Kenai Peninsula, it is difficult to know if these glacial stabilizations necessarily relate to cooling triggered in the North Atlantic Ocean. Rather, they could be related to a number of factors that could cause glacier recession to be interrupted by re-advances or stillstands (e.g. isostatic rebound, solar variability, glacier hypsometric effects). Thus, attributing them *per se* to North Atlantic stadial conditions at this time is premature. In fact, in spite of some interruptions, there was overall significant

recession of glaciers throughout HS-1 in Alaska. Most glaciers in Alaska with reasonable chronological constraints experienced net retreat during HS-1.

5.4 Cordilleran Ice Sheet and the North Cascades

Alpine glaciers receded from maximum positions during the Port Moody interstade, which began after 21.4 ka (Riedel et al., 2010). Two glacial events in this region correlate with HS-1: construction of alpine glacier end moraines and the advance of the CIS to its maximum limit. Deposition of ice-rafted detritus at a deep-sea core site west of Vancouver Island began about 17 ka and abruptly terminated at about 16.2 ka, recording the rapid advance and retreat of the western margin of the CIS (Cosma et al., 2008). Studies west of Haida Gwaii (Blaise et al., 1990) and near the southwestern margin of the CIS (Porter and Swanson, 1998; Troost, 2016) also indicate that it reached its maximum extent several thousand years after the GLGM. Glaciers in two mountain valleys in the southern North Cascades retreated from moraines closely nested inside the GLGM moraines. However, ^{36}Cl ages on the Domerie II (17.9-14.7 ka) and the Leavenworth II moraines (17.2-15.0 ka) have large uncertainties, and the moraine ages may or may not be associated with HS-1 (Porter, 1976; Kaufman et al., 2004; Porter and Swanson, 2008).

The climate in the North Cascades during HS-1 is not well understood due to a lack of age control on landforms, limited paleoecological data, and the large influence of the continental ice sheets on climate. However, glacial ELAs associated with potential HS-1 moraines located well to the south of the CIS terminus were slightly above the GLGM maximum (Porter, 1976; Kaufman et al., 2004; Porter and Swanson, 2008). In areas inundated by the CIS to the north, alpine glaciers retreated to valley heads, presumably due to lower precipitation as the continental ice sheets expanded to cover most of Canada and northern Washington. Climate models and pollen data indicate that at 16 ka mean annual air temperature was 4-7ºC cooler than today (Heusser, 1977; Kutzbach, 1987; Liu et al., 2009).

5.5 Rocky Mountain/Yellowstone region

In some areas of this region, glacier retreat began toward the end of the GLGM; in other areas, glaciers maintained their fronts or re-advanced at ~16.5 ka, although with a great degree of local variability, and then immediately retreated. Glaciers in some valleys near the margins of the Yellowstone Ice Cap reached their local maximum extent at ~17 ka, then rapidly retreated at ca. 15 ka when several external climate forcings coincided

(Licciardi and Pierce, 2018) (Figs. 11 and 12). Moraines dated to the HS-1 period are common in valleys along the eastern slope of the Teton Range (Licciardi and Pierce, 2018) and in the Wind River Range (Dahms et al., 2018, 2019; Marcott et al., 2019). In the Wind River Range, these moraines are ~1-2 km downvalley from cirque headwalls in 14 valleys (Dahms et al., 2010). Ages from these moraines in Stough Basin, Cirque of the Towers and Temple Lake cluster around ~15.5 ka (Fig. 10) (Dahms et al., 2018; Marcott et al., 2019). Subsequently, a second period of regional deglaciation was well under way after ~15 ka (Larsen et al., 2016; Dahms et al., 2018; Pierce et al., 2018).

Glaciers in some valleys in the Colorado Rocky Mountains receded during HS-1. In contrast, many other valleys contain end moraines dating to 17-16 ka. Ages on polished bedrock surfaces up-valley of these moraines have yielded ages that show that the glaciers retreated shortly thereafter (Young et al., 2011; Shakun et al., 2015a; Leonard et al., 2017a, 2017b; Laabs et al., 2020, submitted). Ward et al. (2009) suggest that there was a stillstand or possible re-advance around 17-15 ka in the Colorado Front Range, interrupting overall post-GLGM recession.

5.6 Sierra Nevada

There is strong evidence for an advance of glaciers in the Sierra Nevada during HS-1 – the Tioga 4 advance in local terminology (Phillips et al., 1996) – but HS-1 was not a time of extensive glaciation. As described in Section 3.5, retreat from the GLGM maximum began gradually at about 19 ka. It accelerated rapidly after 18 ka, and glaciers receded past Tioga 4 glacier margins by about 17 ka (Phillips, 2017). Retreat then reversed and glaciers readvanced to Tioga 4 positions by 16.2 ka (Fig. 14). The ELA depression for this advance was about 900 m, compared to the GLGM ELA depression of about 1200 m. The Tioga 4 advance apparently was short-lived; by 15.5 ka, the range was effectively deglaciated. It is clear from the simultaneous expansion of Lake Lahontan and the Tioga 4 glaciers that increased precipitation played a major role in glacier expansion at this time.

The fact that Lake Lahontan was relatively small during Tioga 3 (21-19 ka, the LLGM), while glaciers were more extensive, shows that Tioga 3 was colder and drier than Tioga 4. Plummer (2002) estimated that Tioga 4 precipitation was 160% greater than today and temperature was 3°C cooler based on the inferred size of Searles Lake at that time. Had he used the extent of Lake Lahontan in his analysis, the increase in precipitation would have been even larger. Phillips (2017) suggested that the large extent of sea ice in the North Atlantic during HS-1 led to greatly increased precipitation and cooler temperatures

in California through an atmospheric teleconnection. An impediment to further analysis of these topics is the chronological inconsistencies between the dating of the Sierra glacial record, nearby marine cores, and lacustrine records (Phillips, 2017). More confidence in the chronology could allow researchers to resolve questions of climate leads and lags, and determine whether the apparent differences in timing are the result of chronological imprecision or latitudinal paleoclimate gradients.

5.7 Mexico and Central America

Glaciers in central Mexico remained at or near their maximum positions throughout HS-1. In the interior mountains (e.g. Iztaccíhuatl), glaciers were slightly smaller during HS-1 (ELA = 4040 m asl) than at the LLGM (ELA = 3940 m asl, from 21 ka to 17 ka) (Vázquez-Selem and Lachniet, 2017). Recession at this time is not recorded in mountains near the Pacific Ocean, where a low ELA persisted until 15-14 ka. Indeed, during HS-1, ELAs were ca. 400-650 m lower on mountains near the coast than in the interior, which suggests a strong precipitation gradient from the coast to the interior and overall drier conditions in the interior during HS-1 (Lachniet et al., 2013). In general, the end of HS-1 is coeval with the onset of glacier recession ~14.5 ka in central Mexico. Existing evidence at Cerro Chirripó, Costa Rica, indicates moraine formation between 18.5 ka and 17 ka (Cunningham et al., 2019), potentially during the earlier part of HS-1. If the summit area was ice-free by 15.2 ka, as suggested by Cunningham et al. (2019), glacier recession prevailed during the second part of HS-1 (as defined by Hodell et al., 2017).

5.8 Northern Andes

Most of the glacier advances in the northern tropical Andes were dated between the end of the GLGM and the end of HS-1 (~15 ka). In the Sierra Nevada of the Venezuelan Andes, some valleys were completely deglaciated by ~16.5 ka (Angel et al., 2016). In others, glaciers advanced ~17 ka (modified ages of Angel, 2016). In the Sierra Santo Domingo, maximum advances are dated to ~17.5 ka (modified ages from Wesnousky et al., 2012; Angel, 2016). In the Sierra del Norte they date to between 18 ka and 15.5 ka (modified ages from Wesnousky et al., 2012; Angel, 2016), and in the Cordillera de Trujillo, to around 18 ka (^{10}Be ages modified ages from those of Angel, 2016). Some advances in the Colombian Andes may be related to HS-1. This is the case in the Bogotá Plain, where a moraine complex has been dated to between 18 ka and 14.5 ka (Helmens, 1988; Helmens et al., 1997b), and in the Central Cordillera, where peat overlying a moraine complex yielded a minimum age of 16-15 ka (Thouret et al., 1996). There are

moraines in the Ecuadorian Andes that are related to HS-1, for example in Cajas National Park, vicinity of Pallcacocha lake above 3700 m asl, where a moraine was radiocarbon dated to 17-14.5 cal ka BP (Hansen et al., 2003).

Most glacier advances in the northern tropical Andes have been dated to ~18-15 ka based on ^{10}Be ages. However, the scarcity of paleoclimatic information limits our ability to estimate the regional HS-1 climate and to compare it to GLGM conditions. Rull (1998) proposed a cold event (~7°C cooler than today), locally called as El Caballo Stadial, at 16.5 ka based on a palynological record from the central Mérida Andes in Venezuela. Similarly, Hooghiemstra et al. (1993) proposed the Fúquene Stadial at a similar time in the Colombian Andes based on a palynological study in the Bogotá Plain. In contrast, Brunschön and Behling (2009) concluded that both temperature and precipitation in the southern Ecuadorian Andes were higher during the period 16.2-14.7 cal yr BP than during the GLGM.

5.9 Peru and Bolivia

Three moraines near Lake Junín have cosmogenic ages of ~21 ka to 18 ka (Smith et al., 2005), providing evidence of an advance prior to HS-1. In contrast, the Galeno moraines in the Cajamarca region have slightly younger ages and have complete inset lateral/terminal loops with an average age of 19 ka. The Juellesh and Tuco valleys in the Cordillera Blanca have inner and outer moraine loops that date, respectively, to ~18.8±2.0 ka and ~18.7±1.6 ka (Smith and Rodbell, 2010). Glasser et al. (2009) presented similar ages (~18.3±1.4 ka) for an outer lateral moraine in the Tuco valley. An inner lateral moraine (M4 of Smith and Rodbell, 2010) has been dated to ~18.8±2.3 ka, and Glasser et al. (2009) reported similar ages on the same moraine (~17.9±0.9 ka). Revised ages on various stages of deglaciation of the Cordillera Huayhuash are centered on ~17.8-16.5 ka (Hall et al., 2009). Similarly, dated boulders on the Huara Loma, Coropuna, and Wara Wara moraines in Bolivia may record post-GLGM advances between 19.4 ka and 18.2 ka (Zech et al., 2010; May et al., 2011; Martin et al., 2018).

Many valleys in central Peru and Bolivia contain evidence of glacier advances or persistent stillstands during HS-1 (~17.5-14.6 ka) (syntheses in Mark et al., 2017, and Martin et al., 2018). The mean exposure ages of all groups of moraine boulders in this region that fall within HS-1 is 16.1±1.1 ka. A stillstand synchronous with HS-1 is also indicated by cosmogenic ^{3}He ages of moraines on the Coropuna volcano, southern Peru (Bromley et al., 2009). Radiocarbon and cosmogenic ages from the Cordillera Vilcanota

and the HualcaHualca volcano (Fig. 17) provide independent evidence that glaciers in southern Peru advanced sometime after ~18.0-16.8 ka (Mercer and Palacios, 1977; Alcalá-Reygosa et al., 2017), and radiocarbon ages from the Altiplano indicate an advance occurred there from ~17 ka to 15.4 ka (Clapperton et al., 1997b; Clapperton, 1998).

Ice core records from Huascarán, Peru, suggest that HS-1 was the coldest period of the past ~19 ka (Thompson et al., 1995), but researchers have argued recently that the $\delta^{18}O$ signal in tropical ice does not provide a pure temperature signal (Quesada et al., 2015). The cooling inferred from reconstructions of paleo-ELAs during HS-1 is around 3°C in the central Altiplano (Martin et al., 2018).

The northern equatorial Andes of Peru appear to have been wetter during most of HS-1 (Mollier-Vogel et al., 2013), whereas speleothem records in central Peru suggest that the local climate became abruptly drier at ~16 ka (Kanner et al., 2012; Mollier-Vogel et al., 2013). Lake-level fluctuations provide strong evidence for pronounced shifts in precipitation across the central Andes during this period (Baker et al., 2001a, 2001b; Placzek et al., 2006; Blard et al., 2011). Farther south, over the Altiplano, shoreline reconstructions demonstrate that the first part of HS-1 (~18-16.5 ka) was similar to or drier than today. However, during the Lake Tauca highstand in the second part of HS-1 (16.5-14.5 ka) precipitation was ca. 130% higher than today (Placzek et al., 2013; Martin et al., 2018). Some of the GLGM and older moraines in this part of the Altiplano may have been overridden during this wet phase. Martin et al. (2018) established that the downward shift in ELA at this time was amplified in valleys that are near the latitudinal center of paleo-lake Tauca, resulting from a significant local increase in precipitation.

5.10 Southern Bolivia and Northern Chile

During HS-1, there was a sharp spatial gradient in climate between Cerro Tunupa, which is located at the geographic center of Lake Tauca, and Cerro Uturuncu (Bolivia) and elsewhere north of the Arid Diagonal (Ward et al., 2017; Martin et al., 2018). Blard et al. (2014) describe a 900 m gradient in ELAs between Cerro Tunupa and Cerro Uturuncu based on the Tauca-phase moraines at each site. The spatial gradient in temperature between these sites (Ammann et al., 2001) is not sufficient to explain the ELA difference, which implies the existence of a strong spatial gradient in precipitation across the southern margin of Lake Tauca. Further work by Martin et al. (2018) quantified this precipitation gradient, confirming that it was significantly drier in the southern portion of

the Lake Tauca basin. The presence of this drying trend to the south and west is supported by the lack of a clear Tauca-phase transgression at Pozuelos Basin in the Puna region, which is at a similar latitude to Cerro Uturuncu and El Tatio (McGlue et al., 2013). Based on the clustering of ^{10}Be and ^{36}Cl exposure ages on LLGM moraines (Section 4.10), Tauca-phase moraines appear to be either absent or restricted to higher parts of valleys at El Tatio, Cerro La Torta, and Chajnantor Plateau (Ward et al., 2017), as well as at several sites on the central Puna Plateau (Luna et al., 2018) and the western slope of Nevado Chañi (24ºS) in Argentina (Martini et al., 2017a). The precipitation gradient is consistent with paleo-vegetation proxy records that indicate an approximate doubling of modern precipitation, from ~300 to ~600 mm/yr (Grosjean et al., 2001; Maldonado et al., 2005; Gayo et al., 2012), in the northern Arid Diagonal and adjacent Andes during the Tauca highstand. South of the Arid Diagonal, at Valle de Encierro and Cordón de la Rosa, ages of 17 ka from highly recessed locations indicate a stillstand or minor advance during HS-1, followed by full deglaciation (Ward et al., 2017).

5.11. Central Andes of Argentina

Initial deglaciation in the Central Andes after the LLGM was followed by renewed glacier expansion during HS-1. Moraines that mark the HS-1 limit are found up-valley of those constructed during the GLGM. North of the Arid Diagonal, glacier expansion during HS-1 coincided with the Tauca paleo-lake (Blard et al., 2011; Placzek et al., 2013). Glaciers advanced in the Laguna Grande valley in the Tres Lagunas area between ~17 ka and ~15 ka (Zech et al., 2017), the east and west sides of Nevado de Chañi ~15 ka (Fig. 19) (Martini et al., 2017a), and in the Sierra de Quilmes, between ~18 ka and ~15 ka (Zech et al., 2017). An exception to these findings comes from Sierra de Aconquija where renewed glacier growth appears to have occurred after the HS-1 stadial (D'Arcy et al., 2019). South of the Arid Diagonal, there is almost no evidence of glacial limits dating to HS-1. Just one sample from the La Angostura I moraine in the Cordon del Plata has been dated to ~15 ka (Moreiras et al., 2017). Moraines up-valley of the GLGM limit in the Las Leñas valley and Ansilta Range have not yet been dated (Terrizzano et al., 2017; Zech et al., 2017).

5.12 Patagonia

At the time of the HS-1 stadial, the Patagonian region was experiencing widespread warming and deglaciation (Moreno et al., 2015; Bertrand et al., 2008). Rapid warming began at 17.8 ka in northwestern Patagonia and approached average interglacial

temperatures by 16.8 ka (Moreno et al., 2015). Glaciers in northwestern Patagonia retreated out of the lowlands shortly before ~17.8 ka and into high mountain cirques above 800 m asl by 16.7 ka (Denton et al., 1999a; Moreno et al., 2015). The abrupt and synchronous withdrawal of many glacier lobes in northwestern Patagonia was contemporaneous with the rapid expansion of temperate rainforests (Heusser et al., 1999; Moreno et al., 1999), suggesting pronounced warming at 17.8 ka coupled with a poleward shift of the southern westerlies between 17.8 ka and 16.8 ka (Pesce and Moreno, 2014; Moreno et al., 2018). However, on the east flank of the Andes (Cisnes valley, 44°S), it has been suggested that glaciers started retreating somewhat earlier, at ~19 ka. At this site, it has been estimated that the ice had diminished to 40% of its local maximum extent by ~16.9 ka (Weller et al., 2017; Garcia et al., 2019).

Farther south, in central Patagonia, lake cores from two small basin (Villa-Martínez et al., 2012; Henríquez et al., 2017) show that the Lago Cochrane/Pueyrredón ice lobe (47.5°S) retreated over 90 km into the Chacabuco Valley between ~21 ka (Río Blanco moraines; Hein et al., 2010a) and 19.4 ka. Ice receded an additional ~60 km to reach a position close to modern glacier limits by around 16-15 ka (Turner et al., 2005; Hein et al., 2010; Boex et al., 2013; Mendelova et al., 2017; Davies et al., 2018; Thorndycraft et al., 2019). Retreat east of the shrinking ice sheet in the Lago Cochrane sector of central Patagonia occurred without discernable warming (Henríquez et al., 2017). Almost certainly, however, this retreat was facilitated by calving in deep proglacial lakes that formed in the over-deepened Cochrane/Pueyrredón and General Carrera/Buenos Aires basins as the glaciers withdrew (Turner et al., 2005; Bell, 2008; Hein et al., 2010; Borgois et al., 2016; Glasser et al., 2016; Davies et al., 2018; Thorndycraft et al., 2019). At Lago General Carrera/Buenos Aires (46.5°S), glacier retreat from the Fenix I moraine commenced ~18 ka, but was interrupted by a readvance to the Menucos moraines at ~17.7 ka. An annually resolved lake sediment record, tied to a calendar-year timescale by the presence of the well dated Ho tephra erupted from Volcán Hudson (17,378±118 cal yr BP), indicates that ice remained close to the east end of the lake until after 16.9 ka, before retreating back into the mountains (Kaplan et al., 2004; Douglass et al., 2006; Bendle et al., 2017, 2019). Bendle et al. (2019) suggest that the onset of deglaciation in central Patagonia was a direct result of the HS-1 event. They hypothesize that warming at the start of HS-1 occurred due to rapid poleward migration of southern westerly winds, which increased solar radiation and ablation at the ice sheet surface. They linked warming and

accelerated deglaciation to the oceanic bipolar seesaw, which delayed Southern Hemisphere warming following the slowdown of the Atlantic meridional overturning at the start of HS-1 (Bendle et al., 2019).

Determining whether "early LGM" and "early deglaciation" are correct interpretations of glacier activity in central Patagonia (44°-49°S) (Van Daele et al., 2016; García et al., 2019) is important for determining whether local (glaciological, reworking of old organic matter) or regional (climatic) mechanisms are responsible for apparent differences in timing, rate, and magnitude of glacier fluctuations prior to and during the GLGM and Termination I (Vilanova et al., 2019). Another problem emerges from studies of lake sediments from the eastern slopes of the Andes in central Patagonia. Based on an analysis of seismic data and lake sediment cores from Lago Castor (Fig. 1), Van Daele et al. (2016) concluded that the Coyhaique glacier lobe achieved its maximum extent and retreated before the GLGM. The concepts of 'early LGM' and 'early deglaciation' rely heavily on the interpretation and selective rejection of anomalously old radiocarbon ages, which include results as old as 43,100±3600 ^{14}C yr BP in the clastic-dominated and intensely reworked portion of the Lago Castor cores beneath the H0 tephra, which has been radiocarbon dated to 17,300 cal yr BP (Weller et al., 2014). This enigmatic radiocarbon chronology has not been corroborated by more recent studies in the Río Pollux valley, where Moreno et al. (2019) and Vilanova et al. (2019) have reported stratigraphic, geochronologic, and palynological results from small, closed-basin lakes to constrain the timing and extent of the Coyhaique glacier lobe during Termination I. These studies point to the abandonment of the final LLGM margins at ~17.9 ka, ~600 years before the reported age of the H0 tephra. The similarities between northern and southern Patagonia (see below), and contrasts with the Río Cisnes and Lago Cochrane/Pueyrredón glacier lobes, suggest that the different behavior of the latter might arise from differences in their topographic setting, ice divide migration (Mendelova et al., 2019), or differential calving in large proglacial lakes in the Central Patagonian Andes during the final stage of the LLGM.

In southern Patagonia, the Lago Argentino lobe (50°S) retreated at least 60 km from its LLGM by 16.2 ka (Strelin et al., 2011). A nearby mountain glacier at Río Guanaco (50°S) retreated to half its extent between 18.9 ka and 17 ka, suggesting a temperature increase of ~1.5°C, or about one-third of the total deglacial warming relative to today (Murray et

al., 2012). Similarly, the Última Esperanza ice lobe retreated after 17.5 ka, but with a short period of stabilization at ~16.9-16.2 ka (Sagredo et al., 2011).

5.13 Tierra del Fuego

HS-1 in the Cordillera Darwin was characterized by very rapid glacier recession with no evidence of stillstands (Hall et al., 2013, 2017a). Surface exposure ages on boulders indicate that ice was at the innermost GLGM moraine at the shore of Bahía Inútil at ~18 ka (McCulloch et al., 2005b; Kaplan et al., 2008; Hall et al., 2013), but retreated shortly thereafter (McCulloch et al., 2005b). Radiocarbon ages from peat bogs near present-day sea level indicate that the Cordillera Darwin icefield had retreated inside fjords by 16.8 ka (Hall et al., 2013, 2017b). On the north side of the Cordillera Darwin, this recession was ~130 km from its LLGL. In the Fuegian Andes, two ^{10}Be ages from glacially eroded bedrock in front of an alpine glacier indicate that recession was well underway by ~17.8 ka and had reached the late-glacial position as early as ~16.7 ka (Menounos et al., 2013). Whether this glacier was part of the Cordillera Darwin icefield or a separate ice mass at the GLGM remains uncertain (Coronato, 1995; Menounos et al., 2013). In any case, glaciers in the region responded to HS-1 by rapidly retreating, as was the case at some other Southern Hemisphere locations (Putnam et al., 2013).

5.14 Synthesis

Glaciers in most of North and Central America began to retreat from their GLGM positions by about 21 ka (Table 2 and Fig. 4). In some areas (e.g. Wind River Range), they suffered the same mass losses after ~21 ka as other glaciers, but apparently re-advanced during HS-1. In other regions (e.g. Yellowstone Ice Cap, the Colorado Rocky Mountains and on some Mexican volcanoes), glaciers reached their maximum extents during HS-1. Some of these glaciers may have advanced from the GLGM to HS-1 and surpassed their GLGM limits. This possibility, however, must be considered hypothetical, as it is inherently difficult to verify.

Interestingly, one of the Northern Hemisphere regions that appears to have been least affected by the HS-1 event, at least in terms of the ice-marginal fluctuations, is the LIS. Rather, the ice sheet thinned and retreated during this period. It is likely that internal flow patterns and ice divides were impacted by drawdown induced by the Hudson Strait ice stream. There are few data from Alaska to evaluate the effects of HS-1 on glaciers, but there is some evidence of advances interrupting overall retreat during this interval. The

southern sector of the CIS and a number of glaciers in Colorado and those proximal to the Yellowstone Ice Cap area reached their maximum extents during HS-1. In a few valleys in the North Cascades south of the CIS limit, possible HS-1 moraines lie upvalley of GLGM moraines, although data are sparse. A clear advance immediately following HS-1 has been documented in the Sierra Nevada and the Wind River Range. In the Sierra, HS-1 moraines, locally termed Tioga 4, lie well inside GLGM moraines. These moraines record an ELA depression of 900 m, which is 300 m less than during the GLGM. In the Wind River Range, the Older Dryas/HS-1 moraines lie 19-27 km upvalley of LLGM/GLGM moraines. In the interior mountains of Central Mexico and Costa Rica, moraines dating to near HS-1 lie inside GLGM moraines. However, glaciers in mountains close to the oceans remained at, or advanced past, their GLGM limits until the end of HS-1.

In the Sierra Nevada, temperatures were 3ºC lower than today during HS-1, but clearly precipitation was increased. In other regions, data appear to confirm the decrease in temperature in the Sierra Nevada, but there is little information on precipitation.

Glaciers in the tropical Andes built significant moraine complexes during HS-1, attesting to a significant stillstand or readvance. In the northern Andes, numerous moraines have been dated to this period, reflecting an interruption of the longer-term of trend glacier retreat. HS-1 advances are widespread and significant in central and southern Peru and in Bolivia. Although the first part of the HS-1 stadial in these areas was dry, the second part was wet, with, on average, a two-fold increase in precipitation above modern values. The precipitation increase may have been five-fold around the Altiplano paleo-lakes (Tauca highstand from 16.5 ka to 14.5 ka). This precipitation control on glacier mass balance is a strong driver of the spatial variability of ELA reductions during HS-1. Several of the HS-1 moraines in the region appear to have been constructed by glaciers that were very close to LLGM moraines. HS-1 moraines are also present in the Arid Diagonal, although aridity increased towards the south, resulting in a more limited glacier extent in that area. In some cases, glaciers in the Arid Diagonal disappeared during HS-1. Glaciers advanced during HS-1 in the Central Andes of Argentina after a long period of retreat, and at the same time as the Tauca highstand.

In contrast, glaciers in the temperate and subpolar Andes abandoned their LGM positions and underwent sustained or step-wise recession during HS-1. In northwestern Patagonia, climate warmed rapidly and experienced a significant decline in precipitation, driven by

a southward shift of the southern westerly winds (Pesce and Moreno, 2014; Moreno et al., 2015, 2018; Henríquez et al., 2017; Vilanova et al., 2019). The magnitude of these changes appears to decline south of 45°S, modulated by the regional cooling effect of residual ice masses in sectors adjacent to the eastern margins of the Patagonian ice sheet (Henríquez et al., 2017). The difference in glacier behavior between the tropical Andes and Patagonia and Tierra del Fuego during HS-1 could be due to two causes. First, the significant increase in precipitation in the tropical Andes during HS-1 could be the main cause of the glacier advances in that region. Second, Patagonia and Tierra del Fuego may have been too distant from the events responsible for HS-1, which are closely related to North Atlantic circulation; rather they may have been more affected by Antarctica and southern westerly winds. The two effects may have even converged, dividing the continent into two different glacial regimes during HS-1 (Sugden et al., 2005).

6. Evolution of American Glaciers during the Bølling-Allerød Interstadial (B-A) and the Antarctic Cold Reversal (ACR) (14.6-12.9 ka)

6.1 Bølling-Allerød Interstadial and the Antarctic Cold Reversal

The term 'Bølling-Allerød' (B-A) is derived from recognition of two warm Late Glacial palynological zones (the Bølling and the Allerød) between the HS-1 and Younger Dryas. The use of this term for a chronological period has been criticized from a palynological point of view (De Klerk, 2004). Nevertheless, warming during this period has been identified (Lowe et al., 2001) and firmly dated in the GI-1 Greenland ice core to 14.6 ka to 12.9 ka (Rasmussen et al., 2014), and the term Bølling-Allerød interstadial (abbreviated 'B-A') is customarily applied to this period.

The B-A period began with reinforcement of the AMOC (McManus et al., 2004) and a marked increase in atmospheric CO_2 (Chen et al., 2015) and methane (Rosen et al., 2014); these conditions persisted through this period (Monnin et al., 2001). Climate rapidly warmed, at least around the North Atlantic (Clark et al., 2012). The AMOC remained vigorous throughout the B-A period (Deaney et al., 2017), and only a few cold events interrupted it in the Northern Hemisphere (Rasmussen et al., 2014). Sea ice retreated to the north (Denton et al., 2005), and glaciers in Europe thinned and retreated (for example in the Alps; Ivy-Ochs, 2015). The Asian monsoon strengthened to a level similar to the present (Sinha et al., 2005; Wang et al., 2008). It seems that the changes in the oceans

preceded changes in the atmosphere, and the oceans had a decisive influence on Northern Hemisphere warming (Thiagarajan et al., 2014). The changes in the oceans were possibly caused by a period of intense melt in Antarctica just before the B-A (Weaver et al., 2003; Weber et al., 2014). The process that drove the B-A would then be the opposite of that which caused HS-1, when the melting of the northern ice sheets led to warming in the Southern Hemisphere (Zhang et al., 2016). During the B-A, cooling in Antarctica caused increased sea ice cover in the surrounding ocean, causing the southern westerlies and the Intertropical Convergence Zone (ITCZ) to migrate northward, and strengthening the AMOC, which in turn caused warming in the Northern Hemisphere (Pedro et al., 2015; Zhang et al., 2016).

The cold period in the south has been called the Antarctic Cold Reversal (ACR). We analyze the B-A and ACR together because they occurred around the same time, although the boundary between cooling in the south and the warming in the north is not well defined (Pedro et al., 2015). The ACR has been well documented in Antarctic ice cores, and a clear bipolar seesaw is observed in relation to Greenland ice cores (Blunier et al., 1997, 1998; Pedro et al., 2011). Cooling in the Southern Hemisphere is apparent up to 40º S (Pedro et al., 2015), resulting in widespread glacier advance (Putnam et al., 2010; Shulmeister et al., 2019). There is also a clear cooling signal in tropical areas, at least in high Andean regions (Jomelli et al., 2014, 2016).

6.2 Laurentide Ice Sheet

The hemispheric extent of glaciation during the B-A is summarized in Figure 5. The Bølling-Allerød interstadial is characterized by enhanced ablation in marginal areas of the LIS (Ullman et al., 2015b) and a marked acceleration in the rate of retreat, most notably along the southern and western margins, but with minimal retreat along its northern margin (Dyke and Prest, 1987; Dyke, 2004; Stokes, 2017). As a result, the LIS is likely to have fully separated from the CIS by the end of the interstadial, although precise dating of the opening of the 'ice-free corridor' remains a challenge (Dyke and Prest, 1987; Gowan, 2013; Dixon, 2015; Pedersen et al., 2016). It is worth noting, however, that positive feedback mechanisms related to ice surface lowering and surface mass balance are likely to have resulted in the rapid 'collapse' of the saddle between the LIS and the CIS, which some have hypothesized was the source of Meltwater Pulse 1A (Gregoire et al., 2012).

The rapid retreat of the southern and western margins of the LIS was also likely aided by the development of proglacial lakes that facilitated calving and the draw-down of ice, particularly at the southern margin (Andrews, 1973; Dyke and Prest, 1987; Cutler et al., 2001). Moreover, the rapid retreat of the LIS during this time period led to major changes in the trajectory of ice streams at the western and southern margins, with associated changes in the location of the major ice divide in Keewatin, which migrated several hundred kilometers east towards Hudson Bay (Dyke and Prest, 1987; Margold et al., 2018).

There is also clear evidence for an overall acceleration in the rate of retreat and thinning of the ice sheet in the southeastern sector. This has been characterized as a two-phase pattern of deglaciation (Barth et al., 2019), with steady retreat starting ~20 ka and then increasing around 14.5 ka, coincident with the B-A warming. A clear example of this is seen in an extensive suite of 21 ^{36}Cl ages from boulder and bedrock samples along vertical transects spanning ~1000 m of relief in the Adirondack Mountains of the northeastern USA (Barth et al., 2019). These data suggest gradual ice sheet thinning of 200 m initiated around 20 ka, followed by a rapid surface lowering of 1000 m, coincident with the onset of the B-A warming (Barth et al., 2019). Similarly high rates of thinning are also recorded on Mt. Mansfield, Vermont's highest peak, although they appear to have initiated around 13.9±0.6 ka, which slightly post-dates the abrupt onset of the B-A (Corbett et al., 2019).

Despite an acceleration in the overall rate of recession, there appears to have been minimal recession of the LIS along its northern margin (Dyke, 2004). Also, there is evidence for readvances/oscillations of some of the lobes in the vicinity of the Great Lakes (Dyke, 2004), perhaps related to internal 'surge' dynamics and short-lived ice stream activity, rather than any external climatic forcing (Clayton et al., 1985; Patterson, 1997; Cutler et al., 2001; Margold et al., 2015, 2018; Stokes et al., 2016). There is also some evidence of climatically induced readvances of parts of the LIS during the B-A. For example, recession of the ice margin in northern New Hampshire was interrupted by the Littleton-Bethlehem readvance and deposition of the extensive White Mountain moraine system (Thompson et al., 2017). Based on a suite of approaches (glacial stratigraphy and sedimentology, radiocarbon dating, varve chronology, and cosmogenic-nuclide exposure dating), Thompson et al. (2017) constrained the age of this readvance to ~14.0-13.8 ka, coincident with Older Dryas cooling.

6.3 *Alaska*

Glaciers in the Brooks Range were smaller than today by 15 ka in some valleys and ~14 ka in others (Badding et al., 2013; Pendleton et al., 2015), suggesting widespread glacier retreat around the time of the B-A onset. In southeast Alaska, there was widespread glacier collapse throughout fjords and sounds during this period (Baichtal, 2010; Carlson and Baichtal, 2015; J. Baichtal, unpublished data). Whether this recession was related to an abrupt increase in temperature or to a steady temperature increase during this broader time period is unknown. However, rising lake levels and decreasing aridity at ~15 ka (Abbott et al., 2000; Finkenbinder et al., 2014; Dorfman et al., 2015) suggest that there was a major climate shift in Alaska at this time.

6.4 Cordilleran Ice Sheet and North Cascades

The B-A interstadial began with the rapid disintegration of the CIS and deglaciation in the North Cascades from 14.5 ka to 13.5 ka (Clague, 2017; Menounos et al., 2017; Riedel, 2017). Recent glacio-isostatic adjustment models supported by data calibration from records of sea level, paleo-lake shorelines, and present-day geodetic measurements confirm more than 500 m of thinning of the CIS between 14.5 ka and 14.0 ka (Peltier et al., 2015; Lambeck et al., 2017). The pattern of CIS deglaciation was complex due to the influences of mountain topography, marine waters and regional climate variability. Early deglaciation was marked by rapid eastward frontal retreat across the British Columbia continental shelf and northward retreat up Puget Sound. Rapid down-wasting exposed high-elevation hydrologic divides and led to the isolation of large ice masses in mountain valleys (Riedel, 2017). Lakeman et al. (2008) presented evidence that the CIS in north-central British Columbia thinned and in some areas transformed into a labyrinth of dead or dying ice tongues in valleys. The presence of ice-marginal landforms in most North Cascade valleys is likely related to temporary stillstands of the wasting remnants of the CIS, but the ages of most of these landforms are unknown (Riedel, 2017).

Ice sheet deglaciation temporarily rearranged regional drainage patterns. Frontal retreat of ice back to the north from hydrologic divides led to the formation of proglacial lakes in southern British Columbia and northern Washington (Fulton, 1967; Riedel, 2007). The lakes generally drained to the south, and several major valleys carried Late Glacial outburst floods that crossed low hydrologic divides, connecting rivers and fish migration pathways that later became isolated. The Sumas advances of the CIS diverted Chilliwack and Nooksack rivers to the south into lower Skagit valley (Clague et al., 1997). Fish genetics and geomorphic evidence, including perched deltas and boulder gravel deposits,

indicate that the lower Fraser River may have been diverted through Skagit valley at this time.

CIS deglaciation during the B-A was interrupted by minor advances of the CIS, and some alpine glaciers also advanced. The Sumas I advance of the CIS across Fraser Lowland occurred between 13.6 ka and 13.3 ka (Clague et al., 1997; Kovanen and Easterbrook, 2002). Top-down deglaciation of the ice sheet from mountain divides led to exposure of valley heads and cirques before adjacent valley floors. This set the stage for the formation of new cirque and valley moraines from Yukon Territory to the North Cascades during the B-A (Clague, 2017; Riedel, 2017). Menounos et al. (2017) report 76 ^{10}Be surface exposure ages on bedrock and boulders associated with lateral and end moraines at 26 locations in high mountains of British Columbia and Yukon Territory. At some of these sites, they also obtained radiocarbon ages from lakes impounded by moraines or till. Three older moraines have a combined median age of 13.9 ka, which the authors assigned to the B-A. A moraine near Rocky Creek at Mount Baker was built before 13.4-13.3 ka based on the age of volcanic ash and charcoal on the moraine surface. The Hyak I and Rat Creek I moraines have ^{36}Cl surface exposure ages of 14.6–12.8 ka, but uncertainty in the ^{36}Cl surface exposure ages precludes a definitive correlation with this event (Weaver et al., 2003).

There is sparse geological and paleoecological data on climate during the B-A interval from North Cascades and CIS region. In the North Cascades, the tentatively dated Rat Creek and Hyak alpine glacial moraines had ELAs ~500-700 m below those of modern glaciers or about 200 m above the GLGM advances (Porter et al., 1983). The lower ELAs were caused, in part, by mean July temperatures about 4-6°C below modern values (Heusser, 1977; Kutzbach, 1987; Liu et al., 2009). Rapid loss of the CIS was driven by a positive temperature anomaly of 1-2ºC early in the B-A, while a regional increase in mean annual precipitation of 250 mm and brief cold periods with temperature reductions of 1.5 ºC caused the small glacier advances later in the B-A (Liu et al., 2009).

6.5 Rocky Mountain/Yellowstone region

Although glaciers in some southwestern valleys continued to advance after 16 ka due to their exposure to greater orographic precipitation, the Yellowstone ice cap experienced intense deglaciation from 15 ka to 14 ka in response to a warming climate (Licciardi and Pierce, 2018; Pierce et al., 2018). Glaciers in the Wind River Range retreated behind their HS-1 moraines at this time, possibly as far as cirque headwalls (Dahms et al., 2018;

Marcott et al., 2019) before they began to readvance during the YD (see below). Deglaciation occurred in all ranges in the Colorado Rocky Mountains after about 16 ka, and by 13 ka most glaciers had disappeared (Laabs et al., 2009; Young et al., 2011; Shakun et al., 2015a; Leonard et al, 2017a, 2017b).

6.6 Sierra Nevada

Glaciers in the Sierra Nevada retreated to cirque headwalls by about 15.5 ka, well before the start of the B-A (Phillips, 2016, 2017). This relatively early disappearance is attributable to the southerly latitude and summer-warm, high-insolation Mediterranean climate of the Sierra Nevada. Following the B-A transition, glaciers reappeared for a very short interval prior to the Holocene. This event, named the 'Recess Peak advance', resulted from an approximate 150 m decrease in the ELA, in comparison to a 1200 m decrease during the GLGM maximum advance (Clark and Gillespie, 1997). Unfortunately, the chronological control for the time of this advance is imprecise. Three radiocarbon ages from bulk organic matter in lake cores from two different lake basins that overlie Recess Peak till fall between 14 ka and 13 ka, suggesting correlation with both the Inter-Allerød Cold Period and the ACR (Bowerman and Clark, 2011). However, cosmogenic ages (both ^{10}Be and ^{36}Cl), although somewhat scattered and imprecise, tend to cluster in the 12.7-11.3 ka range, which would be correlative with the Younger Dryas. More recently, Marcott et al. (2019) averaged six new ^{10}Be ages to obtain a date of 12.4±0.8 ka for the Recess Peak advance, which is consistent with the previous cosmogenic ages but does not definitively establish whether it was a YD or ACR event. Most indirect regional indicators of cooling also fall within the Younger Dryas age range. Phillips (2016) performed an in-depth study of this issue, but was unable to arrive at any definitive conclusion. In summary, there is no unequivocal evidence for any glacier presence in the Sierra Nevada during the B-A. It is possible that there was a brief minor advance toward the end of the B-A, but the dating of this event has yet to establish this with any certainty.

6.7 Mexico and Central America

Data from central Mexico, and to some extent Costa Rica, indicate that glaciers receded during the B-A, consistent with warming in the American tropics (Vázquez-Selem and Lachniet, 2017). In central Mexico, slow initial deglaciation from 15 ka to 14 ka was accompanied by the formation of small recessional moraines close to those of the maximum advance (Vázquez-Selem and Lachniet, 2017). Subsequently, glacier recession

accelerated, as evidenced by exposure ages on glacially abraded surfaces from 14 to 13 ka. The ELA increased by at least 200 m during that period (Vázquez-Selem and Lachniet, 2017). According to Cunningham et al. (2019), Cerro Chirripó , in Costa Rica, was ice-free by 15.2 ka, before the onset of the B-A. However, also in Cerro Chirripó, Potter et al. (2019) proposed periods of glacier retreat and stillstand from 15 ka to 10 ka.

6.8 Northern Andes

An advance of Ritacuba Negro Glacier in the Sierra Nevada de Cocuy, Colombia, has been linked to the ACR and an ELA decrease of about 500 m (Jomelli et al., 2014). A model simulation of the last deglaciation in Colombia (Liu et al., 2009; He et al., 2013) suggests a temperature 2.9°±0.8°C lower than today during the ACR, with a 10% increase in annual precipitation (Jomelli et al., 2016). Bracketing radiocarbon ages on laminated proglacial lake sediments indicate that glaciers retreated in the central Mérida Andes of Venezuela under warmer and wetter conditions at the start of the Bølling (14.6 ka) (Rull et al., 2010). Glaciers then briefly advanced under colder conditions from 14.1 ka to 13.9 ka), followed by warm and dry conditions during the Allerød (13.9-12.9 ka) (Stansell et al., 2010).

6.9 Peru and Bolivia

There is evidence for glacier advance at many sites in Peru and Bolivia during the ACR (Jomelli et al., 2014). Mean surface exposure ages on moraines built during this advance are 14.4-12.7 ka; at some sites there is an apparent bimodal distribution of ages (Jomelli et al., 2014). A glacier advance at Nevado Huaguruncho in the Eastern Cordillera of the Peruvian Andes has been dated to 14.1±0.4 ka, based on both exposure ages on moraines and radiocarbon ages on lake sediments, and was followed by retreat by 13.7±0.4 ka (Stansell et al., 2015). Two sets of moraine ridges in valleys within the Cordillera Huayhuash date to the ACR (Hall et al., 2009). However, moraine ages from the Queshque valley in the nearby Cordillera Blanca are at the end of the ACR (Stansell et al., 2017). In Bolivia, the two moraines from Wara Wara and Tres Lagunas (Zech et al., 2009, 2010) may have been constructed during the ACR, but could be older (Jomelli et al., 2014). A moraine of Telata Glacier in Zongo Valley formed during either the ACR or YD (Jomelli et al., 2014). The ACR advance exceeded all subsequent Holocene advances, with an ELA estimated to be 450-550 m below its current level based on glaciological modeling (Jomelli et al., 2014, 2016, 2017). Some glacial valleys contain at least two sets of moraines attributed to the ACR (Jomelli et al., 2014), suggesting multiple advances

related to possible centennial-scale climate fluctuations during this period. However, such patterns must be better documented in other mountain ranges to establish a robust climate interpretation (Figs. 21 and 22).

Paleoclimate records suggest that the central tropical Andes were cold during the ACR (Jomelli et al., 2014), although some contradictory evidence exists. Moreover, fluvial sediment records suggest that northern Peru was wet at the start of the ACR but subsequently became drier (Mollier-Vogel et al., 2013); and speleothem records from Brazil suggest that the ACR was a period of drier monsoon conditions (Novello et al., 2017). Farther south on the Altiplano, lake sediment records also indicate that the ACR was likely a drier interval (Sylvestre et al., 1999; Baker et al., 2001b), as does the shoreline stratigraphy, indicating that Lake Tauca had vanished (Placzek et al., 2006; Blard et al., 2011).

Climate forcings responsible for such glacier trends during the ACR were analyzed using transient simulations with a coupled global climate model (Jomelli et al., 2014). Results suggest that glacial behavior in the tropical Andes was mostly driven by temperature changes related to the AMOC variability superimposed on a deglacial CO_2 rise. During the ACR, temperature fluctuations in the tropical Andes are significantly correlated with other Southern Hemisphere regions (Jomelli et al., 2014), in particular with the southern high-latitudes and the eastern equatorial Pacific. Cold SSTs in the eastern equatorial Pacific were associated with glacier advance.

6.10 Southern Bolivia and Northern Chile

There are no glacial landforms in the Arid Diagonal that have been dated with sufficient precision to permit an ACR age assignment (Ward et al., 2015). There are, however, small undated moraines in the upper headwaters at El Tatio that may date to this period, or perhaps to the Younger Dryas (Ward et al., 2017). Sites to the south and west, even those north of the Arid Diagonal, appear to have been fully deglaciated by this time.

6.11 Central Andes of Argentina

As of yet, there are no firmly documented glacier advances in the Argentine Andes after HS-1. In the Sierra de Aconquija, however, D'Arcy et al. (2019) obtained two ages on a moraine (M3a) that fall within the B-A/ACR. At Tres Lagunas, there are no moraines younger than HS-1 (Zech et al., 2009). Possible B-A/AC moraines at other locations

(Sierra de Quilmes, Ansilta Range and Las Leñas) have not yet been dated (Terrizzano et al., 2017; Zech et al., 2017).

6.12 Patagonia

Many researchers have identified B-A/ACR glacier advances in central and southern Patagonia (Turner et al., 2005; Ackert et al., 2008; Kaplan et al., 2008; Moreno et al., 2009; Glasser et al., 2011; Sagredo et al., 2011, 2018; Strelin et al., 2011; García et al., 2012; Nimick et al., 2016; Davies et al., 2018; Mendelova et al., 2020). Past research on glacier fluctuations in northwestern Patagonia did not focus on the last termination, consequently no evidence of an advance of ACR age has yet been reported. However, paleoecological records from sectors as far north as 41°S suggest cooling during this interval (Hajdas et al., 2003). For example, records from northwestern Patagonia (40°-44°S) show declines in relatively thermophilous trees and increases in the cold-tolerant/hygrophilous conifer *Podocarpus nubigena* during ACR time, suggesting a shift to cold/wet conditions (Jara and Moreno, 2014; Pesce and Moreno, 2014; Moreno and Videla, 2016; Moreno et al., 2018). There is a gap in well-dated glacial geologic studies along a ~600 km length of the Andes between 40°S and 47°S (Fig. 23) covering the time span of the ACR. The only existing study reports a glacial advance in the Cisnes valley (44°S) sometime between 16.9 and 12.3 ka (Garcia et al. 2019), however, the chronological constrains are too broad to reach further conclusions.

Detailed geomorphic studies suggest that glaciers in central and southwestern Patagonia experienced repeated expansion or marginal fluctuations during the ACR period (Strelin et al., 2011; García et al., 2012; Sagredo et al., 2018; Reynhout et al., 2019; Thorndycraft et al., 2019). Multiple ^{10}Be ages from moraines deposited by glaciers on the Mt. San Lorenzo massif (47°S) indicate that glaciers there reached their maximum Late Glacial extents at 13.8±0.5 ka (Tranquilo Glacier; Sagredo et al., 2018), 13.2±0.2 ka (Calluqueo Glacier; Davies et al., 2018), and 13.1±0.6 ka (Lacteo and Belgrano glaciers; Mendelova et al., 2020). An ELA reconstruction based on the data from Tranquilo valley suggests that temperatures were 1.6-1.8°C lower than at present at the peak of the ACR (Sagredo et al., 2018). García et al. (2012) report a mean age of 14.2±0.6 ka for a sequence of moraines farther south, in the Torres del Paine area (51°S). The latter findings support the conclusions of Moreno et al. (2009), based on radiocarbon-dated ice-dammed lake records, that the Río Paine Glacier was near its maximum extent during the ACR.

6.13 Tierra del Fuego

Relatively little work has been done on ACR ice extent on Tierra del Fuego. McCulloch et al. (2005a) propose extensive ice in the Cordillera Darwin as far north as the Isla Dawson adjacent to the Strait of Magellan during the ACR, but subsequent work has failed to support this hypothesis. Rather, evidence from bogs located near sea level up-ice of Isla Dawson suggests that there has not been any major re-expansion of Cordillera Darwin ice towards the Strait of Magellan since initial deglaciation during HS-1 (Hall et al., 2013). Similarly, a radiocarbon age from a bog on the south side of the mountains in front of Ventisquero Holanda indicates that the glacier has not reached more than 2 km beyond its present limit in the past ~15 ka (Hall et al., 2013). In the only confirmed case of ACR moraines in the region, Menounos et al. (2013) used ^{10}Be surface exposure ages of boulders to document an age of ~14 ka for a cirque moraine in the nearby Fuegian Andes. Other moraines in the Cordillera Darwin may date to the same period (Hall, unpublished data), but none has yet been dated adequately.

6.14 Synthesis

Glacier activity in North and Central America was very different from that in South America during the B-A interstadial (Table 3 and Fig. 5). This period was generally a time of rapid glacier retreat throughout North and Central America. Indeed, in many regions, glaciers completely disappeared during the B-A interstadial. Although evidence has been presented in some areas for minor advances during the B-A, uncertainties in numeric ages on which the conclusions are based do not preclude the possibility that the advances happened during the ACR.

The LIS experienced rapid retreat along much of its margin during the B-A. Documented local advances may be related more to surge processes than to climate, although there may be exceptions related to cooling during the Older Dryas (e.g. Thompson et al., 2017). Glaciers in Alaska retreated significantly, even beyond the limits they achieved in the late Holocene. In western Canada and in Washington State, the CIS retreated rapidly, especially from 14.5 ka to 13.5 ka. During this period of general retreat, however, the CIS and many alpine glaciers advanced between 13.9 ka and 13.3 ka. In the Central and Southern Rocky Mountains of Wyoming and Colorado, deglaciation had begun by 14.5 ka, and most glaciers had disappeared by 13.5 ka. Although single-boulder ^{10}Be ages associated with moraines fall between 14.5 ka and 13.3 ka, no evidence of synchronous glacier advances within the B-A have been reported from these areas. In the Sierra

Nevada, glaciers retreated to cirque headwalls by about 15.5 ka. Some moraines within Sierra cirques indicate that there were relatively minor advances, but again, it is not known if they date to the Inter-Allerød Cold Period, the ACR, or even the YD. In central Mexico, recessional moraines close to moraines of the maximum advance date to 15-14 ka; after 14 ka, there was rapid glacier recession. Glaciers in Costa Rica disappeared by 15.2 ka.

Glaciers in the Venezuelan Andes retreated during the B-A, whereas glaciers in several regions of Central and Southern South America advanced during this period. In most cases, these advances have been assigned to the ACR. For example, ACR advances have been proposed in the Colombian Andes, with temperatures about 3ºC lower than today. Multiple ACR advances have also been reported in the Peruvian and Bolivian Andes under a cold and relatively dry climate. There are no conclusive data from northern Chile or the central Andes of Argentina, but it appears that there was a trend towards deglaciation during the B-A. Existing data do not resolve whether minor glacier advances that have been recognized occurred during the ACR or the YD. There were several ACR-related glacier advances in Patagonia, with temperatures almost 2ºC below current levels. Only limited evidence of the ACR has been found in Tierra del Fuego.

7. The Impact of the Younger Dryas (YD) (12.9-11.7 ka) and the Final Stages of Deglaciation

7.1 Younger Dryas concept

The last period we consider in our review extends from the end of the B-A (12.9 ka) to the beginning of the Holocene (11.7 ka). Again, the name coined by palynologists – Younger Dryas (YD) – is now widely used. Although the chronological limits derived from palynology are controversial, this cold interval has now been defined in Greenland ice cores (Rasmussen et al., 2014). Undoubtedly, it is the most widely studied deglacial period. Although climate varied extraordinarily during this period (Naughton et al., 2019), its effects in the Northern Hemisphere are clear – the AMOC weakened (Meissner, 2007; Muschitiello et al., 2019), sea ice expanded, and winter and spring temperatures dropped drastically (Steffensen et al., 2008; Mangerud et al., 2016); summers remained relatively warm (Schenk et al., 2018). Glaciers in Europe advanced (Ivy-Ochs, 2015; Mangerud et al., 2016), and the Asian monsoon weakened (Wang et al., 2008). Although

the ITCZ migrated southward, precipitation changes in the tropics during the YD were complex (Partin et al., 2015). Like HS-1, the YD was accompanied by warming in Antarctica and an increase in atmospheric CO_2 (Broecker et al., 2010; Beeman et al., 2019). The southern continents appear to have cooled slightly (Renssen et al., 2018), although glaciers in New Zealand and Patagonia clearly retreated, an apparent contradiction that has not been resolved (Kaplan et al. 2008, 2011; Martin et al., 2019; Shulmeister et al., 2019).

The causes of the abrupt YD anomaly continue to be a topic of debate. Changes in deep-water circulation in the Nordic seas, weakening of the AMOC (Muschitiello et al., 2019), moderate negative radiative forcing and altered atmospheric circulation (Renseen et al., 2015; Naughton et al., 2019) likely played a role. Draining of Glacial Lake Agassiz after intense melting of the Laurentide Ice Sheet during the B-A would have weakened the AMOC and is supported by geomorphic evidence of this lake draining into the Gulf of St. Lawrence and the North Atlantic at the end of the B-A (Leydet et al., 2018). Additionally or alternatively, Glacial Lake Agassiz may have drained via the Mackenzie River into the Arctic Ocean, also weakening the AMOC (Keigwin et al., 2018). The hypothesis that the cause was external to the planet has recently attracted renewed interest (Wolbach et al., 2018). In any case, the YD ended abruptly, with a 7 ºC warming of some regions in the Northern Hemisphere in only 50 years (Dansgaard et al., 1989; Steffensen et al., 2008).

7.2 Laurentide Ice Sheet

The hemispheric extent of glaciation during the YD is summarized in Figure 6, and that of the early Holocene is shown in Figure 7. The response of the LIS to the abrupt cooling of the YD is complex and difficult to generalize, but most records appear to indicate that recession slowed and that some major moraine systems were built, likely as a result of marginal readvances (Dyke, 2004). For example, the largest end moraine belt along the northwestern margin of the ice sheet, encompassing the Bluenose Lake moraine system on the Arctic mainland and its correlative on Victoria Island, is now thought to have formed due to YD cooling (Dyke and Savelle, 2000; Dyke et al., 2003). Similarly, there are examples of readvances on Baffin Island, most notably in Cumberland Sound (Jennings et al. 1996; Andrews et al. 1998). The large Gold Cove readvance of Labrador ice across the mouth of Hudson Strait has also been assigned to the late stage of the YD,

possibly in response to the rapid retreat of ice along the Hudson Strait (Miller and Kaufmann, 1990; Miller et al., 1999).

It has also been noted that several ice streams switched on during the YD, perhaps in response to a more positive ice sheet mass balance in some sectors (Stokes et al., 2016; Margold et al., 2018). Examples are two large lobes southwest of Hudson Bay (the Hayes and Rainy lobes), which readvanced towards the end of the YD. However, the precise trigger is uncertain; climatic forcing and dynamic instabilities related to meltwater lubrication and/or proglacial lake-level flucutations are possibities (Margold et al., 2018). Elsewhere, the M'Clintock Channel ice stream in the Canadian Arctic Archipelago (Clark and Stokes, 2001) is thought to have been activated during the early part of the YD and may have generated a large (60,000 km^2) ice shelf that occupied Viscount Melville Sound (Hodgson, 1994; Dyke, 2004; Stokes et al., 2009). In contrast, the nearby Amundsen Gulf ice stream appears to have retreated rapidly during the early part of the YD, perhaps triggered by glacier retreat from a bathymetric pinning point into a wider and deeper channel (Lakeman et al., 2018).

The above examples highlight the difficulty of attempting to relate ice stream activity to external climate forcing. Overall, it appears that the LIS receded throughout the YD, but that the pace of recession slowed and there were notable readvances at the scale of individual lobes or ice streams. It should also be noted that while several moraine systems have been robustly linked to YD advances or stillstands, many others might also be correlative but have not yet been precisely dated (Dyke, 2004).

Following the YD, the LIS retreated rapidly in response to both increased summer insolation and increasing levels of carbon dioxide (Carlson et al., 2007, 2008; Marcott et al., 2013). Retreat proceeded back towards the positions of the major ice dispersal centers in the Foxe-Baffin sector, Labrador and Keewatin (Dyke and Prest, 1987; Dyke, 2004; Stokes, 2017). The final retreat of the Labrador Dome has recently been constrained by Ullman et al. (2016) using ^{10}Be surface exposure dating of a series of end moraines that likely relate to North Atlantic cooling (Bond et al., 1997; Rasmussen et al., 2006). Following the last of these cold events at 8.2 ka (Alley et al., 1997; Barber et al., 1999), Hudson Bay became seasonally ice-free and deglaciation was completed by 6.7±0.4 ka (Ullman et al., 2016).

7.3 Alaska

The existing literature offers limited evidence for glacier readvances in Alaska during the YD. There may be many moraines that were deposited during or at the culmination of the YD, but they have not been dated. One way to assess the possibility of there being YD moraines in Alaska is to consider whether or not glaciers extended beyond their present limits during the YD. Of the 14 glaciers throughout Alaska discussed by Briner et al. (2017), nine had retreated up-valley of their late Holocene positions prior to the YD. Thus, in some cases, it appears that glaciers did indeed extend down-valley of modern limits during the YD. This was the case in Denali National Park and several sites in southern Alaska. A notable site that provides the best evidence to date of YD glaciation in the state is at Waskey Mountain in the Ahklun Mountains. The chronology of the moraines at this locality has been updated since the work of Briner et al. (2002). Young et al. (2019) report evidence for an early YD glacier culmination, followed by minor retreat through the remainder of the interval.

In terms of climate, Kokorowski et al. (2008) conclude that evidence for YD cooling is mainly restricted to southern Alaska. Kaufman et al. (2010) argue that the coldest temperatures in southern Alaska were at the beginning of the YD and that warming occurred subsequently. This climatic pattern is consistent with the revised glacier chronology of the Waskey Mountain moraines. Denton et al. (2005) hypothesized that YD cooling was mostly a wintertime phenomenon and hence may have had limited effect on glacier mass balance. This hypothesis is supported in Arctic Alaska with the documentation of extreme winter temperature depression during the YD (Meyer et al., 2010). Most of the pollen records summarized by Kokorowski et al. (2008) show no significant cooling during the YD. In addition to the climate forcing transmitted from the North Atlantic region, the Bering Land Bridge was flooded around the time of the YD (England and Furze, 2008), although it may not have been completely covered by the sea until about 11 ka (Jakobsson, 2017). This flooding event may have led to an increase in precipitation due to more northerly storm tracks (Kaufman et al., 2010), which may have influenced glacier mass balance. Additionally, the decreasing influence of LIS-induced atmospheric reorganization may have affected summer temperature in Beringia during the Late Pleistocene-Holocene transition. Of course, there may have been more glacier fluctuations during the YD than is currently envisioned, because they may have occurred under a climate that was similar to, or warmer than, that of the late Holocene (Kurek et

al., 2009; Kaufman et al., 2016), in which case moraines may have been destroyed by Holocene glacier advances.

7.4 Cordilleran Ice Sheet and the North Cascades

Many alpine glaciers and at least two remnant lobes of the CIS advanced during the YD. In all cases, the advances were much smaller than those during the LGM and HS-1. At alpine sites, most glaciers reached only several hundred meters beyond late Holocene maximum positions attained during the Little Ice Age (Osborn et al., 2012; Menounos et al., 2017). Other glaciers advanced and came into contact with stagnant CIS ice at lower elevations (Lakeman et al., 2008). In the western North Cascades, there are multiple, closely spaced moraines constructed during the YD (Riedel 2017). Radiocarbon dating constrains the time of an advance on Mount Baker in the North Cascades to 13.0-12.3 ka (K. Scott, written communication; Kovanen and Easterbrook, 2001). The Hyak II advance in the southernmost North Cascades near Snoqualmie Pass occurred after 13 ka (Porter, 1976). Menounos et al. (2017) established ^{10}Be ages on 12 high-elevation moraines in western Canada with a median age of 11.4 ka. A lobe of the CIS advanced across central Fraser Lowland one or two times after 12.9 ka (Saunders et al., 1987; Clague et al., 1997; Kovanen and Easterbrook, 2001; Kovanen, 2002), and the final advance of the glacier in the Squamish River valley in the southern Coast Mountains north of Vancouver has been dated to about 12.5 ka (Friele and Clague, 2002). It is not clear how long the CIS persisted in each North Cascade mountain valley, but the middle reaches of Silver Creek were ice-free by 11.6 ka, as were many sites in western Canada (Clague, 2017; Riedel, 2017). By the beginning of the Holocene or shortly thereafter, ice cover in British Columbia was no more extensive than it is today. A radiocarbon age from basal sediments in a pond adjacent to the outermost Holocene moraine at Tiedemann Glacier in the southern Coast Mountains shows that ice cover in one of the highest mountain areas in British Columbia was, at most, only slightly more extensive at 11 ka than today (Clague, 1981; Arsenault et al., 2007). This conclusion is supported by an age of 11.8-11.3 ka on a piece of wood recovered from a placer gold mine near Quesnel, British Columbia, which is located near the center of the former CIS (Lowdon and Blake, 1980).

Alpine glacial ELAs associated with YD advances were 200-400 m below modern values in the North Cascades, but fluctuated 100-200 m (Riedel, 2007). The colder YD climate is also recorded in changes in loss-on-ignition carbon in lake bed sediments in the eastern North Cascades (Riedel, 2017). Changes in pollen zone boundaries led Heusser (1977) to

conclude that YD mean July air temperature was 2-3ºC cooler than today. Liu et al. (2009) suggested that annual precipitation increased by 250 mm, while mean annual air temperature was 4ºC colder compared to the 1960-1990 average, and fluctuated by ±0.5ºC during the YD interval.

7.5 Rocky Mountain/Yellowstone region

A YD glacier advance or stillstand has been documented in the Lake Solitude cirque in the Teton Range. Boulders perched on the small cirque lip date to 12.9±0.7 ka (Licciardi and Pierce, 2008). Glaciers in cirques in the Wind River Range advanced to form moraines or rock glaciers 50-300 m upvalley of Older Dryas/ HS-1 deposits (Fig. 10). Ages on these moraines in Stough Basin, Cirque of the Towers and Titcomb Basin are between 13.3 ka and 11.4 ka (Shakun et al., 2015a; Dahms et al., 2018; Marcott et al., 2019) and provide clear evidence of a glacier advance during the YD period. It is uncertain whether or not these glaciers disappeared prior to re-advancing to their YD positions.

There is clear evidence of a significant glacier advance in the Colorado Mountains during the YD (Marcott et al., 2019), confirming previous age assignments (Menounos and Reasoner, 1997; Benson et al., 2007). Pollen studies (Jiménez-Moreno et al., 2011; Briles et al., 2012) also indicate Younger Dryas cooling in the Colorado Rocky Mountains, as does a study of lacustrine sediment (Yuan et al., 2013) in the San Luis Valley of southern Colorado (Leonard et al., 2017a).

7.6 Sierra Nevada

The only known glacier advance between the retreat of the Tioga 4 glaciers at ~15.5 ka and the late Holocene Matthes ('Little Ice Age') advance in the Sierra Nevada is the Recess Peak advance (Bowerman and Clark, 2011). Both cosmogenic surface exposure ages and independent regional climate records favor a YD age for this minor advance. However, limiting radiocarbon ages on bulk organic matter just above the Recess Peak till in lacustrine cores are between 14 ka and 13 ka (Philips, 2017), suggesting that the advance may be older than the YD. The weight of the evidence appears to still favor the YD age assignment, but the replicated direct radiocarbon measurements are difficult to dismiss. Confirmation of a YD age would support the model that the YD cooling had a detectable, although not major, impact on the deglacial climate of the west coast of North America. Confirmation of a slightly older age would suggest that there was a brief, but

significant episode of cooling there late during the B-A. In either case, the climate signal is small compared to that of the GLGM. The linked glacial/lacustrine modeling of Plummer (2002) yields a match to Recess Peak glacier extent and lake surface area in the paleo-Owens River watershed, with a temperature reduction of 1°C and 140% of modern precipitation. This local combination of glacial and closed-basin lacustrine records offers an unusual opportunity to assess the paleoclimatic drivers of Recess Peak event, but the significance of the event cannot be understood until the chronology is secure. Clearly, additional radiocarbon and high-precision cosmogenic dating of the Recess Peak deposits is a priority.

7.7 Mexico and Central America

Glaciers constructed a distinctive group of closely spaced end moraines in the mountains of central Mexico at 3800-3900 m asl from 13-12 ka to ~10.5 ka (Vázquez-Selem and Lachniet, 2017). ELAs were 4100-4250 m asl, which is 650-800 m below the modern ELA, suggesting temperatures ~4-5°C below modern values. Considering that other proxies generally show relatively dry conditions (Lachniet et al., 2013), the relatively low ELAs were likely controlled by temperature.

The terminal Pleistocene moraines of central Mexico provide clear evidence for Younger Dryas glaciation in the northern tropics. The moraines are closely spaced and relatively small (in general <6 m high near their front), but are well preserved in most mountain valleys at elevations of 3800-3900 m asl. They suggest that glaciers remained near 3800-3900 m asl for 1000-2000 years at the close of the Pleistocene, forming several small ridges only tens of meters apart from one another (Vázquez-Selem and Lachniet, 2017). Cosmogenic ages on glacially abraded surfaces indicate that mountains <4000 m asl in central Mexico were ice-free by 11.5 ka, and mountains <4200 m asl became ice-free between 10.5 ka and 10 ka. South-facing valleys were ice-free even earlier (12 ka) (Vázquez-Selem and Lachniet, 2017). Glaciers on high peaks (Iztaccíhuatl, Nevado de Toluca, La Malinche) receded, exposing polished bedrock surfaces below 4100 m asl, from 10.5 ka to 9 ka. A brief, but distinctive glacier advance is recorded later, from ca. 8.5 ka to 7.5 ka, on the highest peaks of central Mexico (>4400 m asl) (Vázquez-Selem and Lachniet, 2017) (Fig. 24).

Cosmogenic exposure ages from the summit of Cerro Chirripó, Costa Rica, indicate that the mountain was ice-free by 15.2 ka (Cunningham et al., 2019). However, other ages suggest moraine formation around YD time (Potter et al., 2019) and complete

deglaciation thereafter (Orvis and Horn, 2000). The mountains of Costa Rica and likely Guatemala were ice-free before 9.7 ka (Orvis and Horn, 2000).

7.8 Northern Andes

The evidence of possible YD glacier advances in the northern Andes is limited and mainly restricted to elevations above 3800 m asl (Angel et al., 2017). Glacier advances in some valleys in the Venezuelan Andes seem to be related to cooling during the YD. In the Sierra Nevada, climate was dry, but temperatures were 2.2-3.8°C colder than today between 12.9 ka and 11.6 ka (Salgado-Labouriau et al., 1977; Carrillo et al., 2008; Rull et al., 2010; Stansell et al., 2010). Mahaney et al. (2008) suggest glaciers advanced in the Humboldt Massif of this mountain range at 12.4 ka. In the Mucubají valley, also in this range, small moraines located at elevations higher than 3800 m asl have yielded ^{10}Be ages of 12.22±0.60 ka and 12.42±1.05 ka (modified ages from Angel, 2016) and may be related to the YD. Glacier advances have been linked to the YD in the Sierra Nevada del Cocuy, Colombia, based on ^{10}Be dating (Jomelli et al., 2014), and on the Bogota Plain based on ages on lacustrine sediments behind the moraines (Helmens, 1988). There are also moraines that might date to the YD in the Ecuadorian Andes. For example, in the Chimborazo-Carihuairazo Massif, two moraine complexes have been radiocarbon-dated to 13.4-12.7 cal ka BP (Clapperton and McEwan, 1985).

7.9 Peru and Bolivia

The weight of evidence suggests that glaciers were generally in retreat during the YD in Peru and Bolivia. In the Cordillera Oriental of northern Peru, lake sediment records show some evidence of readvance and reoccupation of higher cirques by glaciers, but no moraines have been dated (Rodbell, 1993). Similar evidence from Vilcabamba in southern Peru suggests glaciers advanced at the beginning of the YD, but then retreated (Licciardi et al., 2009). Mercer and Palacios (1977) present evidence that glaciers advanced near Quelccaya near the beginning and end of the YD. Similarly, Rodbell and Seltzer (2000) and Kelly et al. (2012) provide radiocarbon-based evidence that sites in the Cordillera Blanca and the Quelccaya Ice Cap advanced either just prior to or at the start of the YD, followed by retreat. A cirque lake in Bolivia (16ºS, headwall 5650 m asl) formed before 12.7 ka, suggesting that ice had retreated by that time (Abbott et al., 1997). According to Bromley et al. (2011), the ice cap on the Coropuna volcano experienced a strong advance at ~13 ka. Similar glacier activity has been reported at Hualca Hualca volcano (Alcalá-Reygosa et al., 2017) and Sajama (Smith et al., 2009) volcanoes. These

advances coincide with the highest level of the Coipasa paleo-lake cycle, confirming the high sensitivity of the glaciers in this region to shifts in humidity (Blard et al., 2009; Placzek et al., 2013) (Fig. 17).

Many glaciers advanced or experienced stillstands in the Central Andes during the early Holocene. The mean age of all Holocene moraine boulders is 11.0±0.4 ka (Mark et al., 2017). In the Cordillera Huayhuash, ^{10}Be samples from moraine boulders date from 11.4 ka to 10.5 ka (Hall et al., 2009). Early Holocene (11.6-10.5 ka) moraines are also present on Nevado Huaguruncho (Stansell et al., 2015), and a moraine in the Cordillera Vilcabamba in southern Peru has been dated to ~10.5 ka (Licciardi et al., 2009). Basal radiocarbon ages from lake sediments in the Cordillera Raura suggest ice-free conditions after 9.4 ka (Stansell et al., 2013). At Quelccaya in the Cordillera Vilcanota, peat overlain by till has been dated to 11.1 ka and 10.9 ka (Mercer and Palacios, 1977). Similarly, the Taptapa moraine on the Junin plain has been radiocarbon-dated to ~10.1 cal ka BP (Wright, 1984). The Quelccaya Ice Cap reached its present extent by10 cal ka BP, based on dated peat at its margin (Mercer, 1984). Glaciers in Peru seem not to have advanced throughout the remainder of the early Holocene. In Bolivia, however, ^{10}Be ages suggest several advances during the early Holocene period (Jomelli et al., 2011, 2014).

7.10 Southern Bolivia and Northern Chile

As in the case of the ACR, there are no confirmed YD glacial landforms in the Arid Diagonal, but the chronology is insufficent to exclude minor glacial fluctuations in the high headwaters at this time (Ward et al., 2017).

7.11 Central Andes of Argentina

Published evidence of YD glacier activity exists at only two sites in the central Andes of Argentina. In the Nevado de Chañi, glaciers retreated after HS-1, followed by an advance during the YD (Martini et al., 2017a). Four ^{10}Be ages from lateral and frontal moraines in the Chañi Chico valley average 12.1±0.6 ka (Fig. 19) (Martini et al., 2017a). The ELA during the YD advance was at ~5023 m asl, which is 315 m above the GLGM ELA (Martini et al., 2017a). Moraines assigned to the YD have been found in two valleys in the Sierra de Aconquija (D'Arcy et al., 2019). According to D'Arcy et al. (2019), one moraine (M3a) was deposited at 12.5 ka and a second (M3b) at 12.3 ka. YD glacier advances coincided with a period of higher-than-present precipitation at paleo-lake Coipasa on the Altiplano (Blard et al., 2011; Placzek et al., 2013). No general early

Holocene glacier activity has been reported for the region, although two moraine boulders from Sierra de Aconquija yielded ^{10}Be ages of 8.5 ka and 7.9 ka (D'Arcy et al., 2019). In northwestern Argentina, the presence of relict rock glaciers in cirques suggests that YD or early Holocene cooling may have activated rock glaciers instead of causing glaciers to re-form (Martini et al., 2013, 2017b).

7.12 Patagonia

After reaching their maximum Late Glacial extents during the ACR, Patagonian glaciers receded during the YD period. In some regions (47°-52°S), this general trend was interrupted by stillstands or minor readvances that deposited small moraines upvalley from the much larger ACR moraines (Moreno et al., 2009; Sagredo et al., 2011, 2018; Strelin et al., 2011; Glasser et al., 2012; Mendelova et al., 2020). Some of these advances may relate to the end of terminal calving following the draining of paleo-lakes in the region (Davies et al., 2018; Thorndycraft et al., 2019). Again, no evidence of glacier advances during the YD has been reported north of 47°S.

Paleo-vegetation records indicate a decline in precipitation during the YD in northwestern Patagonia (Jara and Moreno, 2014; Pesce and Moreno, 2014; Moreno et al., 2018), warm/wet conditions in central-western sectors (44°-48°S) (Villa-Martínez et al., 2012; Henríquez et al., 2017), and increased precipitation in southwestern sectors (48°-54°S) (Moreno et al., 2012, 2018). A widespread warm/dry interval is evident between 11 ka and 8 ka (Moreno et al., 2010). Although, most studies suggest that Patagonian glaciers retreated through the early Holocene, approaching their present-day configurations (Strelin et al., 2011; Kaplan et al., 2016), recent finding by Reynhout et al. (2019) at Torre glacier (49°S) show robust evidence of early renewed glacial activity during the early Holocene.

7.13 Tierra del Fuego

To our knowledge, there are no published data on glacier behavior during the Northern Hemisphere YD or at the start of the Holocene in the Cordillera Darwin. Glaciers are assumed to be restricted to the inner fjords. In the adjacent Fuegian Andes, an excavation just upvalley of an ACR moraine yielded a calibrated radiocarbon age on peat of ~12.2 ka, indicating that the glacier had receded by that time (Menounos et al., 2013), possibly during the YD. In the same cirque, the presence of the Hudson tephra (7.96-7.34 ka)

within ~100 m of Little Ice Age moraines suggests the glacier had receded to the Little Ice Age limit by the early Holocene.

7.14 Synthesis

Information on glacier activity in the Americas during the YD is limited, but has been improving in recent years (Table 4 and Figs. 6 and 7).

The LIS continued to thin and retreat throughout the YD, although at a lower rate than earlier. Some major moraine systems were built during YD stillstands or re-advances, but it is uncertain if they are a consequence of climate forcing or glacier dynamics related to internally driven instabilities. Evidence for YD advances is sparse in Alaska, and it seems that glacier retreat dominated there. In southern Alaska, however, temperatures decreased during the YD. It is possible that glaciers advanced during this period, but if so, the evidence was destroyed by late Holocene advances. There is evidence of YD glacier advances at the southwestern margin of the CIS and in the North Cascades, where a significant reduction in temperature and an increase in precipitation have been detected. In the Wyoming and Colorado Rocky Mountains, moraines in several cirque basins, which once were thought to be mid-Holocene ('Neoglacial') age, are now attributed to the YD. In the Sierra Nevada a minor advance may be attributed to the YD, although the dating is problematic. Many other small moraine complexes in the western mountains of the U.S. have yet to be dated.

One of the few regions with obvious YD moraines is central Mexico, where reconstructed ELAs suggest temperatures were ~4-5°C below modern values in an environment that was drier than today. The evidence for YD glaciation in the mountains of Costa Rica is inconclusive, but in the Northern Andes at elevations above 3800 m asl, some glaciers advanced during the YD due to a decrease in temperatures of 2.2-3.8°C below present values under a dry climate.

Glaciers continued to retreat in Peru and Bolivia during the YD, except on the Altiplano where the YD coincided with the highest level of the Coipasa paleo-lake cycle and with advances of glaciers in numerous mountain ranges and on high volcanoes. It is questionable whether some late advances in northern Chile occurred during the ACR or the YD, but most of the Arid Diagonal was already ice-free in the YD. Some evidence for YD advances has been found in the central Andes of Argentina, but in Patagonia glacier retreat continued throughout the YD and was interrupted only by stillstands or

minor readvances that deposited small moraines. Glacier retreat also dominated during the YD on Tierra del Fuego, where there is no evidence for advances during this period.

Deglaciation accelerated after the YD in nearly all of North, Central and South America, and most small glaciers reached their current size or disappeared during the early Holocene. In the area of the LIS, deglaciation occurred rapidly following the YD and was largely complete by 7 ka. In Alaska, glaciers reached sizes similar to today in the early Holocene. The CIS had disappeared by the beginning of the Holocene. Most glaciers in the Yellowstone region and the Colorado Rocky Mountains disappeared before the Holocene, and in the Sierra Nevada glaciers were about their current size at that time. In central Mexico, glaciers probably reached their current size or disappeared by the beginning of the Holocene, although a minor advance, probably related to the 8.2 ka event, is recorded on the highest volcanoes. Many glaciers advanced or experienced stillstands in the Central Andes under a wetter climate during the early Holocene, although these glaciers apparently rapidly retreated a short time thereafter. In Patagonia and Tierra del Fuego, glaciers retreated during the early Holocene and most glaciers approached their present size at that time.

8. Discussion

8.1. The climatic meaning of the Last Glacial Termination

Before comparing glacier behavior in the different regions of the Americas, we first summarize the state of knowledge of global climate evolution during the Last Glacial Termination and the mechanisms that caused it. An immediate problem in attempting such a summary is that it is difficult to even define the start and end of this period. It encompasses a set of events that do not begin or end at the same time around the world. In addition, deglaciation may be caused, not only by changes in orbital forcing that regulate the amount of insolation that Earth receives (Broecker and van Donk, 1970), but also by internal forcing mechanisms and feedbacks, including changes in atmospheric circulation and composition, especially in CO_2 and CH_4 (Sigman and Boyle, 2000; Monnin et al., 2001; Sigman et al., 2010; Shakun et al., 2012; Deaney et al., 2017), changes in ocean circulation, the composition of the oceans and sea ice extent (Bereiter et al., 2018), and the interplay between the atmosphere and oceans (Schmittner and Galbraith, 2008; Fogwill et al., 2017). Finally, the Last Glacial Termination is difficult to

define because the two hemispheres experience opposing external forcing and potentially opposing internal forcing mechanisms that might induce a climate compensation effect between the hemispheres termed the "bipolar seesaw" (Broecker and Denton, 1990).

Broadly speaking, glacial terminations initiate when the ice sheets of the Northern Hemisphere are at their maximum extent and with global sea level at its lowest (Birchfield and Broecker, 1990; Imbrie et al., 1993; Raymo, 1997; Paillard, 1998). Additionally, global deglaciation during each termination operates over approximately the same length of time during each glacial cycle and is characterised by short-lived fluctuations of rapid glacier retreat and occasional re-advances (Lea et al., 2003). Given these observations, it is important to determine the mechanisms responsible for the climatic and glacial changes that accompany deglaciations. To that end, several hypotheses have been proposed that are mainly based on the temperatures of the oceans (Voelker, 2002) and the composition of the atmosphere (Severinghaus and Brook, 1999; Stolper et al., 2016).

Any attempt to closely examine the Last Glacial Termination must account for changes in ocean temperature throughout this period. These temperature changes are simultaneous in the two hemispheres, but can shift in opposite directions, for example in the Atlantic Ocean. They are determined by the greater or lesser intensity of the AMOC (see syntheses in Barker et al., 2009, 2010). Even though these changes occur throughout deglaciation, the amount of CO_2 in the atmosphere tends to increase more or less continuously. A possible explanation for this apparent enigma is that the oceans in one hemisphere may cool while those in the other hemisphere warm and emit more CO_2, redistributing heat across the planet (Barker et al., 2009).

Building on previous work (Cheng et al., 2009), Denton et al. (2010) propose that a concatenation of processes, with multiple positive feedbacks, drive deglaciation. They argue that deglaciation is initiated by coincident "excessive" growth of Northern Hemisphere ice sheets and increasing boreal summer insolation due to orbital forcing. The large volume of ice on northern continents results in maximum isostatic depression and an increase in the extent of the ice sheets that are marine-based. Even a small increase in insolation could, under these conditions, enlarge ablation zones and initiate the collapse of Northern Hemisphere ice sheets. Marine-based ice sheets can also be more vulnerable to collapse due to positive feedbacks associated with sea-level rise at the grounding line. Outbursts of meltwater and icebergs from these ice sheets cool the North Atlantic Ocean and weaken the AMOC, leading to an expansion of winter sea ice and very cold winters

on the adjacent continents (Denton et al., 2010). Under these conditions, the northern polar front expands, driving the ITCZ, the southern trade winds, and the southern westerlies to the south (Denton et al., 2010). The Asian monsoon weakens, while the cooling over the North Atlantic intensifies the South American monsoon (Novello et al., 2017) and the southern westerlies. The result is an increase in upwelling in the southern oceans, accompanied by enhanced ocean ventilation and a rise in atmospheric CO_2. During deglaciation, the Southern Hemisphere warms first, followed by warming over the rest of the planet (Broecker, 1998). Southward migration of the southern westerlies also contributes to a temperature rise in the southern oceans, which transfer heat to the south (Denton et al., 2010). The intensive cooling in the Northern Hemisphere ends due to a reduction in meltwater input, northward retreat of sea ice, and renewed warming of the northern oceans, which reestablish the AMOC. Subsequently, the ITCZ returns northward and the Asian monsoon intensifies. The northward migration of the southern westerlies and the intensification of the AMOC cool the southern oceans, completing a cycle in the recurrent bipolar seesaw that ultimately tends toward equilibrium (Denton et al., 2010).

The hypothesis for climate evolution during Last Glacial Termination summarized above can be tested with our dataset on the behavior of glaciers in the Americas. It is clear that sea level depends on how water is distributed between the ocean and Northern Hemisphere ice sheets during glacials and also on the effects of land-based glacier ice cover on the isostatic balance of the northern continents (Lambeck et al., 2014). The hypothesis that deglaciation begins when northern ice sheets are extremely large is still supported (Abe-Ouchi et al., 2013; Deaney et al., 2017). According to Cheng et al. (2016), for example, ice sheets reach their maximum size after five precession cycles, which may explain why glacial cycles finished after similar durations of about 115 ka (Paillard, 1998). In addition, it seems that the time needed for ice sheets to reach this extreme size increased throughout the Pleistocene (Clark et al., 2006), and successively more insolation energy was required to start deglaciation. This might explain why each glacial cycle is longer than its predecessor (Tzedakis et al., 2017). Deglaciation begins when the excessive size of the northern ice sheets coincides with: (i) increasing insolation in boreal summer in the Northern Hemisphere, mainly at 65º N, the average latitude of large northern ice sheets (Kawamura et al., 2007; Brook and Buizert, 2018); (ii) minimum CO_2 in the atmosphere (Shakun et al., 2012); and (iii) maximum sea ice extent (Gildor et al.,

2014). These conditions induce aridity and reduce vegetation cover, which in turn increases atmospheric dust, reducing albedo on northern ice sheets (Ellis and Palmer, 2016). Better knowledge of the activity of glaciers throughout the Americas may confirm the hypothesis that is central to these models, namely that deglaciation begins in the North and is transmitted to the South.

New information from ocean and polar ice cores reinforces the idea of climate compensation between the two hemispheres (the bipolar seesaw) during the Last Glacial Termination. Intensive sea-level rise occurs within the first 2 kyr of deglaciation, inducing retreat of marine-based ice sheets, and acts as a positive feedback for deglaciation (Grant et al., 2014). Fogwill et al. (2017) argue that, once deglaciation starts, it is driven by global oceanic and atmospheric teleconnections. New data support the idea that meltwater cooling of the Northern Hemisphere reduced the AMOC strength (Deaney et al., 2017; Muschitiello et al., 2019) and pushed the northern westerlies southward in Asia (Chen et al., 2019), Europe (Naughton et al., 2019), and North America (Hudson et al., 2019). The Asian summer monsoon weakened during these cold periods in the Northern Hemisphere (Cheng et al., 2016; Chen et al., 2019), and the Indian summer monsoon transferred Southern Hemisphere heat northward, promoting subsequent Northern Hemisphere deglaciation (Nilsson-Kerr et al., 2019).

New data have also highlighted the importance of CO_2 storage in the dense deep waters of the Southern Hemisphere during glacials (Fogwill et al., 2017; Clementi and Sikes, 2019). Ventilation of these waters during deglaciation emits a large amount of CO_2 into the atmosphere and significantly warms the planet (Stephens and Keeling, 2000; Anderson et al., 2009; Skinner et al., 2010; Brook and Buizert, 2018; Clementi and Sikes, 2019), favoring deglaciation (Lee et al., 2011; Shakun et al., 2012). This increase in CO_2 overrides the cooling effect from orbital variations in the Southern Hemisphere (He et al., 2013).

Recent high-resolution data from ice cores in Antarctica and Greenland have helped verify the opposite temperature trends in the two polar areas during deglaciation, at least on a large scale. Moreover, these data confirm that the rise in CO_2 was synchronous with the increase in Antarctic temperatures (Ahn et al., 2012; Beeman et al., 2019). Antarctic temperature seems to be more closely linked to changes in tropical ocean currents, whereas Greenland is less affected by this phenomenon (Wolff et al., 2009; Landais et al., 2015). However, the intimate relationship between AMOC intensity and atmospheric

CO_2 concentrations has been clearly demonstrated (Deaney et al., 2017), and deglaciation largely represents a period of imbalance between these two parameters. Therefore, when the AMOC stabilizes, atmospheric CO_2 concentrations stabilize and the interglacial period begins (Deaney et al., 2017). That said, some exceptions have been detected on a centennial scale (Böhm et al., 2015). A sudden surge in the AMOC may cause a large release of CO_2 into the atmosphere, although only for a few centuries (Chen et al., 2015). New studies propose that mean ocean temperature and the temperature of Antarctica are closely related, underlining the importance of the Southern Hemisphere ocean in orchestrating deglaciation (Bereiter et al., 2018), as it is the main contributor of CO_2 to the atmosphere (Beeman et al., 2019). Inverse temperature evolution and the latitudinal migration of atmospheric circulation systems (fronts, ITCZ, trade winds and westerlies) may have the greatest impact on the planet's glaciers and ice sheets, albeit in opposite directions.

Improved knowledge of the changing extent of glaciers throughout the Americas is necessary to understand how glaciers are affected by the above-described evolution of the climate system during the Last Glacial Termination. However, little attention has been focussed on the differing behavior of glaciers between the hemispheres and how this might reflect global ocean and atmospheric teleconnections during the last deglaciation. Is there a glacial bipolar seesaw reflected in the behavior of mountain glaciers? In that sense, it is necessary to consider that mountain glaciers today contribute about one-third of the ice melt to the oceans (Gardner et al., 2013; Bamber et al., 2018). One of the few studies that compares the behavior of mountain glaciers in both hemispheres is that of Shakun et al. (2015a). These authors analyzed 1116 cosmogenic nuclide exposure ages (mostly ^{10}Be ages) from glacial landforms located between 50ºN and 55ºS on different continents, but mostly from the Americas. Inferred glacier behavior was evaluated using a variety of climate forcings. Their results demonstrate that glaciers responded synchronously throughout deglaciation, mainly due to the global increase of CO_2 in the atmosphere and the subsequent increase in temperature. They note important regional differences related to other factors, such as insolation in the Northern Hemisphere, a seesaw response to changes in the AMOC in the Southern Hemisphere, and changes in precipitation distribution and in tropical ocean currents.

8.2 Glaciers in the Americas during GLGM in a global context

We note the similarity in the times of glacier advances in North and Central America during the GLGM. Most mountain glaciers reached their maximum extent before or during the GLGM, although in some areas (e.g. Teton Range and portions of the Yellowstone Ice Cap), the maximum may also have encompassed HS-1. However, there were many local differences within each region. Similarly, the LIS did not exhibit uniform evolution along all parts of its margin, although it did reach its maximum extent during the GLGM. Based on our synthesis, the LIS began to retreat about 21 ka ago at the same time as the majority of the North and Central American glaciers, as well as European glaciers. The Scandinavian Ice Sheet reached its maximum extent in the GLGM and also started its retreat about 21 ka (Toucanne et al., 2015; Cuzzone et al., 2016; Hughes A.L.C. et al., 2016; Hughes, P. et al., 2016; Stroeven et al., 2016; Patton et al., 2017). As in the case of the LIS, the margins of the Scandinavian Ice Sheet retreated at different times; retreat in some areas was delayed until HS-1. The same timing and behavior has been reported for the Barents, British-Irish, and Icelandic ice sheets (Hormes et al., 2013; Pétursson et al., 2015; Hughes A.L.C. et al., 2016). In all three cases, the maximum was reached during the GLGM and deglaciation began about 21-20 ka, although retreat did not begin in some areas until HS-1. Some sectors of the British-Irish Ice Sheet began their retreat very early in the GLGM, although for reasons related to the dynamics of the ice sheet rather than climate (Ó Cofaigh et al., 2019). In the case of the Icelandic Ice Sheet, sea-level rise caused it to collapse after 19 ka (Pétursson et al., 2015). In summary, the Last Glacial Termination started almost simultaneously in areas covered by the LIS and the Eurasian ice sheets.

Similarities are also evident between North and Central American and many European mountain glaciers. The glacial maximum in Europe extended from 30 ka until the beginning of deglaciation 21-19 ka, for example in the Alps (Ivy-Ochs, 2015), Apennines (Giraudi et al., 2015), Trata Mountains (Makos, 2015; Makos et al., 2018) and the Anatolia peninsula mountains (Akçar et al., 2017). However, glaciers in some mid-latitude mountains in Europe achieved their maximum size much earlier, between MIS 5 to MIS 3, for example, glaciers in the Cantabrian Mountains and central Pyrenees on the Iberian Peninsula (Oliva et al., 2019) and the High Atlas in North Africa (Hughes et al., 2018). In contrast, glaciers in the eastern Pyrenees, the Central Range and the Sierra Nevada on the Iberian Peninsula, which are also located in mid-latitudes, clearly attained their maximum size during the GLGM (Oliva et al., 2019). In summary, mountain

glaciers in Europe and North America evolved in a similar way, in spite of the local differences within each region.

Comparing glacial behavior in South America to glaciers in other continents at similar latitudes is more difficult. The extra-American glaciers of the Southern Hemisphere are located in isolated mountains of Africa and Oceania and, with one exception, have not been well studied. The exception is the Southern Alps of New Zealand, which are located at the about the same latitudes as northern Patagonia.

Unlike most of North and Central America, the maximum advance of the last glacial cycle throughout South America, except perhaps in Tierra del Fuego and in some mountains of Patagonia, was reached long before the GLGM, which is between approximately 60 ka and 40 ka. A similar pattern is also evident in mountains of East Africa (Shanahan and Zreda, 2000; Mahaney, 2011), New Zealand (Schaefer et al., 2015; Darvill et al., 2016) and Kerguelen (Jomelli et al., 2018). Outside the Southern Hemisphere, an early maximum advance during the last glacial cycle has also been proposed in some mountains in Mexico (Heine, 1988), in the central Pyrenees, the Cantabrian Mountains (Oliva et al., 2019), and in the High Atlas (Hughes et al., 2018). However, these cases are exceptional and are not located in any latitudinal zone; rather they are purely regional. Some authors have suggested the idea of an aborted termination around 65-45 ka in the Southern Hemisphere, after glaciers had achieved their maximum extents (Schaefer et al., 2015).

Although the GLGM was not the last time that glaciers advanced in the Southern Hemisphere, it was a period of widespread glacier expansion under a mainly cold and wet climate. As in the Andes, many glaciers in the mountains of East Africa (Shanahan and Zreda, 2000; Mahaney, 2011) and New Zealand (Schaefer et al., 2015; Darvill et al., 2016; Shulmeister et al., 2019) advanced during the GLGM and left outer moraine systems. This advance has been attributed to a southward migration of the ITCZ and westerlies in response to strong cooling in the Northern Hemisphere (Kanner et al., 2012; Schaefer et al., 2015; Darvill et al., 2016). Paleoclimate records from central Chile, northwestern Patagonia, and the southeast Pacific, however, imply a northward shift in southwesterly winds during the GLGM (Heusser, 1990; Villagrán, 1988a, 1988b; Heusser et al., 1999; Lamy et al., 1999; Moreno et al., 1999, 2018).

Deglaciation in the Patagonian Andes began at 17.8 ka, consistent with Antarctic ice core records (Erb et al., 2018) and New Zealand glacial chronologies (Schaefer et al., 2015; Darvill et al., 2016; Barrell et al., 2019; Shulmeister et al., 2019). It occurred two or three

millennia after the inception of deglaciation in the Northern Hemisphere, although researchers have noted that ice recession and moderate warming took place during the Varas Interstade, between ~24 and ~19 ka (Mercer, 1972, 1976; Lowell et al., 1995; Denton et al., 1999; Hein et al., 2010; Mendelova et al., 2017).

The GLGM was more than a climatic period; it was the time when the world's glaciers achieved their maximum extent after the previous interglacial. However, ice masses did not all behave in the same way because their activity was affected by topography, regional changes in ocean and atmospheric circulation, local climatic conditions and climate feedbacks (Liakka et al., 2016; Patton et al., 2017; Liakka and Lofverstrom, 2018; Licciardi and Pierce, 2018). Although many glaciers reached their maximum extent well before the GLGM, especially in the Southern Hemisphere, the northern ice sheets grew more-or-less continuously towards the GLGM. Many glaciers, also in the Northern Hemisphere, achieved their largest size just before the GLGM. Within each region, glaciers advanced many times, conditioned by the geographical constraints arising from their own expansion. When the next warm orbital cycle began to affect the Northern Hemisphere, around 21 ka, deglaciation started in all areas, although it was somewhat delayed in the Southern Hemisphere. Again, the duration and intensity of deglaciation after the GLGM differed greatly and was regional rather than latitudinal.

8.3 Glaciers in the Americas during HS-1 in a global context

Records of glacier behavior in the Americas during HS-1 are consistent with records from other continents, albeit with considerable local variability in each region. HS-1 did not have a strong impact on the LIS and European ice sheets (Patton et al., 2017). Around 17.8 ka, however, some of the margins of these ice sheets stabilized or advanced and moraines were built at their margins. Retreat began again shortly thereafter, around 17.5 ka, with some local oscillations superimposed on overall retreat through the rest of HS-1 (Cuzzone et al., 2016; Hughes A.L.C. et al., 2016; Peters et al., 2016; Stroeven et al., 2016; Gump et al., 2017; Patton et al., 2017). Although there may have been an internal reorganization of flow patterns and ice sheet geometry at this time, we note that there is little evidence for any major readvance of the LIS during during HS-1, and retreat likely continued in most regions including the southern margin (Heath et al., 2018). The European ice sheets evolved in a similar manner (Toucanne et al., 2015), with deglaciation beginning between 21 ka and 19 ka (Patton et al., 2017) and rapidly leading to huge ice losses. The meltwater contribution to the North Atlantic, mainly from the LIS,

was enough to drastically reduce the AMOC (Toucanne et al., 2015; Stroeven et al., 2016).

Knowledge of the impacts of HS-1 on mountain glaciers in Europe is stronger than in North and Central America. Glaciers advanced in the Alps during HS-1 (Gschnitz stadial), occupying valley bottoms that had been deglaciated earlier. The main advance was at the beginning of HS-1, around 17-16 ka, and its moraines are recognized in many valleys (Ivy-Ochs, 2015). An advance of the same age has been documented in the Tatra Mountains, (Makos, 2015; Makos et al., 2018). Up to three readvances have been recognized in the Appenines during HS-1 (Giraudi et al., 2015), and glaciers advanced on the Anatolian Peninsula near the end of HS-1 (Sarıkaya et al., 2014, 2017). Glacial advances around 17-16 ka are recognized in almost all mountain ranges on the Iberian Peninsula (Oliva et al., 2019). As in the Alps, glaciers on the Iberian Peninsula reoccupied the lower reaches of valleys, approaching the moraines of the GLGM (Palacios et al., 2017a). This was the case in the central and eastern Pyrenees, the Central Range and the Sierra Nevada (Oliva et al., 2019). All of these European advances happened at about the same time as the HS-1 glacier advances in North and Central America. In the Rocky Mountains, Mexico and Central America, maximum GLGM advances appear to have extended into HS-1, although it is possible that glaciers readvanced during HS-1, surpassing and erasing GLGM glacial landforms. The most recent summaries of the glacial chronology of the California Sierra Nevada (Phillips, 2017), Wyoming's Wind River Range (Dahms et al., 2018, 2019; Marcott et al., 2019), the European Alps (Ivy-Ochs, 2015), and Iberian Sierra Nevada (Palacios et al., 2016) indicate that the glaciers in these mountain systems behaved in similar ways during HS-1.

The marked glacier advances in the tropical Andes during HS-1 have been attributed to an intensification of the South American monsoon under a colder climate (Kanner et al., 2012). The monsoon produced a wet period on the Altiplano and caused glaciers to advance in the surrounding mountains, in many cases beyond the limits of the GLGM moraines. Again, it is difficult to compare South American tropical glaciers to other glaciers at similar latitudes. There is little information on the glaciers of East Africa; ages bearing on deglaciation have a large margin of error that precludes assigning events to HS-1 with confidence, although many of the glaciers show evidence of large late-glacial oscillations (Shanahan and Zreda, 2000; Mahaney, 2011).

It is much easier to compare glacier behavior between temperate southern latitudes, such as Patagonia and the Southern Alps of New Zealand and Kerguelen Archipelago. In these mountain ranges, deglaciation accelerated during HS-1 (Darvill et al., 2016). The glaciers retreated throughout the entire HS-1 period in the Southern Alps (Putnam et al., 2013; Koffman et al., 2017), Kerguelen (Jomelli et al., 2018) and the same happened in Patagonia (Mendelova et al., 2017) and Tierra del Fuego (Hall et al., 2013). Moraines in some valleys of the Southern Alps dated to 17 ka were built at the end of a prolonged GLGM and mark the beginning of large-scale deglaciation (Barrell et al., 2019; Shulmeister et al., 2019).

On both continents, deglaciation began about 21 ka and became much more widespread after 19-18 ka, resulting in a steady rise in sea level, cooling of the North Atlantic, and reduction of the AMOC. HS-1 was a short period of stabilization and reduction in ice loss. Strong cooling occurred in temperate northern latitudes, and mountain glaciers advanced close to the limits reached during the GLGM, in some cases even surpassing them. This happened in spite of increased aridity, which was a consequence of the southward migration of the polar front. The ITCZ also migrated southward, particularly over the tropical Atlantic, thereby intensifying the South American monsoon and increasing precipitation in tropical latitudes, where glaciers advanced considerably. In contrast, in the temperate latitudes of the Southern Hemisphere, HS-1 was a warm period and glaciers began or continued their rapid retreat under a climate that was opposite that in the temperate latitudes of the Northern Hemisphere.

8.4 Glaciers in the Americas during the B-A and ACR in a global context

We have seen above that the southern and western margins of the LIS retreated during the B-A, whereas there was minimal retreat along its northern margin. In the rest of North and Central America, many glaciers retreated significantly or disappeared altogether by the end of HS-1 and during the B-A. However, some studies have suggested that there were short periods of glacier advance in Europe, as in North America, during this period of general deglaciation. The European ice sheet retreated from the sea and through central Europe during the B-A (Cuzzone et al., 2016) and separated into smaller ice sheets centered on the Scandinavian Peninsula, Svalbard and Novaya Zemlya (Hughes A.L.C. et al., 2016; Patton et al., 2017). Along the southern and northwestern margins of the Scandinavian Peninsula, there are moraine systems that mark the end of GS-2.1, and other moraines inboard of them relate to the cold stage of GI-1d, called the Older Dryas

(Mangerud et al., 2016, 2017; Stroeven et al., 2016; Romundset et al., 2017). Moraines were built at the margin of the British-Irish ice sheet about 14 ka in the Older Dryas, but that ice sheet had nearly disappeared along the B-A (Ballantyne et al., 2009; Hughes A.L.C. et al., 2016; Wilson et al., 2019). The ice sheet covering Iceland retreated and left important parts of the interior of the island free of ice during the B-A, with a climate similar to that of today (Pétursson et al., 2015). In summary, we conclude that European ice-sheets behaved in a similar manner to American glaciers during the B-A.

Glaciers in the European Alps experienced the same rapid deglaciation during the B-A as in North and Central America. After advances during HS-1, alpine glaciers retreated considerably during the B-A and had practically disappeared by the end of this period (Ivy-Ochs, 2015). Older Dryas (Daun stadial) moraines have been identified in many alpine valleys, indicating stagnation or an advance of glaciers between the two interstadials (Ivy-Ochs, 2015). After an advance in the Tatra Mountains at about 15 ka, glaciers retreated rapidly (Makos, 2015; Makos et al., 2018). This retreat was interrupted by readvances of glaciers during the Older Dryas (Marks et al., 2019). Glaciers also rapidly retreated in the eastern Mediterranean during the B-A (Dede et al., 2017; Sarıkaya and Çiner, 2017; Sarıkaya et al., 2017). The same pattern is evident in the Balkans (Styllas et al., 2018), the Apennines (Giraudi et al., 2015), and the Iberian Peninsula where glaciers disappeared from some mountain systems or retreated into the interior of cirques (Oliva et al., 2019). Some moraines in these mountains may have been built in the Older Dryas cold period, but uncertainties in the cosmogenic ages are sufficiently large that this possibility cannot be confirmed. Examples are found in the central Pyrenees (Palacios et al., 2017b).

Conditions were warmer in Venezuela, and glaciers retreated, during B-A. The B-A warm interstadial is not reflected in Central and Southern South American glacier behavior. Rather, there is clear evidence from the northern and tropical Andes of advances during the ACR. These advances occurred under cold and arid conditions caused mainly by temperature changes related to the strengthening of the AMOC (Jomelli et al., 2014). Although there is currently no evidence of these advances in northern Chile and the central Andes of Argentina, they are clear in Patagonia, where after a retreat of glaciers during HS-1, there was an advance during the ACR (Strelin et al., 2011; García et al., 2012). Evidence has been found also of a glacier advance during the ACR in the Fuegian

Andes on Tierra del Fuego (Menounos et al., 2013), although there is no conclusive evidence of an ACR event in the adjacent Cordillera Darwin (Hall et al., 2019).

Again, a comparison of the behavior of South American glaciers to glaciers in other areas of the Southern Hemisphere is almost impossible. In East Africa, as is the case on other continents, it is very difficult to place the ages of some moraines within the ACR or YD (Mahaney, 2011). However, in the Southern Alps of New Zealand, at Kerguelen (Jomelli et al., 2018) as in Patagonia, there is evidence of glacier advances during the ACR, but with large regional variations, possibly related to the westerlies (Darvill et al., 2016). In any case, most of the possible ACR moraines in New Zealand have been dated to 13 ka, at the boundary between the ACR and the YD (Shulmeister et al., 2019). There are indications of a decrease in temperature of 2-3ºC at that time, at least in some areas of the Southern Alps (Doughty et al., 2013). In spite of the limited knowledge of glacier evolution over much of this region, we conclude that South American glaciers evolved in a similar way to glaciers at similar latitudes on other continents and opposite to that of glaciers in the Northern Hemisphere.

Deglaciation of the Northern Hemisphere accelerated under a warm climate in the lead-up to the interglacial period. Again, we observe differences in glacial behavior within each region, in both North America and Europe, but these differences are local and relate to the geography of ice sheets and mountain glaciers and not to latitudinal trends. In the best-studied regions where glacial landforms are well preserved, the impacts of short cold intervals on glaciers have been detected, especially in the Older Dryas. However, in most cases, uncertainties in dating preclude correctly assigning landforms to brief climatic periods. Thus, it is not yet possible to determine whether any moraines in the Northern Hemisphere belong to the ACR or the Older Dryas. Glacier behavior in the Southern Hemisphere is different from that in North America and on other northern continents. The impact of cooling during the ACR is clear in some of its regions. In the Southern Hemisphere, there was no massive, continuous glacier melt, but rather a tendency towards stagnation or glacier advance. As was the case for HS-1, the north and the south responded in opposite ways to climate change during the B-A/ACR period.

8.5 Glaciers in the Americas during the YD in a Global Context

In many cases, the glaciers in North and Central America responded to the YD by advancing. Retreat of the LIS slowed, and some sectors advanced. At the end of the YD period, the LIS renewed its retreat. Similarly, several fronts of the Fennoscandian Ice

Sheet advanced during the YD, although there was great variability in its different margins (Cuzzone et al., 2016; Hughes A.L.C. et al., 2016; Mangerud et al., 2016; Stroeven et al., 2016; Patton et al., 2017; Romundset et al., 2017). It appears that the maximum advance occurred at the end of the YD period, at least at some margins (Mangerud et al., 2016; Romundset et al., 2017). At the beginning of the Holocene, retreat of the Fennoscandian Ice Sheet began anew, although this was interrupted during the short-lived Preboreal oscillation, at 11.4 ka. Afterwards, retreat continued until the ice sheet disappearance at 10-9 ka (Cuzzone et al., 2016; Hughes A.L.C. et al., 2016; Stroeven et al., 2016). During the YD, ice caps in some sectors of Britain, Franz Josef Land and Novaya Zemlya also expanded (Hughes A.L.C. et al., 2016; Patton et al., 2017; Bickerdike et al., 2018). The glaciers in Iceland recovered during the YD and again brought their fronts close to the present shoreline and, in some cases, beyond it (Pétursson et al., 2015). With the Holocene came rapid retreat, interrupted by the Preboreal oscillation at 11.4 ka (Andrés et al., 2019). In summary, the remnant European ice sheets grew during the YD, but similar growth is less evident for the LIS.

The impact on glaciers of the YD is currently being studied in the mountains of North and Central America. In Alaska, the only clear evidence reported to date is in the south. However, it is evident that there were small advances during the YD in many valleys of British Columbia and the North Cascades. Recent dating has provided much more evidence of small advances in the Wyoming and the Colorado Rocky Mountains (Leonard et al., 2017a; Dahms et al., 2018, 2019) and possibly the California Sierra Nevada (Phillips, 2017). YD advances are clear in central Mexico and increasingly certain in Central America. Glaciers advanced throughout the European Alps during the YD (Egesen stadial) and built moraines intermediate in position between those of the Oldest Dryas and those of the Little Ice Age (Ivy-Ochs, 2015). In some valleys, there are moraines dating to the Preboreal oscillation that lie between those of the YD and the Little Ice Age (Ivy-Ochs, 2015). From glacier ELA depressions, it can be inferred that the annual temperature was 3-5ºC cooler in the Alps, the Tatra Mountains and elsewhere in the Carpathians (Rinterknecht et al., 2012; Makos, 2015). New information shows that glaciers advanced in cirques in the Mediterranean mountains, for example in the Anatolian Peninsula (Sarıkaya and Çiner, 2017), the Balkans (Styllas et al., 2018), the Apennines (Giraudi et al., 2015), the Iberian mountains (García-Ruiz et al., 2016; Oliva et al., 2019), the French Pyrenées (Jomelli et al., under review) and the High Atlas

(Hughes et al., 2018). At this time, we can conclude that the activity of glaciers in North America and Europe during the YD is more similar than it appeared a few years ago.

Glaciers also apparently advanced in the northern Andes during the YD. However, in the central Andes, the YD was a period of glacier retreat, with the exception of the Altiplano where the Coipasa wet phase coincided with advances in the surrounding mountains. Glaciers may also have advanced in these mountains at the beginning of the Holocene, around 11 ka, but they all retreated after 10 ka. Glaciers in Patagonia and on Tierra del Fuego retreated after the ACR, in the latter area probably beyond the limits of the Little Ice Age. Glaciers in East Africa retreated immediately after constructing ACR or YD moraines (Mahaney, 2011). In the Southern Alps, as in Patagonia, the YD was a period of glacier retreat (Shulmeister et al., 2019) with temperatures about 1ºC warmer than today (Koffman et al., 2017).

Glaciers in the Northern Hemisphere responded synchronously to YD cooling by either stabilizing or advancing, but the timing of the maximum extent differs spatially, as does the magnitude of advance; in many areas, there is no evidence for YD glacier activity. In the Southern Hemisphere, the South American monsoon intensified, thereby increasing humidity, which caused tropical glaciers to advance. However, in the temperate latitudes of this hemisphere, glaciers retreated, once again showing their antiphase behavior compared to those in the north.

9. Conclusions

The decrease in temperature in the Americas during the GLGM was 4-8 ºC, but changes in precipitation differed considerably throughout this large region. Consequently, many glaciers of North and Central America reached their maximum extent during the GLGM, whereas others reached it later, during the HS-1 period. In the Andes, for example, glaciers advanced during the GLGM, but this advance was not the largest of the Last Glacial, except possibly on Tierra del Fuego. HS-1 was a time of glacier growth throughout most of North and Central America; some glaciers built new moraines beyond those of the GLGM. Glaciers in the tropical Andes stabilized or advanced during HS-1 and, in many cases, overrode GLGM moraines. However, glaciers in the temperate and subpolar Andes retreated during this period. Glaciers retreated throughout North and Central America during the B-A interstadial and, in some cases, disappeared. Glaciers

advanced during the ACR in some parts of the tropical Andes and in the south of South America. This advance was strong in Patagonia. Limited advances have been documented in high mountain valleys in North and Central America during the YD. In contrast, glaciers retreated during this interval in South America, except in some sectors of the northern Andes and on the Altiplano where glacier advances coincided with the highest level of the Coipasa paleo-lake cycle.

In summary, the GLGM was the culmination of glacier growth during the last glacial cycle. Glaciers achieved their maximum extent in many sectors before the GLGM, and even in individual sectors at different times, but the main northern ice sheets were largest within the GLGM. The latter explains why orbital forcing triggered deglaciation beginning about 21 ka across the Northern Hemisphere and somewhat later in the Southern Hemisphere.

Glaciers in North America and Europe exhibit common behavior at all latitudes through the Last Glacial Termination. This synchronous behavior extended almost to the Equator. This commonality was clearly influenced by pronounced shifts in ocean circulation (e.g. the AMOC), but probably also reflected proximity to the great Northern Hemisphere ice sheets that profoundly affected atmospheric circulation and temperature.

Glaciers at temperate latitudes in the Southern Hemisphere fluctuated synchronously, especially those in Patagonia and the Southern Alps of New Zealand. Their behavior is generally opposite to that of Northern Hemisphere glaciers during HS-1 and the B-A/ACR, but the two are similar at the beginning and end of Last Glacial Termination.

Glaciers at tropical latitudes in the Southern Hemisphere show greater diversity in their behavior, which is most likely related to shifts in the ITCZ. A striking feature of the glacial history of Central America and the tropical Andes is the persistence of relatively extensive mountain glaciers through the Younger Dryas, long after those in North America and Europe had retreated close to Holocene limits. One significant difference between much of the Andes and the Northern Hemisphere is that the combination of extreme elevation and aridity produces a larger sensitivity to precipitation than for the lower and wetter mountain ranges of North America and Europe.

Once deglaciation began, there was a seesaw between the hemispheres, which affected not only marine currents but also atmospheric circulation and glacier behavior. This seesaw explains the opposing behavior of many glaciers in the Northern and Southern

Hemispheres during HS-1 and the B-A/ACR. At the end of the B-A, it appears that many mountain glaciers and minor ice sheets had achieved sizes similar to those of the early Holocene. Subsequently, the YD ended deglaciation in the south and led to the re-advance of some glaciers in the north.

Acknowledgements

This paper was supported by Project CGL2015-65813-R (Spanish Ministry of Economy and Competitiveness). David Palacios thanks the Institute of Alpine and Arctic Research, at the University of Colorado, for providing the facilities to coordinate this work during his Fulbright Grant stay there in 2019. We thank Eric Leonard and Joe Licciardi for corrections of some sections of the text, and two anonymous reviewers for their valuable suggestions that have greatly improved the paper.

References

Abbott, M.B., Finney, B.P., Edwards, M.E., Kelts, K.R. 2000. Lake-level reconstruction and paleohydrology of Birch Lake, central Alaska, based on seismic reflection profiles and core transects. Quat. Res. 53, 154–166. 10.1006/qres.1999.2112

Abbott, M.B., Seltzer, G.O., Kelts, K.R., Southon, J. 1997. Holocene paleohydrology of the tropical Andes from lake records. Quat. Res. 47, 70–80. 10.1006/qres.1996.1874

Abe-Ouchi, A., Saito, F., Kawamura, K., Raymo, M.E., Okuno, J.I., Takahashi, K., Blatter, H. 2013. Insolation-driven 100,000-year glacial cycles and hysteresis of ice-sheet volume. Nature 500(7461), 190–193. 10.1038/nature12374

Ackert, R.P., Becker, R.A., Singer, B.S., Kurz, M.D., Caffee, M.W., Mickelson, D.M. 2008. Patagonian glacier response during the Late Glacial–Holocene transition. Science, 321(5887), 392–395. 10.1126/science.1157215

Ahn, J., Brook, E.J., Schmittner, A., Kreutz, K. 2012. Abrupt change in atmospheric CO_2 during the last ice age. Geophys. Res. Lett. 39, L18711. 10.1029/ 2012GL053018

Akçar, N., Yavuz, V., Yeşilyurt, S., Ivy-Ochs, S., Reber, R., Bayrakdar, C., Kubik, P.W., Zahno, C., Schlunegger, F., Schlüchter, C. 2017. Synchronous Last Glacial Maximum across the Anatolian Peninsula. In: Hughes, P.D., Woodward, J.C. (eds.) Quaternary Glaciation in the Mediterranean Mountains. Geol. Soc. London Spec. Publ. 433, 251–269. 10.1144/SP433.7

Alcalá-Reygosa, J., Palacios, D., Vázquez-Selem, L. 2017. A preliminary investigation of the timing of the local last glacial maximum and deglaciation on HualcaHualca volcano – Patapampa Altiplano (arid Central Andes, Peru). Quat. Int. 449, 149–160. 10.1016/j.quaint.2017.07.036

Alley, R.B., Mayewski, P.A., Sowers, T., Stuiver, M., Taylor, K.C., Clark, P.U. 1997. Holocene climatic instability: A prominent, widespread event 8200 yr ago. Geology 25, 483–486. 10.1130/0091-7613(1997)025<0483:HCIAPW>2.3.CO;2

Ammann, C., Jenny, B., Kammer, K., Messerli, B. 2001. Late Quaternary glacier response to humidity changes in the arid Andes of Chile (18–29º S). Palaeogeogr. Palaeoclimatol. Palaeoecol. 172, 313–326. 10.1016/S0031-0182(01)00306-6

Anderson, R.F., Ali, S., Bradtmiller, L.I., Nielsen, S.H.H., Fleisher, M.Q., Anderson, B.E. Burckle, L.H. 2009. Wind-driven upwelling in the Southern Ocean and the deglacial rise in atmospheric CO_2. Science 323(5920), 1443–1448. 10.1126/science.1167441

Andrés, N., Palacios, D., Saemundsson, Þ., Brynjólfsson, S., Fernández-Fernández, J.M. 2019. The rapid deglaciation of the Skagafjörður fjord, northern Iceland. Boreas 48, 92–106. 10.1111/bor.12341

Andrews, J.T. 1973. The Wisconsin Laurentide Ice Sheet: Dispersal centres, problems of rates of retreat, and climatic implications. Arct. Alp. Res. 5, 185–199. 10.1080/00040851.1973.12003700

Andrews, J.T., Voelker, A.H. 2018. “Heinrich events” (& sediments): A history of terminology and recommendations for future usage. Quat. Sci. Rev. 187, 31–40. 10.1016/j.quascirev.2018.03.017

Andrews, J.T., Barber, D.C., Jennings, A.E., Eberl, D.D., Maclean, B., Kirby, M.E., Stoner, J.S. 2012. Varying sediment sources (Hudson Strait, Cumberland

Sound, Baffin Bay) to the NW Labrador Sea slope between and during Heinrich events 0 to 4. J. Quat. Sci. 27, 475–484. 10.1002/jqs.2535

Andrews, J.T., Kirby, M.E., Jennings, A.E., Barber, D.C. 1998. Late Quaternary stratigraphy, chronology, and depositional processes on the SE Baffin Island slope, detrital carbonate and Heinrich events: Implications for onshore glacial history. Géogr. phys. Quat. 52, 91–105. 10.7202/004762ar

Angel, I. 2016. Late Pleistocene Deglaciation Histories in the Central Mérida Andes (Venezuela). Ph.D. thesis, Université de Grenoble Alpes – Universidad Central de Venezuela, Francia, Venezuela, 234 pp.

Angel, I., Audemard, F.A., Carcaillet, J., Carrillo, E., Beck, C., Audin, L. 2016. Deglaciation chronology in the Mérida Andes from cosmogenic ^{10}Be dating, (Gavidia valley, Venezuela). J. South Am. Earth Sci. 71, 235–247. 10.1016/j.jsames.2016.08.001

Angel, I., Carrillo, E., Carcaillet, J., Audemard, F.A., Beck, C. 2013. Geocronología con el isótopo cosmogénico ^{10}Be, aplicación para el estudio de la dinámica glaciar cuaternaria en la región central de los Andes de Mérida. GEOS 44, 73–82.

Angel, I., Guzmán, O., Carcaillet, J. 2017. Pleistocene glaciations in the northern tropical Andes, South America (Venezuela, Colombia and Ecuador). Geogr. Res. Lett. 43, 571–590. 10.18172/cig.3202

Arsenault, T.A., Clague, J.J., Mathewes, R.W. 2007. Late Holocene vegetation and climate change at Moraine Bog, Tiedemann Glacier, southern Coast Mountains, British Columbia. Can. J. Earth Sci. 44, 707–719. 10.1139/e06-135

Badding, M.E., Briner, J.P., Kaufman, D.S. 2013. ^{10}Be ages of late Pleistocene deglaciation and Neoglaciation in the north-central Brooks Range, Arctic Alaska. J. Quat. Sci. 28, 95–102. 10.1002/jqs.2596

Baichtal, J.F., Carlson, R.J. 2010. Development of a model to predict the location of early Holocene habitation sites along the western coast of Prince of Wales Island and the outer islands, Southeast Alaska. Curr. Res. Pleistocene 27(64), 64–67.

Baker, P.A., Rigsby, C.A., Seltzer, G.O., Fritz, S.C., Lowenstein, T.K., Bacher, N.P., Veliz, C. 2001a. Tropical climate changes at millennial and orbital timescales on the Bolivian Altiplano. Nature 409(6821), 698–701. 10.1038/35055524

Baker, P.A., Dunbar, R.B., Cross, S.L., Seltzer, G.O., Grove, M.J., Rowe, H.D., Fritz, S.C., Tapia, P.M., Broda, J.P. 2001b. The history of South American tropical precipitation for the past 25,000 years. Science 291, 640–643. 10.1126/science.291.5504.640

Balco, G., Schaefer, J.M. 2006. Cosmogenic-nuclide and varve chronologies for the deglaciation of southern New England. Quat. Geochronol. 1, 15–28. 10.1016/j.quageo.2006.06.014

Balco, G., Stone, J.O., Lifton, N.A., Dunai, T.J. 2008. A complete and easily accessible means of calculating surface exposure ages or erosion rates from ^{10}Be and ^{26}Al measurements. Quat. Geochronol. 3(3), 174–195. 10.1016/j.quageo.2007.12.001

Ballantyne, C.K., Schnabel, C., Xu, S. 2009. Readvance of the last British-Irish ice sheet during Greenland Interstade 1 (GI-1): The Wester Ross readvance, NW Scotland. Quat. Sci. Rev. 28, 783–789. 10.1016/j.quascirev.2009.01.011

Bamber, J.L., Westaway, R.M., Marzeion, B., Wouters, B. 2018. The land ice contribution to sea level during the satellite era. Environ. Res. Lett. 13(6), 063008. 10.1088/1748-9326/aadb2c

Barber, D.C., Dyke, A., Hillaire-Marcel, C., Jennings, A.E., Andrews, J.T., Kerwin, M.W., Bilodeau, G., McNeely, R., Southon, J., Morehead, M.D., Gagnon, J.-M. 1999. Forcing the cold event of 8,200 years ago by catastrophic drainage of Laurentide lakes. Nature 400(6742), 344–348. 10.1038/22504

Barker, S., Chen, J., Gong, X., Jonkers, L., Knorr, G., Thornalley, D. 2015. Icebergs not the trigger for North Atlantic cold events. Nature 520(7547) 333–336. 10.1038/nature14330

Barker, S., Diz, P., Vautravers, M.J., Pike, J., Knorr, G., Hall, I.R., Broecker, W.S. 2009. Interhemispheric Atlantic seesaw response during the last deglaciation. Nature 457(7233), 1097–1102. 10.1038/nature07770

Barker, S., Knorr, G., Vautravers, M.J., Diz, P., Skinner, L.C. 2010. Extreme deepening of the Atlantic overturning circulation during deglaciation. Nature Geosci. 3, 567–571.

Barnosky, C.W., Anderson, P.M., Bartlein, P.J. 1987. The northwestern U.S. during deglaciation: Vegetational history and paleoclimatic implications. In: North America and Adjacent Oceans during the Last Deglaciation, Ruddiman, W.F., Wright, H.E., Jr. (eds.) Geol. Soc. Am., Geol. North Am. K-3, 289–321.

Barrell, D.J., Putnam, A.E., Denton, G.H. 2019. Reconciling the onset of deglaciation in the upper Rangitata valley, Southern Alps, New Zealand. Quat. Sci. Rev. 203, 141–150. 10.1016/j.quascirev.2018.11.003

Barth, A.M., Marcott, S.A., Licciardi, J.M., Shakun, J.D. 2019. Deglacial thinning of the Laurentide Ice Sheet in the Adirondack Mountains, New York, USA, revealed by ^{36}Cl exposure dating. Paleoceanogr. Paleoclim. 34, 946–953. 10.1029/2018PA003477

Bartlein, P.J., Anderson, K.H., Anderson, P.M., Edwards, M.E., Mock, C.J., Thompson, R.S., Webb, R.S., Webb, T., III, Whitlock, C. 1998. Paleoclimate simulations for North America over the past 21,000 years: Features of the simulated climate and comparisons with paleoenvironmental data. Quat. Sci. Rev. 17, 549–585. 10.1016/S0277-3791(98)00012-2

Bartlein, P.J., Harrison, S.P., Brewer, S., Connor, S., Davis, B.A.S., Gajewski, K., Guiot, J., Harrison-Prentice, T.I., Henderson, A., Peyron, O., Prentice, L.C., Scholze, M., Seppa, H., Shuman, B., Sugita, S., Thompson, R.S., Viau, A.E., Williams, J., Wu, H. 2011. Pollen-based continental climate reconstructions at 6 and 21 ka: A global synthesis. Clim. Dynam. 37, 775–802. 10.1007/s00382-010-0904-1

Beeman, C.J., Gest, L., Parrenin, F., Raynaud, D., Fudge, T.J., Buizert, C., Brook, E.J. 2019. Antarctic temperature and CO_2: Near-synchrony yet variable phasing during the last deglaciation. Clim. Past 15, 913–926. 10.5194/cp-15-913-2019

Bendle, J.M., Palmer, A.P., Thorndycraft, V.R., Matthews, I.P. 2017. High-resolution chronology for deglaciation of the Patagonian Ice Sheet at Lago

Buenos Aires (46.5 S) revealed through varve chronology and Bayesian age modelling. Quat. Sci. Rev. 177, 314–339. 10.1016/j.quascirev.2017.10.013

Bendle, J.M., Palmer, A.P., Thorndycraft, V.R., Matthews, I.P. 2019. Phased Patagonian Ice Sheet response to Southern Hemisphere atmospheric and oceanic warming between 18 and 17 ka. Sci. Rep. 9, 4133.

Benson, L., Madole, R., Kubik, P, McDonald, R. 2007. Surface-exposure ages of Front Range moraines that may have formed during the Younger Dryas, 8.2 cal ka, and Little Ice Age events. Quat. Sci. Rev. 26, 1638–1649. 10.1016/j.quascirev.2007.02.015

Benson, L.V., Lund, S.P., Burdett, J.W., Kashgarian, M., Rose, T.P., Smoot, J.P., Schwartz, M. 1998a. Correlation of late-Pleistocene lake-level oscillations in Mono Lake, California, with North Atlantic climate events. Quat. Res. 49, 1–10. 10.1006/qres.1997.1940

Benson, L.V., May, H.M., Antweiler, R.C., Brinton, T.I., Kashgarian, M., Smoot, J.P., Lund, S.P. 1998b. Continuous lake-sediment records of glaciation in the Sierra Nevada between 52,600 and 12,500 ^{14}C yr B.P. Quat. Res. 50, 113–127. 10.1006/qres.1998.1993

Bentley, M.J., Sugden, D., Hulton, N.R.J., McCulloch, R.D. 2005. The landforms and pattern of deglaciation in the Strait of Magellan and Bahía Inútil, southernmost South America. Geogr. Ann., Ser. A, Phys. Geogr. 87A, 313–333. 10.1111/j.0435-3676.2005.00261.x

Bereiter, B., Shackleton, S., Baggenstos, D., Kawamura, K., Severinghaus, J. 2018. Mean global ocean temperatures during the last glacial transition. Nature 553(7686), 39–44. 10.1038/nature25152

Bertrand, S., Charlet, F., Charlier, B., Renson, V., Fagel, N. 2008. Climate variability of southern Chile since the Last Glacial Maximum: Continuous sedimentological record from Lago Puyehue (40 S). J. Paleolimnol. 39(2), 179–195. 10.1007/s10933-007-9117-y

Bezada, M. 1989. Geología Glacial del Cuaternario de la Región de Santo Domingo –Pueblo Llano–Las Mesitas (Estados Mérida y Trujillo). Ph.D. thesis, Instituto Venezolano de Investigaciones Científicas, Venezuela, 245 pp.

Bickerdike, H.L., Ó Cofaigh, C., Evans, D.J., Stokes, C.R. 2018. Glacial landsystems, retreat dynamics and controls on Loch Lomond Stadial (Younger Dryas) glaciation in Britain. Boreas 47, 202–224. 10.1111/bor.12259

Birchfield, G.E., Broecker, W.S. 1990. A salt oscillator in the glacial Atlantic? 2. A "scale analysis" model. Paleoceanogr. Paleoclim. 5, 835–843. 10.1029/PA005i006p00835

Blaise, B., Clague, J.J., Mathewes, R.W. 1990. Time of maximum Late Wisconsinan glaciation, west coast of Canada. Quat. Res. 47, 282–295. 10.1016/0033-5894(90)90041-I

Blard, P.H., Braucher, R., Lavé, J., Bourlès, D. 2013a. Cosmogenic ^{10}Be production rate calibrated against ^{3}He in the high tropical Andes (3800–4900 m, 20–22° S). Earth Planet. Sci. Lett. 382, 140–149. 10.1016/j.epsl.2013.09.010

Blard, P.H., Lave, J., Sylvestre, F., Placzek, C.J., Claude, C., Galy, V., Condom, T., Tibari, B. 2013b. Cosmogenic ^{3}He production rate in the high tropical Andes (3800 m, 20ºS): Implications for the local Last Glacial Maximum. Earth Planet. Sci. Lett. 377-378, 260–275. 10.1016/j.epsl.2013.07.006

Blard, P.H., Lavé, J., Farley, K.A., Fornari, M., Jiménez, N., Ramírez, V. 2009. Late local glacial maximum in the Central Altiplano triggered by cold and locally-wet conditions during the paleolake Tauca episode (17-15 ka, Heinrich 1). Quat. Sci. Rev. 28, 3414–3427. 10.1016/j.quascirev.2009.09.025

Blard, P.H., Lave, J., Farley, K.A., Ramirez, V., Jiménez, N., Martin, L., Charreau, J., Tibari, B., Fornari, M. 2014. Progressive glacial retreat in the Southern Altiplano (Uturuncu volcano, 22°S) between 65 and 14 ka constrained by cosmogenic ^{3}He dating. Quat. Res. 82, 209–221. 10.1016/j.yqres.2014.02.002

Blard, P.H., Sylvestre, F., Tripati, A.K., Claude, C., Causse, C., Coudrain, A., Condom, T., Seidel, J.L., Vimeux, F., Moreau, C., Dumoulin, J.P., Lavé, J. 2011. Lake highstands on the Altiplano (tropical Andes) contemporaneous with Heinrich 1 and the Younger Dryas: New insights from ^{14}C, U-Th dating and δ^{18}O of carbonates. Quat. Sci. Rev. 30, 3973–3989. 10.1016/j.quascirev.2011.11.001

Blunier, T., Chappellaz, J., Schwander, J., Dällenbach, A., Stauffer, B., Stocker, T.F., Johnsen, S.J. 1998. Asynchrony of Antarctic and Greenland climate change during the last glacial period. Nature 394(6695), 739–743. 10.1038/29447

Blunier, T., Schwander, J., Stauffer, B., Stocker, T., Dällenbach, A., Indermühle, A., Tschumi, J., Chappellaz, J., Raynaud, D., Barnola, J.M. 1997. Timing of the Antarctic Cold Reversal and the atmospheric CO_2 increase with respect to the Younger Dryas event. Geophys. Res. Lett. 24, 2683–2686. 10.1029/97GL02658

Boex, J., Fogwill, C., Harrison, S., Glasser, N.F., Hein, A., Schnabel, C., Xu, S. 2013. Rapid thinning of the late Pleistocene Patagonian Ice Sheet followed migration of the Southern Westerlies. Sci. Rep. 3, 2118. 10.1038/srep02118

Böhm, E., Lippold, J., Gutjahr, M., Frank, M., Blaser, P., Antz, B., Deininger, M. 2015. Strong and deep Atlantic meridional overturning circulation during the last glacial cycle. Nature 517(7532), 73–76. 10.1038/nature14059

Bond, G., Showers, W., Cheseby, M., Lotti, R., Almasi, P., deMenocal, P., Priore, P., Cullen, H., Hajda, I., Bonani, G. 1997. A pervasive millennial-scale cycle in North Atlantic Holocene and glacial climates. Science 278, 1257–1266. 10.1126/science.278.5341.1257

Borchers, B., Marrero, S., Balco, G., Caffee, M., Goehring, B., Lifton, N., Stone, J. 2016. Geological calibration of spallation production rates in the CRONUS-Earth project. Quat. Geochronol. 31, 188–198. 10.1016/j.quageo.2015.01.009

Bowerman, N.D., Clark, D.H. 2011. Holocene glaciation of the central Sierra Nevada, California. Quat. Sci. Rev. 30, 1067–1085. 10.1016/j.quascirev.2010.10.014

Briles, C.E., Whitlock, C., Meltzer, D.J. 2012. Last glacial–interglacial environments in the southern Rocky Mountains, USA and implications for Younger Dryas-age human occupation. Quat. Res. 77, 96–103. 10.1016/yqres2011.10.002.

Briner, J.P. 2009. Moraine pebbles and boulders yield indistinguishable ^{10}Be ages: A case study from Colorado, USA. Quat. Geochronol. 4, 299–305. 10.1016/j.quageo.2009.02.010

Briner, J.P., Goehring, B.M., Mangerud, J., Svendsen, J.I. 2016. The deep accumulation of ^{10}Be at Utsira, southwestern Norway: Implications for cosmogenic nuclide exposure dating in peripheral ice sheet landscapes. Geophys. Res. Lett. 43, 9121–9129. 10.1002/2016GL070100

Briner, J.P., Kaufman, D.S., Manley, W.F., Finkel, R.C., Caffee, M.W. 2005. Cosmogenic exposure dating of late Pleistocene moraine stabilization in Alaska. Geol. Soc. Am. Bull. 117, 1108–1120. 10.1130/B25649.1

Briner, J.P., Kaufman, D.S., Werner, A., Caffee, M., Levy, L., Manley, W.F., Kaplan, M.R., Finkel, R.C. 2002. Glacier readvance during the late glacial (Younger Dryas?) in the Ahklun Mountains, southwestern Alaska. Geology 30, 679–682. 10.1130/0091-7613(2002)030<0679:GRDTLG>2.0.CO;2

Briner, J.P., Tulenko, J.P., Kaufman, D.S., Young, N.E., Baichtal, J.F., Lesnek, A. 2017. The last deglaciation of Alaska. Geogr. Res. Lett. 43, 429–448. 10.18172/cig.3229

Broccoli, A.J., Manabe, S. 1987a. The effects of the Laurentide Ice Sheet on North American climate during the last glacial maximum. Geogr. phys. Quat. 41, 291–299. 10.7202/032684ar

Broccoli, A.J., Manabe, S. 1987b. The influence of continental ice, atmospheric CO_2, and land albedo on the climate of the Last Glacial Maximum. Clim. Dynam. 1, 87–99. 10.1007/BF01054478

Broecker, W.S. 1998. Paleocean circulation during the last deglaciation: A bipolar seesaw? Paleoceanogr. Paleoclim. 13, 119–121. 10.1029/97PA03707

Broecker, W.S., Denton, G.H. 1990. The role of ocean-atmosphere reorganizations in glacial cycles. Quat. Sci. Rev. 9, 305–341. 10.1016/0277-3791(90)90026-7

Broecker, W.S., van Donk, J. 1970. Insolation changes, ice volumes and the O^{18} in deep-sea cores. Rev. Geophys. 8, 169–198. 10.1029/RG008i001p00169

Broecker, W.S., Denton, G.H., Edwards, R.L., Cheng, H., Alley, R.B., Putnam, A.E. 2010. Putting the Younger Dryas cold event into context. Quat. Sci. Rev. 29, 1078–1081. 10.1016/j.quascirev.2010.02.019

Bromley, R.M., Hall, B.L., Schaefer, J.M., Winckeler, G., Todd, C.E., Rademaker, K.M. 2011. Glacier fluctuations in the southern Peruvian Andes during the Late-glacial period, constrained with cosmogenic ^{3}He. J. Quat. Sci. 26, 37–43. 10.1002/jqs.1424

Bromley, R.M., Schaefer, J.M., Hall, B.L., Rademaker, K.M., Putnam, A.E., Todd, C. E., Hegland, M., Winckler, G., Jackson, M.S., Strand, P.D. 2016. A cosmogenic ^{10}Be chronology for the local last glacial maximum and termination in the Cordillera Oriental, southern Peruvian Andes: Implications for the tropical role in global climate. Quat. Sci. Rev. 148, 54–67. 10.1016/j.quascirev.2016.07.010

Bromley, G.R.M., Schaefer, J.M., Winckeler, G., Hall, B.L., Todd, C.E., Rademaker, K.M. 2009. Relative timing of last glacial maximum and late-glacial events in the central tropical Andes. Quat. Sci. Rev. 28, 2514–2526. 10.1016/j.quascirev.2009.05.012

Bromley, G.R.M., Thouret, J.C., Schimmelpfennig, I., Mariño, J., Valdivia, D., Rademaker, K., Vivanco Lopez, S. P., ASTER Team, Aumaître, G., Bourlès, D., Keddadouche. K. 2019. In situ cosmogenic ^{3}He and ^{36}Cl and radiocarbon dating of volcanic deposits refine the Pleistocene and Holocene eruption chronology of SW Peru. Bull. Volcanology 81, 64. 10.1007/s00445-019-1325-6

Brook, E.J., Buizert, C. 2018. Antarctic and global climate history viewed from ice cores. Nature 558(7709), 200–208. 10.1038/s41586-018-0172-5

Brugger, K.A. 2006. Late Pleistocene climate inferred from the reconstruction of the Taylor River glacier complex, southern Sawatch Range, Colorado. Geomorphology 75, 318–329. 10.1016/j.geomorph.2005.07.020

Brugger, K.A. 2010. Climate in the southern Sawatch Range and Elk Mountains, Colorado, USA, during the Last Glacial Maximum: Inferences using a simple degree-day model. Arct. Antarct. Alp. Res. 42, 164–178. 10.1657/1938-4246-42.2.164

Brugger, K.A., Goldstein, B.S. 1999. Paleoglacier reconstruction and late-Pleistocene equilibrium-line altitudes, southern Sawatch Range, Colorado. In: Mickelson, D.M., Attig, J.W. (eds.) Glacial Processes Past and Present. Geol. Soc. Am. Spec. Pap. 337, 103–112. 10.1130/0-8137-2337-X.103

Brugger, K.A., Laabs, B., Reimers, A., Bensen, N. 2019. Late Pleistocene glaciation in the Mosquito Range, Colorado, USA: Chronology and climate. J. Quat. Sci. 34, 187–202. 10.1002/jqs.3090

Brunschön, C., Behling, H. 2009. Reconstruction and visualization of upper forest line and vegetation changes in the Andean depression region of southeastern Ecuador since the last glacial maximum – A multi-site synthesis. Rev. Palaeobot. Palynol. 163, 139–152. 10.1016/j.revpalbo.2010.10.005

Caldenius, C.C. 1932. Las glaciaciones Cuaternarias en la Patagonia y Tierra del Fuego. Geogr. Ann. 14, 164 pp. (English summary, pp. 144–157). 10.1080/20014422.1932.11880545

Carcaillet, J., Angel, I., Carrillo, E., Audemard, F.A., Beck, C. 2013. Timing of the last deglaciation in the Sierra Nevada of the Mérida Andes, Venezuela. Quat. Res. 80, 482–494. 10.1016/j.yqres.2013.08.001

Carlson, A.E., Clark, P.U., Raisbeck, G.M., Brook, E.J. 2007. Rapid Holocene deglaciation of the Labrador sector of the Laurentide ice sheet. J. Climate 20, 5126–5133. 10.1175/JCLI4273.1

Carlson, A.E., LeGrande, A.N., Oppo, D.W., Came, R.E., Schmidt, G.A., Anslow, F.S., Licciardi, J.M., Obbink, E.A. 2008. Rapid early Holocene deglaciation of the Laurentide Ice Sheet. Nature Geosci. 1, 620–624.

Carlson, R.J., Baichtal, J.F. 2015. A predictive model for locating early Holocene archaeological sites based on raised shell-bearing strata in southeast Alaska, USA. Geoarchaeology 30, 120–138. 10.1002/gea.21501

Carrillo, E., Beck, C., Audemard, F.A., Moreno, E., Ollarves, R. 2008. Disentangling late Quaternary climatic and seismo-tectonic controls on Lake Mucubají sedimentation (Mérida Andes, Venezuela). Palaeogeogr. Palaeoclimatol. Palaeoecol. 259, 284–300. 10.1016/j.palaeo.2007.10.012

Casassa, G., Haeberli, W., Jones, G., Kaser, G., Ribstein, P., Rivera, A., Schneider, C. 2007. Current status of Andean glaciers. Global Planet. Change. 59, 1–9. 10.1016/j.gloplacha.2006.11.013

Cesta, J.M., Ward, D.J. 2016. Timing and nature of alluvial fan development along the Chajnantor Plateau, northern Chile. Geomorphology 273, 412–427. 10.1016/j.geomorph.2016.09.003

Chen, H., Xu, Z., Clift, P.D., Lim, D., Khim, B.K., Yu, Z. 2019. Orbital-scale evolution of the Indian summer monsoon since 1.2 Ma: Evidence from clay mineral records at IODP Expedition 355 Site U1456 in the eastern Arabian Sea. J. Asian Earth Sci. 174, 11–22. 10.1016/j.jseaes.2018.10.012

Chen, T., Robinson, L.F., Burke, A., Southon, J., Spooner, P., Morris, P.J., Ng, H.C. 2015. Synchronous centennial abrupt events in the ocean and atmosphere during the last deglaciation. Science 349(6255), 1537–1541. 10.1126/science.aac6159

Cheng, H., Edwards, R.L., Broecker, W.S., Denton, G.H., Kong, X., Wang, Y., Zhang, R., Wang, X. 2009. Ice Age Terminations. Science 326(5950), 248–252. 10.1126/science.1177840

Cheng, H., Edwards, R.L., Sinha, A., Spötl, C., Yi, L., Chen, S., Kelly, M., Kathayat, G., Wang, X., Li, X., Kong, X., Wang, Y., Ning, Y., Zhang, H. 2016. The Asian monsoon over the past 640,000 years and Ice Age Terminations. Nature 534(7609), 640–646. 10.1038/nature18591

Cheng, H., Sinha, A. Cruz, F.W., Wang, X., Edwards, R.L., d'Horta, F.M., Ribas, C.C..,Vuille, M., Stott, L.D., Auler, A.S. 2013. Climate change patterns in Amazonia and biodiversity. Nature Commun. 4, 1411. 10.1038/ncomms2415

Çiner, A., Sarıkaya, M.A., Yıldırım, C. 2017. Misleading old age on a young landform? The dilemma of cosmogenic inheritance in surface exposure dating: Moraines vs. rock glaciers. Quat. Geochronol. 42, 76–88. 10.1016/j.quageo.2017.07.003

Clague, J.J. 1981. Late Quaternary Geology and Geochronology of British Columbia. Part 2: Summary and Discussion of Radiocarbon-Dated Quaternary History. Geol. Surv. Can. Pap. 80-35, 41 pp. 10.4095/119439

Clague, J.J. 2017. Deglaciation of the Cordillera of Western Canada at the end of the Pleistocene. Geogr. Res. Lett. 43, 449–466. 10.18172/cig3232

Clague, J.J., Mathewes, R.W., Guilbault, J.-P., Hutchinson, I., Ricketts, B.D. 1997. Pre-Younger Dryas resurgence of the southwestern margin of the Cordilleran ice sheet, British Columbia, Canada. Boreas 26, 261–278. 10.1111/j.1502-3885.1997.tb00855.x

Clapperton, C.M. 1998. Late Quaternary glacier fluctuations in the Andes: Testing the synchrony of global change. Quat. Proc. 6, 65–74.

Clapperton, C.M. 2000. Interhemispheric synchroneity of Marine Oxygen Isotope Stage 2 glacier fluctuations along the American Cordilleras transect. J. Quat. Sci. 15, 435–468. 10.1002/1099-1417(200005)15:4<435::AID-JQS552>3.0.CO;2-R

Clapperton, C.M., McEwan, C. 1985. Late Quaternary moraines in the Chimborazo area, Ecuador. Arct. Alp. Res. 17, 135–142. 10.1080/00040851.1985.12004459

Clapperton, C.M., Hall, M., Mothes, P., Hole, M.J., Still, J.W., Helmens, K.F., Kuhry, P., Gemmelle, A.M.D. 1997a. A Younger Dryas icecap in the equatorial Andes. Quat. Res. 47, 13–28. 10.1006/qres.1996.1861

Clapperton, C.M., Clayton, J.D., Benn, D.I., Marden, C.J., Argollo, J. 1997b. Late Quaternary glacier advances and paleolake highstands in the Bolivian Altiplano. Quat. Int. 38-39, 49–59. 10.1016/s1040-6182(96)00020-1

Clapperton, C., Sugden, D., Kaufman, D.S., McCulloch, R.D. 1995. The last glaciation in central Magellan Strait, southernmost Chile. Quat. Res. 44, 133–148. 10.1006/qres.1995.1058

Clark, C.D., Stokes, C.R. 2001. Extent and basal characteristics of the M'Clintock Channel ice stream. Quat. Int. 86, 81–101. 10.1016/S1040-6182(01)00052-0

Clark D.H. and Gillespie A.R. (1997) Timing and significance of late-glacial and Holocene cirque glaciation in the Sierra Nevada, California. Quat. Int., 38/39, 21–38. 10.1016/S1040-6182(96)00024-9

Clark, P.U. 1994. Unstable behavior of the Laurentide Ice Sheet over deforming sediment and its implications for climate change. Quat. Res. 41, 19–25. 10.1006/qres.1994.1002

Clark, P.U., Archer, D., Pollard, D., Blum, J.D., Rial, J.A., Brovkin, V., Mix, A.C., Pisias, N.G., Roy, M. 2006. The Middle Pleistocene transition: Characteristics, mechanisms, and implications for long-term changes in atmospheric pCO_2. Quat. Sci. Rev. 25, 3150–3184. 10.1016/j.quascirev.2006.07.008

Clark, P.U., Dyke, A.S., Shakun, J.D., Carlson, A.E., Clark, J., Wohlfarth, B., Mitrovica, J.X., Hostetler, S.W., McCabe, A. 2009. The Last Glacial Maximum. Science 325, 710–714. 10.1126/science.1172873

Clark, P.U., Shakun, J.D., Baker, P.A., Bartlein, P.J., Brewer, S., Brook, E., Carlson, A.E., Cheng, H., Kaufman, D.S., Liu, Z., Marchitto, T.M., Mix, A.C., Morrill, C., Otto-Bliesner, B.L., Pahnke, K., Russell, J.M., Whitlock, C., Adkins, J.F., Blois, J.L., Clark, J., Colman S.M., Curry, W.B., Flower, B.P., He, F., Johnson, T.C., Lynch-Stieglitz, J., Markgraf, V., McManus, J., Mitrovica, J.X., Moreno, P.I., Williams, J.W. 2012. Global climate evolution during the last deglaciation. Proc. Natl. Acad. Sci. 109(19), E1134–E1142. 10.1073/pnas.1116619109

Clayton, J.D., Clapperton, C.M. 1997. Broad synchrony of a Late-glacial glacier advance and the highstand of palaeolake Tauca in the Bolivian Altiplano. J. Quat. Sci. 12, 169–182. 10.1002/(SICI)1099-1417(199705/06)12:3<169::AID-JQS304>3.0.CO;2-S

Clayton, L., Teller, J.T., Attig, J.W. 1985. Surging of the southwestern part of the Laurentide Ice Sheet. Boreas 14, 235–241. 10.1111/j.1502-3885.1985.tb00726.x

Clementi, V.J., Sikes, E.L. 2019. Southwest Pacific vertical structure influences on oceanic carbon storage since the Last Glacial Maximum. Paleoceanogr. Paleoclim. 34, 734–754. 10.1029/2018PA003501

Cofaigh, C.Ó., Weilbach, K., Lloyd, J.M., Benetti, S., Callard, S.L., Purcell, C., Chiverrell, R.C., Dunlop, P., Saher, M., Livingstone, S.J., Van Landeghem, K.J.J., Moreton, S.G., Clarke, C.D., Fabelg, D. 2019. Early deglaciation of the British-Irish Ice Sheet on the Atlantic shelf northwest of Ireland driven by glacioisostatic depression and high relative sea level. Quat. Sci. Rev. 208, 76–96. 10.1016/j.quascirev.2018.12.022

COHMAP Members. 1988. Climatic changes of the last 18,000 years: Observations and model simulations. Science 241, 1043–1052. 10.1126/science.241.4869.1043

Corbett, L.B., Bierman, P.R., Wright, S.F., Shakun, J.D., Davis, P.T., Goehring, B.M., Halsted, C.T., Koester, A.J., Caffee, M.W., Zimmerman, S.R. 2019. Analysis of multiple cosmogenic nuclides constrains Laurentide Ice Sheet history and process on Mt. Mansfield, Vermont's highest peak. Quat. Sci. Rev., 205, 234–246. 10.1016/j.quascirev.2018.12.014

Coronato, A. 1995. The last Pleistocene glaciation in tributary valleys of the Beagle Channel, southernmost South America. In: Rabassa, J., Salemme, M. (eds.) Quaternary of South America and Antarctic Peninsula, Vol. 9. Balkema: Amsterdam, 173–182.

Coronato, A., Meglioli, A., Rabassa, J. 2004. Glaciations in the Magellan Straits and Tierra del Fuego, southernmost South America. In: Elhers, J., Gibbard, P., Coronato, A.M.J., Meglioli, A., Rabassa, J. (eds.) Quaternary Glaciations: Extent and Chronology. Part III: South America, Asia, Africa, Australia and Antarctica. Quaternary Book Series, Elsevier, Amsterdam, 45–48.

Coronato, A., Seppälä, M., Ponce, J.F., Rabassa, J. 2009. Glacial geomorphology of the Pleistocene Lake Fagnano ice lobe, Tierra del Fuego, southern South America. Geomorphology 112, 67–81. 10.1016/j.geomorph.2009.05.005

Cosma, T.N., Hendy, I.L., Chang, A.S. 2008. Chronological constraints on Cordilleran Ice Sheet glaciomarine sedimentation from Core MD02-2496 off Vancouver Island (Western Canada). Quat. Sci. Rev. 27, 941–955. 10.1016/j.quascirev.2008.01.013

Cruz, F.W., Jr., Burns, S.J., Karmann, I., Sharp, W.D., Vuille, M., Cardoso, A.O., Ferrari, J.A., Silva Dias, P.L., Viana, O., Jr. 2005. Insolation-driven changes in atmospheric circulation over the past 116,000 years in subtropical Brazil. Nature 434, 63–66. 10.1038/nature03365

Cunningham, M.T., Stark, C.P., Kaplan, M.R., Schaefer, J.M. 2019. Glacial limitation of tropical mountain height. Earth Surf. Dynam. 7, 147–169. 10.5194/esurf-7-147-2019

Cutler, P.I., Mickelson, D.M., Colgan, P.M., MacAyeal, D.R., Parizek, B.R. 2001. Influence of the Great Lakes on the dynamics of the southern Laurentide Ice sheet: Numerical experiments. Geology 29, 1039–1042. 10.1130/0091-7613(2001)029<1039:IOTGLO>2.0.CO;2

Cuzzone, J.K., Clark, P.U., Carlson, A.E., Ullman, D.J., Rinterknecht, V.R., Milne, G. A., Lunkka, J-P., Wohlfarth, B., Marcot, S.A., Caffee, M. 2016. Final deglaciation of the Scandinavian Ice Sheet and implications for the Holocene global sea-level budget. Earth Planet. Sci. Lett. 448, 34–41. 10.1016/j.epsl.2016.05.019

D'Arcy, M., Schildgen, T.F., Strecker, M.R., Wittmann, H., Duesing, W., Mey, J., Tofelde, S., Weissmann, P., Alonso, R.N. 2019. Timing of past glaciation at the Sierra de Aconquija, northwestern Argentina, and throughout the Central Andes. Quat. Sci. Rev. 204, 37–57. 10.1016/j.quascirev.2018.11.022

Dahms, D.E. 2002. Glacial stratigraphy of Stough Creek basin, Wind River Range, Wyoming. Geomorphology 42(1/2), 59–83. 10.1016/S0169-555X(01)00073-3

Dahms, D.E. 2004. Relative and numeric age-data for Pleistocene glacial deposits and diamictons in and Near Sinks Canyon, Wind River Range, Wyoming. Arct. Antarct. Alp. Res. 36(1), 59–77. 10.1657/1523-0430(2004)036[0059:RANADF]2.0.CO;2

Dahms, D.E., Birkeland, P.W., Shroba, R.R., Miller, C. Dan, Kihl, R. 2010. Latest glacial and periglacial stratigraphy, Wind River Range, Wyoming. Geol. Soc. Am. Digital Maps Charts Ser. 7, 46 pp. 10.1130/2010.DMCH007.TXT

Dahms, D.E., Egli, M. Fabel, D., Harbor, J., Brandova, D., de Castro Portes, R. D.B., Christl, M. 2018. Revised Quaternary glacial succession and post-LGM recession, southern Wind River Range, Wyoming, USA. Quat. Sci. Rev. 192, 167–184. 10.1016/j.quascirev.2018.05.020

Dahms, D.E., Egli, M., Fabel, D., Harbor, J., Brandova, D., de Castro Portes, R., Christl, M. 2019. Corrigendum to "Revised Quaternary glacial successioin and post-LGM recession, southern Wind River Range, Wyoming, USA". Quat. Sci. Rev. 212, 219–220. 10.1016/j.quascirev.2019.03.029

Dansgaard, W., White, J.W.C., Johnsen, S.J. 1989. The abrupt termination of the Younger Dryas climate event. Nature 339(6225), 532–534. 10.1038/339532a0

Darvill, C.M., Bentley, M.J., Stokes, C.R., Hein, A.S., Rodés, Á. 2015a. Extensive MIS 3 glaciation in southernmost Patagonia revealed by cosmogenic nuclide dating of outwash sediments. Earth Planet. Sci. Lett. 429, 157–169. 10.1016/j.epsl.2015.07.030

Darvill, C.M., Bentley, M.J., Stokes, C.R. 2015b. Geomorphology and weathering characteristics of erratic boulder trains on Tierra del Fuego, southernmost South America: Implications for dating of glacial deposits. Geomorphology 228, 382–397. 10.1016/j.geomorph.2014.09.017

Darvill, C.M., Bentley, M.J., Stokes, C.R., Shulmeister, J. 2016. The timing and cause of glacial advances in the southern mid-latitudes during the last glacial cycle based on a synthesis of exposure ages from Patagonia and New Zealand. Quat. Sci. Rev. 149, 200–214. 10.1016/j.quascirev.2016.07.024

Darvill, C.M., Stokes, C.R., Bentley, M.J., Lovell, H. 2014. A glacial geomorphological map of the southernmost ice lobes of Patagonia: The Bahía Inútil – San Sebastían, Magellan, Otway, Skyring, and Río Gallegos lobes. J. Maps 10, 500–520. 10.1080/17445647.2014.890134

Davies, B.J., Thorndycraft, V.R., Fabel, D., Martin, J.R.V. 2018. Asynchronous glacier dynamics during the Antarctic Cold Reversal in central Patagonia. Quat. Sci. Rev. 200, 287–312. 10.1016/j.quascirev.2018.09.025

De Klerk, P. 2004. Confusing concepts in Lateglacial stratigraphy and geochronology: Origin, consequences, conclusions (with special emphasis on the type locality Bøllingsø). Rev. Palaeobot. Palynol. 129, 265–298. 10.1016/j.revpalbo.2004.02.006

De Martonne, E. 1934. The Andes of the north-west Argentine. Geogr. J. 84, 1–14. 10.2307/1786827

de Porras, M.E., Maldonado, A., Quintana, F.A., Martel Cea, A., Reyes, O., Méndez Melgar, C. 2014. Environmental and climatic changes in central Chilean Patagonia since the Late Glacial (Mallín El Embudo, 44º S). Clim. Past. 10, 1063–1078. 10.5194/cp-10-1063-2014

Deaney, E.L., Barker, S., Van De Flierdt, T. 2017. Timing and nature of AMOC recovery across Termination 2 and magnitude of deglacial CO_2 change. Nature Commun. 8, 14595. 10.1038/ncomms14595

Dede, V., Çiçek, I., Sarıkaya, M.A., Çiner, A., Uncu, L. 2017. First cosmogenic geochronology from the Lesser Caucasus: Late Pleistocene glaciation and rock glacier development in the Karçal Valley, NE Turkey. Quat. Sci. Rev. 164, 54–67. 10.1016/j.quascirev.2017.03.025

Denton, G.H., Alley, R.B., Comer, G.C., Broecker, W.S. 2005. The role of seasonality in abrupt climate change. Quat. Sci. Rev. 24, 1159–1182. 10.1016/j.quascirev.2004.12.002

Denton, G.H., Anderson, R.F., Toggweiler, J.R., Edwards, R.L., Schaefer, J.M., Putnam, A.E. 2010. The Last Glacial Termination. Science 328(5986), 1652–1656. 10.1126/science.1184119

Denton, G.H., Broecker, W.S., Alley, R.B. 2006. The mystery interval 17.5 to 14.5 kyrs ago. PAGES News 14, 14–16. 10.22498/pages.14.2.14

Denton, G.H., Lowell, T.V., Heusser, C.J., Schluchter, C., Andersen, B.G., Heusser, L.E., Moreno, P.I., Marchant, D.R. 1999a. Geomorphology, stratigraphy, and radiocarbon chronology of Llanquihue drift in the area of the southern Lake District, Seno Reloncavi, and Isla Grande de Chiloe, Chile. Geogr. Ann., Ser. A, Phys. Geogr. 81A, 167–229. 10.1111/1468-0459.00057

Denton, G.H., Heusser, C.J., Lowell, T.V., Moreno, P.I., Andersen, B.G., Heusser, L.E., Schlühter, C., Marchant, D.R. 1999b. Interhemispheric linkage of paleoclimate during the last glaciation. Geogr. Ann., Ser. A, Phys. Geogr. 81A, 107–153. 10.1111/1468-0459.00055

Dirszowsky, R.W., Mahaney, W.C., Hodder, K.R., Milner, M.W., Kalm, V., Bezada, M., Beukens, R.P. 2005. Lithostratigraphy of the Merida (Wisconsinan) glaciation and Pedregal interstade, Merida Andes, northwestern Venezuela. J. South Am. Earth Sci. 19, 525–536. 10.1016/j.jsames.2005.07.001

Dixon, E.J. 2015. Late Pleistocene colonization of North America from Northeast Asia: New insights from large-scale paleogeographic reconstructions. In: Frachetti, M.D., Spengler III, R.N. (eds.) Mobility and Ancient Society in

Asia and the Americas. Springer Intern. Publ., pp. 169–184. 10.1007/978-3-319-15138-0

Dorfman, J.M., Stoner, J.S., Finkenbinder, M.S., Abbott, M.B., Xuan, C., St-Onge, G. 2015. A 37,000-year environmental magnetic record of aeolian dust deposition from Burial Lake, Arctic Alaska. Quat. Sci. Rev. 128, 81–97. 10.1016/j.quascirev.2015.08.018

Doughty, A.M., Anderson, B.M., Mackintosh, A.N., Kaplan, M.R., Vandergoes, M.J., Barrell, D.J., Denton, G.H., Schaefer, J.M., Chinn, T.J.H., Putnam, A.E. 2013. Evaluation of Lateglacial temperatures in the Southern Alps of New Zealand based on glacier modelling at Irishman Stream, Ben Ohau Range. Quat. Sci. Rev. 74, 160–169. 10.1016/j.quascirev.2012.09.013

Douglass, D.C., Singer, B.S., Kaplan, M.R., Mickelson, D.M., Caffee, M.W. 2006. Cosmogenic nuclide surface exposure dating of boulders on Last Glacial and Late Glacial moraines, Lago Buenos Aires, Argentina: Interpretive strategies and paleoclimate implications. Quat. Geochronol. 1, 43–58. 10.1016/j.quageo.2006.06.001

Dühnforth, M., Anderson, R.S. 2011. Reconstructing the glacial history of Green Lakes valley, North Boulder Creek, Colorado Front Range. Arct. Antarct. Alp. Res. 43, 527–542. 10.1657/1938-4246-43.4.527

Dyke, A.S. 2004. An outline of North American deglaciation with emphasis on central and northern Canada. In: Ehlers, J., Gibbard, P.L. (eds.) Quaternary Glaciations – Extent and Chronology. Elsevier, Amsterdam, 2, 371–406. 10.1016/S1571-0866(04)80209-4

Dyke, A.S., Prest, V.K. 1987. Late Wisconsinan and Holocene history of the Laurentide Ice Sheet. Géogr. phys. Quat. 41, 237–263. 10.7202/032681ar

Dyke, A.S., Savelle, J.M. 2000. Major end moraines of Younger Dryas age on Wollaston Peninsula, Victoria Island, Canadian Arctic: Implications for paleoclimate and for formation of hummocky moraine. Can. J. Earth Sci. 37, 601–619. 10.1139/e99-118

Dyke, A.S., Andrews, J.T., Clark, P.U., England, J.H., Miller, G.H., Shaw, J., Veillette, J.J. 2002. The Laurentide and Innuitian ice sheets during the Last Glacial Maximum. Quat. Sci. Rev. 21, 9–31. 10.1016/S0277-3791(01)00095-6

Dyke, A.S., Moore, A., Robertson, L. 2003. Deglaciation of North America. Geol. Surv. Can. Open File 1574. 10.4095/214399

Ellis, R., Palmer, M. 2016. Modulation of ice ages via precession and dust-albedo feedbacks. Geosci. Front. 7, 891–909. 10.1016/j.gsf.2016.04.004

Emiliani, C. 1955. Pleistocene temperatures. J. Geol. 63, 538–578. 10.1086/626295

England, J.H., Furze, M.F.A. 2008. New evidence from the western Canadian Arctic Archipelago for the resubmergence of Bering Strait. Quat. Res. 70, 60–67. 10.1016/j.yqres.2008.03.001

Erb, M.P., Jackson, C.S., Broccoli, A.J., Lea, D.W., Valdes, P.J., Crucifix, M., DiNezio, P.N. 2018. Model evidence for a seasonal bias in Antarctic ice cores. Nature Commun. 9, 1361. 10.1038/s41467-018-03800-0

Evenson, E., Burkhart, P., Gosse, J., Baker, G., Jackofsky, D., Meglioli, A., Dalziel, I., Kraus, S., Alley, R., Berti, C. 2009. Enigmatic boulder trains, supraglacial rock avalanches, and the origin of "Darwin's boulders," Tierra del Fuego. GSA Today 19, 4–10. 10.1130/GSATG72A.1

Finkenbinder, M.S., Abbott, M.B., Edwards, M.E., Langdon, C.T., Steinman, B.A., Finney, B.P. 2014. A 31,000 year record of paleoenvironmental and lake-level change from Harding Lake, Alaska, USA. Quat. Sci. Rev. 87, 98–113. 10.1016/j.quascirev.2014.01.005

Fogwill, C.J., Turney, C.S.M., Golledge, N.R., Etheridge, D.M., Rubino, M., Thornton, D.P., Baker, A., Woodward, J., Winter, K., van Ommen, T.D., Moy, A.D., Curran, M.A.J., Davies, S.M., Weber, M.E., Bird, M.I., Munksgaard, N.C., Menviel, L., Rootes, C.M., Ellis, B., Millman, H., Vohra, J., Rivera, A., Cooper A. 2017. Antarctic ice sheet discharge driven by atmosphere-ocean feedbacks at the Last Glacial Termination. Sci. Rep. 7, 39979. 10.1038/srep39979

Friele, P.A., Clague, J.J. 2002. Younger Dryas readvance in Squamish River valley, southern Coast Mountains, British Columbia. Quat. Sci. Rev. 21, 1925–1933. 10.1016/S0277-3791(02)00081-1

Fulton, R.J. 1967. Deglaciation in Kamloops Region, An Area of Moderate Relief, British Columbia. Geol. Surv. Can. Bull. 154. 10.4095/101467

García, J.L., Hall, B.L., Kaplan, M.R., Vega, R.M., Strelin, J.A. 2014. Glacial geomorphology of the Torres del Paine region (southern Patagonia): Implications for glaciation, deglaciation and paleolake history. Geomorphology 204, 599–616. 10.1016/j.geomorph.2013.08.036

García, J.L., Hein, A.S., Binnie, S.A., Gómez, G.A., González, M.A., Dunai, T.J. 2018. The MIS 3 maximum of the Torres del Paine and Última Esperanza ice lobes in Patagonia and the pacing of southern mountain glaciation. Quat. Sci. Rev. 185, 9–26. 10.1016/j.quascirev.2018.01.013

García, J.L., Kaplan, M.R., Hall, B.L., Schaefer, J.M., Vega, R.M., Schwartz, R., Finkel, R. 2012. Glacier expansion in southern Patagonia throughout the Antarctic Cold Reversal. Geology 40, 859–862. 10.1130/G33164.1

García, J.L., Maldonado, A., de Porras, M.E., Delaunay, A.N., Reyes, O., Ebensperger, C.A., Binnie, S.A., Lüthgens, C., Méndez, C. 2018. Early deglaciation and paleolake history of Río Cisnes Glacier, Patagonian Ice Sheet (44º S). Quat. Res. 91, 194–217. 10.1017/qua.2018.93

García-Ruiz, J.M., Palacios, D., González-Sampériz, P., de Andrés, N., Moreno, A., Valero-Garcés, B., Gómez-Villar, A. 2016. Mountain glacier evolution in the Iberian Peninsula during the Younger Dryas. Quat. Sci. Rev. 138, 16–30. 10.1016/j.quascirev.2016.02.022

Gardner, A.S., Moholdt, G., Cogley, J.G., Wouters, B., Arendt, A.A., Wahr, J., Berthier, E., Hock, R., Pfeffer, W.T., Kaser, G., Ligtenberg, S.R., Bolch, T., Sharp, M.J., Hagen, J.O., Ove, J., van den Broeke, M.R., Paul, P. 2013. A reconciled estimate of glacier contributions to sea level rise: 2003 to 2009. Science 340(6134), 852–857. 10.1126/science.1234532

Gayo, E.M., Latorre, C., Jordan, T.E., Nester, P.L., Estay, S.A., Ojeda, K.F., Santoro, C.M. 2012. Late Quaternary hydrological and ecological changes in the

hyperarid core of the northern Atacama Desert (~21 S). Earth-Sci. Rev. 113, 120–140. 10.1016/j.earscirev.2012.04.003

Gildor, H., Ashkenazy, Y., Tziperman, E., Lev, I. 2014. The role of sea ice in the temperature-precipitation feedback of glacial cycles. Clim. Dynam. 43, 1001–1010. 10.1007/s00382-013-1990-7

Gillespie, A.R., Clark, D.H. 2011. Glaciations of the Sierra Nevada, California, USA. In: Ehlers, J., Gibbard, P.L., Hughes, P.D. (eds.) Quaternary Glaciations - Extent and Chronology. A Closer Look. Elsevier, Amsterdam, 15, 447–462. 10.1016/B978-0-444-53447-7.00034-9

Gillespie, A.R., Zehfuss, P.H. 2004. Glaciations of the Sierra Nevada, California, USA. In: Ehlers, J., Gibbard, P.L. (eds.) Quaternary Glaciations – Extent and Chronology. Part II: North America. Elsevier, Amsterdam, 2, 51–62. 10.1016/S1571-0866(04)80185-4

Giraudi, C. 2015. The upper Pleistocene deglaciation on the Apennines (peninsular Italy). Geogr. Res. Lett. 41, 337–358. 10.18172/cig.2696

Glasser, N.F., Clemmens, S., Schnabel, C., Fenton, C.R., Mchargue, L. 2009. Tropical glacier fluctuations in the Cordillera Blanca, Peru between 12.5 and 7.6 ka from cosmogenic ^{10}Be dating. Quat. Sci. Rev. 28, 3448–3458. 10.1016/j.quascirev.2009.10.006

Glasser, N.F., Harrison, S., Schnabel, C., Fabel, D., Jansson, K.N. 2012. Younger Dryas and early Holocene age glacier advances in Patagonia. Quat. Sci. Rev. 58, 7–17. 10.1016/j.quascirev.2012.10.011

Glasser, N.F., Harrison, S., Winchester, V., Aniya, M. 2004. Late Pleistocene and Holocene palaeoclimate and glacier fluctuations in Patagonia. Glob. Planet. Change. 43, 79–101. 10.1016/j.gloplacha.2004.03.002

Glasser, N.F., Jansson, K.N., Duller, G.A.T., Singarayer, J., Holloway, M., Harrison, S., 2016. Glacial lake drainage in Patagonia (13-8 kyr) and response of the adjacent Pacific Ocean. Sci. Rep. 6, 21064. 10.1038/srep21064

Glasser, N.F., Jansson, K.N., Goodfellow, B.W., de Angelis, H., Rodnight, H., Rood, D.H. 2011. Cosmogenic nuclide exposure ages for moraines in the Lago

San Martin Valley, Argentina. Quat. Res. 75, 636–646. 10.1016/j.yqres.2010.11.005

Glasser, N.F., Jansson, K.N., Harrison, S., Kleman, J. 2008. The glacial geomorphology and Pleistocene history of South America between 38º S and 56º S. Quat. Sci. Rev. 27, 365–390. 10.1016/j.quascirev.2007.11.011

Gowan, E.J. 2013. An assessment of the minimum timing of ice free conditions of the western Laurentide Ice Sheet. Quat. Sci. Rev. 75, 100–113. 10.1016/j.quascirev.2013.06.001

Grant, K.M. Rohling, E.J., Ramsey, C.B., Cheng, H., Edwards, R.L., Florindo, F., Heslop, D., Marra, F., Roberts, A.P., Tamisiea, M.E., Williams, F. 2014. Sea-level variability over five glacial cycles. Nature Commun. 5, 5076. 10.1038/ncomms6076

Gregoire, L.J., Payne, A.J., Valdes, P.J. 2012. Deglacial rapid sea level rises caused by ice sheet saddle collapses. Nature 487, 219–222. 10.1038/nature11257

Gregoire, L.J., Valdes, P.J., Payne, A.J. 2015. The relative contribution of orbital forcing and greenhouse gases to the North American deglaciation. Geophys. Res. Lett. 42, 9970-9979. 10.1002/2015GL066005

Grigg, L.D., Whitlock, C. 2002. Patterns and causes of millennial scale climate change in the Pacific Northwest during Marine Isotope Stages 2 and 3. Quat. Sci. Rev. 21, 2067–2083. 10.1016/S0277-3791(02)00017-3

Grosjean, M., Van Leeuwen, J.F.N., Van der Knaap, W.O., Geyh, M.A., Ammann, B., Tanner, W., Messerli, B., Núñez, L.A., Valero-Garcés, B.L., Veit, H. 2001. A 22,000 ^{14}C year BP sediment and pollen record of climate change from Laguna Miscanti (23º S), northern Chile. Glob. Planet. Change 28, 35–51. 10.1016/S0921-8181(00)00063-1

Gump, D.J., Briner, J.P., Mangerud, J., Svendsen, J.I. 2017. Deglaciation of Boknafjorden, south-western Norway. J. Quat. Sci. 32, 80–90. 10.1002/jqs.2925

Guzmán, O. 2013. Timing and Dynamics of River Terraces Formation in Moderate Uplifted Ranges: The Example of Venezuela and Albania. Ph.D. thesis, Université de Grenoble, France, 269 pp.

Hajdas, I., Bonani, G., Moreno, P.I., Ariztegui, D. 2003. Precise radiocarbon dating of Late-Glacial cooling in mid-latitude South America. Quat. Res. 59, 70–78. 10.1016/S0033-5894(02)00017-0

Hall, B.L., Denton, G., Lowell, T., Bromley, G.R.M., Putnam, A.E. 2017a. Retreat of the Cordillera Darwin Icefield during Termination I. Geogr. Res. Lett. 43, 751–766. 10.18172/cig.3158

Hall, B.L., Borns, H.W.Jr., Bromley, G.R., Lowell, T.V. 2017b. Age of the Pineo Ridge system: Implications for behavior of the Laurentide Ice Sheet in eastern Maine, USA, during the last deglaciation. Quat. Sci. Rev. 169, 344–356. 10.1016/j.quascirev.2017.06.011

Hall, B.L., Lowell, T. V, Bromley, G.R.M., Denton, G.H., Putnam, A.E. 2019. Holocene glacier fluctuations on the northern flank of Cordillera Darwin, southernmost South America. Quat. Sci. Rev. 222, 105904. 10.1016/j.quascirev.2019.105904

Hall, B.L., Porter, C.T., Denton, G.H., Lowell, T.V., Bromley, G.R.M. 2013. Collapse of Cordillera Darwin glaciers in southernmost South America during Heinrich Stadial 1. Quat. Sci. Rev. 62, 49–55. 10.1016/j.quascirev.2012.11.026

Hall, S.R., Farber, D.L., Ramage, J.M., Rodbell, D.T., Finkel, R.C., Smith, J.A., Mark, B.G., Kassel, C. 2009. Geochronology of Quaternary glaciations from the tropical Cordillera Huayhuash, Peru. Quat. Sci. Rev. 28, 2991–3009. 10.1016/j.quascirev.2009.08.004

Hansen, B.C.S., Rodbell, D.T., Seltzer, G.O., León, B., Young, K.R., Abbott, M. 2003. Late Glacial and Holocene vegetational history from two sites in the western Cordillera of southwestern Ecuador. Palaeogeogr. Palaeoclimatol. Palaeoecol. 194, 79–108. 10.1016/S0031-0182(03)00272-4

Harrison, S., Glasser, N.F. 2011. The Pleistocene glaciations of Chile. In: Ehlers, J., Gibbard, P.L., Hughes, P.D. (eds.) Quaternary Glaciations - Extent and Chronology. A Closer Look. Elsevier, Amsterdam, 15, 739–756. 10.1016/B978-0-444-53447-7.00054-4

He, F., Shakun, J.D., Clark, P.U., Carlson, A.E., Liu, Z., Otto-Bliesner, B.L., Kutzbach, J.E. 2013. Northern Hemisphere forcing of Southern Hemisphere

climate during the last deglaciation. Nature 494(7435), 81–85. 10.1038/nature11822

Heath, S.L., Loope, H.M., Curry, B.B., Lowell, T.V. 2018. Pattern of southern Laurentide Ice Sheet margin position changes during Heinrich Stadials 2 and 1. Quat. Sci. Rev. 201, 362–379. 10.1016/j.quascirev.2018.10.019

Hein, A.S. 2009. Quaternary Glaciations in the Lago Pueyrredón Valley, Argentina. Ph.D. thesis, University of Edinburgh: Edinburgh, 236 pp.

Hein, A.S., Cogez, A., Darvill, C.M., Mendelova, M., Kaplan, M.R., Herman, F., Dunai, T.J., Norton, K., Xu, S., Christl, M., Rodés, A. 2017. Regional mid-Pleistocene glaciation in central Patagonia. Quat. Sci. Rev. 164, 77–94. 10.1016/j.quascirev.2017.03.023

Hein, A.S., Hulton, N.R., Dunai, T.J., Sugden, D.E., Kaplan, M.R., Xu, S. 2010. The chronology of the Last Glacial Maximum and deglacial events in central Argentine Patagonia. Quat. Sci. Rev. 29, 1212–1227. 10.1016/j.quascirev.2010.01.020

Heine, K. 1988. Late Quaternary glacial chronology of the Mexican volcanoes. Die Geowissenschaften 6, 197-205.

Heine, K., Heine, J.T. 1996. Late glacial climatic fluctuations in Ecuador: Glacier retreat during Younger Dryas time. Arct. Alp. Res. 28, 496–501.

Heinrich, H. 1988. Origin and consequences of cyclic ice rafting in the northeast Atlantic Ocean during the past 130,000 years. Quat. Res. 29, 143–152. 10.1016/0033-5894(88)90057-9

Helmens, K.F. 1988. Late Pleistocene glacial sequence in the area of the high plain of Bogotá (Eastern Cordillera, Colombia). Palaeogeogr. Palaeoclimatol. Palaeoecol. 67, 263–283. 10.1016/0031-0182(88)90156-3

Helmens, K.F. 2004. The Quaternary glacial record of the Colombian Andes. In: Ehlers, J., Gibbard, P.L. (eds.) Quaternary Glaciations – Extent and Chronology, Part III: South America, Asia, Africa, Australasia, Antarctica. Elsevier, Amsterdam, 115–134. 10.1016/S1571-0866(04)80117-9

Helmens, K.F. 2011. Quaternary glaciations of Colombia. In: Ehlers, J., Gibbard, P.L., Hughes, P.D. (eds.) Quaternary Glaciations – Extent and

Chronology. A Closer Look. Elsevier, Amsterdam, 15, 815–834. 10.1016/B978-0-444-53447-7.00058-1

Helmens, K.F., Barendregt, R.W., Enkin, R.J., Bakker, J., Andriessen, P.A.M. 1997a. Magnetic polarity and fission track chronology of a Late Pliocene–Pleistocene paleoclimatic proxy record in the tropical Andes. Quat. Res. 48, 15–28. 10.1006/qres.1997.1886

Helmens, K.F., Rutter, N.W., Kuhry, P. 1997b. Glacier fluctuations in the eastern Andes of Colombia (South America) during the last 45,000 radiocarbon years. Quat. Int. 38, 39–48. 10.1016/S1040-6182(96)00021-3

Hemming, S.R. 2004. Heinrich events: Massive late Pleistocene detritus layers the North Atlantic and their global climate imprint. Rev. Geophys. 42, 2003RG000128. 10.1029/2003RG000128

Henríquez, W.I., Moreno, P.I., Alloway, B.V., Villarosa, G. 2015. Vegetation and climate change, fire-regime shifts and volcanic disturbance in Chiloé Continental (43º S) during the last 10,000 years. Quat. Sci. Rev. 123, 158–167. 10.1016/j.quascirev.2015.06.017

Henríquez, W.I., Villa-Martínez, R., Vilanova, I., Pol-Holz, R.D., Moreno, P.I. 2017. The Last Glacial Termination on the eastern flank of the central Patagonian Andes (47º S). Clim. Past. 13, 879–895. 10.5194/cp-13-879-2017

Heusser, C.J. 1977. Quaternary palynology of the Pacific slope of Washington. Quat. Res. 8, 282–306. 10.1016/0033-5894(77)90073-4

Heusser, C.J. 1989. Climate and chronology of Antarctica and adjacent South America over the past 30,000 yr. Palaeogeogr. Palaeoclimatol. Palaeoecol. 76, 31–37. 10.1016/0031-0182(89)90101-6

Heusser, C.J., 1990. Ice age vegetation and climate of subtropical Chile. Palaeogeogr. Palaeoclimatol. Palaeoecol. 80, 107–127. 10.1016/0031-0182(90)90124-P

Heusser, C.J., Heusser, L.E., Lowell, T.V. 1999. Paleoecology of the southern Chilean Lake District – Isla Grande de Chiloé during middle–Late Llanquihue glaciation and deglaciation. Geogr. Ann., Ser. A, Phys. Geogr. 81A, 231–284. 10.1111/1468-0459.00058

Heyman, J., Stroeven, A.P., Harbor, J.M., Caffee, M.W. 2011. Too young or too old: Evaluating cosmogenic exposure dating based on an analysis of compiled boulder exposure ages. Earth Planet. Sci. Lett. 302, 71–80. 10.1016/j.epsl.2010.11.040

Hicock, S.R., Armstrong, J.E. 1981. Coquitlam Drift: A pre-Vashon Fraser glacial formation in the Fraser Lowland, British Columbia. Can. J. Earth Sci. 18, 1443–1451. 10.1139/e81-135

Hicock, S.R., Lian, O.B. 1995. The Sisters Creek Formation: Pleistocene sediments representing a nonglacial interval in southwestern British Columbia at about 18 ka. Can. J. Earth Sci. 32, 758–767. 10.1139/e95-065

Hicock, S.R., Hebda, R.J., Armstrong, J.E. 1982. Lag of the Fraser glacial maximum in the Pacific Northwest: Pollen and macrofossil evidence from western Fraser Lowland, B.C. Can. J. Earth Sci. 19, 2288–2296. 10.1139/e82-201

Hicock, S.R., Lian, O.B., Mathewes, R.W. 1999. 'Bond cycles' recorded in terrestrial Pleistocene sediments of southwestern British Columbia, Canada. J. Quat. Sci. 14, 443–449. 10.1002/(SICI)1099-1417(199908)14:5<443::AID-JQS459>3.0.CO;2-6

Hodell, D.A., Nicholl, J.A., Bontognali, T.R.R., Danino, S. Dorador, J., Dowdeswell, J.A., Einsle, J., Kuhlmann, H., Martrat, B., Mleneck-Vautravers, M.J., Rodríguez-Tovar, F.J., Röhl, U. 2017. Anatomy of Heinrich Layer 1 and its role in the last deglaciation. Paleoceanogr. Paleoclim. 32, 284–303. 10.1002/2016PA003028

Hodgson, D.A. 1994. Episodic ice streams and ice shelves during retreat of the northwesternmost sector of the late Wisconsinan Laurentide Ice Sheet over the central Canadian Arctic Archipelago. Boreas 23, 14–28. 10.1111/j.1502-3885.1994.tb00582.x

Hormes, A., Gjermundsen, E.F., Rasmussen, T.L. 2013. From mountain top to the deep sea – Deglaciation in 4D of the northwestern Barents Sea ice sheet. Quat. Sci. Rev. 75, 78–99. 10.1016/j.quascirev.2013.04.009

Hudson, A.M., Hatchett, B.J., Quade, J., Boyle, D.P., Bassett, S.D., Ali, G., De los Santos, M.G. 2019. North-south dipole in winter hydroclimate in the western United States during the last deglaciation. Sci. Rep. 9, 4826. 10.1038/s41598-019-41197-y

Hughes, A.L.C., Gyllencreutz, R., Lohne, Ø.S., Mangerud, J., Svendsen, J.I. 2016. The last Eurasian ice sheets - A chronological database and time-slice reconstruction, DATED-1. Boreas 45, 1–45. 10.1111/bor.12142

Hughes, P.D., Fink, D., Rodés, Á., Fenton, C.R., Fujioka, T. 2018. Timing of Pleistocene glaciations in the High Atlas, Morocco: New ^{10}Be and ^{36}Cl exposure ages. Quat. Sci. Rev. 180, 193–213. 10.1016/j.quascirev.2017.11.015

Hughes, P.D., Gibbard, P.L., Ehlers, J. 2013. Timing of glaciation during the last glacial cycle: Evaluating the concept of a global 'Last Glacial Maximum' (LGM). Earth-Sci. Rev. 125, 171–198. 10.1016/j.earscirev.2013.07.003

Hughes, P.D., Glasser, N.F., Fink, D. 2016. Rapid thinning of the Welsh Ice Cap at 20-19 ka based on ^{10}Be ages. Quat. Res. 85, 107–117. 10.1016/j.yqres.2015.11.003

Imbrie, J., Berger, A., Boyle, E.A., Clemens, S.C., Duffy, A., Howard, W.R., Kukla, G., Kutzbach, J., Martinson, D.G., McIntyre, A., Mix, A.C., Molfino, B., Morley, J.J., Peterson, L.C., Pisias, N.G., Prell, W.L., Raymo, M.E., Shackleton, N.J., Toggweiler, J.R. 1993. On the structure and origin of major glaciation cycles. Paleoceanogr. Paleoclim. 8, 699–735. 10.1029/93PA02751

Ivy-Ochs, S. 2015. Glacier variations in the European Alps at the end of the last glaciation. Geogr. Res. Lett. 41, 295–315. 10.18172/cig.2750

Jakobsson, M., Pearce, C., Cronin, T.M., Backman, J., Anderson, L.G., Barrientos, N., Björk, G., Coxall, H., de Boer, A., Mayer, L.A., Mörth, C.-M., Nilsson, J., Rattray, J.E., Stranne, C., Semiletov, I., O'Regan, M. 2017. Post-glacial flooding of the Bering Land Bridge dated to 11 cal ka BP based on new geophysical and sediment records. Clim. Past. 13, 991–1005. 10.5194/cp-13-991-2017

Jara, I.A., Moreno, P.I. 2014. Climatic and disturbance influences on the temperate rainforests of northwestern Patagonia (40º S) since ~14,500 yr BP. Quat. Sci. Rev. 90, 217–228. 10.1016/j.quascirev.2014.01.024

Jennings, A.E., Tedesco, K.A., Andrews, J.T., Kirby, M.E. 1996. Shelf erosion and glacial ice proximity in the Labrador Sea during and after Heinrich events (H-3 or 4 to H-0) as shown by foraminifera. In: Andrews, J.T., Austin, W.E.N., Bergstrom, H., Jennings, A.E. (eds.) Palaeoceanography of the North Atlantic Margins. Geol. Soc. London Spec. Publ. 111, 29–49. 10.1144/GSL.SP.1996.111.01.04

Jenny, B., Kammer, K., Ammann, C. 1996. Climate Change in den Trockenen Anden. Universität Bern, Verlag des Geographischen Institutes, Bern, Switzerland.

Jiménez-Moreno, G., Anderson, R.S., Atudorei, V., Toney, J.L. 2011. A high-resolution record of climate, vegetation, and fire in the mixed conifer forest of northern Colorado, USA. Geol. Soc. Am. Bull. 123, 240–254. 10.1130/B30240.1

Jomelli V., Chapron E., Favier V., Rinterknecht V., Braucher R., Tournier N., Gascoin S., Marti R., Galop D., Binet S., Deschamps-Berger C., Tissoux H., ASTER Team. 2020. Glacier fluctuations during the Late Glacial and Holocene on the Ariege valley, northern slope of the Pyrenees and reconstructed climatic conditions. Mediterranean. Geosci. Rev. (in revision).

Jomelli, V., Favier, V., Brunstein, D., He, F., Liu, Z. 2016. High altitude temperature changes in the tropical Andes over the last 15000 years estimated from a glaciological model. In: Doyle, N. (ed.) Glaciers: Formation, Climate Change and Their Effects. Nova Science, USA, pp. 53–70.

Jomelli, V., Favier, V., Vuille, M., Braucher, R., Martin, L., Blard, P.H., Colose, C., Brunstein, D., He, F., Khodri, M., Bourles, D.L., Leanni, L., Rinterknecht, V., Grancher, D., Francou, B., Ceballos, J.L., Fonseca, H., Liu, Z., Otto-Bliesner, B.L. 2014. A major advance of tropical Andean glaciers during the Antarctic Cold Reversal. Nature 513, 224–228. 10.1038/nature13546

Jomelli, V., Khodri, M., Favier, V., Brunstein, D., Ledru, M-P., Wagnon, P., Blard, P-H., Sicart, J-E., Braucher, R., Grancher, D., Bourlès, D., Braconnot, P.,

Vuille, M. 2011. Irregular tropical glacier retreat over the Holocene driven by progressive warming. Nature 474, 196–199. 10.1038/nature10150

Jomelli, V., Martin, L., Blard, P.H., Favier, V., Vuille, M., Ceballos, J.L. 2017. Revisiting the Andean tropical glacier behavior during the Antarctic Cold Reversal. Geogr. Res. Lett. 43, 629–648. 10.18172/cig.3201

Jomelli, V., Schimmelpfennig, I., Favier, V., Mokadem, F., Landais, A., Rinterknecht, V., Brunstein, D., Verfaillie, D., Legentil, C., Aster Team. 2018. Glacier extent in sub-Antarctic Kerguelen Archipelago from MIS 3 period: Evidence from ^{36}Cl dating. Quat. Sci. Rev. 183, 110–123. 10.1016/j.quascirev.2018.01.008

Kaiser, J., Schefuß, E., Lamy, F., Mohtadi, M., Hebbeln, D. 2008. Glacial to Holocene changes in sea surface temperature and coastal vegetation in north central Chile: High versus low latitude forcing. Quat. Sci. Rev. 27, 2064–2075. 10.1016/j.quascirev.2008.08.025

Kanner, L.C., Burns, S.J., Cheng, H., Edwards, R.L. 2012. High-latitude forcing of the South American summer monsoon during the last glacial. Science 335(6068), 570–573. 10.1126/science.1213397

Kaplan, M.R., Ackert, R.P. Jr., Singer, B.S., Douglass, D.C., Kurz, M.D. 2004. Cosmogenic nuclide chronology of millennial-scale glacial advances during O-isotope stage 2 in Patagonia. Geol. Soc. Am. Bull. 116, 308–321. 10.1130/B25178.1

Kaplan, M.R., Coronato, A., Hulton, N.R.J., Rabassa, J.O., Kubik, P.W., Freeman, S.P.H.T. 2007. Cosmogenic nuclide measurements in southernmost South America and implications for landscape change. Geomorphology 87, 284–301. 10.1016/j.geomorph.2006.10.005

Kaplan, M.R., Fogwill, C.J., Sugden, D.E., Hulton, N.R.J., Kubik, P.W., Freeman, S.P.H.T. 2008. Southern Patagonian glacial chronology for the Last Glacial period and implications for Southern Ocean climate. Quat. Sci. Rev. 27, 284–294. 10.1016/j.quascirev.2007.09.013

Kaplan, M.R., Schaefer, J.M., Strelin, J.A., Denton, G.H., Anderson, R.F., Vandergoes, M.J., Finkel, R.C., Schwartz, R., Travis, S.G., Garcia, J.L., Martini,

M.A., Nielsen, S.H.H. 2016. Patagonian and southern South Atlantic view of Holocene climate. Quat. Sci. Rev. 141, 112–125. 10.1016/j.quascirev.2016.03.014

Kaplan, M.R., Strelin, J.A., Schaefer, J.M., Denton, G.H., Finkel, R. C., Schwartz, R., Putnam, A.E., Vandergoes, M.J., Goehring, B.M., Travis, S.G. 2011. In-situ cosmogenic ^{10}Be production rate at Lago Argentino, Patagonia: Implications for Late-Glacial climate chronology. Earth Planet. Sci. Lett. 309, 21–32. 10.1016/j.epsl.2011.06.018

Kaufman, D.S., Anderson, R.S., Hu, F.S., Berg, E., Werner, A. 2010. Evidence for a variable and wet Younger Dryas in southern Alaska. Quat. Sci. Rev. 29, 1445–1452. 10.1016/j.quascirev.2010.02.025

Kaufman, D.S., Axford, Y.L., Henderson, A.C.G., McKay, N.P., Oswald, W.W., Saenger, C., Anderson, R.S., Bailey, H.L., Clegg, B., Gajewski, K., Hu, F.S., Jones, M.C., Massa, C., Routson, C.C., Werner, A., Wooller, M.J., Yu, Z. 2016. Holocene climate changes in eastern Beringia (NW North America) – A systematic review of multi-proxy evidence. Quat. Sci. Rev. 147, 312–339. 10.1016/j.quascirev.2015.10.021

Kaufman, D.S., Hu, F.S., Briner, J.P., Werner, A., Finney, B.P., Gregory-Eaves, I. 2003. A ~33,000 year record of environmental change from Arolik Lake, Ahklun Mountains, Alaska, USA. J. Paleolimnolo. 30, 343–361. 10.1023/B:JOPL.0000007219.15604.27

Kaufman, D.S., Jensen, B.J.L., Reyes, A.V., Schiff, C.J., Froese, D.G., Pearce, N.J.G. 2012. Late Quaternary tephrostratigraphy, Ahklun Mountains, SW Alaska. J. Quat. Sci. 27, 344–359. 10.1002/jqs.1552

Kaufman, D.S., Porter, S.C., Gillespie, A.R. 2004. Quaternary alpine glaciation in Alaska, the Pacific Northwest, Sierra Nevada and Hawaii. In: Gillespie, A.R., Porter, S.C., Atwater, B.F. (eds.) The Quaternary Period in the United States. Elsevier, Amsterdam 1, 77–103. 10.1016/S1571-0866(03)01005-4

Kawamura, K. Parrenin, F., Lisiecki, L., Uemura, R., Vimeux, F., Severinghaus, J.P., Hutterli, M.A., Nakazawa, T., Aoki, S., Jouzel, J., Raymo, M.E., Matsumoto, K., Nakata, H., Motoyama,H., Fujita,S., Goto-Azuma, K., Fujii, Y., Watanabe, O. 2007. Northern Hemisphere forcing of climatic cycles in

Antarctica over the past 360,000 years. Nature 448, 912–916. 10.1038/nature06015

Keigwin, L.D., Klotsko, S., Zhao, N., Reilly, B., Giosan, L., Driscoll, N.W. 2018. Deglacial floods in the Beaufort Sea preceded Younger Dryas cooling. Nature Geosci. 11, 599–604. 10.1038/s41561-018-0169-6

Kelly, M.A., Lowell, T.V., Applegate, P.J., Phillips, F.M., Schaefer, J.M., Smith, C.A., Kim, H., Leonard, K.L., Hudson, A.M. 2015. A locally calibrated, late glacial ^{10}Be production rate from a low-latitude, high-altitude site in the Peruvian Andes. Quat. Geochronol. 26, 70–85. 10.1016/j.quageo.2013.10.007

Kelly, M.A., Lowell, T.V., Applegate, P.J., Smith, C.A., Phillips, F.M., Hudson, A.M. 2012. Late glacial fluctuations of Quelccaya Ice Cap, southeastern Peru. Geology 40, 991–994. 10.1130/G33430.1

Kennedy, K.E., Froese, D.G., Zazula, G.D., Lauriol, B. 2010. Last Glacial Maximum age for the northwest Laurentide maximum from the Eagle River spillway and delta complex, northern Yukon. Quat. Sci. Rev. 29, 1288–1300. 10.1016/j.quascirev.2010.02.015

Kirkbride, M.P., Winkler, S. 2012. Correlation of Late Quaternary moraines: Impact of climate variability, glacier response, and chronological resolution. Quat. Sci. Rev. 46, 1–29. 10.1016/j.quascirev.2012.04.002

Koester, A.J., Shakun, J.D., Bierman, P.R., Davis, P.T., Corbett, L.B., Braun, D., Zimmerman, S.R. 2017. Rapid thinning of the Laurentide Ice Sheet in coastal Maine, USA, during late Heinrich Stadial 1. Quat. Sci. Rev. 163, 180–192. 10.1016/j.quascirev.2017.03.005

Koffman, T.N., Schaefer, J.M., Putnam, A.E., Denton, G.H., Barrell, D.J., Rowan, A.V., Finkel, R.C., Rood, D.H., Schwartz, R., Plummer, M.A., Brocklehurst, S.H. 2017. A beryllium-10 chronology of Late-glacial moraines in the upper Rakaia valley, Southern Alps, New Zealand supports Southern Hemisphere warming during the Younger Dryas. Quat. Sci. Rev. 170, 14–25. 10.1016/j.quascirev.2017.06.012

Kokorowski, H.D., Anderson, P.M., Mock, C.J., Lozhkin, A.V. 2008. A re-evaluation and spatial analysis of evidence for a Younger Dryas climatic

reversal in Beringia. Quat. Sci. Rev. 27, 1710–1722. 10.1016/j.quascirev.2008.06.010

Kopczynski, S.E., Kelley, S.E., Lowell, T.V., Evenson, E.B., Applegate, P.J. 2017. Latest Pleistocene advance and collapse of the Matanuska-Knik glacier system, Anchorage lowland, southern Alaska. Quat. Sci. Rev. 156, 121–134. 10.1016/j.quascirev.2016.11.026

Kovanen, D.J. 2002. Morphologic and stratigraphic evidence for Allerød and Younger Dryas age glacier fluctuations of the Cordilleran Ice Sheet, British Columbia, Canada and northwest Washington, USA. Boreas 31, 163–184. 10.1111/j.1502-3885.2002.tb01064.x

Kovanen, D.J., Easterbrook, D.J. 2001. Late Pleistocene, post-Vashon, alpine glaciation of the Nooksack drainage, North Cascades, Washington. Geol. Soc. Am. Bull. 113, 247–288. 10.1130/0016-7606(2001)113<0274:LPPVAG>2.0.CO;2

Kovanen, D.J., Easterbrook, D.J. 2002. Timing and extent of Allerod and Younger Dryas age (ca. 12,500-10,000 ^{14}C yr B.P.) oscillations of the Cordilleran ice sheet in the Fraser Lowland, western North America. Quat. Res. 57, 208–224. 10.1006/qres.2001.2307

Kull, C., Grosjean, M. 2000. Late Pleistocene climate conditions in the north Chilean Andes drawn from a climate-glacier model. J. Glaciol. 46, 622–632. 10.3189/172756500781832611

Kull, C., Grosjean, M., Veit, H. 2002. Modeling modern and Late Pleistocene glacio-climatological conditions in the north Chilean Andes (29-30º). Clim. Change. 52, 359–381. 10.1023/A:1013746917257

Kurek, J., Cwynar, L.C., Ager, T.A., Abbott, M.B., Edwards, M.E. 2009. Late Quaternary paleoclimate of western Alaska inferred from fossil chironomids and its relation to vegetation histories. Quat. Sci. Rev. 28, 799–811. 10.1016/j.quascirev.2008.12.001

Kutzbach, J.E. 1987. Model simulations of the climatic patterns during the deglaciation of North America. In: Ruddiman, W.F., Wright, H.E. (eds.) North

America and Adjacent Oceans during the Last Deglaciation. Geol. Soc. Am., Geol. North Am. K-3, 425–446. 10.1130/DNAG-GNA-K3.425

La Frenierre, J., Huh, K.I., Mark, B.G. 2011. Ecuador, Peru and Bolivia. In: Ehlers, J., Gibbard, P.L., Hughes, P.D. (eds.) Quaternary Glaciations – Extent and Chronology. Elsevier, Amsterdam, 15, 773–802. 10.1016/B978-0-444-53447-7.00056-8

Laabs, B.J.C., Licciardi, J.M., Leonard, E.M., Munroe, J.S. (in preparation) Cosmogenic ^{10}Be chronology of latest Pleistocene moraines in the western U.S.: Reconsidering production rates and inferences of climate change. Quat. Sci. Rev. (In revision)

Laabs, B.J.C., Refsnider, K.A., Munroe, J.S., Mickelson, D.M., Applegate, P.M., Singer, B.S., Caffee, M.W. 2009. Latest Pleistocene glacial chronology of the Uinta Mountains: Support for moisture-driven asynchrony of the last deglaciation. Quat. Sci. Rev. 28, 1171–1187. 10.1016/j.quascirev.2008.12.012

Lacelle, D., Lauroil, B., Zazula, G., Ghaleb, B., Utting, N., Clark, I.D. 2013. Timing of advance and basal condition of the Laurentide Ice Sheet during the Last Glacial Maximum in the Richardson Mountains, NWT. Quat. Res. 80, 274–283. 10.1016/j.yqres.2013.06.001

Lachniet, M.S., Seltzer, G.O. 2002. Late Quaternary glaciation of Costa Rica. Geol. Soc. Am. Bull. 114, 547–558. 10.1130/0016-7606(2002)114<0547:LQGOCR>2.0.CO;2

Lachniet, M.S., Vazquez-Selem, L. 2005. Last glacial maximum equilibrium line altitudes in the circum-Caribbean (Mexico, Guatemala, Costa Rica, Colombia, and Venezuela). Quat. Int. 138, 129–144. 10.1016/j.quaint.2005.02.010

Lachniet, M.S., Asmerom, Y., Bernal, J.P., Polyak, V.J., Vazquez-Selem, L. 2013. Orbital pacing and ocean circulation-induced collapses of the Mesoamerican monsoon over the past 22,000 yr. Proc. Natl. Acad. Sci. 110, 9255–9260. 10.1073/pnas.1222804110

Lakeman, T.R., Clague, J.J., Menounos, B. 2008. Advance of alpine glaciers during final retreat of the Cordilleran ice sheet in the Finlay River area, northern British Columbia, Canada. Quat. Res. 69, 188–200. 10.1016/j.yqres.2008.01.002

Lakeman, T.R., Pieńkowski, A.J., Nixon, F.C., Furze, M.F.A., Blasco, S., Andrews, J.T., King, E.L. 2018. Collapse of a marine-based ice stream during the early Younger Dryas chronozone, western Canadian Arctic. Geology 46, 212–214. 10.1130/G39665.1

Lal, D. 1991. Cosmic ray labeling of erosion surfaces: In situ nuclide production rates and erosion rates. Earth Planet. Sci. Lett. 104, 424–439. 10.1016/0012-821X(91)90220-C

Lambeck, K., Purcell, A., Zhao, S. 2017. The North American Late Wisconsin ice sheet and mantle viscosity from glacial rebound analyses. Quat. Sci. Rev. 158, 172–210. 10.1016/j.quascirev.2016.11.033

Lambeck, K., Rouby, H., Purcell, A., Sun, Y., Sambridge, M. 2014. Sea level and global ice volumes from the Last Glacial Maximum to the Holocene. Proc. Natl. Acad. Sci. 111, 15296–15303. 10.1073/pnas.1411762111

Lamy, F., Hebblen, D., Wefer, G. 1999. High-resolution marine record of climate change in mid-latitude Chile during the last 28,000 years based on terrigenous sediment parameters. Quat. Res. 51, 83–93. 10.1006/qres.1998.2010

Landais, A., Masson-Delmotte, V., Stenni, B., Selmo, E., Roche, D. M., Jouzel, J., Lambert, F., Guillevic, M., Bazin, L., Arzel, O., Vinther, B., Gkinis, V., Popp, T. 2015. A review of the bipolar see-saw from synchronized and high resolution ice core water stable isotope records from Greenland and East Antarctica. Quat. Sci. Rev. 114, 18–32. 10.1016/j.quascirev.2015.01.031

Larsen, D.J., Finkenbinder, M.S., Abbott, M.B., Ofstun, A.R. 2016. Deglaciation and postglacial environmental changes in the Teton Mountain Range recorded at Jenny Lake, Grand Teton National Park, WY. Quat. Sci. Rev. 138, 62–75. 10.1016/j.quascirev.2016.02.024

Lea, D.W., Pak, D.K., Peterson, L.C., Hughen, K.A. 2003. Synchroneity of tropical and high-latitude Atlantic temperatures over the Last Glacial Termination. Science 301(5638), 1361–1364. 10.1126/science.1088470

Lee, S., Chiang, J.C.H., Matsumoto, K., Tokos, K.S. 2011. Southern Ocean wind response to North Atlantic cooling and the rise in atmospheric CO_2: Modeling perspective and paleoceanographic implications. Paleoceanography 26, PA1214. 10.1029/2010PA002004

Leonard, E.M. 1989. Climatic change in the Colorado Rocky Mountains: Estimates based on modern climate at late Pleistocene equilibrium lines. Arct. Alp. Res. 21, 245–255. 10.1080/00040851.1989.12002736

Leonard, E.M. 2007. Modeled patterns of Late Pleistocene glacier inception and growth in the southern and central Rocky Mountains, USA: Sensitivity to climate change and paleoclimatic implications. Quat. Sci. Rev. 26, 2152–2166. 10.1016/j.quascirev.2007.02.013

Leonard, E.M., Laabs, B.J.B., Schweinsberg, A.D., Russell, C.M., Briner, J.P., Young, N.E. 2017a. Deglaciation of the Colorado Rocky Mountains following the Last Glacial Maximum. Geogr. Res. Lett. 43, 497–526. 10.18172/cig.3234

Leonard, E.M., Laabs, B.J.C., Kroner, R.K., Plummer, M.A., Brugger, K.A., Refsnider, K.A., Spiess, V.M., Caffee, M.W. 2017b. Late Pleistocene glaciation and deglaciation in the Crestone Peaks area, Colorado Sangre de Cristo Range – Chronology and paleoclimate. Quat. Sci. Rev. 158, 127–144. 10.1016/j.quascirev.2016.11.024

Leydet, D.J., Carlson, A.E., Teller, J.T., Breckenridge, A., Barth, A.M., Ullman, D.J., Sinclair, G., Milne, G.A., Cuzzone, J.K., Caffee, M.W. 2018. Opening of glacial Lake Agassiz's eastern outlets by the start of the Younger Dryas cold period. Geology 46, 155–158. 10.1130/G39501.1

Liakka, J., Lofverstrom, M. 2018. Arctic warming induced by the Laurentide Ice Sheet topography. Clim. Past. 14, 887–900. 10.5194/cp-14-887-2018

Liakka, J., Löfverström, M., Colleoni, F. 2016. The impact of the North American glacial topography on the evolution of the Eurasian ice sheet over the last glacial cycle. Clim. Past. 12, 1225–1241. 10.5194/cp-12-1225-2016

Lian, O.B., Mathewes, R.W., Hicock, S.R. 2001. Paleo-environmental reconstruction of the Port Moody interstade, a nonglacial interval in

southwestern British Columbia at about 18,000 ^{14}C yr B.P. Can. J. Earth. Sci. 38, 943–952. 10.1139/e00-114

Licciardi, J.M., Pierce, K.L. 2008. Cosmogenic exposure-age chronologies of Pinedale and Bull Lake glaciations in greater Yellowstone and the Teton Range, USA. Quat. Sci. Rev. 27, 814–831. 10.1016/j.quascirev.2007.12.005

Licciardi, J.M., Pierce, K.L. 2018. History and dynamics of the greater Yellowstone glacial system during the last two glaciations. Quat. Sci. Rev. 200, 1–33. 10.1016/j.quascirev.2018.08.027

Licciardi, J.M., Clark, P.U., Brook, E.J., Elmore, D., Sharma, P. 2004. Variable responses of western US glaciers during the last deglaciation. Geology 32, 81–84. 10.1130/G19868.1

Licciardi, J.M., Clark, P.U., Brook, E.J., Pierce, K.L., Kurz, M.D., Elmore, D., Sharma, P. 2001. Cosmogenic ^{3}He and ^{10}Be chronologies of the late Pinedale northern Yellowstone ice cap, Montana, USA. Geology 29, 1095–1098. 10.1130/0091-7613(2001)029<1095:CHABCO>2.0.CO;2

Licciardi, J.M., Schaefer, J.M., Taggart, J.R., Lund, D.C. 2009. Holocene glacier fluctuations in the Peruvian Andes indicate northern climate linkages. Science 325, 1677–1679. 10.1126/science.1175010

Liu, A., Otto-Bliesner, B.L., He, F., Brady, E.C., Tomas, R., Clark, P.U., Carlson, A.E., Lynch-Stieglitz, J., Curry, W., Brook, E., Erickson, D., Jacob, R., Kutzbach, J., Cheng, J. 2009. Transient simulation of last deglaciation with a new mechanism for Bølling-Allerød warming. Science 325, 310–314. 10.1126/science.1171041

Lowell, T.V., Heusser, C.J., Andersen, B.G., Moreno, P.I., Hauser, A., Heusser, L.E., Schluchter, C., Marchant, D.R., Denton, G.H. 1995. Interhemispheric correlation of Late Pleistocene glacial events. Science 269, 1541–1549. 10.1126/science.269.5230.1541

Löfverström, M., Liakka, J. 2016. On the limited ice intrusion in Alaska at the LGM. Geophys. Res. Lett. 43, 11,030–11,038. 10.1002/2016GL071012

Lowdon, J.A, Blake, W., Jr. 1980. Geological Survey of Canada Radiocarbon Dates XX. Geol. Surv. Can. Pap. 80-7, 28 pp. 10.4095/119073

Lowe, J.J., Hoek, W.Z., INTIMATE group. 2001. Inter-regional correlation of palaeoclimatic records for the Last Glacial–Interglacial transition: A protocol for improved precision recommended by the INTIMATE project group. Quat. Sci. Rev. 20, 1175–1187. 10.1016/S0277-3791(00)00183-9

Luna, L.V., Bookhagen, B., Niedermann, S., Rugel, G., Scharf, A., Merchel, S. 2018. Glacial chronology and production rate cross-calibration of five cosmogenic nuclide and mineral systems from the southern central Andean Plateau. Earth Planet. Sci. Lett. 500, 242–253. 10.1016/j.epsl.2018.07.034

Mahaney, W.C. 2011. Quaternary glacial chronology of Mount Kenya massif. In: Ehlers, J., Gibbard, P.L., Hughes, P.D. (eds.) Quaternary Glaciations – Extent and Chronology. A Closer Look. Elsevier, Amsterdam, 15, 1075–1080. 10.1016/B978-0-444-53447-7.00077-5

Mahaney, W.C., Milner, M.W., Kalm, V. Dirszowsky, R.W., Hancock, R.G.V., Beukens, R.P. 2008. Evidence for a Younger Dryas glacial advance in the Andes of northwestern Venezuela. Geomorphology 96, 199–211. 10.1016/j.geomorph.2007.08.002

Mahaney, W.C., Milner, M.W., Voros, J., Kalm, V., Hütt, G., Bezada, M., Hancock, R.G.V., Aufreiter, S. 2000. Stratotype for the Merida Glaciation at Pueblo Llano in the northern Venezuelan Andes. J. South Am. Earth. Sci. 13, 761–774. 10.1016/S0895-9811(00)00054-7

Makos, M. 2015. Deglaciation of the high Tatra Mountains. Geogr. Res. Lett. 41, 317–335. 10.18172/cig.vol41iss2

Makos, M., Rinterknecht, V., Braucher, R., Tołoczko-Pasek, A., ASTER Team. 2018. Last Glacial Maximum and Lateglacial in the Polish high Tatra Mountains – Revised deglaciation chronology based on the ^{10}Be exposure age dating. Quat. Sci. Rev. 187, 130–156. 10.1016/j.quascirev.2018.03.006

Maldonado, A., Betancourt, J.L., Latorre, C., Villagran, C. 2005. Pollen analyses from a 50 000-yr rodent midden series in the southern Atacama Desert (25° 30′ S). J. Quat. Sci. 20, 493–507. 10.1002/jqs.936

Mangerud, J., Aarseth, I., Hughes, A.L., Lohne, Ø.S., Skår, K., Sønstegaard, E., Svendsen, J.I. 2016. A major re-growth of the Scandinavian Ice Sheet in western

Norway during Allerød-Younger Dryas. Quat. Sci. Rev. 132, 175–205. 10.1016/j.quascirev.2015.11.013

Mangerud, J., Briner, J.P., Goslar, T., Svendsen, J.I. 2017. The Bølling-age Blomvåg Beds, western Norway: Implications for the Older Dryas glacial readvance and the age of the deglaciation. Boreas 46, 162–184. 10.1111/bor.12208

Manley, W.F., Kaufman, D.S., Briner, J.P. 2001. Pleistocene glacial history of the southern Ahklun Mountains, southwestern Alaska: Soil-development, morphometric, and radiocarbon constraints. Quat. Sci. Rev. 20, 353–370. 10.1016/S0277-3791(00)00111-6

Marcott, S.A., Clark, P.U., Shakun, J.D., Brook, E.J., Davis, P.T., Caffee, M.W. 2019. ^{10}Be age constraints on latest Pleistocene and Holocene cirque glaciation across the western United States. Clim. Atmos. Sci. 2(5). 10.1038/s41612-019-0062-z

Marcott, S.A., Shakun, J.D., Clark, P.U., Mix, A.C. 2013. A reconstruction of regional and global temperature for the past 11,300 years. Science 339(6124), 1198–1201. 10.1126/science.1228026

Margold, M., Stokes, C.R., Clark, C.D. 2015. Ice streams in the Laurentide Ice Sheet: Identification, characteristics and comparison to modern ice sheets. Earth-Sci. Rev. 143, 117–146. 10.1016/j.earscirev.2015.01.011

Margold, M., Stokes, C.R., Clark, C.D. 2018. Reconciling records of ice streaming and ice margin retreat to produce a palaeogeographic reconstruction of the deglaciation of the Laurentide Ice Sheet. Quat. Sci. Rev. 189, 1–30. 10.1016/j.quascirev.2018.03.013

Mark, B.G., Helmens, K.F. 2005. Reconstruction of glacier equilibrium-line altitudes for the Last Glacial Maximum on the High Plain of Bogotá, Eastern Cordillera, Colombia: Climatic and topographic implications. J. Quat. Sci. 20 (7-8), 789–800. 10.1002/jqs.974

Mark, B.G., Seltzer, G.O. 2005. Evaluation of recent glacier recession in the Cordillera Blanca, Peru (AD 1962-1999): Spatial distribution of mass loss and

climatic forcing. Quat. Sci. Rev. 24, 2265–2280. 10.1016/j.quascirev.2005.01.003

Mark, B.G., Harrison, S.P., Spessa, A., New, M., Evans, D.J.E., Helmens, K.F. 2005. Tropical snowline changes at the LGM: A global assessment. Quat. Int. 138-139, 168–201. 10.1016/j.quaint.2005.02.012

Mark, B.G., Stansell, N., Zeballos, G. 2017. The last deglaciation of Peru and Bolivia. Geogr. Res. Lett. 43, 591–628. 10.18172/cig.3265

Marks, L., Makos, M., Szymanek, M., Woronko, B., Dzierżek, J., Majecka, A. 2019. Late Pleistocene climate of Poland in the mid-European context. Quat. Int. 504, 24–39. 10.1016/j.quaint.2018.01.024

Marrero, S.M., Phillips, F.M., Caffee, M.W., Gosse, J.C. 2016. CRONUS – Earth cosmogenic ^{36}Cl calibration. Quat. Geochronol. 31, 199–219. 10.1016/j.quageo.2015.10.002

Martin, J.R.V., Davies B.J., Thorndycraft, V.R. 2019. Glacier dynamics during a phase of Late Quaternary warming in Patagonia reconstructed from sediment-landform associations. Geomorphology 337, 111–133. 10.1016/j.geomorph.2019.03.007

Martin, L.C, Blard, P.-H., Balco, G., Lavé, J., Delunel, R., Lifton, N., Laurent, V. 2017. The CREp program and the ICE-D production rate calibration database: A fully parameterizable and updated online tool to compute cosmic ray exposure ages. Quat. Geochronol. 38, 25–49. 10.1016/j.quageo.2016.11.006

Martin, L.C., Blard, P.H., Lavé, J., Braucher, R., Lupker, M., Condom, T., Charreau, J., Mariotti, V., ASTER Team, Davy, E. 2015. In situ cosmogenic ^{10}Be production rate in the high tropical Andes. Quat. Geochronol. 30, 54–68. 10.1016/j.quageo.2015.06.012

Martin, L.C., Blard, P.H., Lavé, J., Condom, T., Prémaillon, M., Jomelli, V., Brunstein, D., Lupker, M., Charreau, J., Mariotti, V., Tibari, B., ASTER Team, Davy, E. 2018. Lake Tauca highstand (Heinrich Stadial 1a) driven by a southward shift of the Bolivian High. Sci. Adv. 4(8), eaar2514. 10.1126/sciadv.aar2514

Martini, M.A., Kaplan, M.R., Strelin, J.A., Astini, R.A., Schaefer, J.M., Caffee, M.W., Schwartz, R. 2017a. Late Pleistocene glacial fluctuations in Cordillera Oriental, subtropical Andes. Quat. Sci. Rev. 171, 245–259. 10.1016/j.quascirev.2017.06.033

Martini, M.A., Strelin, J.A., Flores, E., Astini, R.A., Kaplan, M.R., 2017b. Recent climate warming and the Varas rock glacier activity, Cordillera Oriental, Central Andes of Argentina. Geol. Res. J. 14, 67–79. 10.1016/j.grj.2017.08.002

Martini, M.A., Strelin, J.A., Astini, R.A., 2013. Inventario y caracterización morfoclimática de los glaciares de roca en la Cordillera Oriental Argentina (entre 22° y 25° S). Rev. Mex. Ciencias Geol. 30, 569–581.

May, J.H., Zech, J., Zech, R., Preusser, F., Argollo, J., Kubik, P.W., Veit, H. 2011. Reconstruction of a complex late Quaternary glacial landscape in the Cordillera de Cochabamba (Bolivia) based on a morphostratigraphic and multiple dating approach. Quat. Res. 76, 106–118. 10.1016/j.yqres.2011.05.003

McCulloch, R.D., Fogwill, C., Sugden, D., Bentley, M.J., Kubik, P. 2005a. Chronology of the last glaciation in the central Strait of Magellan and Bahía Inútil, southernmost South America. Geogr. Ann., Ser. A, Phys. Geogr. 87A, 289–312. 10.1111/j.0435-3676.2005.00260.x

McCulloch, R.D., Bentley, M.J., Tipping, R.M., Clapperton, C.M. 2005b. Evidence for late-glacial ice dammed lakes in the central Strait of Magellan and Bahía Inútil, southernmost South America. Geogr. Ann., Ser. A, Phys. Geogr. 87A, 335–362. 10.1111/j.0435-3676.2005.00262.x

McGlue, M.M., Cohen, A.S., Ellis, G.S., Kowler, A.L. 2013. Late Quaternary stratigraphy, sedimentology and geochemistry of an underfilled lake basin in the Puna Plateau (northwest Argentina). Basin Res. 25, 638–658. 10.1111/bre.12025

McManus, J.F., Francois, R., Gherardi, J.M., Keigwin, L.D., Brown-Leger, S. 2004. Collapse and rapid resumption of Atlantic meridional circulation linked to deglacial climate changes. Nature 428, 834–837. 10.1038/nature02494

Meissner, K.J. 2007. Younger Dryas: A data to model comparison to constrain the strength of the overturning circulation. Geophys. Res. Lett. 34, L21705. 10.1029/2007GL031304

Mendelova, M., Hein, A.S., McCulloch, R., Davies, B. 2017. The Last Glacial Maximum and deglaciation in central Patagonia, 44°S–49°S. Geogr. Res. Lett. 43, 719–750. 10.18172/cig.3263

Menounos, B., Reasoner, M.A. 1997. Evidence for cirque glaciation in the Colorado Front Range during the Younger Dryas Chronozone. Quat. Res. 48, 38–47. 10.1006/qres.1997.1902

Menounos, B., Clague, J.J., Osborn, G., Thompson Davis, P., Ponce, F., Goehring, B., Maurer, M., Rabassa, R., Coronato, A., Marr, R. 2013. Latest Pleistocene and Holocene glacier fluctuations in southernmost Tierra del Fuego, Argentina. Quat. Sci. Rev. 77, 70–79. 10.1016/j.quascirev.2013.07.008

Menounos, B.M., Goehring, B.M., Osborn, G., Margold, M., Ward, B., Bond, J., Clarke, G.K.C., Clague, J.J., Lakeman, T., Koch, J., Caffee, M.W., Gosse, J., Stroeven, A.P., Seguinot, J., Heman, J. 2017. Cordilleran Ice Sheet mass loss preceded climate reversals near the Pleistocene Transition. Science 358, 781–784. 10.1126/science.aan3001

Mercer, J.H. 1972. Chilean glacial chronology 20,000 to 11,000 carbon-14 years ago: Some global comparisons. Science 172, 1118–1120. 10.1126/science.176.4039.1118

Mercer, J.H. 1976. Glacial history of southernmost South America. Quaternary Research 6, 125–166. 10.1016/0033-5894(76)90047-8

Mercer, J.H. 1984. Late Cainozoic glacial variations in South America south of the equator. In: Vogel, J.C. (ed.) Late Cainozoic Palaeoclimates of the Southern Hemisphere. Proc. SASQUA Symp., Swaziland, pp. 45–58.

Mercer, J.H., Palacios, O. 1977. Radiocarbon dating of the last glaciation in Peru. Geology 5, 600–604. 10.1130/0091-7613(1977)5<600:RDOTLG>2.0.CO;2

Meyer, H., Schirrmeister, L., Yoshikawa, K., Opel, T., Wetterich, S., Hubberten, H.-W., Brown, J. 2010. Permafrost evidence for severe winter cooling during the Younger Dryas in northern Alaska. Geophys. Res. Lett. 37, L03501. 10.1029/2009GL041013

Miller, G.H., Kaufman, D.S. 1990. Rapid fluctuations of the Laurentide Ice Sheet at the mouth of Hudson Strait: New evidence for ocean/ice-sheet interactions as a control on the Younger Dryas. Paleoceanography 5, 907–919. 10.1029/PA005i006p00907

Miller, G.H., Mode, W.N., Wolfe, A.P., Sauer, P.E., Bennike, O., Forman, S.L., Short, S.K., Stafford, T.W., Jr. 1999. Stratified interglacial lacustrine sediments from Baffin Island, Arctic Canada: Chronology and paleoenvironmental implications. Quat. Sci. Rev. 18, 789–810. 10.1016/S0277-3791(98)00075-4

Mitchell, S.G., Humphries, E.E. 2015. Glacial cirques and the relationship between equilibrium line altitudes and mountain range height. Geology 43, 35–38. 10.1130/G36180.1

Mollier-Vogel, E., Leduc, G., Böschen, T., Martínez, P., Schneider, R.R. 2013. Rainfall response to orbital and millennial forcing in northern Peru over the last 18 ka. Quat. Sci. Rev. 76, 29–38. 10.1016/j.quascirev.2013.06.021

Monnin, E., Indermühle, A., Dällenbach, A., Flückiger, J., Stauffer, B., Stocker, T.F., Raynaud, D., Barnola, J.M. 2001. Atmospheric CO_2 concentrations over the Last Glacial Termination. Science 291(5501), 112–114. 10.1126/science.291.5501.112

Mooers, H.D., Lehr, J.D. 1997. Terrestrial record of Laurentide Ice Sheet reorganization during Heinrich events. Geology 25, 987–990. 10.1130/0091-7613(1997)025<0987:TROLIS>2.3.CO;2

Moreiras, S.M., Páez, M.S., Lauro, C., Jeanneret, P. 2017. First cosmogenic ages for glacial deposits from the Plata Range (33º S): New inferences for Quaternary landscape evolution in the Central Andes. Quat. Int. 438, 50–64. 10.1016/j.quaint.2016.08.041

Moreno, P.I., Videla, J. 2016. Centennial and millennial-scale hydroclimate changes in northwestern Patagonia since 16,000 yr BP. Quat. Sci. Rev. 149, 326–337. 10.1016/j.quascirev.2016.08.008

Moreno, P.I., Denton, G.H., Moreno, H., Lowell, T.V., Putnam, A.E., Kaplan, M.R. 2015. Radiocarbon chronology of the Last Glacial Maximum and its

termination in northwestern Patagonia. Quat. Sci. Rev. 122, 233–249. 10.1016/j.quascirev.2015.05.027

Moreno, P.I., Francois, J.P., Moy, C.M., Villa-Martínez, R. 2010. Covariability of the Southern Westerlies and atmospheric CO_2 during the Holocene. Geology 38, 727–730. 10.1130/G30962.1

Moreno, P.I., Kaplan, M.R., François, J.P., Villa-Martínez, R., Moy, C.M., Stern, C.R., Kubik, P.W. 2009. Renewed glacial activity during the Antarctic Cold Reversal and persistence of cold conditions until 11.5 ka in southwestern Patagonia. Geology 37, 375–378. 10.1130/G25399A.1

Moreno, P.I., Lowell, T.V., Jacobson, G.L., Denton, G.H. 1999. Abrupt vegetation and climate changes during the Last Glacial Maximum and the last termination in the Chilean Lake District: A case study from Canal de la Puntilla (41° S). Geogr. Ann., Ser. A, Phys. Geogr. 81A, 285–311. 10.1111/1468-0459.00059

Moreno, P.I., Simi, E., Villa-Martínez, R.P., Vilanova, I. 2019. Early arboreal colonization, postglacial resilience of deciduous Nothofagus forests, and the Southern Westerly wind influence in central-east Andean Patagonia. Quat. Sci. Rev. 218, 61–74. 10.1016/j.quascirev.2019.06.004

Moreno, P.I., Videla, J., Valero-Garcés, B., Alloway, B.V, Heusser, L.E. 2018. A continuous record of vegetation, fire-regime and climatic changes in northwestern Patagonia spanning the last 25,000 years. Quat. Sci. Rev. 198, 15–36. 10.1016/j.quascirev.2018.08.013

Moreno, P.I., Vilanova, I., Villa-Martínez, R., Dunbar, R.B., Mucciarone, D.A., Kaplan, M.R., Garreaud, R.D., Rojas, M., Moy, C.M., De Pol-Holz, R. 2018. Onset and evolution of southern annular mode-like changes at centennial timescale. Sci. Rep. 8, 3458. 10.1038/s41598-018-21836-6

Moreno, P.I., Villa-Martínez, R., Cárdenas, M.L., Sagredo, E.A. 2012. Deglacial changes of the southern margin of the Southern Westerly winds revealed by terrestrial records from SW Patagonia (52° S). Quat. Sci. Rev. 41, 1–21. 10.1016/j.quascirev.2012.02.002

Munroe, J.S., Laabs, B.J., Shakun, J.D., Singer, B.S., Mickelson, D.M., Refsnider, K.A., Caffee, M.W. 2006. Latest Pleistocene advance of alpine glaciers in the southwestern Uinta Mountains, Utah, USA: Evidence for the influence of local moisture sources. Geology 34, 841–844. 10.1130/G22681.1

Murray, D.S., Carlson, A.E., Singer, B.S., Anslow, F.S., He, F., Caffee, M., Marcott, S.A., Liu, Z., Otto-Bliesner, B.L. 2012. Northern Hemisphere forcing of the last deglaciation in southern Patagonia. Geology 40, 631–634. 10.1130/G32836.1

Murton, J.B, Bateman, M.D, Waller, R.I., Whiteman, C.A. 2015. Late Wisconsin glaciation of Hadwen and Summer islands, Tuktoyaktuk coastlands, NWT, Canada. In: GEOQuébec2015. 7th Can. Permafrost Conf., 20–23 September 2015, Quebec City, PQ.

Murton, J.B., Frenchen, M., Maddy, D. 2007. Luminescence dating of Mid- to Late Wisconsinan aeolian sand as a constraint on the last advance of the Laurentide Ice Sheet across the Tuktoyaktuk coastlands, western Arctic Canada. Can. J. Earth Sci. 44, 857–869. 10.1139/e07-015

Muschitiello, F., D'Andrea, W.J., Schmittner, A., Heaton, T.J., Balascio, N.L., deRoberts, N., Caffee, M.W., Woodruff, T.E., Welten, K.C., Skinner, L.C., Simon, M.H., Dokken, T.M. 2019. Deep-water circulation changes lead North Atlantic climate during deglaciation. Nature Commun. 10, 1272. 10.1038/s41467-019-09237-3

Naughton, F., Costas, S., Gomes, S.D., Desprat, S., Rodrigues, T., Sánchez-Goñi, M.F., Renssen, H., Trigo, R., Bronk-Ramsey, C., Oliveira, D., Salgueiro, E., Voelker, A.H.L., Abrantes, F. 2019. Coupled ocean and atmospheric changes during Greenland Stadial 1 in southwestern Europe. Quat. Sci. Rev. 212, 108–120. 10.1016/j.quascirev.2019.03.033

Nilsson-Kerr, K., Anand, P., Sexton, P.F., Leng, M.J., Misra, S., Clemens, S.C., Hammond, S.J. 2019. Role of Asian summer monsoon subsystems in the inter-hemispheric progression of deglaciation. Nature Geosci. 12, 290–295. 10.1038/s41561-019-0319-5

Nimick, D.A., McGrath, D., Mahan, S.A., Friesen, B.A., Leidich, J. 2016. Latest Pleistocene and Holocene glacial events in the Colonia valley, northern Patagonia icefield, southern Chile. J. Quat. Sci. 31, 551–564. 10.1002/jqs.2847

Novello, V.F., Cruz, F.W., Vuille, M., Stríkis, N.M., Edwards, R.L., Cheng, H., Emerick, S., De Paula, M.S., Li, X., Barreto, E.D.S., Karmann, I., Santos, R.V. 2017. A high-resolution history of the South American Monsoon from Last Glacial Maximum to the Holocene. Sci. Rep. 7, 44267. 10.1038/srep44267

Oliva, M., Ruiz-Fernández, J. 2015. Coupling patterns between paraglacial and permafrost degradation responses in Antarctica. Earth Surf. Process. Landf. 40, 1227–1238. 10.1002/esp.3716

Oliva, M., Palacios, D., Fernández-Fernández, J.M., Rodríguez-Rodríguez, L., García-Ruiz, J.M., Andrés, N., Carrasco, R.M., Pedraza, J., Pérez-Alberti, A., Valcárcel, M., Hughes, P.D. 2019. Late Quaternary glacial phases in the Iberian Peninsula. Earth-Sci. Rev. 192, 564–600. 10.1016/j.earscirev.2019.03.015

Orvis, K.H., Horn, S.P. 2000. Quaternary glaciers and climate on Cerro Chirripó, Costa Rica. Quat. Res. 54, 24–37. 10.1006/qres.2000.2142

Osborn, G. 1986. Lateral-moraine stratigraphy and Neoglacial history of Bugaboo Glacier, British Columbia. Quat. Res. 26, 171–178. 10.1016/0033-5894(86)90102-X

Osborn, G., Menounous, B., Ryane, C., Riedel, J., Clague, J.J., Koch, J., Clark, D., Scott, K., Davis, P.T. 2012. Latest Pleistocene and Holocene glacier fluctuations on Mount Baker, Washington. Quat. Sci. Rev. 49, 33–51. 10.1016/j.quascirev.2012.06.004

Oster, J.L., Ibarra, D.E., Winnick, M.J., Maher, K. 2015. Steering of westerly storms over western North America at the Last Glacial Maximum. Nature Geosci. 8, 201–205. 10.1038/ngeo2365

Otto-Bliesner, B.L., Brady, E.C., Clauzet, G., Tomas, R., Levis, S., Kothavala, Z. 2006. Last Glacial Maximum and Holocene climate in CCSM3. J. Clim. 19, 2526–2544. 10.1175/JCLI3748.1

Paillard, D. 1998. The timing of Pleistocene glaciations from a simple multiple-state climate model. Nature 391, 378–381. 10.1038/34891

Palacios, D. 2017. The state of knowledge on the deglaciation of America in 2017. Geogr. Res. Lett. 43, 361–376. 10.18172/cig.3318

Palacios, D., Andrés, N., Gòmez-Ortiz, A., García-Ruiz, J.M. 2017a. Evidence of glacial activity during the Oldest Dryas in the mountain of Spain. In: Hughes, P., Woodward, J. (eds.) Quaternary Glaciation in the Mediterranean Mountains. Geol. Soc. London Spec. Publ. 433, 87–110. 10.1144/SP433.10

Palacios, D., García-Ruiz, J.M., Andrés, N., Schimmelpfennig, I., Campos, N., Leanni, L., ASTER Team 2017b. Deglaciation in the central Pyrenees during the Pleistocene-Holocene transition: Timing and geomorphological significance. Quat. Sci. Rev. 162, 111–127. 10.1016/j.quascirev.2017.03.007

Palacios, D., Gómez-Ortiz, A., Andrés, N., Salvador, F., Oliva, M. 2016. A timing and new geomorphologic evidence of the last deglaciation stages in Sierra Nevada (southern Spain). Quat. Sci. Rev. 150, 110–129. 10.1016/j.quascirev.2016.08.012

Partin, J.W., Quinn, T.M., Shen, C.C., Okumura, Y., Cardenas, M.B., Siringan, F.P., Banner, J.L., Lin, K., Hu, H.-M., Taylor, F.W. 2015. Gradual onset and recovery of the Younger Dryas abrupt climate event in the tropics. Nature Commun. 6, 8061. 10.1038/ncomms9061

Patterson, C.J. 1997. Southern Laurentide ice lobes were created by ice streams: Des Moines lobe in Minnesota, USA. Sediment. Geol. 111, 249–261. 10.1016/S0037-0738(97)00018-3

Patton, H., Hubbard, A., Andreassen, K., Auriac, A., Whitehouse, P.L., Stroeven, A.P., Shackleton, C., Winsborrow, M., Heyman, J., Hall, A.M. 2017. Deglaciation of the Eurasian ice sheet complex. Quat. Sci. Rev. 169, 148–172. 10.1016/j.quascirev.2017.05.019

Pedersen, M.W., Ruetr, A., Schweger, C., Friebe, H., Staff, R.A., Kjeldsen, K.K., Mendoza, M.L.Z., Beaudoin, A.B., Zutter, C., Larsen, N.K., Potter, B.A., Nielsen, R., Rainville, R.A., Orlando, L., Meltzer, D.J., Kjaer, K.H., Willerslev, E. 2016. Postglacial viability and colonization in North America's Ice-free Corridor. Nature 537, 45–49. 10.1038/nature19085

Pedro, J.B., Bostock, H.C., Bitz, C.M., He, F., Vandergoes, M.J., Steig, E.J., Chase, B.M., Krause, C.E., Rasmussen, S.O., Markle, B.R., Cortese, G. 2015. The spatial extent and dynamics of the Antarctic Cold Reversal. Nature Geosci. 9, 51–55. 10.1038/ngeo2580

Pedro, J.B., Van Ommen, T.D., Rasmussen, S.O., Morgan, V.I., Chappellaz, J., Moy, A.D., Masson-Delmotte, V., Delmotte, M. 2011. The last deglaciation: Timing the bipolar seesaw. Clim. Past 7, 671–683. 10.5194/cp-7-671-2011

Peltier, W.R., Argus, D.F., Drummond, R. 2015. Space geodesy constrains ice age terminal deglaciation; the global ICE-6G C (VM5a) model. J. Geophys. Res., Solid Earth 120, 450–487. 10.1002/2014JB011176

Pendleton, S.L., Ceperley, E.G., Briner, J.P., Kaufman, D.S., Zimmerman, S. 2015. Rapid and early deglaciation in the central Brooks Range, Arctic Alaska. Geology 43, 419–422. 10.1130/G36430.1

Pesce, O.H., Moreno, P.I. 2014. Vegetation, fire and climate change in central-east Isla Grande de Chiloé (43°S) since the Last Glacial Maximum, northwestern Patagonia. Quat. Sci. Rev. 90, 143–157. 10.1016/j.quascirev.2014.02.021

Peters, J.L., Benetti, S., Dunlop, P., Cofaigh, C.Ó., Moreton, S.G., Wheeler, A.J., Clark, C.D. 2016. Sedimentology and chronology of the advance and retreat of the last British-Irish Ice Sheet on the continental shelf west of Ireland. Quat. Sci. Rev. 140, 101–124. 10.1016/j.quascirev.2016.03.012

Pétursson, H.G., Norddahl, H., Ingólfsson, O. 2015. Late Weichselian history of relative sea level changes in Iceland during a collapse and subsequent retreat of marine-based ice sheet. Geogr. Res. Lett. 41, 261–277. 10.18172/cig.2741

Phillips, F.M. 2016. Cosmogenic nuclide data sets from the Sierra Nevada, California, for assessment of nuclide production models: I. Late Pleistocene glacial chronology. Quat. Geochronol. 35, 119–129. 10.1016/j.quageo.2015.12.003

Phillips, F. 2017. Glacial chronology of the Sierra Nevada, California, from the Last Glacial Maximum to the Holocene. Geogr. Res. Lett. 43, 527–552. 510.18172/cig.13233

Phillips, F.M., Argento, D.C., Balco, G., Caffee, M.W., Clem, J.M., Dunai, T.J., Finkel, R., Goehring, B., Gosse, J.C., Hudson, A., Jull, A.J.T., Kelly, M., Kurz, M.D., Lal, D., Lifton, N., Marrero, S.M., Nishiizumi, K., Reedy, R., Schaefer, J., Stone, J.O.H., Swanson, T., Zreda, M.G. 2016. The CRONUS-Earth project: A synthesis. Quat. Geochronol. 31 119–154. 10.1016/j.quageo.2015.09.006

Phillips, F.M., Zreda, M.G., Benson, L.V., Plummer, M.A., Elmore, D., Sharma, P. 1996. Chronology for fluctuations in late Pleistocene Sierra Nevada glaciers and lakes. Science 274, 749–751. 10.1126/science.274.5288.749

Phillips, F.M., Zreda, M.G., Gosse, J.C., Klein, J., Evenson, E.B., Hall, R.D., Chadwick, O.A., Sharma, P. 1997. Cosmogenic ^{36}Cl and ^{10}Be ages of Quaternary glacial and fluvial deposits of the Wind River Range, Wyoming. Geol. Soc. Am. Bull. 109, 1453–1463. 10.1130/0016-7606(1997)109<1453:CCABAO>2.3.CO;2

Phillips, F.M., Zreda, M., Plummer, M.A., Elmore, D., Clark, D.H. 2009. Glacial geology and chronology of Bishop Creek and vicinity, eastern Sierra Nevada, California. Geol. Soc. Am. Bull. 121, 1013–1033. 10.1130/B26271.1

Pierce, K.L., Licciardi, J.M., Good, J.M., Jaworowski, C. 2018. Pleistocene Glaciation of the Jackson Hole Area, Wyoming. U.S. Geol. Surv. Prof. Pap. 1835. 10.3133/pp1835

Piper, D.J.W., Skene, K.I. 1998. Latest Pleistocene ice-rafting events on the Scotian margin (eastern Canada) and their relationship to Heinrich events. Palaeoceanogr. Paleoclim. 13, 205–214. 10.1029/97PA03641

Placzek, C., Quade, J., Patchett, P.J. 2006. Geochronology and stratigraphy of late Pleistocene lake cycles on the southern Bolivian Altiplano: Implications for causes of tropical climate change. Geol. Soc. Am. Bull. 118, 515–532. 10.1130/B25770.1

Placzek, C.J., Quade, J., Patchett, P.J. 2013. A 130 ka reconstruction of rainfall on the Bolivian Altiplano. Earth Planet. Sci. Lett. 363, 97–108. 10.1016/j.epsl.2012.12.017

Plummer, M.A. 2002. Paleoclimatic Conditions during the Last Deglaciation Inferred from Combined Analysis of Pluvial and Glacial Records. Ph.D. thesis, New Mexico Institute of Mining & Technology, Socorro, NM, 308 pp.

Porter, S.C. 1976. Pleistocene glaciation in the southern part of the North Cascade Range, Washington. Geol. Soc. Am. Bull. 87, 61–75. 10.1130/0016-7606(1976)87<61:PGITSP>2.0.CO;2

Porter, S.C., Swanson, T.W. 1998. Radiocarbon age constraints on rates of advance and retreat of the Puget lobe of the Cordilleran Ice Sheet during the last glaciation. Quat. Res. 50, 205–213. 10.1006/qres.1998.2004

Porter, S.C., Swanson, T.W. 2008. ^{36}Cl dating of the classic Pleistocene glacial record in the northeastern Cascade Range, Washington. Am. J. Sci. 308, 130–166. 10.2475/02.2008.02

Porter, S.C., Pierce, K.L., Hamilton, T.D. 1983. Late Wisconsin mountain glaciation in the western United States. In: Porter, S.C. (ed.) Late Quaternary Environments, Volume 1, The Late Pleistocene. Univ. Minnesota Press, Minneapolis, MN, pp. 71–111.

Potter, R., Li, Y., Horn, S.P., Orvis, K.H. 2019. Cosmogenic Cl-36 surface exposure dating of late Quaternary glacial events in the Cordillera de Talamanca, Costa Rica. Quat. Res. 92, 216–231. 10.1017/qua.2018.133

Putkonen, J., Connolly, J., Orloff, T. 2008. Landscape evolution degrades the geologic signature of past glaciations. Geomorphology 97, 208–217. 10.1016/j.geomorph.2007.02.043

Putnam, A.E., Schaefer, J.M., Denton, G.H., Barrell, D.J., Andersen, B.G., Koffman, T.N., Rowan, A.V., Finkel, R.C., Rood, D.H., Schwartz, R., Vandergoes, M.J. Plummer. M.A., Brocklehurst, S.H., Kelley, S.E., Ladig, K.L. 2013. Warming and glacier recession in the Rakaia valley, Southern Alps of New Zealand, during Heinrich Stadial 1. Earth Planet. Sci. Lett. 382, 98–110. 10.1016/j.epsl.2013.09.005

Quesada, B., Sylvestre, F., Vimeux, F., Black, J., Pailles, C., Sonzogni, C., Alexandre, A., Blard, P.H., Tonetto, A., Mazura, J.C. Bruneton, H. 2015. Impact of Bolivian paleolake evaporation on the δ^{18}O of the Andean glaciers during the

last deglaciation (18.5–11.7 ka): Diatom-inferred $\delta^{18}O$ values and hydro-isotopic modeling. Quat. Sci. Rev., 120, 93–106. 10.1016/j.quascirev.2015.04.022

Quincey, D.J., Braun, M., Glasser, N.F., Bishop, M.P., Hewitt, K., Luckman, A. 2011. Karakoram glacier surge dynamics. Geophys. Res. Lett. 38, L18504. 10.1029/2011GL049004

Rabassa, J., Coronato, A. 2009. Glaciations in Patagonia and Tierra del Fuego during the Ensenadan Stage/age (Early Pleistocene–earliest Middle Pleistocene). Quat. Int. 210, 18–36. 10.1016/j.quaint.2009.06.019

Rabassa, J., Coronato, A., Bujalesky, C., Roig, F., Salemme, M., Meglioli, A., Heusser, C., Gordillo, S., Borromei, A., Quatrocchio, M.J. 2000. Quaternary of Tierra del Fuego, southernmost South America: An updated review. Quat. Int. 68, 217–240. 10.1016/S1040-6182(00)00046-X

Rabassa, J., Coronato, A., Martínez, O. 2011. Late Cenozoic glaciations in Patagonia and Tierra del Fuego: An updated review. Biol. J. Linn. Soc. 103, 316–335. 10.1111/j.1095-8312.2011.01681.x

Rashid, H., Saint-Ange, F., Barber, D.C., Smith, M.E., Devalia, N. 2012. Fine scale sediment structure and geochemical signature between eastern and western North Atlantic during Heinrich events 1 and 2. Quat. Sci. Rev. 46, 136–150. 10.1016/j.quascirev.2012.04.026

Rasmussen, S.O., Anderson, K.K., Svensson, A.M., Steffensen, J.P., Vinther, B.M., Clausen, H.B., Siggaard-Andersen, M-L., Johnsen, S.J., Larsen, L.B., Dahl-Jensen, D., Bigler, M., Röthlisberger, R., Fischer, H., Goto-Azuma, K., Hansson, M.E., Ruth, U. 2006. A new Greenland ice core chronology for the Last Glacial Termination. J. Geophys. Res. 111, D06102. 10.1029/2005JD006079

Rasmussen, S.O., Bigler, M., Blockley, S.P., Blunier, T., Buchardt, S.L., Clausen, H. B., Cvijanovic, I., Dahl-Jensen, D., Johnsen, S.J., Fischer, H., Gkinis, V., Guillevic, M., Hoek, W.Z., Lowe, J.J., Pedro, J.B., Popp, T., Seierstad, I.K., Steffensen, J.P., Svensson, A.M., Vallelonga, P., Vinther, B.M., Walker, M.J.C., Wheatley, J.J., Winstrup, M. 2014. A stratigraphic framework for abrupt climatic changes during the Last Glacial period based on three synchronized Greenland ice-core records: Refining and extending the

INTIMATE event stratigraphy. Quat. Sci. Rev. 106, 14–28. 10.1016/j.quascirev.2014.09.007

Raymo, M. 1997. The timing of major climate terminations. Paleoceanogr. Paleoclim. 12, 577–585. 10.1029/97PA01169

Rea, B.R. 2009. Defining modern day Area-Altitude Balance Ratios (AABRs) and their use in glacier-climate reconstructions. Quat. Sci. Rev. 28, 237–248. 10.1016/j.quascirev.2008.10.011

Refsnider, K.A., Laabs, B.J.C., Plummer, M.A., Mickelson, D.M., Singer, B.S., Caffee, M.W. 2008. Last Glacial Maximum climate inferences from cosmogenic dating and glacier modeling of the western Uinta ice field, Uinta Mountains, Utah. Quat. Res. 69, 130–144. 10.1016/j.yqres.2007.10.014

Reger, R.D., Sturmann, A.G., Berg, E.E., Burns, P.A.C. 2007. A Guide to the Late Quaternary History of Northern and Western Kenai Peninsula, Alaska. Alaska Div. Geol. Geophys. Surv. Guideb. 8, 112 pp.

Renssen, H., Goosse, H., Roche, D.M., Seppä, H. 2018. The global hydroclimate response during the Younger Dryas event. Quat. Sci. Rev. 193, 84–97. 10.1016/j.quascirev.2018.05.033

Renssen, H., Mairesse, A., Goosse, H., Mathiot, P., Heiri, O., Roche, D.M., Nisancioglu, K.H., Valdes, P.J. 2015. Multiple causes of the Younger Dryas cold period. Nature Geosci. 8, 946–949. 10.1038/ngeo2557

Reynhout, S.A., Sagredo, E.A., Kaplan, M.R., Aravena, J.C., Martini, M.A., Moreno, P.I., Rojas, M., Schwartz, R., Schaefer, J.M. 2019. Holocene glacier fluctuations in Patagonia are modulated by summer insolation intensity and paced by Southern Annular Mode-like variability. Quat. Sci. Rev. 220, 178–187. doi.org/10.1016/j.quascirev.2019.05.029

Ridge, J.C. 2004. The Quaternary glaciation of western New England with correlations to surrounding areas. In: Ehlers, J., Gibbard. P.L. (eds.) Quaternary Glaciations – Extent and Chronology: Part II: North America. Elsevier, Amsterdam, pp. 169-199.

Riedel, J.L. 2007. Late Pleistocene Glacial and Environmental History of Skagit Valley, Washington and British Columbia. Ph.D. thesis, Simon Fraser University, Burnaby, BC.

Riedel, J.L. 2017. Deglaciation of the North Cascade Range, Washington and British Columbia, from the Last Glacial Maximum to the Holocene. Geogr. Res. Lett. 43, 467–496. 10.18172/cig.3236

Riedel, J.L., Clague, J.J., Ward, B.C. 2010. Timing and extent of early marine isotope stage 2 alpine glaciation in Skagit valley, Washington. Quat. Res. 73, 313–323. 10.1016/j.yqres.2009.10.004

Rinterknecht, V., Braucher, R., Böse, M., Bourlès, D., Mercier, J.L. 2012. Late Quaternary ice sheet extents in northeastern Germany inferred from surface exposure dating. Quat. Sci. Rev. 44, 89–95. 10.1016/j.quascirev.2010.07.026

Robel, A.A., Tziperman, E. 2016. The role of ice stream dynamics in deglaciation. J. Geophys. Res., Earth Surf. 121, 1540–1554. 10.1002/2016JF003937

Rodbell, D.T., Seltzer, G.O. 2000. Rapid ice margin fluctuations during the Younger Dryas in the tropical Andes. Quat. Res. 54, 328–338. 10.1006/qres.2000.2177

Rodbell, D.T., Bagnato, S., Nebolini, J.C., Seltzer, G.O., Abbott, M.B. 2002. A late glacial Holocene tephrochronology for glacial lakes in southern Ecuador. Quat. Res. 57, 343–354. 10.1006/qres.2002.2324

Rodbell, D.T., Seltzer, G.O., Mark, B.G., Smith, J.A., Abbott, M.B. 2008. Clastic sediment flux to tropical Andean lakes: Records of glaciation and soil erosion. Quat. Sci. Rev. 27, 1612–1626. 10.1016/j.quascirev.2008.06.004

Rodbell, D.T., Smith, J.A., Mark, B.G. 2009. Glaciation in the Andes during the Lateglacial and Holocene. Quat. Sci. Rev. 28, 2165–2212. 10.1016/j.quascirev.2009.03.012

Roger, J., Saint-Ange, F., Lajeunesse, P., Duchesne, M.J., St-Onge, G. 2013. Late Quaternary glacial history and meltwater discharges along the northeastern Newfoundland shelf. Can. J. Earth Sci. 50, 1178−1194. 10.1139/cjes-2013-0096

Romundset, A., Akçar, N., Fredin, O., Tikhomirov, D., Reber, R., Vockenhuber, C., Christl, M., Schlüchter, C. 2017. Lateglacial retreat chronology of the Scandinavian Ice Sheet in Finnmark, northern Norway, reconstructed from surface exposure dating of major end moraines. Quat. Sci. Rev. 177, 130–144. 10.1016/j.quascirev.2017.10.025

Rosen, J.L., Brook, E.J., Severinghaus, J.P., Blunier, T., Mitchell, L.E., Lee, J.E., Edwards, J.S., Gkinis, V. 2014. An ice core record of near-synchronous global climate changes at the Bølling transition. Nature Geosci. 7, 459–463. 10.1038/ngeo2147

Roy, A.J., Lachniet, M.S. 2010. Late Quaternary glaciation and equilibrium-line altitudes of the Mayan Ice Cap, Guatemala, Central America. Quat. Res. 74, 1–7. 10.1016/j.yqres.2010.04.010

Rull, V., Stansell, N.D., Montoya, E., Bezada, M., Abbott, M.B. 2010. Palynological signal of the Younger Dryas in the tropical Venezuelan Andes. Quat. Sci. Rev. 29, 3045–3056. 10.1016/j.quascirev.2010.07.012

Sagredo, E.A., Kaplan, M.R., Araya, P.S., Lowell, T.V., Aravena, J.C., Moreno, P.I., Kelly, M.A., Schaefer, J.M. 2018. Trans-Pacific glacial response to the Antarctic Cold Reversal in the southern mid-latitudes. Quat. Sci. Rev. 188, 160–166. 10.1016/j.quascirev.2018.01.011

Sagredo, E.A., Moreno, P.I., Villa-Martínez, R., Kaplan, M.R., Kubik, P.W., Stern, C.R. 2011. Fluctuations of the Última Esperanza ice lobe (52º S), Chilean Patagonia, during the Last Glacial Maximum and Termination 1. Geomorphology 125, 92–108. 10.1016/j.geomorph.2010.09.007

Salgado-Labouriau, M.L., Schubert, C., Valastro S., Jr. 1977. Paleoecologic analysis of a late-Quaternary terrace from Mucubají, Venezuelan Andes. J. Biogeogr. 4, 313–325. 10.2307/3038190

Sarıkaya, M.A., Çiner, A. 2017. The late Quaternary glaciation in the eastern Mediterranean. In: Huges, P., Woodward, J. (eds.) Quaternary Glaciation in the Mediterranean Mountains. Geol. Soc. London Spec. Publ. 433, 289–305. 10.1144/SP433.4

Sarıkaya, M.A., Çiner, A., Haybat, H., Zreda, M. 2014. An early advance of glaciers on Mount Akdağ, SW Turkey, before the global Last Glacial Maximum; Insights from cosmogenic nuclides and glacier modeling. Quat. Sci. Rev. 88, 96–109. 10.1016/j.quascirev.2014.01.016

Sarıkaya, M.A., Çiner, A., Yıldırım, C. 2017. Cosmogenic ^{36}Cl glacial chronologies of the Late Quaternary glaciers on Mount Geyikdağ in the eastern Mediterranean. Quat. Geochronol. 39, 189–204. 10.1016/j.quageo.2017.03.003

Saunders, I.R., Clague, J.J., Roberts, M.C. 1987. Deglaciation of Chilliwack River valley, British Columbia. Can. J. Earth Sci. 24, 915–923. 10.1139/e87-089

Schaefer, J.M., Putnam, A.E., Denton, G.H., Kaplan, M.R., Birkel, S., Doughty, A.M., Kelley, S., Barrell, D.J.A., Finkel, R.C., Winckler, G., Anderson, R.F., Ninneman, U.S., Barker, S., Schwartz, R., Andersen, B.G., Schluechter, C. 2015. The southern glacial maximum 65,000 years ago and its unfinished termination. Quat. Sci. Rev. 114, 52–60. 10.1016/j.quascirev.2015.02.009

Schenk, F., Väliranta, M., Muschitiello, F., Tarasov, L., Heikkilä, M., Björck, S., Brandefelt, J., Johansson, A.V., Näslund, J-O., Wohlfarth, B. 2018. Warm summers during the Younger Dryas cold reversal. Nature Commun. 9, 1634. 10.1038/s41467-018-04071-5

Schildgen, T.F., Phillips,W.M., Purves, R.S. 2005. Simulation of snow shielding corrections for cosmogenic nuclide surface exposure studies. Geomorphology 64, 67–85. 10.1016/j.geomorph.2004.05.003

Schimmelpfennig, I. 2009. Cosmogenic ^{36}Cl in Ca and K Rich Minerals: Analytical Developments, Production Rate Calibrations and Cross Calibration with ^{3}He and ^{21}Ne. Ph.D. thesis, Universite Paul Cezanne Aix-Marseille III, CEREGE, 324 pp.

Schimmelpfennig, I., Benedetti, L., Finkel, R., Pik, R., Blard, P.H., Bourlès, D., Burnard, P., Williams, A. 2009. Sources of in-situ ^{36}Cl in basaltic rocks. Implications for calibration of production rates. Quat. Geochronol. 4, 441–461. 10.1016/j.quageo.2009.06.003

Schimmelpfennig, I., Schaefer, J.M., Akçar, N., Koffman, T., Ivy-Ochs, S., Schwartz, R., Finkel, R.C., Zimmerman, S., Schlüchter, C. 2014. A chronology

of Holocene and Little Ice Age glacier culminations of the Steingletscher, Central Alps, Switzerland, based on high sensitivity beryllium-10 moraine dating. Earth Planet. Sci. Lett. 393, 220–230. 10.1016/j.epsl.2014.02.046

Schmittner, A., Galbraith, E.D. 2008. Glacial greenhouse-gas fluctuations controlled by ocean circulation changes. Nature 456, 373–376. 10.1038/nature07531

Schubert, C. 1974. Late Pleistocene Merida Glaciation, Venezuelan Andes. Boreas 3, 147–151. 10.1111/j.1502-3885.1974.tb00673.x

Schubert, C., Rinaldi, M. 1987. Nuevos datos sobre la cronología del estadio tardio de la Glaciacion Mérida, Andes Venezolanos. Acta Científica Venezolana 38, 135–136.

Schweinsberg, A.D., Briner, J.P., Shroba, R.R., Licciardi, J.M., Leonard, E.M., Brugger, K.A., Russell, C.M. 2016. Pinedale glacial history of the upper Arkansas River valley: New moraine chronologies, modeling results, and geologic mapping. In: Keller, S.M., Morgan, M.L. (eds.) Unfolding the Geology of the West. Geol. Soc. Am. Field Guide 44, 335–353 10.1130/2016.0044(14)

Seltzer, G., Rodbell, D., Burns, S. 2000. Isotopic evidence for late Quaternary climate change in tropical South America. Geology 28, 35–38. 10.1130/0091-7613(2000)28<35:IEFLQC>2.0.CO;2

Seltzer, G.O., Rodbell, D.T., Baker, P.A., Fritz, S.C., Tapia, P.M., Rowe, H.D., Dunbar, R.B. 2002. Early warming of tropical South America at the Last Glacial–Interglacial transition. Science 296, 1685–1686. 10.1126/science.1070136

Severinghaus, J.P., Brook, E.J. 1999. Abrupt climate change at the end of the last glacial period inferred from trapped air in polar ice. Science 286, 930–934. 10.1126/science.286.5441.930

Shakun, J.D., Clark, P.U., He, F., Marcott, S.A., Mix, A.C., Liu, Z., Otto-Bliesner, B., Schmittner, A., Bard, E. 2012. Global warming preceded by increasing carbon dioxide concentrations during the last deglaciation. Nature 484(7392), 49–54. 10.1038/nature10915

Shakun, J.D., Clark, P.U., He, F., Lifton, N.A., Liu, Z., Otto-Bliesner, B.L. 2015a. Regional and global forcing of glacier retreat during the last deglaciation. Nature Commun. 6, 8059. 10.1038/ncomms9059

Shakun, J.D., Clark, P.U., Marcott, S.A., Brook, E.J., Lifton, N.A., Caffee, M., Shakun, W.R. 2015b. Cosmogenic dating of Late Pleistocene glaciation, southern tropical Andes, Peru. J. Quat. Sci. 30, 841–847. 10.1002/jqs.2822

Shanahan, T.M., Zreda, M. 2000. Chronology of quaternary glaciations in East Africa. Earth Planet. Sci. Lett. 177, 23–42. 10.1016/S0012-821X(00)00029-7

Shaw, J., Piper, D.J.W., Fader, G.B.J., King, E.L., Todd, B.J., Bell, T., Batterson, M.J., Liverman, D.G.E. 2006. A conceptual model of the deglaciation of Atlantic Canada. Quat. Sci. Rev. 25, 2059–2081. 10.1016/j.quascirev.2006.03.002

Shulmeister, J., Thackray, G.D., Rittenour, T.M., Fink, D., Patton, N.R. 2019. The timing and nature of the last glacial cycle in New Zealand. Quat. Sci. Rev. 206, 1–20. 10.1016/j.quascirev.2018.12.020

Sigman, D.M., Boyle, E.A. 2000. Glacial/interglacial variations in atmospheric carbon dioxide. Nature 407, 859–869. 10.1038/35038000

Sigman, D.M., Hain, M.P., Haug, G.H. 2010. The polar ocean and glacial cycles in atmospheric CO_2 concentration. Nature 466, 47–55. 10.1038/nature09149

Sinha, A., Cannariato, K.G., Stott, L.D., Li, H.C., You, C.F., Cheng, H., Edwards, R.L., Singh, I.B. 2005. Variability of southwest Indian summer monsoon precipitation during the Bølling-Allerød. Geology 33, 813–816. 10.1130/G21498.1

Skinner, L., Fallon, S., Waelbroeck, C., Michel, E., Barker, S. 2010. Ventilation of the deep Southern Ocean and deglacial CO_2 rise. Science 328, 1147–1151. 10.1126/science.1183627

Smedley, R.K., Glasser, N.F., Duller, G.A.T. 2016. Luminescence dating of glacial advances at Lago Buenos Aires (~46º S), Patagonia. Quat. Sci. Rev. 134, 59–73. 10.1016/j.quascirev.2015.12.010

Smith, C.A., Lowell, T.V., Caffee, M.W. 2009. Late glacial and Holocene cosmogenic surface exposure age glacial chronology and geomorphological

evidence for the presence of cold-based glaciers at Nevado Sajama, Bolivia. J. Quat. Sci. 24, 360–372. 10.1002/jqs.1239

Smith, G.I., Bischoff, J.L. 1997. Core OL-92 from Owens Lake: Project rationale, geologic setting, drilling procedures, and summary. In: Smith, G.I., Bischoff, J.L. (eds.) An 800,000-year Paleoclimatic Record from Core OL-92, Owens Lake, Southeast California. Geol. Soc. Am., Spec. Pap. 317, 1–8. 10.1130/0-8137-2317-5.1

Smith, J.A., Rodbell, D.T. 2010. Cross-cutting moraines reveal evidence for North Atlantic influence on glaciers in the tropical Andes. J. Quat. Sci. 25, 243–248. 10.1002/jqs.1393

Smith, J.A., Mark, B.G., Rodbell, D.T. 2008. The timing and magnitude of mountain glaciation in the tropical Andes. J. Quat. Sci. 23, 609–634. 10.1002/jqs.1224

Smith, J.A., Seltzer, G.O., Farber, D.L., Rodbell, D.T., Finkel, R.C. 2005. Early Local Last Glacial Maximum in the tropical Andes. Science 308, 678–681. 10.1126/science.1107075

Sowers, T., Bender, M. 1995. Climate records covering the last deglaciation. Science 269, 210–214. 10.1126/science.269.5221.210

Stansell, N.D., Abbott, M.B., Rull, V., Rodbell, D.T., Bezada, M., Montoya, E. 2010. Abrupt Younger Dryas cooling in the northern tropics recorded in lake sediments from the Venezuelan Andes. Earth Planet. Sci. Lett. 293, 154–163. 10.1016/j.epsl.2010.02.040

Stansell, N.D., Licciardi, J.M., Rodbell, D., Mark, B.G. 2017. Tropical ocean-atmospheric forcing of Late Glacial and Holocene glacier fluctuations in the Cordillera Blanca, Peru. Geophys. Res. Lett. 44, 4176–4185. 10.1002/2016GL072408

Stansell, N.D., Polissar, P.J., Abbott, M.B. 2007. Last glacial maximum equilibrium-line altitude and paleo–temperature reconstructions for the Cordillera de Mérida, Venezuelan Andes. Quat. Res. 67, 115–127. 10.1016/j.yqres.2006.07.005

Stansell, N.D. Rodbell, D.T., Abbott, M.B., Mark, B.G. 2013. Proglacial lake sediments records of Holocene climate change in the western Cordillera of Peru. Quat. Sci. Rev. 70, 1–14. 10.1016/j.quascirev.2013.03.003

Stansell, N.D., Rodbell, D., Licciardi, J.M., Sedlak, C.M., Schweinsberg, A.D., Huss, E.G., Delgado, G.M., Zimmerman, S.H., Finkel, R.C. 2015. Late Glacial and Holocene glacier fluctuations at Nevado Huaguruncho in the eastern Cordillera of the Peruvian Andes. Geology 43, 747–750. 10.1130/G36735.1

Steffensen, J.P., Andersen, K.K., Bigler, M., Clausen, H.B., Dahl-Jensen, D., Fischer, H., Goto-Azuma, K., Hansson, M., Johnsen, S.J., Jouzel, J., Masson-Delmotte, V., Popp, T., Rasmussen, S.O., Röthlisberger, R., Ruth, U., Stauffer, B., Siggaard-Andersen, M-L., Sveinbjörnsdóttir, A.E., Svensson, A., White, J. W.C. 2008. High-resolution Greenland ice core data show abrupt climate change happens in few years. Science 321(5889), 680–684. 10.1126/science.1157707

Stephens, B.B., Keeling, R.F. 2000. The influence of Antarctic sea ice on glacial-interglacial CO_2 variations. Nature 404, 171–174. 10.1038/35004556

Stokes, C.R. 2017. Deglaciation of the Laurentide Ice Sheet from the Last Glacial Maximum. Geogr. Res. Lett. 43, 377–428. 10.18172/cig.3237

Stokes, C.R., Clark, C.D., Darby, D.A., Hodgson, D. 2005. Late Pleistocene ice export events into the Arctic Ocean from the M'Clure Strait Ice Stream, Canadian Arctic Archipelago. Glob. Planet. Change. 49, 139–162. 10.1016/j.gloplacha.2005.06.001

Stokes, C.R., Clark, C.D., Storrar, R. 2009. Major changes in ice stream dynamics during deglaciation of the north-western margin of the Laurentide Ice Sheet. Quat. Sci. Rev. 28, 721–738. 10.1016/j.quascirev.2008.07.019

Stokes, C.R., Margold, M., Clark, C.D., Tarasov, L. 2016. Ice stream activity scaled to ice sheet volume during Laurentide Ice Sheet deglaciation. Nature 530, 322–326. 10.1038/nature16947

Stolper, D., Bender, M., Dreyfus, G., Yan, Y., Higgins, J.A. 2016. Pleistocene ice core record of atmospheric O_2 concentrations. Science 353, 1427–1430. 10.1126/science.aaf5445

Stone, J.O. 2000. Air pressure and cosmogenic isotope production. J. Geophys. Res. 105, 23,753–23,759. 10.1029/2000JB900181

Strelin, J.A., Denton, G.H., Vandergoes, M.J., Ninnemann, U.S., Putnam, A.E. 2011. Radiocarbon chronology of the late-glacial Puerto Bandera moraines, Southern Patagonian Icefield, Argentina. Quat. Sci. Rev. 30, 2551–2569. 10.1016/j.quascirev.2011.05.004

Stríkis, N.M., Chiessi, C.M., Cruz, F.W., Vuille, M., Cheng, H., de Sousa Barreto, E.A., Mollenhauer, G., Kasten, S., Karmann, I., Edwards, R.L., Bernal, J.P., dos Reis Sales, H. 2015. Timing and structure of Mega-SACZ events during Heinrich Stadial 1. Geophys. Res. Lett. 42, 5477–5484, 10.1002/2015GL064048

Stríkis, N.M., Cruz, F.W., de Souza Barreto, E.A., Naughton, F., Vuille, M., Cheng, H., Voelker, A.H.L., Zhang, H., Karmann, I., Edwards, R.L., Auler, A.S., Ventura, R.S., dos Reis Sales, H. 2018. South American monsoon response to iceberg discharge in the North Atlantic. Proc. Natl. Acad. Sci. 115, 3788–3793. 10.1073/pnas.1717784115

Stroeven, A.P., Hättestrand, C., Kleman, J., Heyman, J., Fabel, D., Fredin, O., Goodfellow, B.W., Harbor, J.M., Jansen, J.D., Olsen, L., Caffee, M.W., Fink, D., Lundqvist, J., Rosqvist, G.C., Strömberg, B., Jansson, K.N. 2016. Deglaciation of Fennoscandia. Quat. Sci. Rev. 147, 91–121. 10.1016/j.quascirev.2015.09.016

Styllas, M.N., Schimmelpfennig, I., Benedetti, L., Ghilardi, M., ASTER Team. 2018. Late-glacial and Holocene history of the northeast Mediterranean mountains – New insights from in situ-produced ^{36}Cl-based cosmic ray exposure dating of paleo-glacier deposits on Mount Olympus, Greece. Quat. Sci. Rev. 193, 244–265. 10.1016/j.quascirev.2018.06.020

Sugden, D.E., Bentley, M.J., Fogwill, C.J., Hulton, N.R.J., McCulloch, R.D., Purves, R.S. 2005. Late-glacial glacier events in southernmost South America: A blend of 'northern' and 'southern' hemispheric climatic signals? Geogr. Ann., Ser. A, Phys. Geogr. 87A, 273–288. 10.1111/j.0435-3676.2005.00259.x

Sylvestre, F., Servant, M., Servant-Vildary, S., Causse, C., Fournier, M., Ybert, J.P. 1999. Lake-level chronology on the southern Bolivian Altiplano (18º-23º S)

during Late-Glacial time and the early Holocene. Quat. Res. 51, 54–66. 10.1006/qres.1998.2017

Terrizzano, C.M., García Morabito, E., Christl, M., Likerman, J., Tobal, J., Yamin, M., Zech, R. 2017. Climatic and tectonic forcing on alluvial fans in the southern Central Andes. Quat. Sci. Rev. 172, 131–141. 10.1016/j.quascirev.2017.08.002

Thackray, G.D. 2001. Extensive early and middle Wisconsin glaciation on the western Olympic Peninsula, Washington, and the variability of Pacific moisture delivery to the northwestern United States. Quat. Res. 55, 257–270. 10.1006/qres.2001.2220

Thackray, G.D. 2008. Varied climatic and topographic influences on late Pleistocene mountain glaciations in the western United States. J. Quat. Sci. 23, 671–681. 10.1002/jqs.1210

Thiagarajan, N., Subhas, A.V., Southon, J.R., Eiler, J.M., Adkins, J.F. 2014. Abrupt pre-Bølling-Allerød warming and circulation changes in the deep ocean. Nature 511(7507), 75–78. 10.1038/nature13472

Thompson, L.G., Thompson-Mosley, E., Davis, M.E., Lin, P.N., Henderson, K.A., Coledai, J., Bolzan, J.F., Liu, K.B. 1995. Late Glacial stage and Holocene tropical ice core records from Huascarán, Peru. Science 269, 46–50. 10.1126/science.269.5220.46

Thompson, W.B., Dorion, C.C., Ridge, J.C., Balco, G., Fowler, B.K., Svendsen, K.M. 2017. Deglaciation and late-glacial climate change in the White Mountains, New Hampshire, USA. Quat. Res. 87, 96–120. 10.1017/qua.2016.4

Thornalley, D.J., McCave, I.N., Elderfield, H. 2010. Freshwater input and abrupt deglacial climate change in the North Atlantic. Paleoceanography 25, PA1201. 10.1029/2009PA001772

Thorndycraft, V.R., Bendle, J.M., Benito, G., Davies, B.J., Sancho, C., Palmer, A.P., Fabel, D., Medialdea, A., Martin, J.R.V. 2019. Glacial lake evolution and Atlantic-Pacific drainage reversals during deglaciation of the Patagonian Ice Sheet. Quat. Sci. Rev. 203, 102–127. 10.1016/j.quascirev.2018.10.036

Thornton, R.M. 2019. ^{36}Cl Chronologies and ELA Reconstructions from the Northern Boundary of the South American Arid Diagonal. M.S. thesis, University of Cincinnati, Cincinnati, OH.

Thouret, J.-C., van der Hammen, T., Salomons, B. 1996. Paleoenvironmental changes and stades of the last 50,000 years in the Cordillera Central, Colombia. Quat. Res. 46, 1–18. 10.1006/qres.1996.0039

Toucanne, S., Soulet, G., Freslon, N., Jacinto, R.S., Dennielou, B., Zaragosi, S., Eynaud, F., Bourillet, J-F., Bayon, G. 2015. Millennial-scale fluctuations of the European Ice Sheet at the end of the last glacial, and their potential impact on global climate. Quat. Sci. Rev. 123, 113–133. 10.1016/j.quascirev.2015.06.010

Tripsanas, E.K., Piper, D.J.W. 2008. Late Quaternary stratigraphy and sedimentology of Orphan Basin: Implications for meltwater dispersal in the southern Labrador Sea. Palaeogeogr. Palaeoclimatol. Palaeoecol. 260, 521–539. 10.1016/j.palaeo.2007.12.016

Troost, K.G. 2016. Chronology, Lithology, and Paleo-environmental Interpretations of the Penultimate Ice-sheet Advance into Puget Lowland. Ph.D. thesis, University of Washington, Seattle, WA.

Tulenko, J.P., Briner, J.P., Young, N.E., Schaefer, J.M. 2018. Beryllium-10 chronology of early and late Wisconsinan moraines in the Revelation Mountains, Alaska: Insights into the forcing of Wisconsinan glaciation in Beringia. Quat. Sci. Rev. 197, 129–141. 10.1016/j.quascirev.2018.08.009

Turner, K.J., Fogwill, C.J., Mcculloch, R.D., Sugden D.E. 2005. Deglaciation of the eastern flank of the North Patagonian Icefield and associated continental-scale lake diversions. Geogr. Ann., Ser. A, Phys. Geogr. 87A, 363–374. 10.1111/j.0435-3676.2005.00263.x

Tzedakis, P.C., Crucifix, M., Mitsui, T., Wolff, E.W. 2017. A simple rule to determine which insolation cycles lead to interglacials. Nature 542(7642), 427–432. 10.1038/nature21364

Ullman, D.J., Carlson, A.E., LeGrande, A.N., Anslow, F.S., Moore, A.K., Caffee, M., Syverson, K.M., Licciardi, J.M. 2015a. Southern Laurentide ice-

sheet retreat synchronous with rising boreal summer insolation. Geology 43, 23–26. 10.1130/G36179.1

Ullman, D.J., Carlson, A.E., Anslow, F.S., LeGrande, A.N., Licciardi, J.M. 2015b. Laurentide ice-sheet instability during the last deglaciation. Nature Geosci. 8, 534–537. 10.1038/ngeo2463

Ullman, D.J., Carlson, A.E., Hostetler, S.W., Clark, P.U., Cuzzone, J., Milne, G.A., Winsor, K., Caffee, M. 2016. Final Laurentide ice-sheet deglaciation and Holocene climate–sea level change. Quat. Sci. Rev. 152, 49–59. 10.1016/j.quascirev.2016.09.014

Van Daele, M., Bertrand, S., Meyer, I., Moernaut, J., Vandoorne, W., Siani, G., Tanghe, N., Ghazoui, Z., Pino, M., Urrutia, R., De Batist, M. 2016. Late Quaternary evolution of Lago Castor (Chile, 45.6°S): Timing of the deglaciation in northern Patagonia and evolution of the southern westerlies during the last 17 kyr. Quat. Sci. Rev. 133, 130–146. 10.1016/j.quascirev.2015.12.021

van der Hammen, T. 1981. Glaciares y glaciaciones en el Cuaternario de Colombia: Paleoecología y estratigrafía. Revista CIAF (Centro Interamericano de Fotointerpretación) 6, 635–638.

Vázquez-Selem, L., Heine, K. 2011. Late Quaternary glaciation in Mexico. In: Ehlers, J., Gibbard, P.L., Hughes, P.D. (eds.) Quaternary Glaciations – Extent and Chronology. Elsevier, Amsterdam, pp. 849–861. 10.1016/B978-0-444-53447-7.00061-1

Vázquez-Selem, L., Lachniet, M.S. 2017. The deglaciation of the mountains of Mexico and Central America. Geogr. Res. Lett. 43, 553–570. 10.18172/cig.3238

Veillette, J.J., Dyke, A.S., Roy, M. 1999. Ice-flow evolution of the Labrador sector of the Laurentide Ice Sheet: A review, with new evidence from northern Quebec. Quat. Sci. Rev. 18, 993–1019. 10.1016/S0277-3791(98)00076-6

Viau, A.E., Gajewski, K., Sawada, M.C., Bunbury, J. 2008. Low- and high-frequency climate variability in eastern Beringia during the past 25 000 years. Can. J. Earth Sci. 45, 1435–1453. 10.1139/E08-036

Vilanova, I., Moreno, P.I., Miranda, C.G., Villa-Martínez, R.P. 2019. The last glacial termination in the Coyhaique sector of central Patagonia. Quat. Sci. Rev. 224, 105976. 10.1016/j.quascirev.2019.105976

Villagrán, C. 1988a. Expansion of Magellanic moorland during the Late Pleistocene: Palynological evidence from northern Isla Grande de Chiloé, Chile. Quat. Res. 30, 304–314. 10.1016/0033-5894(88)90006-3

Villagrán, C. 1988b. Late Quaternary vegetation of southern Isla Grande de Chiloé, Chile. Quat. Res. 29, 294–306. 10.1016/0033-5894(88)90037-3

Villa-Martínez, R., Moreno, P.I., Valenzuela, M,A. 2012. Deglacial and postglacial vegetation changes on the eastern slopes of the central Patagonian Andes (47º S). Quat. Sci. Rev. 32, 86–99. 10.1016/j.quascirev.2011.11.008

Voelker, A.H. 2002. Global distribution of centennial-scale records for Marine Isotope Stage (MIS) 3: A database. Quat. Sci. Rev. 21, 1185–1212. 10.1016/S0277-3791(01)00139-1

Wang, X., Auler, A.S., Edwards, R.L., Cheng, H., Ito, E., Wang, Y., Kong, X., Solheid, M. 2007. Millennial-scale precipitation changes in southern Brazil over the past 90,000 years. Geophys. Res. Lett. 34, L23701. 10.1029/2007GL031149

Wang, Y., Cheng, H., Edwards, R.L., Kong, X., Shao, X., Chen, S., Wu, J., Juang, X., Wang, X., An, Z. 2008. Millennial- and orbital-scale changes in the East Asian monsoon over the past 224,000 years. Nature 451, 1090–1093. 10.1038/nature06692

Ward, D., Thornton, R., Cesta, J. 2017. Across the Arid Diagonal: Deglaciation of the western Andean Cordillera in southwest Bolivia and northern Chile. Geogr. Res. Lett. 43, 667–696. 10.18172/cig.3209

Ward, D.J., Cesta, J.M., Galewsky, J., Sagredo, E. 2015. Late Pleistocene glaciations of the arid subtropical Andes and new results from the Chajnantor Plateau, northern Chile. Quat. Sci. Rev. 128, 98–116. 10.1016/j.quascirev.2015.09.022

Ward, D.W., Anderson, R.S., Briner, J.P., Guido., Z.S. 2009. Numerical modeling of cosmogenic deglaciation records, Front Range and San Juan

Mountains, Colorado. J. Geophys. Res., Earth Surf. 114, F01026. 10.1029/2008JF001057

Weaver, A.J., Saenko, O.A., Clark, P.U., Mitrovica, J.X. 2003. Meltwater pulse 1A from Antarctica as a trigger of the Bølling-Allerød warm interval. Science 299(5613), 1709–1713. 10.1126/science.1081002

Weber, M.E., Clark, P.U., Kuhn, G., Timmermann, A., Sprenk, D., Gladstone, R., Zhang, X., Lohmann, G., Menviel, L., Chikamoto, M.O., Friedrich, T., Ohlwein, C. 2014. Millennial-scale variability in Antarctic ice-sheet discharge during the last deglaciation. Nature 510, 134–138. 10.1594/PANGAEA.819646.

Weller, D., Miranda, C.G., Moreno, P.I., Villa-Martínez, R., Stern, C.R. 2014. The large late-glacial Ho eruption of the Hudson volcano, southern Chile. Bull. Volcanol. 76(6), 831–xxx. 10.1007/s00445-014-0831-9

Wesnousky, S.G., Aranguren, R., Rengifo, M., Owen, L.A., Caffee, M.W., Krishna Murari, M., Pérez, O.J. 2012. Toward quantifying geomorphic rates of crustal displacement, landscape development, and the age of glaciation in the Venezuelan Andes. Geomorphology 141-142, 99–113. 10.1016/j.geomorph.2011.12.028

Whitlock, C., Sarna-Wojcicki, A., Bartlein, P.J., Nickmann, R.J. 2000. Environmental history and tephrostratigraphy at Carp Lake, southwestern Columbia Basin, Washington, USA. Palaeogeogr. Palaeoclimatol. Palaeoecol. 155, 7–29. 10.1016/S0031-0182(99)00092-9

Williams, C., Flower, B.P., Hastings, D.W. 2012. Seasonal Laurentide Ice Sheet melting during the “Mystery Interval” (15.5-14.5 ka). Geology 40, 955–958. 10.1130/G33279.1

Wilson, P., Ballantyne, C.K., Benetti, S., Small, D., Fabel, D., Clark, C.D. 2019. Deglaciation chronology of the Donegal Ice Centre, north-west Ireland. J. Quat. Sci. 34, 16–28. 10.1002/jqs.3077

Winkler, S., Matthews, J.A. 2010. Observations on terminal moraine-ridge formation during recent advances of southern Norwegian glaciers. Geomorphology 116, 87–106. 10.1016/j.geomorph.2009.10.011

Wolbach, W.S., Ballard, J.P., Mayewski, P.A., Adedeji, V., Bunch, T.E., Firestone, R.B., French, T.A., Howard, G.A., Israde-Alcántara, I., Johnson, J.R., Kimbel, D., Kinzie, C.R., Kurbatov, A., Kletetschka, G., LeCompte, M.A., Mahaney, W.C., Melott, A.L., Maiorana-Boutilier, A. Mitra, S., Moore, C.R., Napier, W.M., Parlier, J., Tankersley, K.B., Thomas, B.C., Wittke, J.H., West, A., Kennett, J.P. 2018. Extraordinary biomass-burning episode and impact winter triggered by the Younger Dryas cosmic impact~12,800 years ago. 1. Ice cores and glaciers. J. Geol. 126, 165–184. 10.1086/695704

Wolff, E., Fischer, H., Röthlisberger, R. 2009. Glacial terminations as southern warmings without northern control. Nature Geosci. 2, 206–209. 10.1038/ngeo442

Woolfenden, W.B. 2003. A 180,000-year pollen record from Owens Lake, CA: Terrestrial vegetation change on orbital scales. Quat. Res. 59, 430–444. 10.1016/S0033-5894(03)00033-4

Wright, H.E. 1984. Late glacial and late Holocene moraines in the Cerros Cuchpanga, central Peru. Quat. Res. 21, 275–285. 10.1016/0033-5894(84)90068-1

Young, N.E., Briner, J.P., Leonard, E.M., Licciardi, J.M., Lee. K. 2011. Assessing climatic and non-climatic forcing of Pinedale glaciation and deglaciation in the western United States. Geology 39, 171–174. 10.1130/G31527.1

Young, N.E., Briner, J.P., Schaefer, J., Zimmerman, S., Finkel, R.C. 2019. Early Younger Dryas glacier culmination in southern Alaska: Implications for North Atlantic climate change during the last deglaciation. Geology 47, 550–554. 10.1130/G46058.1

Yuan, F., Koran, M.R., Valdez, A. 2013. Late Glacial and Holocene record of climatic change in the southern Rocky Mountains from sediments in San Luis Lake, Colorado, USA. Palaeogeogr. Palaeoclimatol. Palaeoecol. 392, 146–160. 10.1016/j.palaeo.2013.09.016

Zech, J., Terrizzano, C.M., García Morabito, E., Veit, H., Zech, R. 2017. Timing and extent of late Pleistocene glaciation in the arid Central Andes of Argentina and Chile (22°-41°S). Geogr. Res. Lett. 43, 697–718. 10.18172/cig.3235

Zech, J., Zech, R., Kubik, P.W., Veit, H. 2009. Glacier and climate reconstruction at Tres Lagunas, NW Argentina, based on ^{10}Be surface exposure dating and lake sediment analyses. Palaeogeogr. Palaeoclimatol. Palaeoecol. 284, 180–190. 10.1016/j.palaeo.2009.09.023

Zech, J., Zech, R., May, J.H., Kubik, P.W., Veit, H. 2010. Lateglacial and early Holocene glaciation in the tropical Andes caused by la Niña-like conditions. Palaeogeogr. Palaeoclimatol. Palaeoecol. 293, 248–254. 10.1016/j.palaeo.2010.05.026

Zech, R., May, J.H., Kull, C., Ilgner, J., Kubik, P.W., Veit, H. 2008. Timing of the late Quaternary glaciation in the Andes from~15 to 40°S. J. Quat. Sci. 23, 635–647. 10.1002/jqs.1200

Zhang, H., Griffiths, M.L., Huang, J., Cai, Y., Wang, C., Zhang, F., Cheng, H., Ning, Y., Hu, C., Xie, S. 2016. Antarctic link with East Asian summer monsoon variability during the Heinrich Stadial–Bølling interstadial transition. Earth Planet. Sci. Lett. 453, 243–251. 10.1016/j.epsl.2016.08.008

Figure captions

Figure 1. Locations of the main sites in North and Central America cited in the text.

Figure 2. Locations of the main sites in South America cited in the text.

Figure 3. Glacier extent during the Global Last Glacial Maximum in the Americas. Coloured areas represent regions containing glaciated mountain ranges and in many cases are, for purposes of visibility, much larger than actual glaciated areas. AK = Alaska, BC = British Columbia (Cordilleran Ice Sheet and northern Cascades), CS = central/southern Cascades, SN = Sierra Nevada, NRM = northern Rocky Mountains, SRM = southern Rocky Mountains, MX = Mexico, CA = Central America, NA = Northern Andes, PB = Peru/Bolivia, NCA = north-central Andes, ACA = arid central Andes, PA = Patagonia, TdF = Tierra del Fuego. The coastline corresponds to the GLGM sea-level low. Figure information comes from author interpretations and refecences cited in Table 1.

Figure 4. Glacier extent during H-1 in the Americas. See Figure 3 for full caption. Figure information come from author interpretations and refecences cited in Table 2.

Figure 5. Glacier extent during the B-A and ACR in the Americas. See Figure 3 for full caption. Figure information comes from author interpretations and refecences cited in Table 3.

Figure 6. Glacier extent during the YD in the Americas. See Figure 3 for full caption. Figure information comes from author interpretations and references cited in Table 4.

Figure 7. Glacier extent during the early Holocene in the Americas. See Figure 3 for full caption. Figure information comes from author interpretation and references cited in Table 4.

Figure 8. Glacial landforms at Deming Glacier on Mount Baker in the North Cascade Range, Washington State. Late-glacial moraines below the present-day terminus of Deming Glacier are numbered 1 through 7. Moraines 1 and 7 and the dashed black line represent the maximum late glacial (Bølling?) limit of Deming Glacier. Moraine number 4 marks the YD limit with its associated adiocarbon ages. Note Neoglacial - Little Ice Age terminus.

Figure 9. GLGM moraines in in the Beartooth Range, Rocky Mountains, Montana. A) Location of the photos. B) Moraines; view west. C) Moraines; view east. The moraines have been dated to 19.8 ka (Licciardi and Pierce, 2018). Photos by Nuria Andrés.

Figure 10. A) Location of the Wind River Range in the Rocky Mountains of Wyoming, Montana and Idaho, and the Middle and North forks of the Popo Agie River (red box) on the southeast flank of the range. B) Overview of LLGM and Late-glacial (pre-Holocene) moraines in the Middle and North fork catchments of the Popo Agie River. Only the farthest extents of the dated moraines are indicated in the main valleys. Yellow – Positions and ^{10}Be ages of terminal LGM and post-LGM (Pinedale and post-Pinedale) moraines. Green – Positions and ^{10}Be ages of moraines associated with glacial activity during the H-1/Oldest Dryas period. Red – Positions and ^{10}Be ages of moraines associated with the YD period. The glacial geology and chronology of this area were originally described by Dahms (2002, 2004) and Dahms et al. (2010), and were subsequently revised by Dahms et al. (2018, 2019). Source: Google Earth images.

Figure 11. LLGM moraines on the east side of the Teton Range, Wyoming, near Taggart and Jenny lakes. A) Locations of photos. B) Moraines east of Taggart Lake. C) Moraines west of Jenny Lake. The moraines have been dated to between 14.4 and 15.2 ka (Licciardi and Pierce, 2018). Photos by Nuria Andrés.

Figure 12. Recessional moraines along the Yellowstone River in the Rocky Mountains of Montana. A) Locations of photo. B) Moraines; view from the northeast. The moraines have been dated to between 14.4 and 15.1 ka (Licciardi and Pierce, 2018). Photo by Nuria Andrés.

Figure 13. GLGM moraines in the Clear Creek watershed, Sawatch Range, central Colorado Rocky Mountains). A) Location of photos. B) Moraines; view to the West. C) Moraines; view to the east. The moraines have been dated to between 19.1 and 21.7 ka (Young et al., 2011). Photos by Nuria Andrés.

Figure 14. Overview of late Pleistocene moraines at Bishop Creek, eastern Sierra Nevada, California. Extents of preserved moraines are indicated for the Tioga 1 (early GLGM), Tioga 2/3 (late GLGM), and Tioga 4 (H-1) advances. Recess Peak moraines (B-A or YD) are numerous throughout the headwaters area, but only one representative moraine is shown. The obvious terminal moraines northeast of the Tioga 1 moraine date to MIS 6 age. The geology and chronology of this drainage are described in Phillips et al. (2009) and updated in Phillips (2017).

Figure 15. Glacial landforms between ~3100 and 4200 m a.s.l. in Gavidia Valley in the Mérida Andes The valley has a U-shaped cross-profile, and has numerous outcrops of

striated and polished bedrock (roches moutonnées). Deglaciation happened in two stages: slow retreat between ~22 and 16.5 ka, followed by the complete deglaciation at ~16 ka (Angel et al., 2016). Photo by Eduardo Barreto.

Figure 16. LLGM and H-1 glacial landforms at the top of Cerro Tunupa (19.8°S, 67.6°W; 5110 m asl); view toward the southeast (Blard et al, 2013a; Martin et al., 2018). In the background is the Salar de Uyuni. Photo by Pierre Henri Blard.

Figure 17. Glacial landforms on Hualcahualca volcano, southern Peru. A) Locations of photos. B) Prominent well-preserved LLGM moraine on the east flank of the volcano. C) H-1 and YD moraines on the north flank of the volcano (Alcalá-Reygosa et al., 2017). Photos by Jesus Alcalá-Reygosa.

Figure 18. Glacial landforms in the arid Chilean Andes, from north to south: A) Glacial valley at El Tatio (22.3° S), view upvalley from the LGM right-lateral moraine that has yielded ^{36}Cl ages of 20-35 ka (Ward et al., 2017). Truck circled for scale. B) View upvalley from LGM right-lateral/frontal moraine near Co. La Torta (22.45° S) dated to 25-30 ka (Ward et al., 2015). Dirt track visible for scale. C) Inner ridge of the western terminal complex of the former Chajnantor ice cap (23.0° S), last occupied at the LLGM (Ward et al., 2015; 2017). View to the southwest; backpack circled for scale. D) Eastern terminal moraine complex at Chajnantor, likely MIS 3 (Ward et al., 2015, 2017). View to the north; largest visible boulders are ~1.5 m in diameter. E) View upvalley from likely MIS 6 terminal moraine of the southern outlet glacier of the former ice field at Cordón de Puntas Negras (23.85° S). Sharper inner lateral/frontal moraines have yielded ages that support an LGM and/or MIS 3 age (Thornton, 2019). Locations of photos: 1 - A; 2 -B , 3 - C and D, 4 - E. Photos by Dylan J. Ward.

Figure 19. Glacial landforms on the east side of Nevado de Chañi in the central Argentina Andes. A) Locations of the photos. B) View to the east (down-valley) of Refugio Valley showing the GLGM l (red) and H-1 (purple) moraines. The green circle marks a hut for scale. C) YD lateral/frontal moraines in the Chañi Chico valley, which is a tributary of Refugio Valley. These moraines are located inboard of those shown in panel A. Photos by Mateo Martini.

Figure 20. Glacial landforms on Tierra de Fuego. A) Locations of photos B-E. B) The inner LGM-age moraine at Bahía Inútil, southern Chile. View to the east, parallel to the moraine (marked by the white dashed line). The large boulders are granite derived from

the Cordillera Darwin. C) Ice-scoured terrain in the Cordillera Darwin characteristic of areas deglaciated during H-I. View to the north along the Beagle Channel. D) Aerial view to the southwest of Marinelli fjord. The dashed line shows the location of a late Holocene moraine, marking a historic glacial margin. The white dot shows the approximate location of a core site that provides evidence that ice receded from the Strait of Magellan and back into the fjord by ~17 ka. The black dot shows the location of photo E. E) Bog in Marinelli fjord; view to the south. The late Holocene moraine is visible in the background. Ice had cleared this site, within view of the historic position, by 16 ka. Photos by Brenda Hall.

Figure 21. ACR moraine in Gueshgue valley in the Cordillera Blanca, Peru (dated by Stansell et al., 2017). Photo by Joseph Licciardi.

Figure 22. ACR moraine at Nevado Huaguruncho in the Eastern Cordillera of Peru (dated by Stansell et al., 2015). Photo by Joseph Licciardi.

Figure 23. ACR (continuous white line) and Holocene (dashed line) moraines in the Tranquilo Valley, close to Mount San Lorenzo, Patagonia. Photo by Esteban Salgedo.

Figure 24. Glacial landforms in Alcalican Valley, southwest of Iztaccíhuatl in central Mexico. Moraine from the Late Pleistocene-Holocene transition. Elevations are ~3865 m at the bottom of the valley at the end of the moraine and ~5200 m a.s.l. on the mountain summit. Moraines of this group have been ^{36}Cl-dated at 13-12 to ~10.5 ka and could be YD in age. Note the three moraine ridges on the right side of the valley. Photo by Lorenzo Vázquez.

Table captions

Table 1. The main climate and glacial evolution features during the Global Last Glacial Maximum (26.5-19 ka) in the Americas.

Table 2. The main climate and glacial evolution features during the Heinrich 1 Stadial (17.5-14.6 ka) in the Americas.

Table 3. The main climate and glacial evolution features during the Bølling-Allerød interstadial and Antarctic Cold Reversal (14.6-12.9 ka) in the Americas.

Table 4. The main climate and glacial evolution features during the Younger Dryas (12.9-11.7 ka) in the Americas.


Arctic Ocean
Viscount Melville Sound
Victoria Island
Baffin Island
Beaufort Sea
Bering Strait
Mackenzie River delta
Brooks Range
Yukon Territory
Keewatin
Foxe Pen.
Cumberland Sound
Hudson Strait
Ankun Mts.
Alaska Range
Hudson Bay
Labrador
Coast Mountains
Kenai Peninsula
Elmendorf Moraine
Fraser River
Vancouver Island
Mt.Baker
North Cascades
Yellowstone
San Juan Mts.
Rocky Mountains
Front Range
Great Lakes
Lake Lahontan
Mono Lake
Owens Lake
Searles Lake
San Luis Valley
S. Nevada
Pacific Ocean
Atlantic Ocean
Cofre de Perote
Iztaccíhuatl
Altos Cuchumatanes
Cordillera de Talamanca
Km
0 500 1000 2000 3000 4000 5000
60°
40°
20° N
0°
160°
140°
120°
100°
80°
60°
40°W

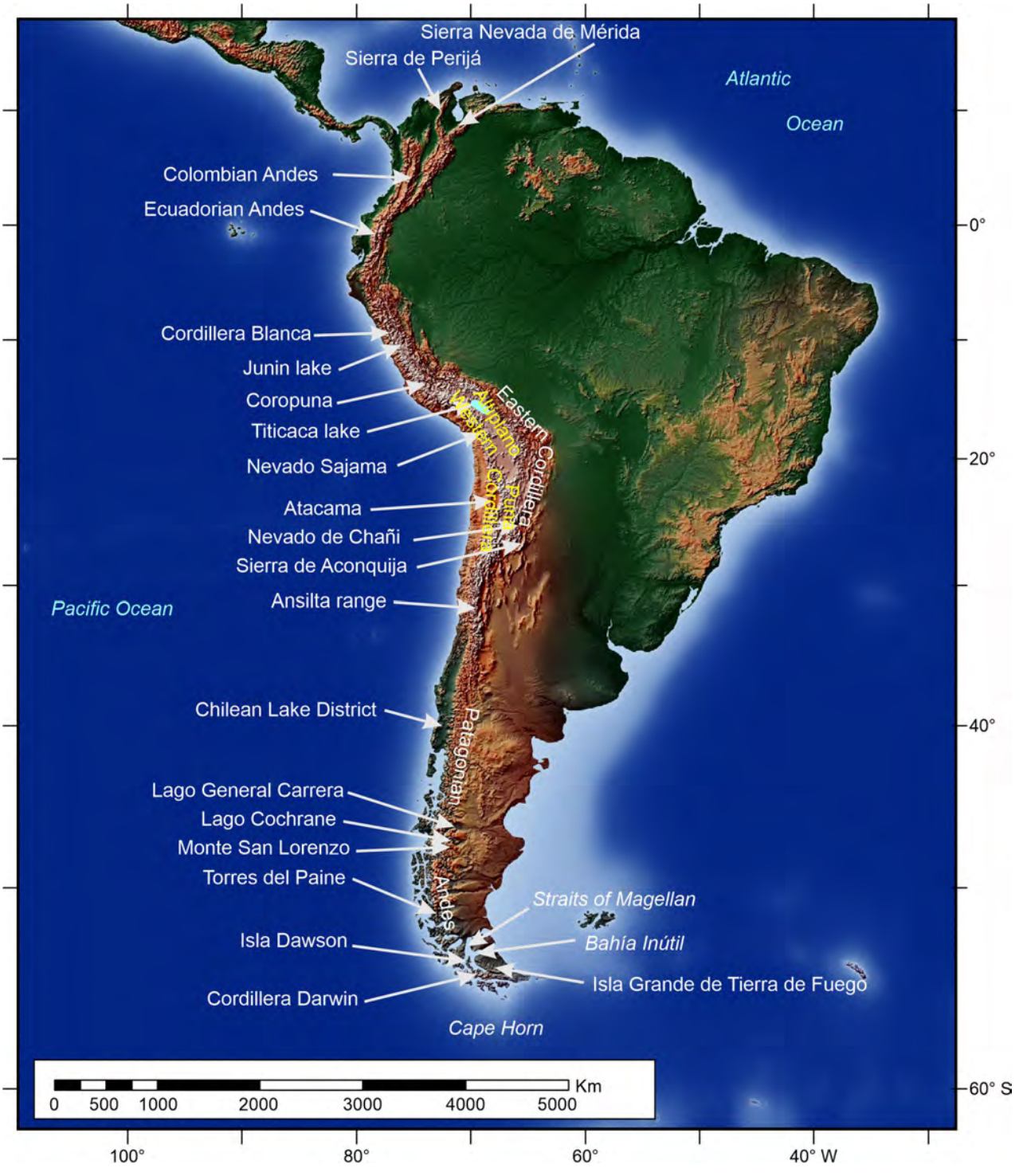
Sierra Nevada de Mérida
Sierra de Perijá
Atlantic
Ocean
Colombian Andes
Ecuadorian Andes
Cordillera Blanca
Junin lake
Coropuna
Titicaca lake
Nevado Sajama
Atacama
Nevado de Chañi
Sierra de Aconquija
Ansilta range
Pacific Ocean
Chilean Lake District
Lago General Carrera
Lago Cochrane
Monte San Lorenzo
Torres del Paine
Isla Dawson
Cordillera Darwin
Cape Horn
Straits of Magellan
Bahía Inútil
Isla Grande de Tierra de Fuego
Eastern Cordillera
Altiplano Puna
Western Cordillera
Patagonian Andes
0°
20°
40°
60° S
100°
80°
60°
40° W
0 500 1000 2000 3000 4000 5000 Km

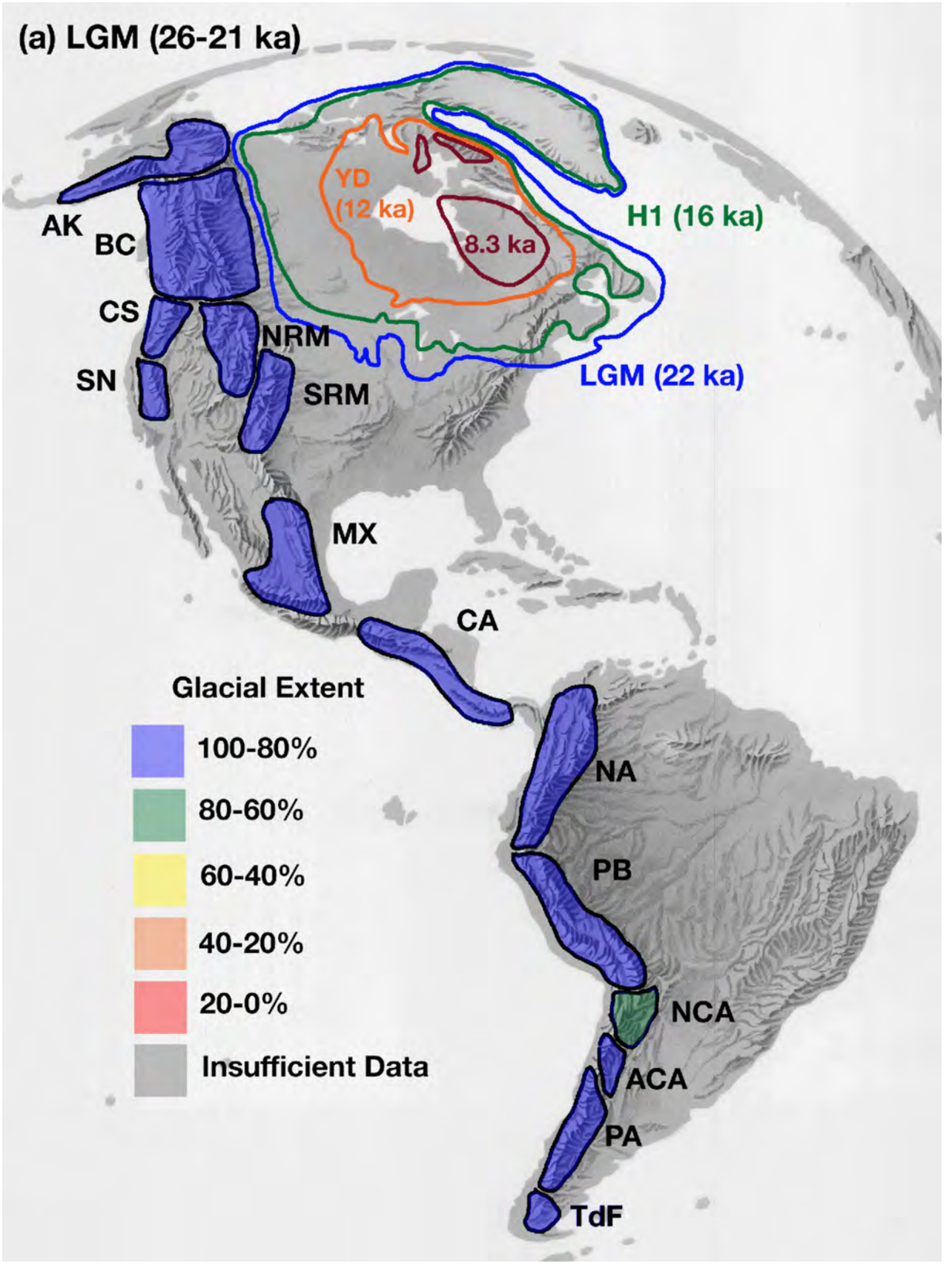
(a) LGM (26-21 ka)
YD
(12 ka)
8.3 ka
H1 (16 ka)
LGM (22 ka)
AK
BC
CS
SN
NRM
SRM
MX
CA
NA
PB
NCA
ACA
PA
TdF
Glacial Extent
100-80%
80-60%
60-40%
40-20%
20-0%
Insufficient Data

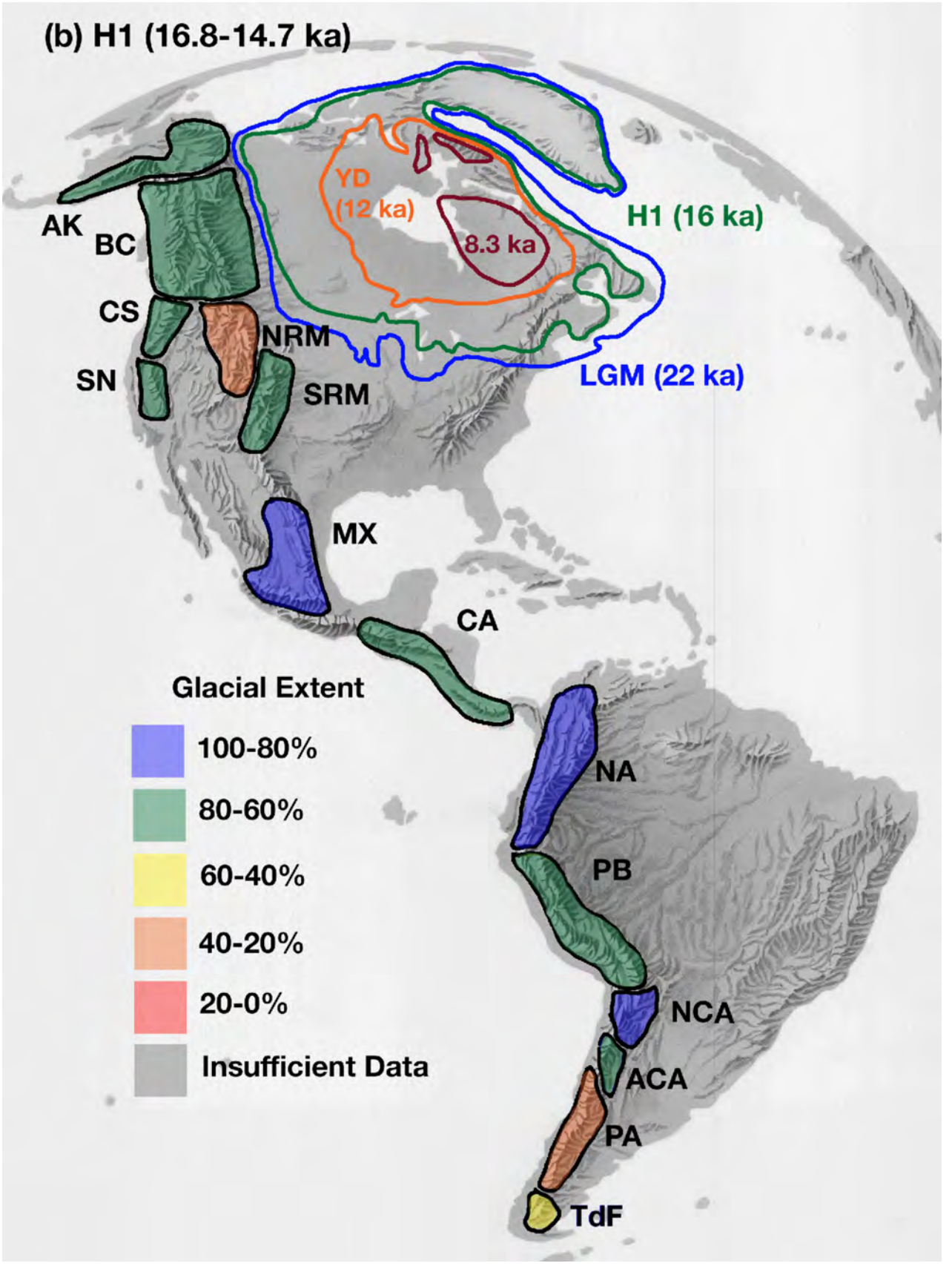
(b) H1 (16.8-14.7 ka)
YD
(12 ka)
8.3 ka
H1 (16 ka)
LGM (22 ka)
AK
BC
CS
NRM
SN
SRM
MX
CA
NA
PB
NCA
ACA
PA
TdF
Glacial Extent
100-80%
80-60%
60-40%
40-20%
20-0%
Insufficient Data

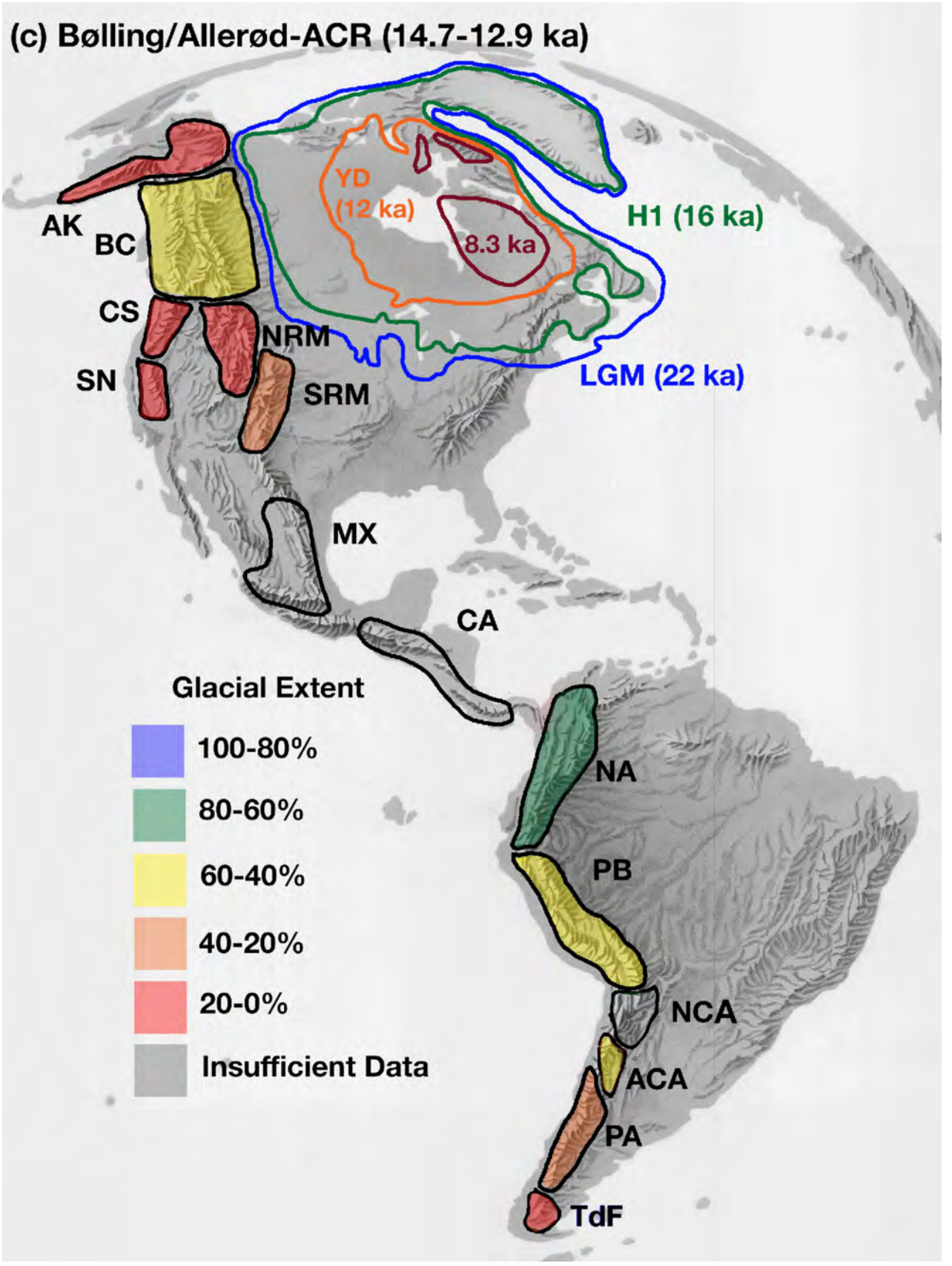
(c) Bølling/Allerød-ACR (14.7-12.9 ka)
YD
(12 ka)
8.3 ka
H1 (16 ka)
LGM (22 ka)
AK
BC
CS
NRM
SN
SRM
MX
CA
NA
PB
NCA
ACA
PA
TdF
Glacial Extent
100-80%
80-60%
60-40%
40-20%
20-0%
Insufficient Data

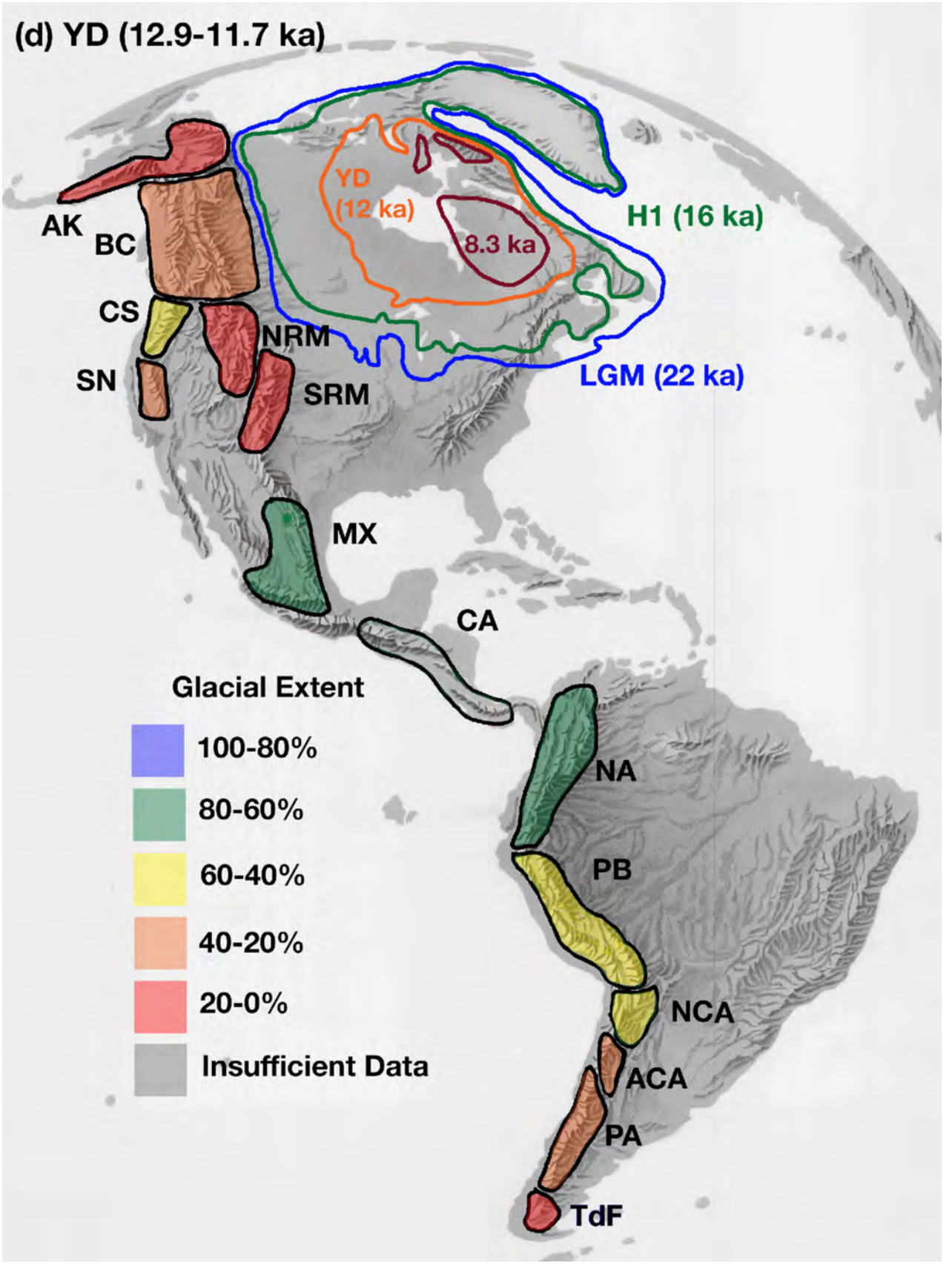
(d) YD (12.9-11.7 ka)
YD
(12 ka)
8.3 ka
H1 (16 ka)
LGM (22 ka)
AK
BC
CS
NRM
SN
SRM
MX
CA
NA
PB
NCA
ACA
PA
TdF
Glacial Extent
100-80%
80-60%
60-40%
40-20%
20-0%
Insufficient Data

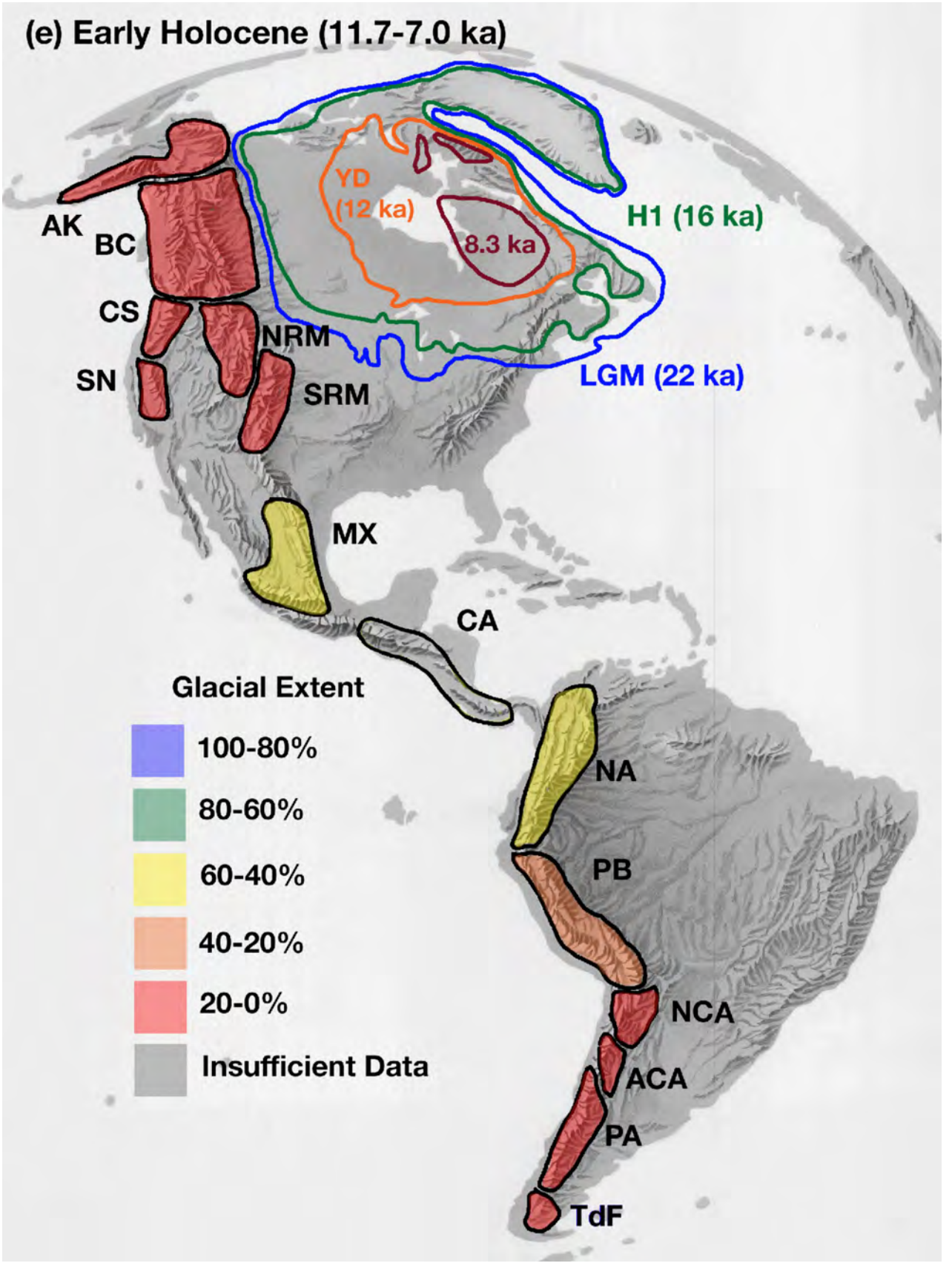
(e) Early Holocene (11.7-7.0 ka)
YD
(12 ka)
8.3 ka
H1 (16 ka)
LGM (22 ka)
AK
BC
CS
NRM
SN
SRM
MX
CA
NA
PB
NCA
ACA
PA
TdF
Glacial Extent
100-80%
80-60%
60-40%
40-20%
20-0%
Insufficient Data

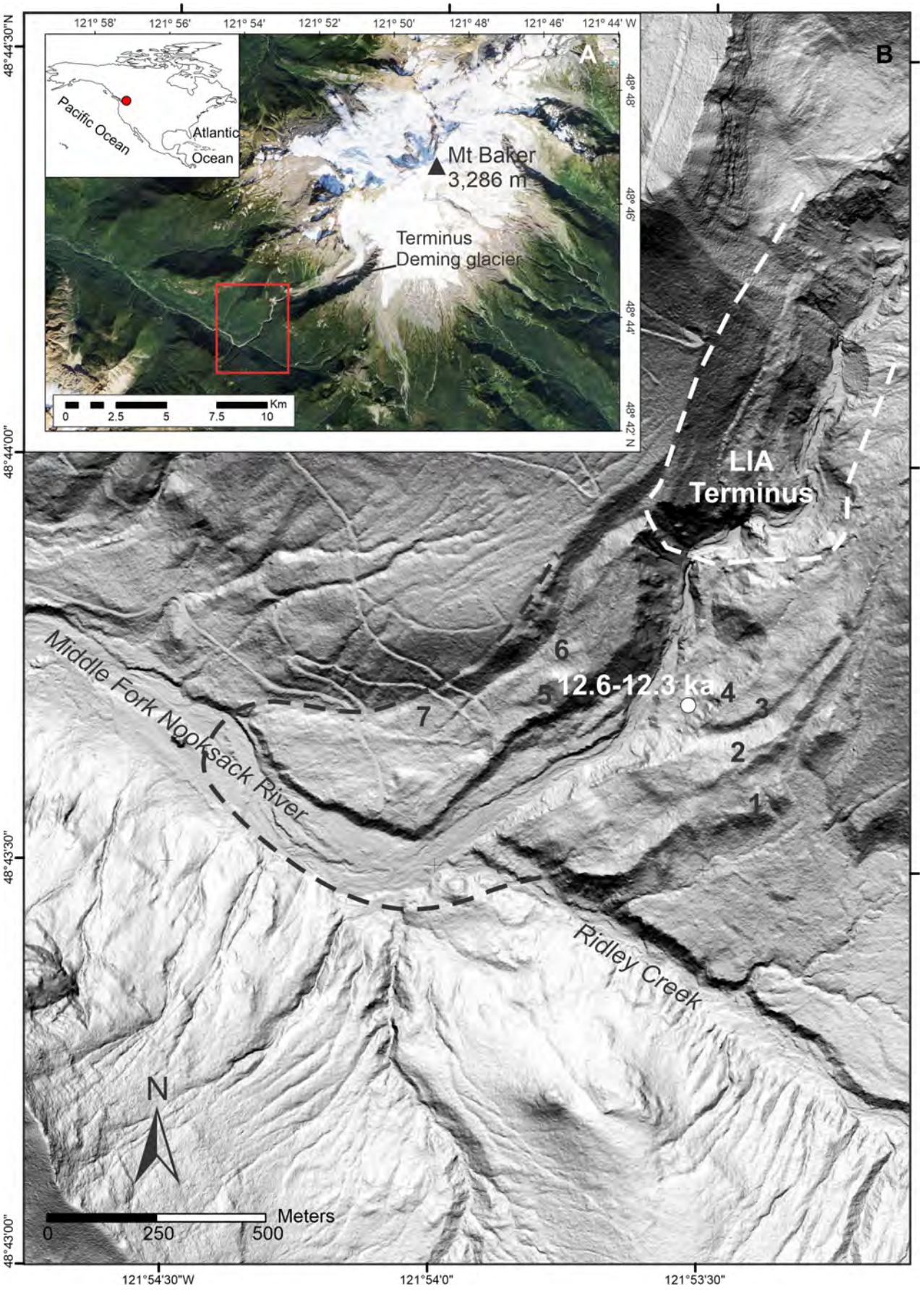
121° 58'
121° 56'
121° 54'
121° 52'
121° 50'
121° 48'
121° 46'
121° 44' W
48° 44'30"N
48° 44'00"
48° 43'30"
48° 43'00"
48° 48'
48° 46'
48° 44'
48° 42' N
A
B
Pacific Ocean
Atlantic Ocean
Mt Baker
3,286 m
Terminus
Deming glacier
0
2.5
5
7.5
10
Km
LIA
Terminus
6
5
12.6-12.3 ka
4
3
2
1
7
Middle Fork Nooksack River
Ridley Creek
N
0
250
500
Meters
121°54'30"W
121°54'0"
121°53'30"

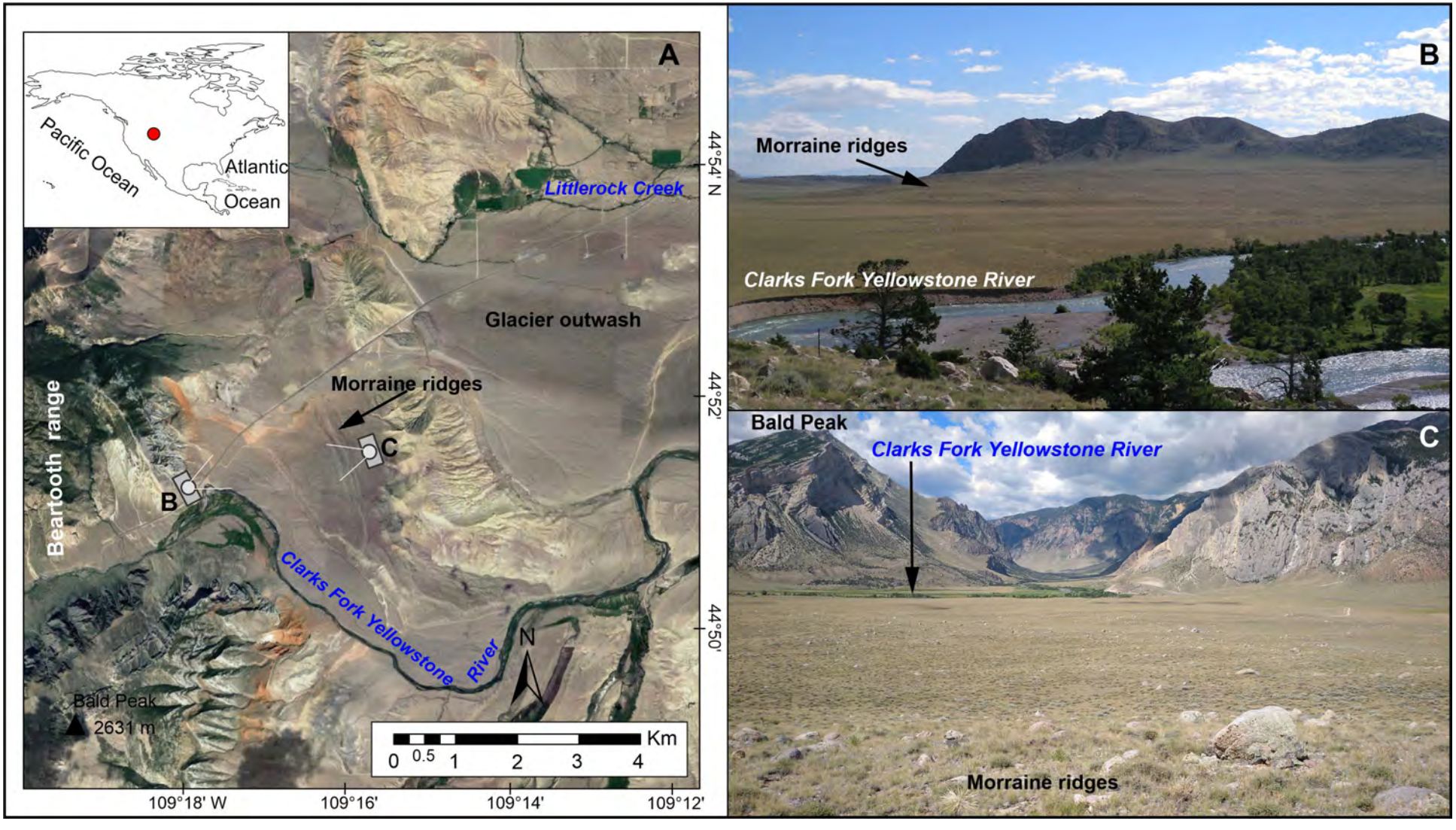
A
Pacific Ocean
Atlantic Ocean
Littlerock Creek
Glacier outwash
Morraine ridges
C
B
Beartooth range
Clarks Fork Yellowstone River
N
Bald Peak
2631 m
0 0.5 1 2 3 4 Km
44°54' N
44°52'
44°50'
109°18' W
109°16'
109°14'
109°12'
B
Morraine ridges
Clarks Fork Yellowstone River
Bald Peak
C
Clarks Fork Yellowstone River
Morraine ridges

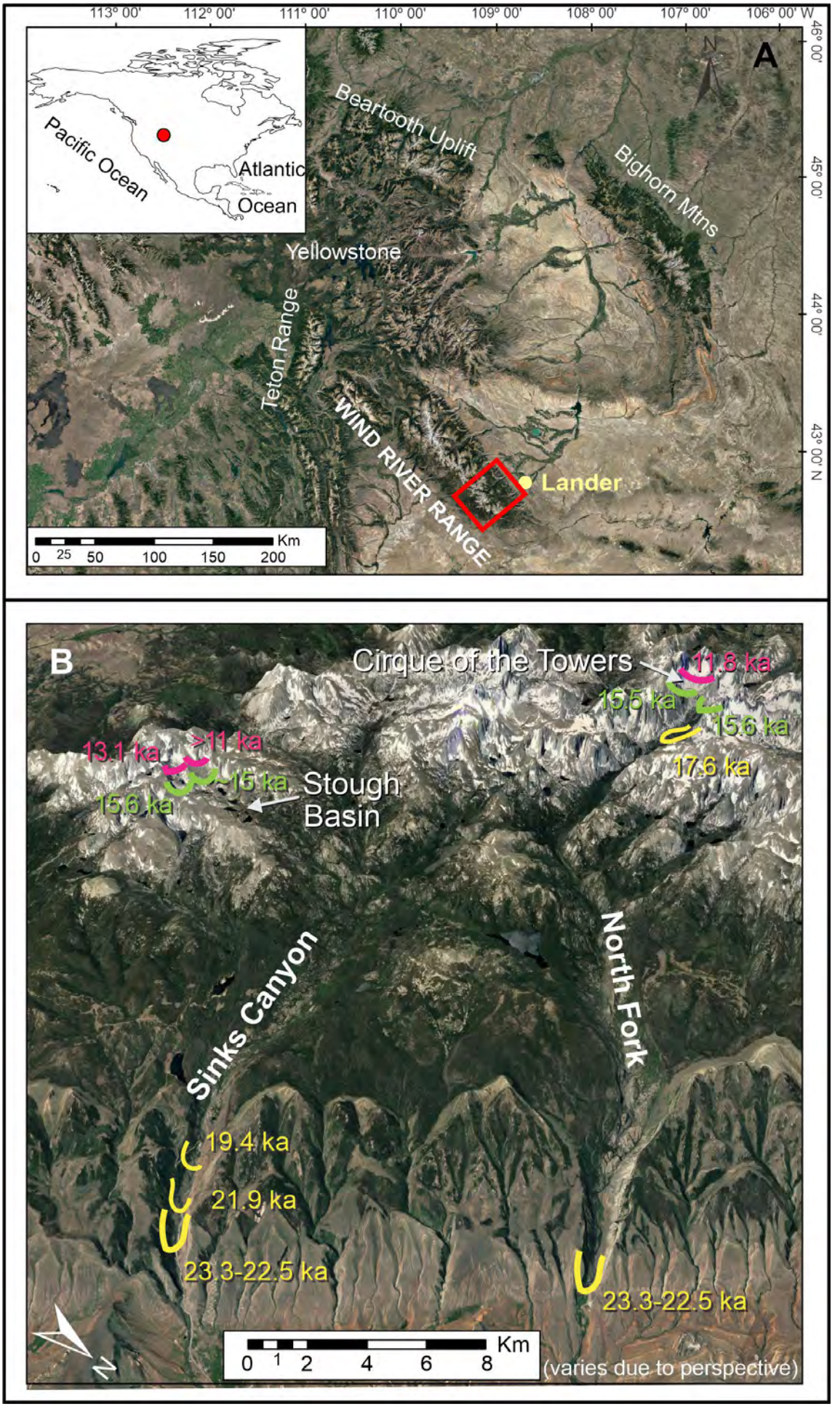
A
113° 00'
112° 00'
111° 00'
110° 00'
109° 00'
108° 00'
107° 00'
106° 00' W
46° 00'
45° 00'
44° 00'
43° 00' N
N
Pacific Ocean
Atlantic Ocean
Beartooth Uplift
Bighorn Mtns
Yellowstone
Teton Range
WIND RIVER RANGE
Lander
Km
0 25 50 100 150 200
B
Cirque of the Towers
11.8 ka
15.5 ka
15.6 ka
17.6 ka
13.1 ka
>11 ka
~15 ka
15.6 ka
Stough Basin
Sinks Canyon
North Fork
19.4 ka
21.9 ka
23.3-22.5 ka
23.3-22.5 ka
N
Km
0 1 2 4 6 8
(varies due to perspective)

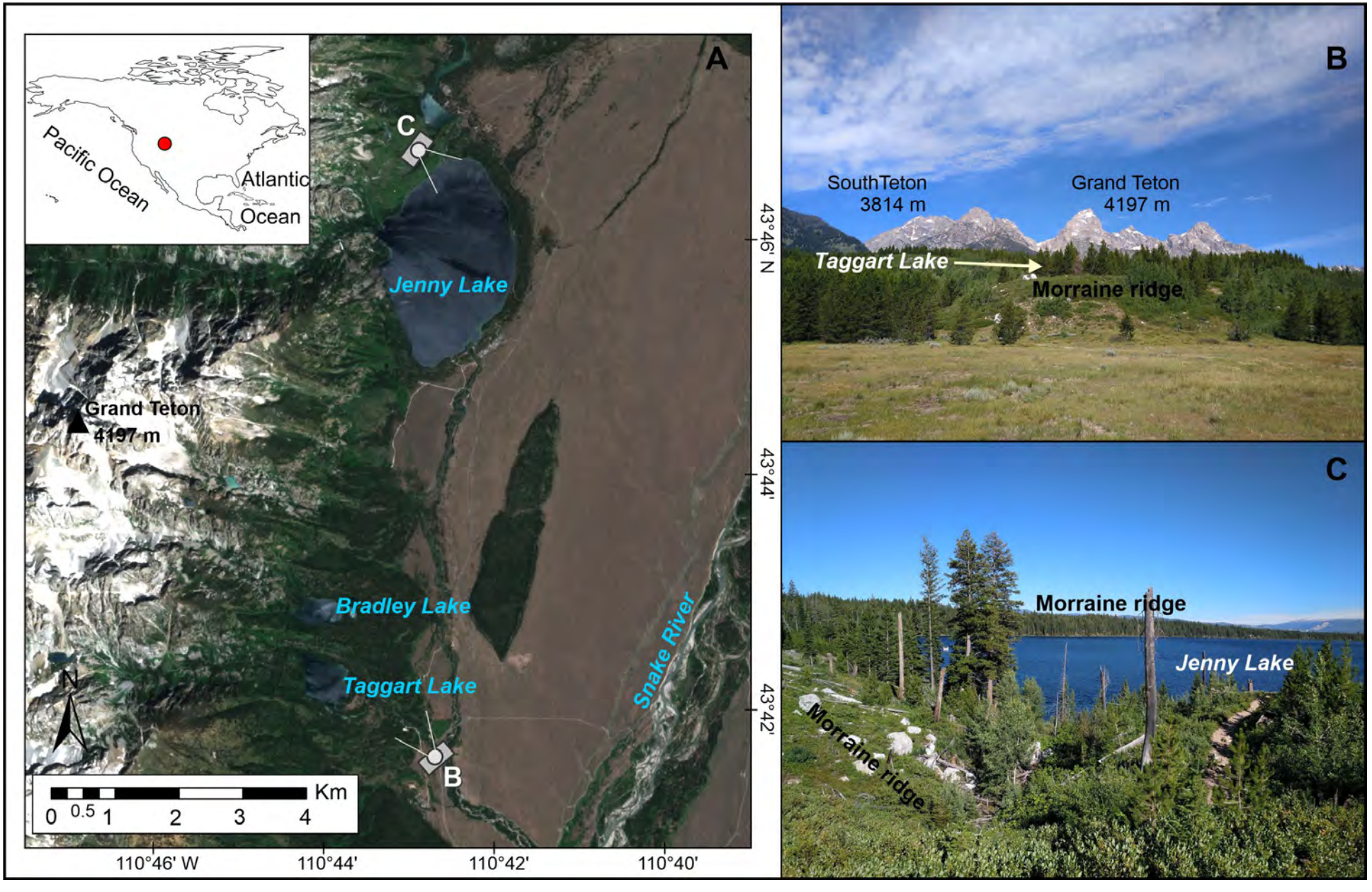
A
Pacific Ocean
Atlantic Ocean
C
B
Jenny Lake
Grand Teton
4197 m
Bradley Lake
Taggart Lake
Snake River
N
0 0.5 1 2 3 4 Km
110°46' W
110°44'
110°42'
110°40'
43°46' N
43°44'
43°42'
B
SouthTeton
3814 m
Grand Teton
4197 m
Taggart Lake
Morraine ridge
C
Morraine ridge
Jenny Lake
Morraine ridge

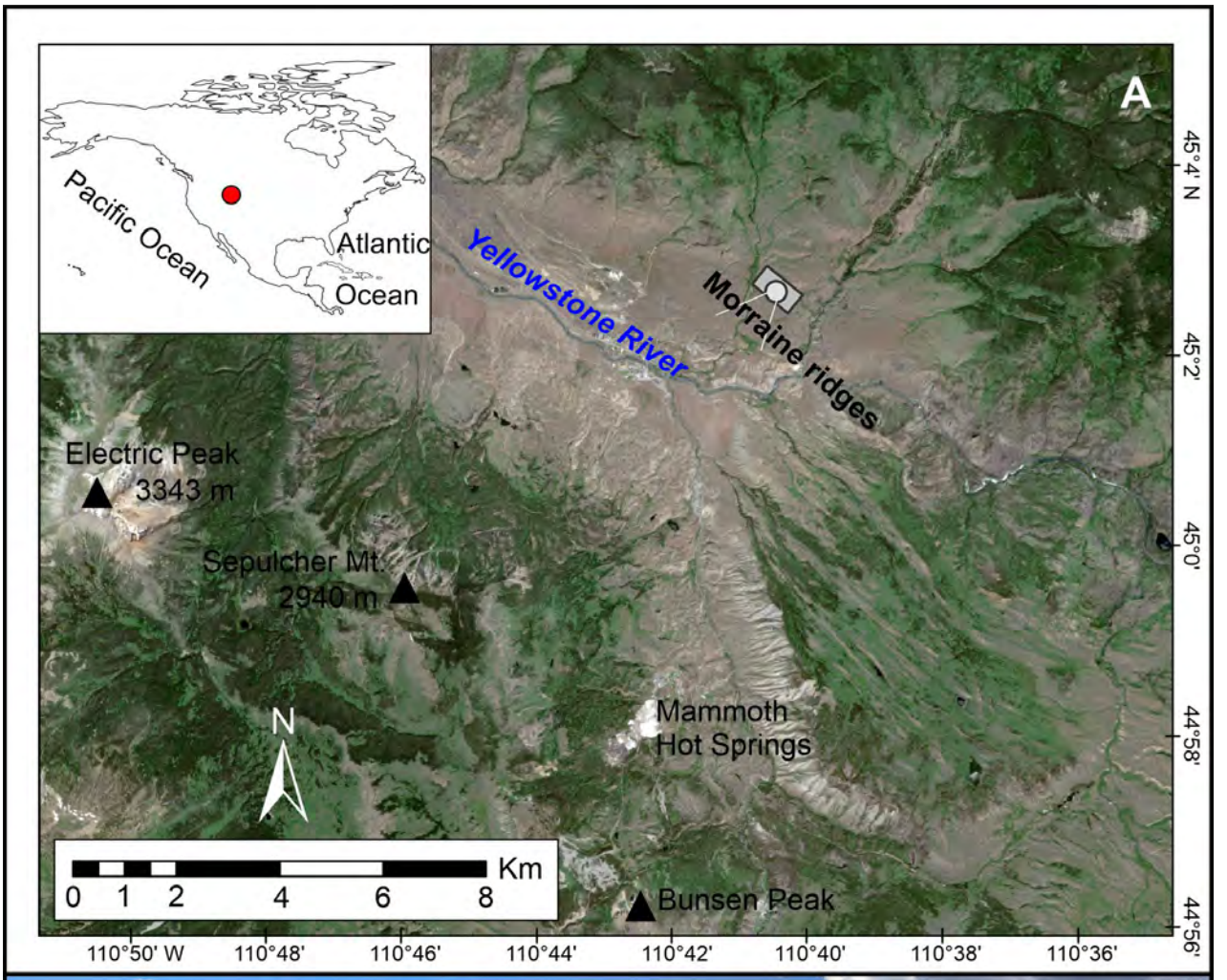
A
Pacific Ocean
Atlantic Ocean
Yellowstone River
Morraine ridges
Electric Peak
3343 m
Sepulcher Mt.
2940 m
Mammoth
Hot Springs
Bunsen Peak
N
0 1 2 4 6 8 Km
45°4' N
45°2'
45°0'
44°58'
44°56'
110°50' W
110°48'
110°46'
110°44'
110°42'
110°40'
110°38'
110°36'

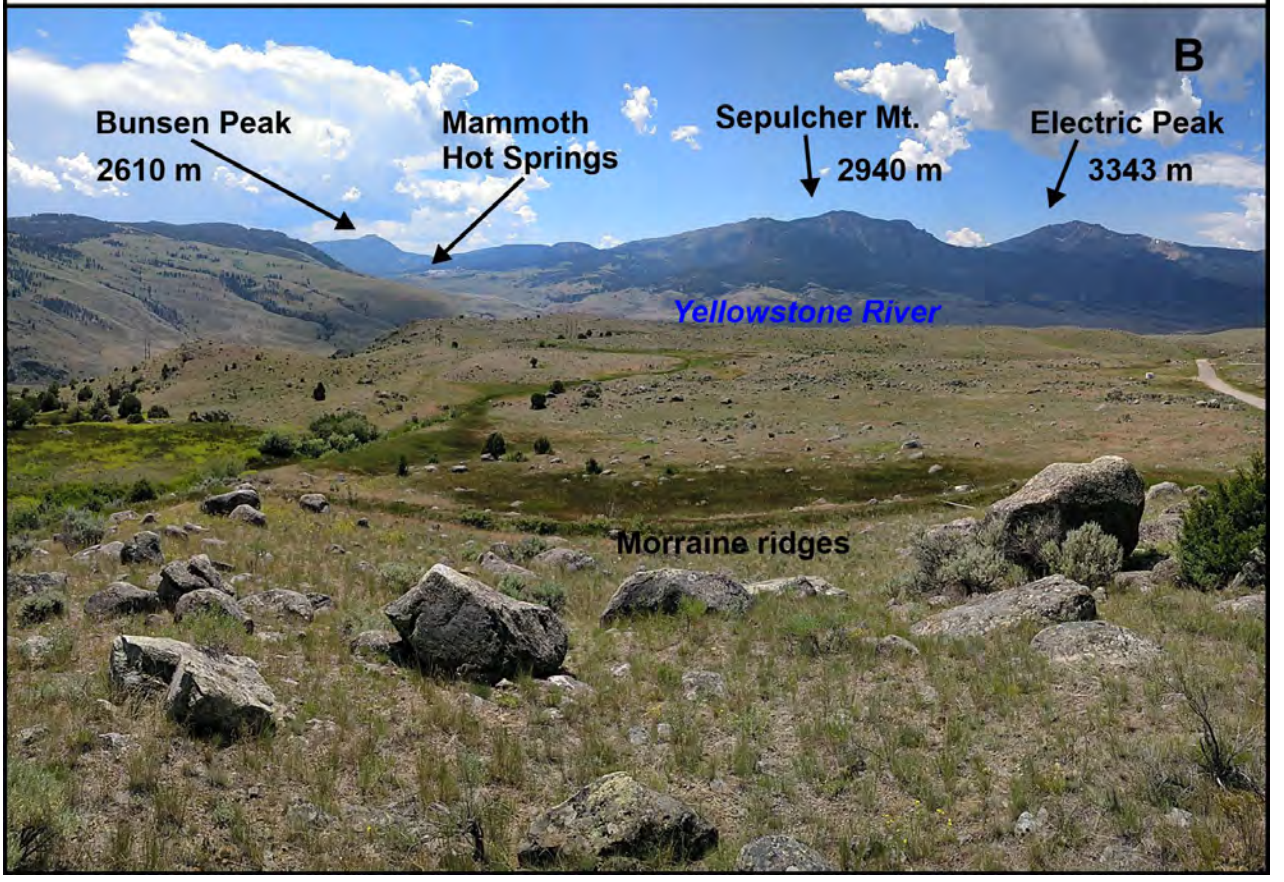
B
Bunsen Peak
2610 m
Mammoth
Hot Springs
Sepulcher Mt.
2940 m
Electric Peak
3343 m
Yellowstone River
Morraine ridges

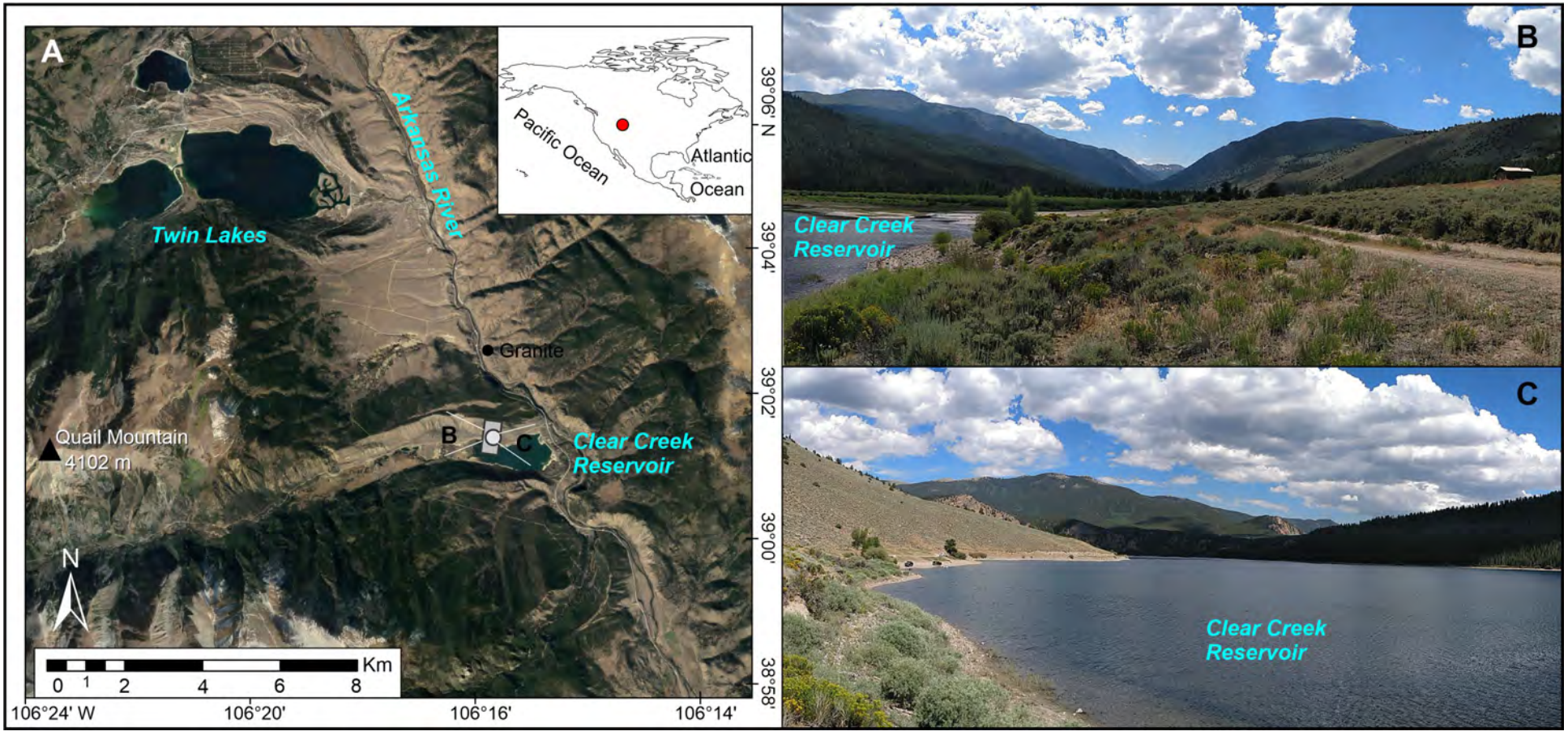
A
Twin Lakes
Arkansas River
Granite
Quail Mountain
4102 m
B
C
Clear Creek
Reservoir
Pacific Ocean
Atlantic
Ocean
N
0 1 2 4 6 8 Km
106°24' W
106°20'
106°16'
106°14'
39°06' N
39°04'
39°02'
39°00'
38°58'
B
Clear Creek
Reservoir
C
Clear Creek
Reservoir

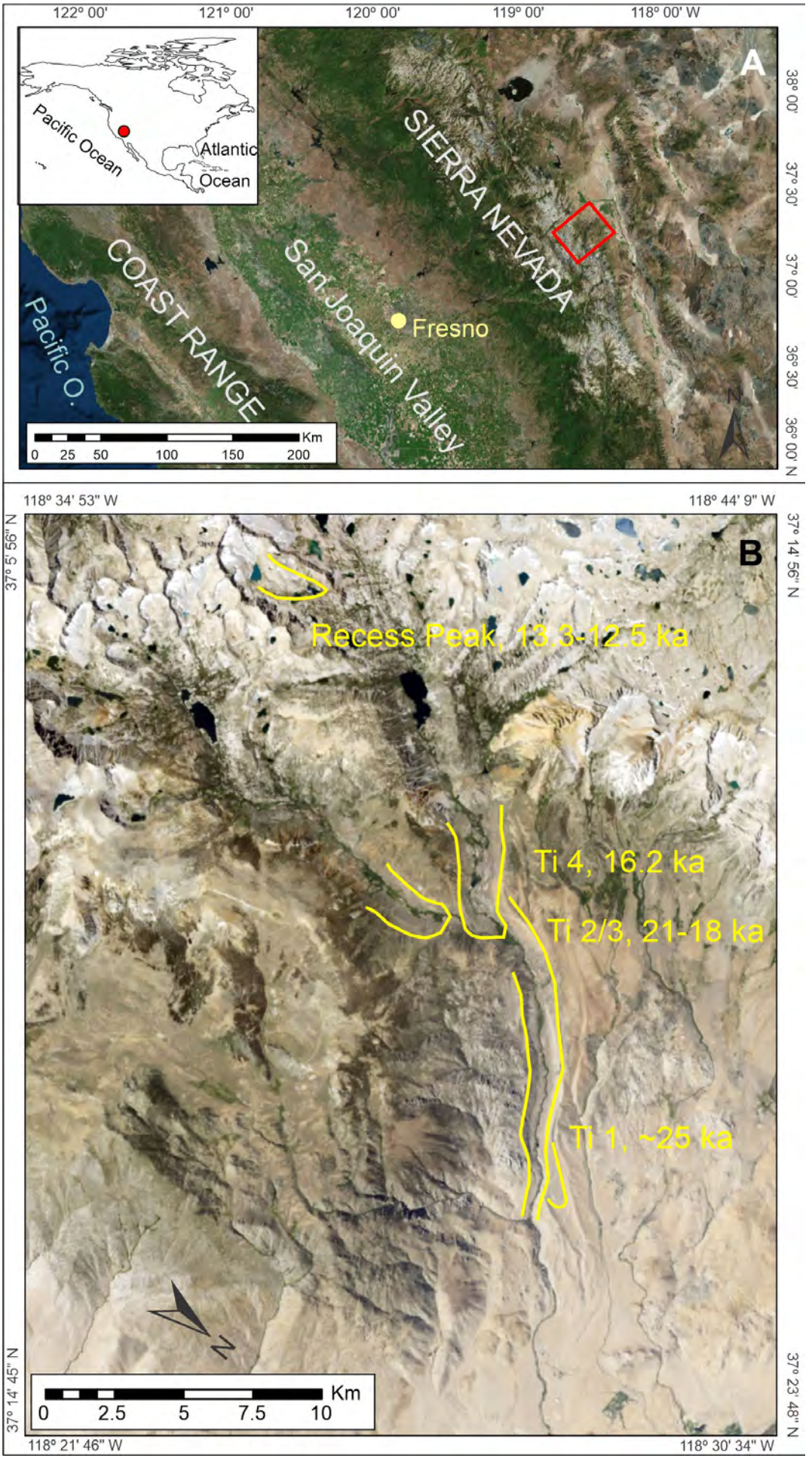
122° 00'
121° 00'
120° 00'
119° 00'
118° 00' W
A
Pacific Ocean
Atlantic Ocean
SIERRA NEVADA
COAST RANGE
San Joaquin Valley
Fresno
Pacific O.
Km
0 25 50 100 150 200
38° 00'
37° 30'
37° 00'
36° 30'
36° 00' N
118° 34' 53" W
118° 44' 9" W
37° 5' 56" N
37° 14' 56" N
B
Recess Peak, 13.3-12.5 ka
Ti 4, 16.2 ka
Ti 2/3, 21-18 ka
Ti 1, ~25 ka
N
Km
0 2.5 5 7.5 10
37° 14' 45" N
37° 23' 48" N
118° 21' 46" W
118° 30' 34" W

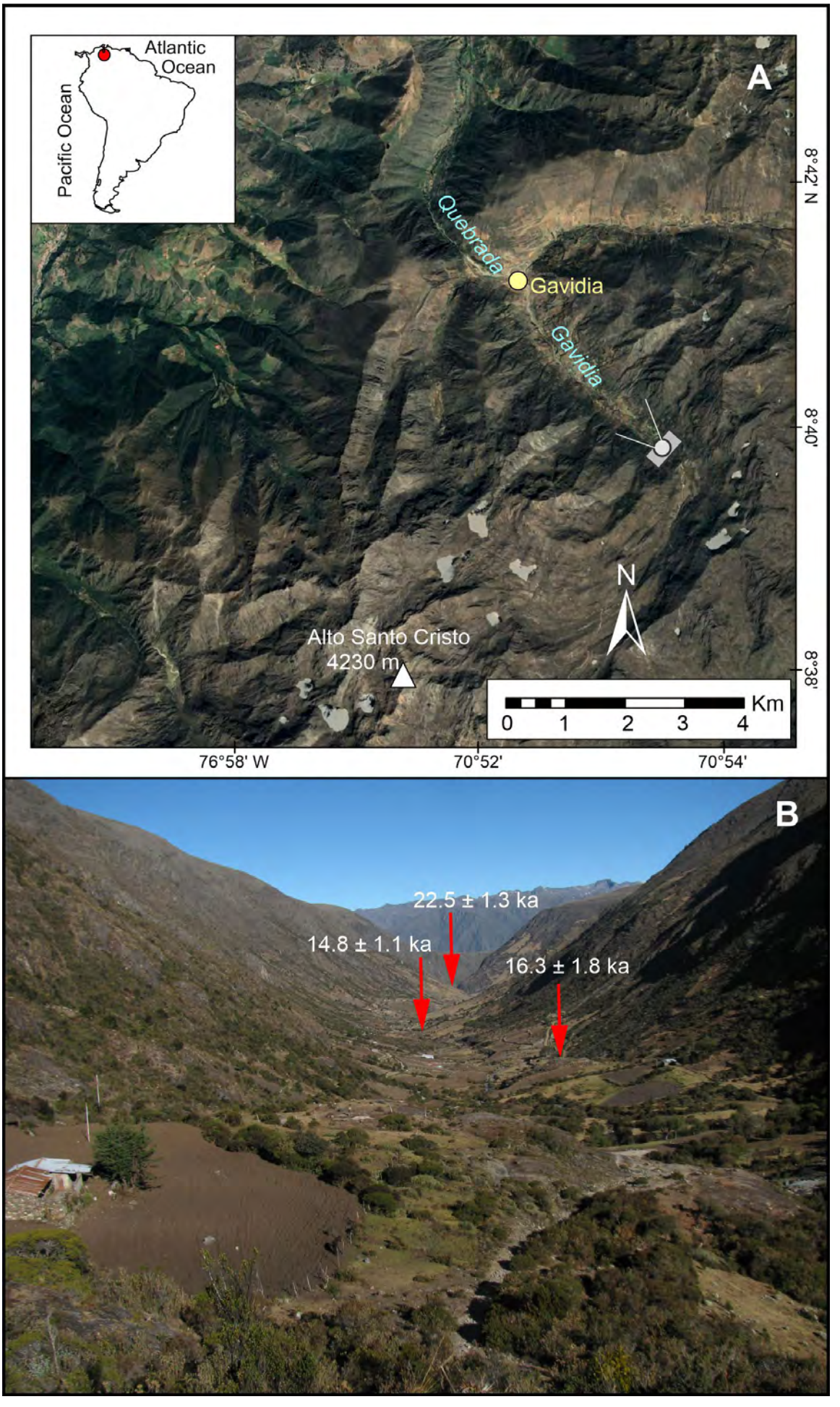
A
Atlantic Ocean
Pacific Ocean
Quebrada Gavidia
Gavidia
Alto Santo Cristo
4230 m
N
Km
0 1 2 3 4
8°42' N
8°40'
8°38'
76°58' W
70°52'
70°54'
B
22.5 ± 1.3 ka
14.8 ± 1.1 ka
16.3 ± 1.8 ka

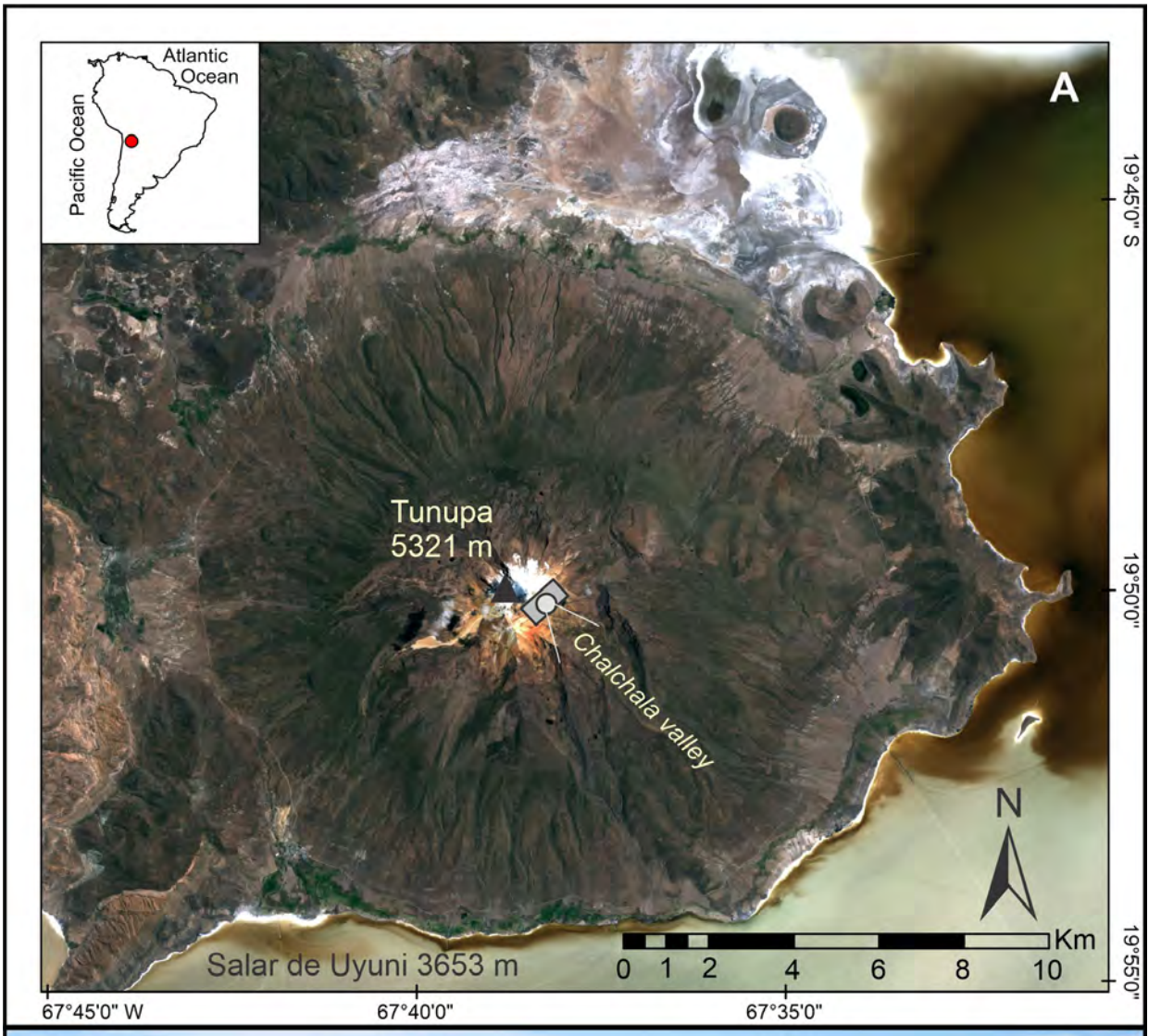
A
Atlantic Ocean
Pacific Ocean
Tunupa
5321 m
C
Chalchala valley
N
Km
0 1 2 4 6 8 10
Salar de Uyuni 3653 m
19°45'0" S
19°50'0"
19°55'0"
67°45'0" W
67°40'0"
67°35'0"

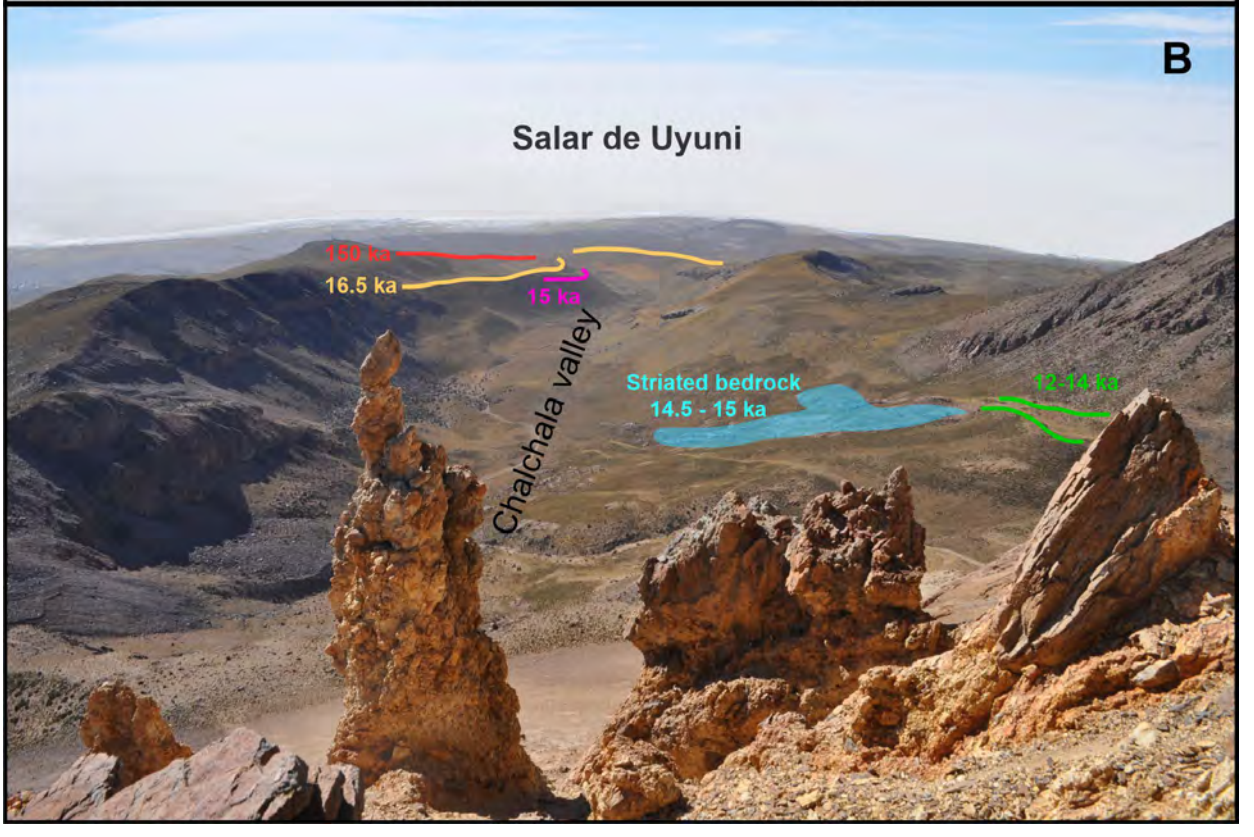
B
Salar de Uyuni
150 ka
16.5 ka
15 ka
Chalchala valley
Striated bedrock
14.5 - 15 ka
12-14 ka

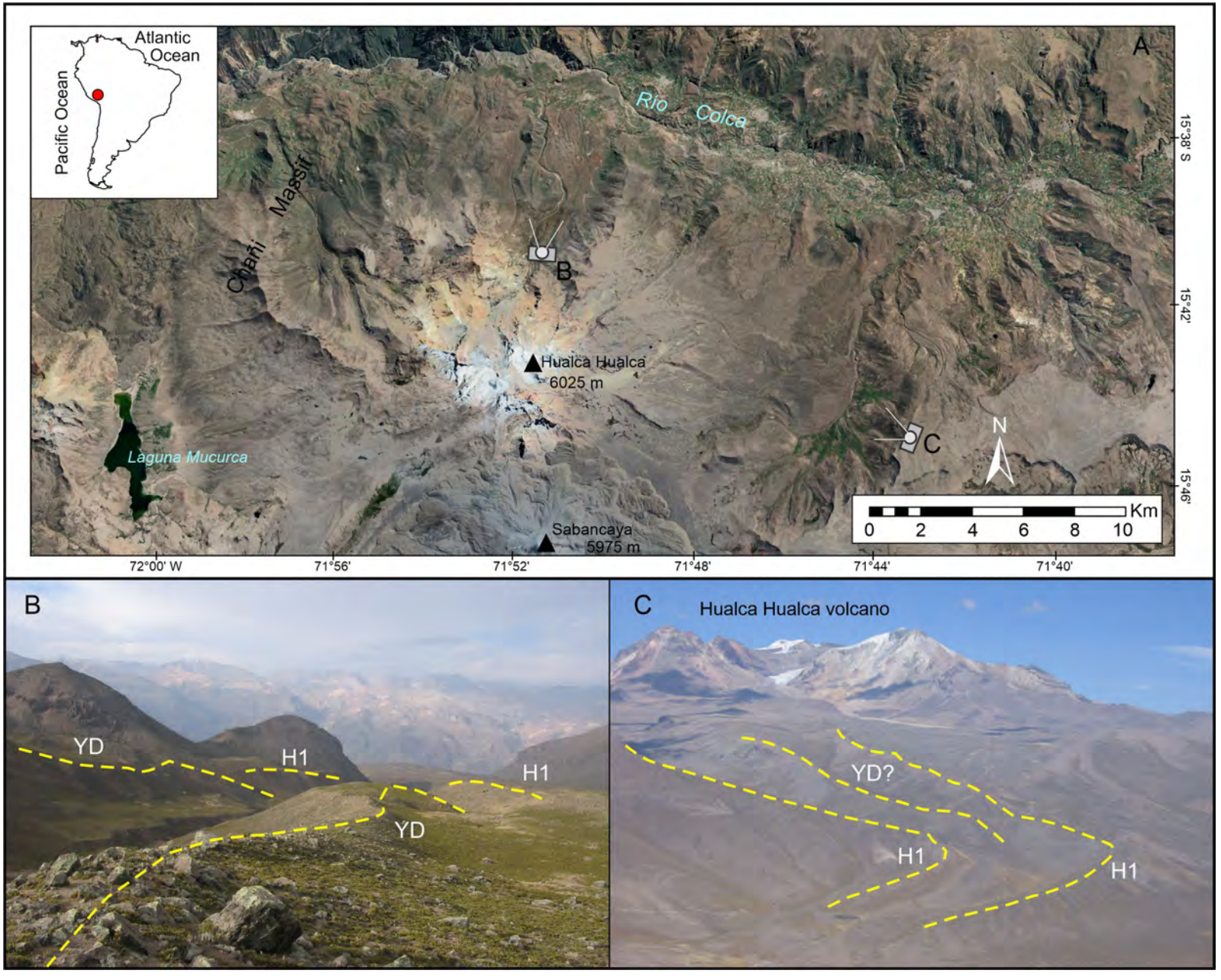
Atlantic Ocean
Pacific Ocean
A
Rio Colca
Chani Massif
B
Hualca Hualca
6025 m
Laguna Mucurca
Sabancaya
5975 m
C
N
Km
0 2 4 6 8 10
15°38' S
15°42'
15°46'
72°00' W
71°56'
71°52'
71°48'
71°44'
71°40'
B
YD
H1
H1
YD
C
Hualca Hualca volcano
YD?
H1
H1

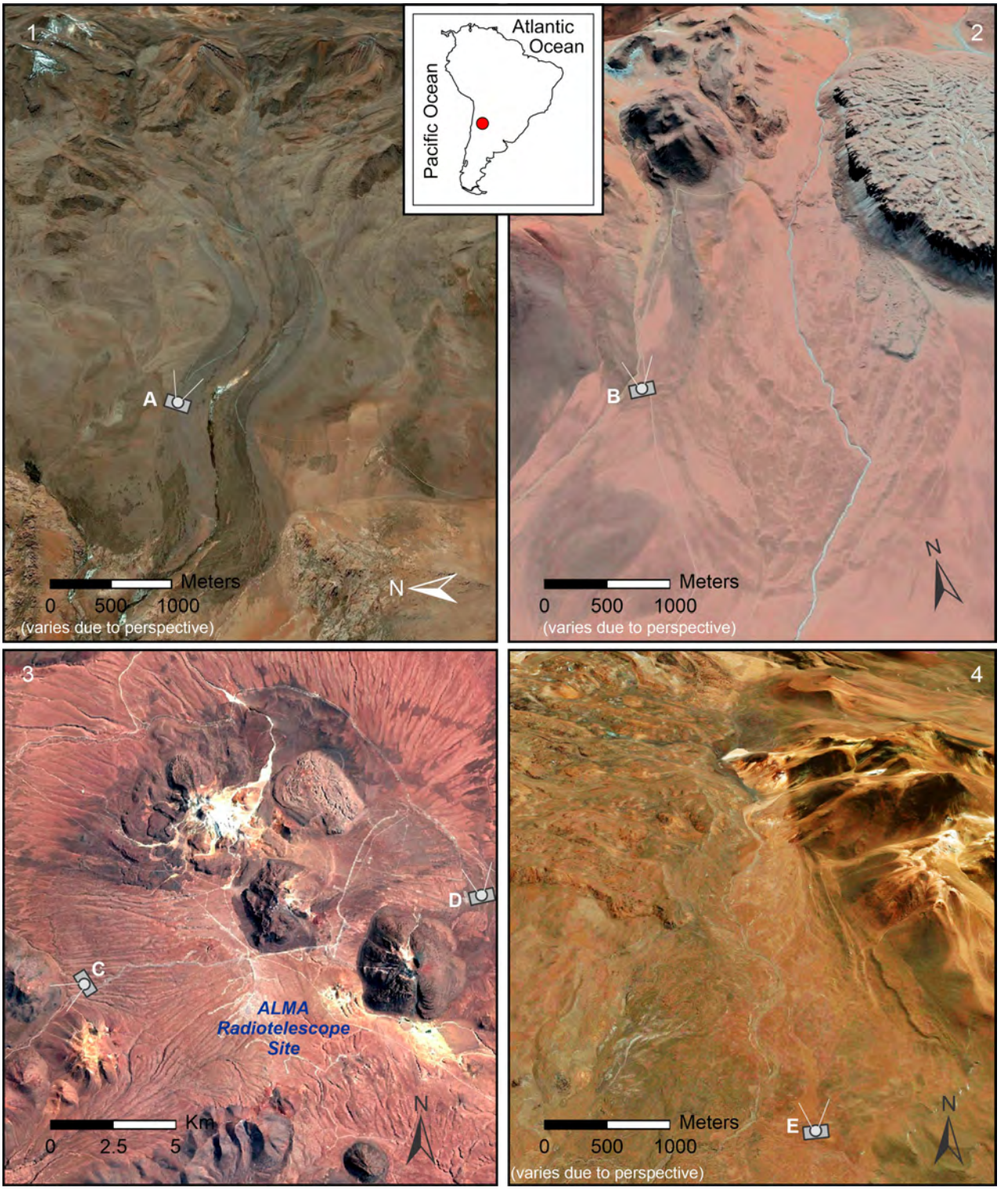
1
A
Meters
0 500 1000
(varies due to perspective)
N
Atlantic Ocean
Pacific Ocean
2
B
Meters
0 500 1000
(varies due to perspective)
N
3
D
C
ALMA
Radiotelescope
Site
Km
0 2.5 5
N
4
E
Meters
0 500 1000
(varies due to perspective)
N

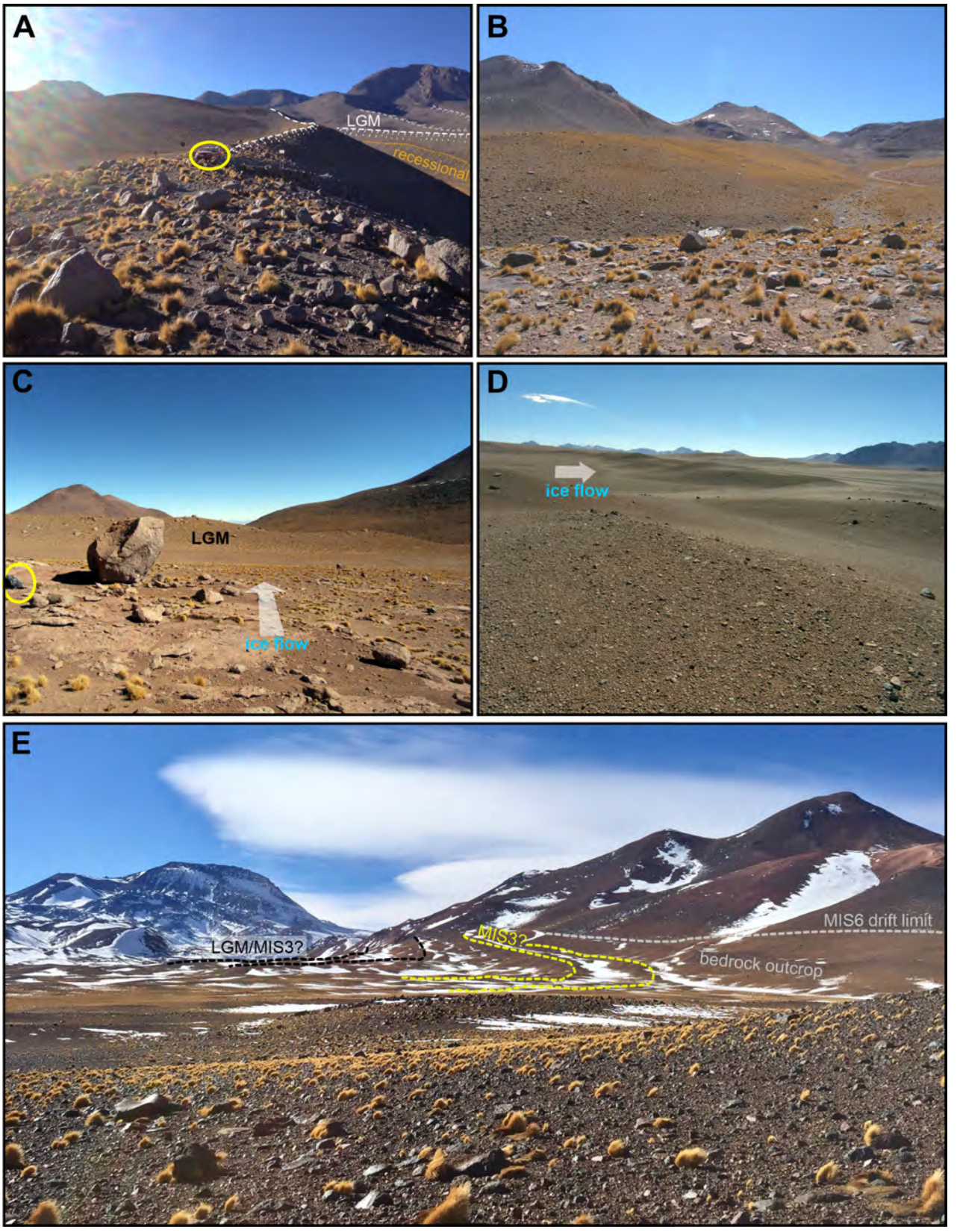
A
LGM
recessional
B
C
LGM
ice flow
D
ice flow
E
LGM/MIS3?
MIS3?
MIS6 drift limit
bedrock outcrop

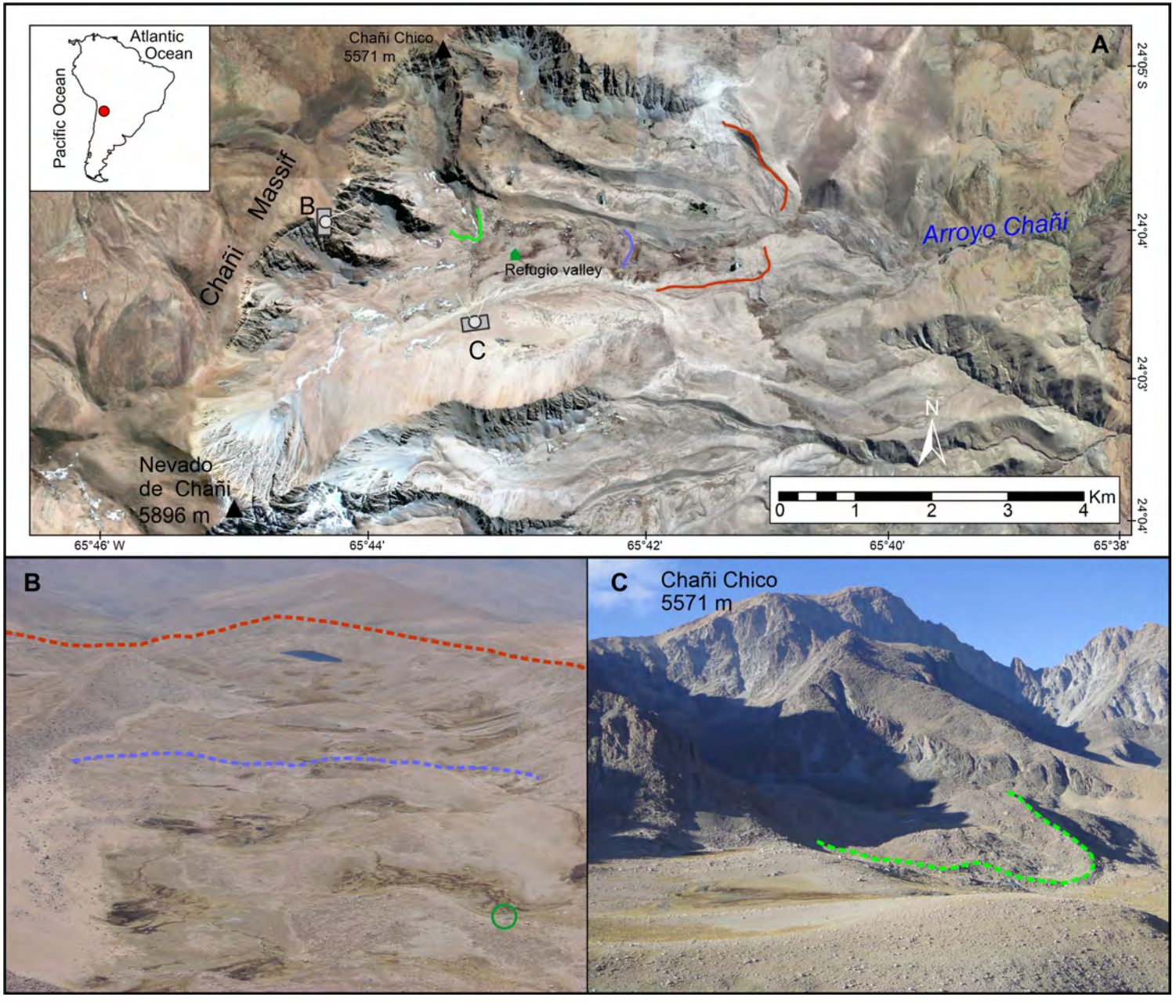
A
Atlantic Ocean
Pacific Ocean
Chañi Chico
5571 m
Chañi Massif
B
C
Refugio valley
Arroyo Chañi
Nevado
de Chañi
5896 m
N
0 1 2 3 4 Km
24°05' S
24°04'
24°03'
24°04'
65°46' W
65°44'
65°42'
65°40'
65°38'
B
C
Chañi Chico
5571 m

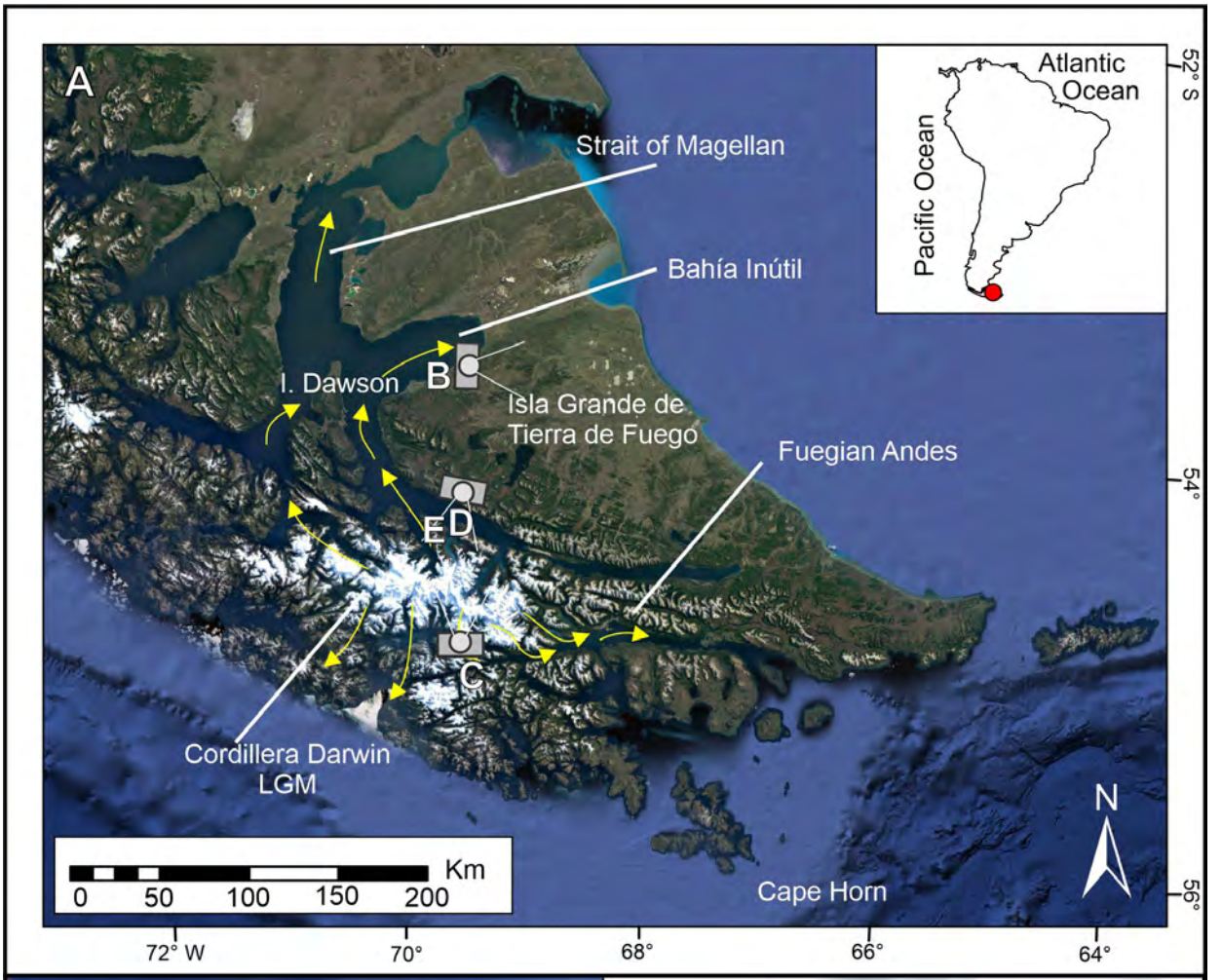
A
Strait of Magellan
Bahía Inútil
I. Dawson
B
C
Isla Grande de
Tierra de Fuego
Fuegian Andes
E
D
C
Cordillera Darwin
LGM
Km
0
50
100
150
200
Cape Horn
N
Atlantic
Ocean
Pacific Ocean
52° S
54°
56°
72° W
70°
68°
66°
64°


LGM moraine
B


C

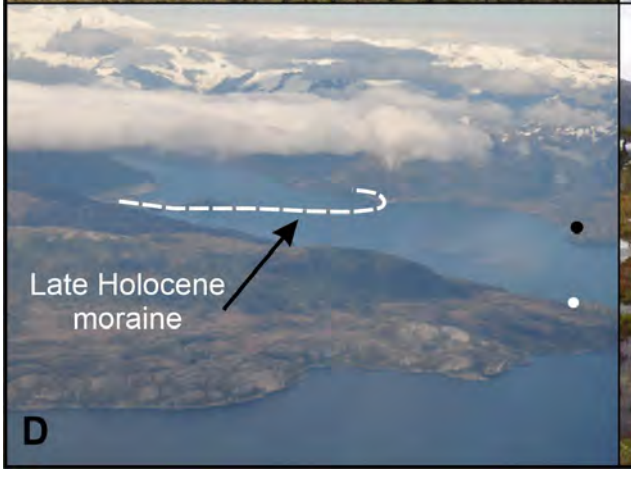
Late Holocene
moraine
D


Late Holocene
moraine
E

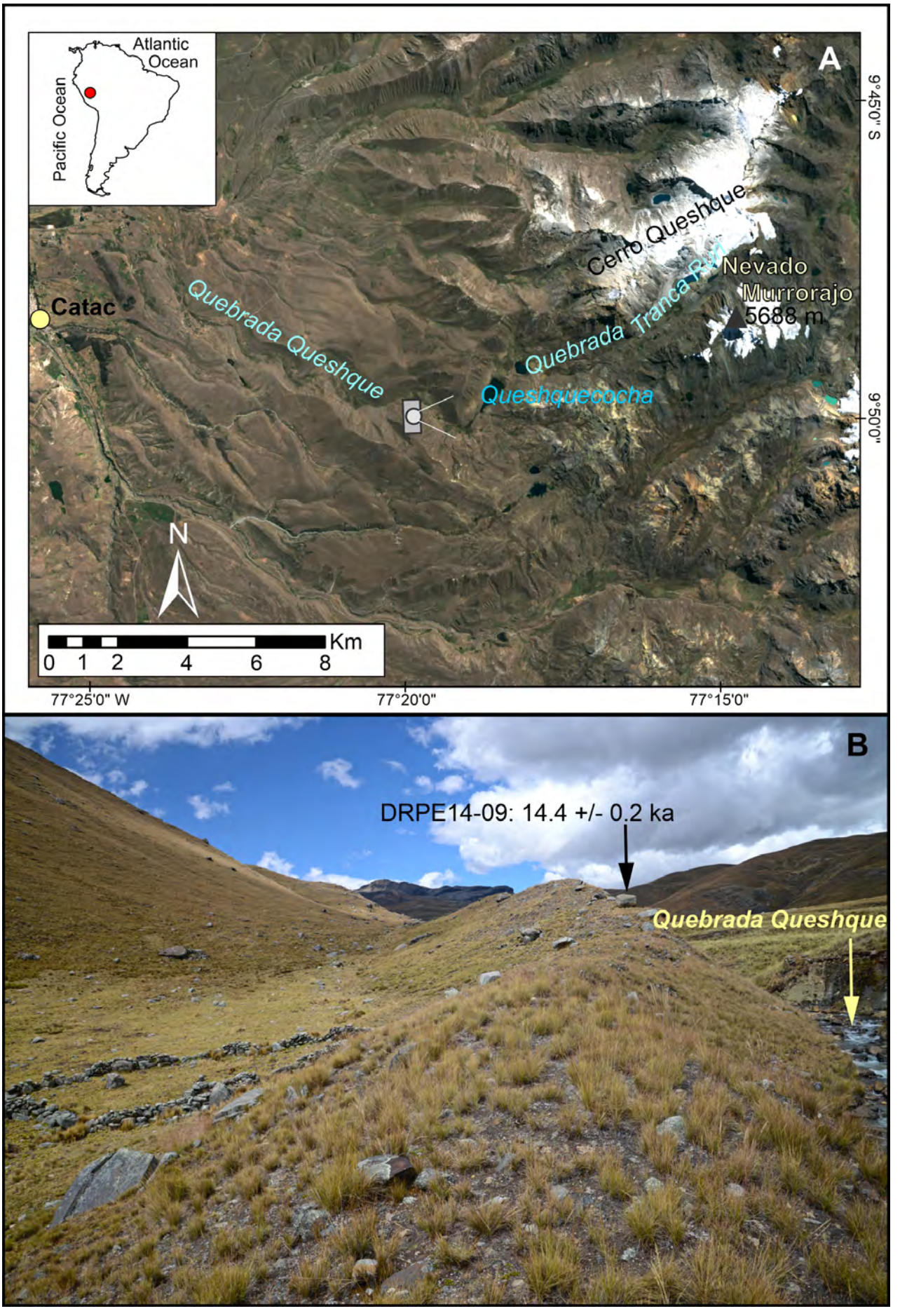
A
Atlantic Ocean
Pacific Ocean
Catac
Quebrada Queshque
Cerro Queshque
Nevado Murrorajo 5688 m
Quebrada Tranca-Rua
Queshquecocha
C
N
Km
0 1 2 4 6 8
9°45'0" S
9°50'0"
77°25'0" W
77°20'0"
77°15'0"
B
DRPE14-09: 14.4 +/- 0.2 ka
Quebrada Queshque

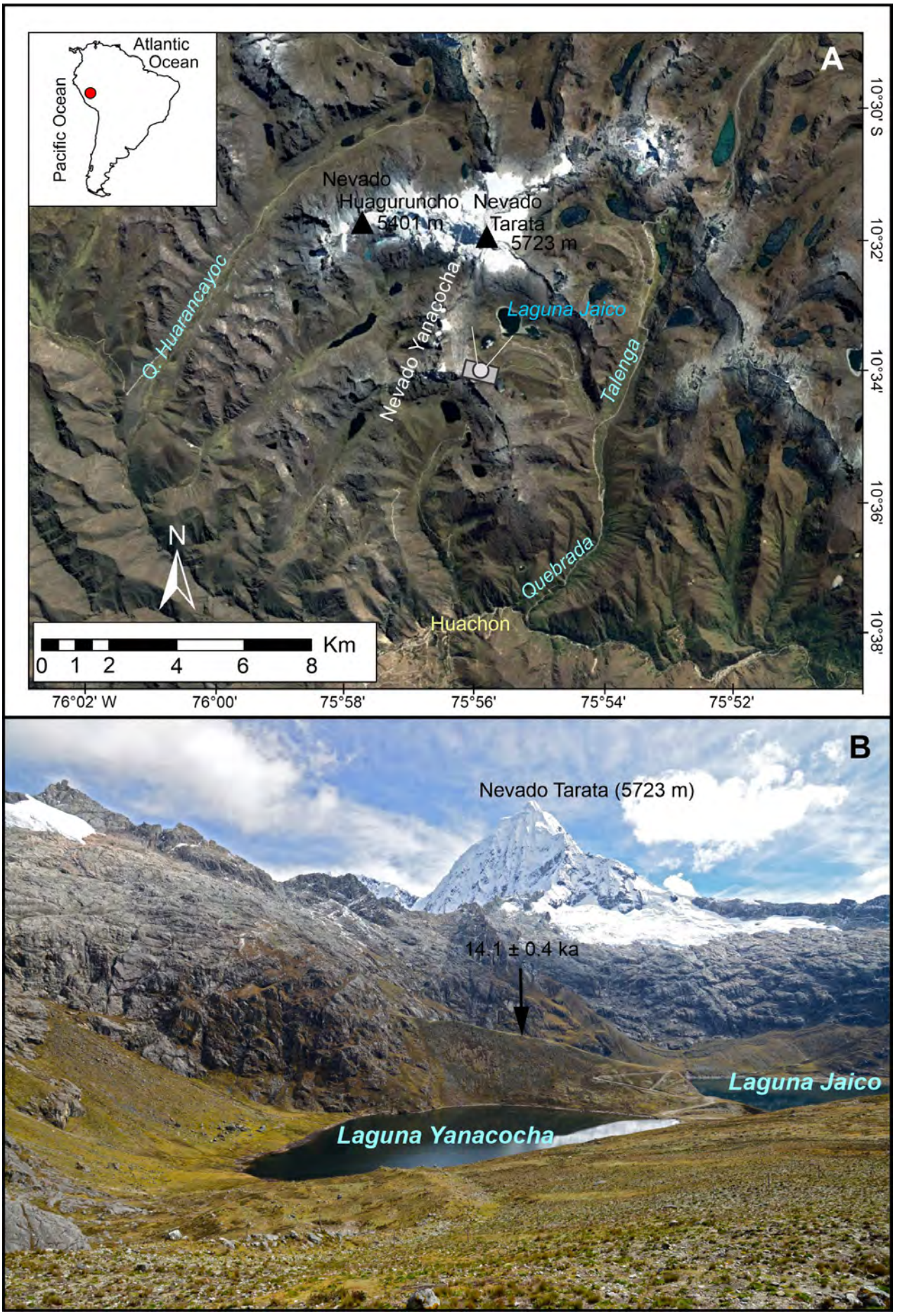
A
Atlantic Ocean
Pacific Ocean
Nevado Huaguruncho 5401 m
Nevado Tarata 5723 m
Q. Huarancayoc
Nevado Yanacocha
Laguna Jaico
Talenga
Quebrada
Huachon
N
0 1 2 4 6 8 Km
10°30' S
10°32'
10°34'
10°36'
10°38'
76°02' W
76°00'
75°58'
75°56'
75°54'
75°52'
B
Nevado Tarata (5723 m)
14.1 ± 0.4 ka
Laguna Jaico
Laguna Yanacocha

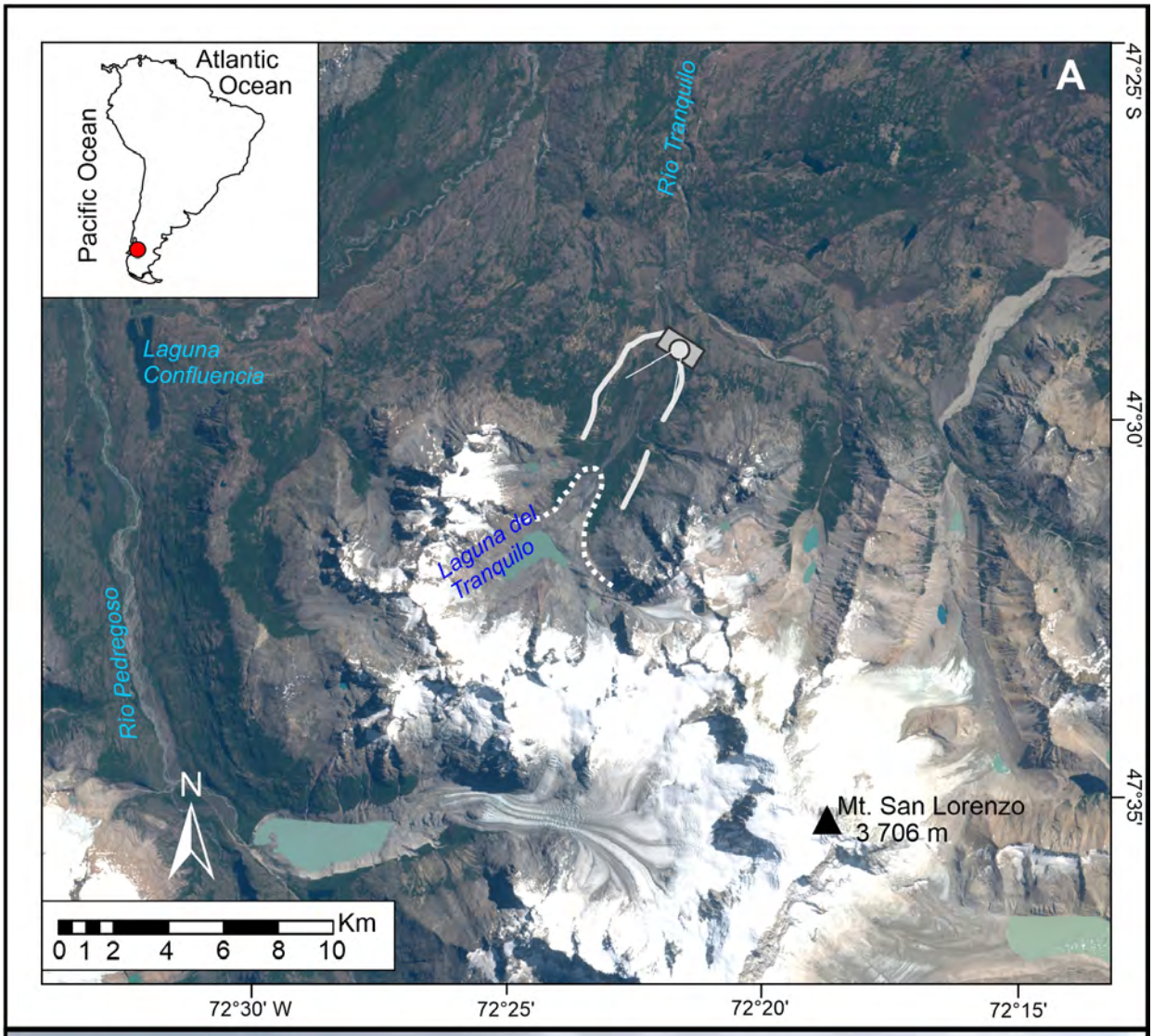
A
Atlantic Ocean
Pacific Ocean
Río Tranquilo
Laguna Confluencia
Laguna del Tranquilo
Río Pedregoso
N
Mt. San Lorenzo
3 706 m
Km
0 1 2 4 6 8 10
47°25' S
47°30'
47°35'
72°30' W
72°25'
72°20'
72°15'


B
Mt. San Lorenzo summit
3 706 m
Landslide
Río Tranquilo

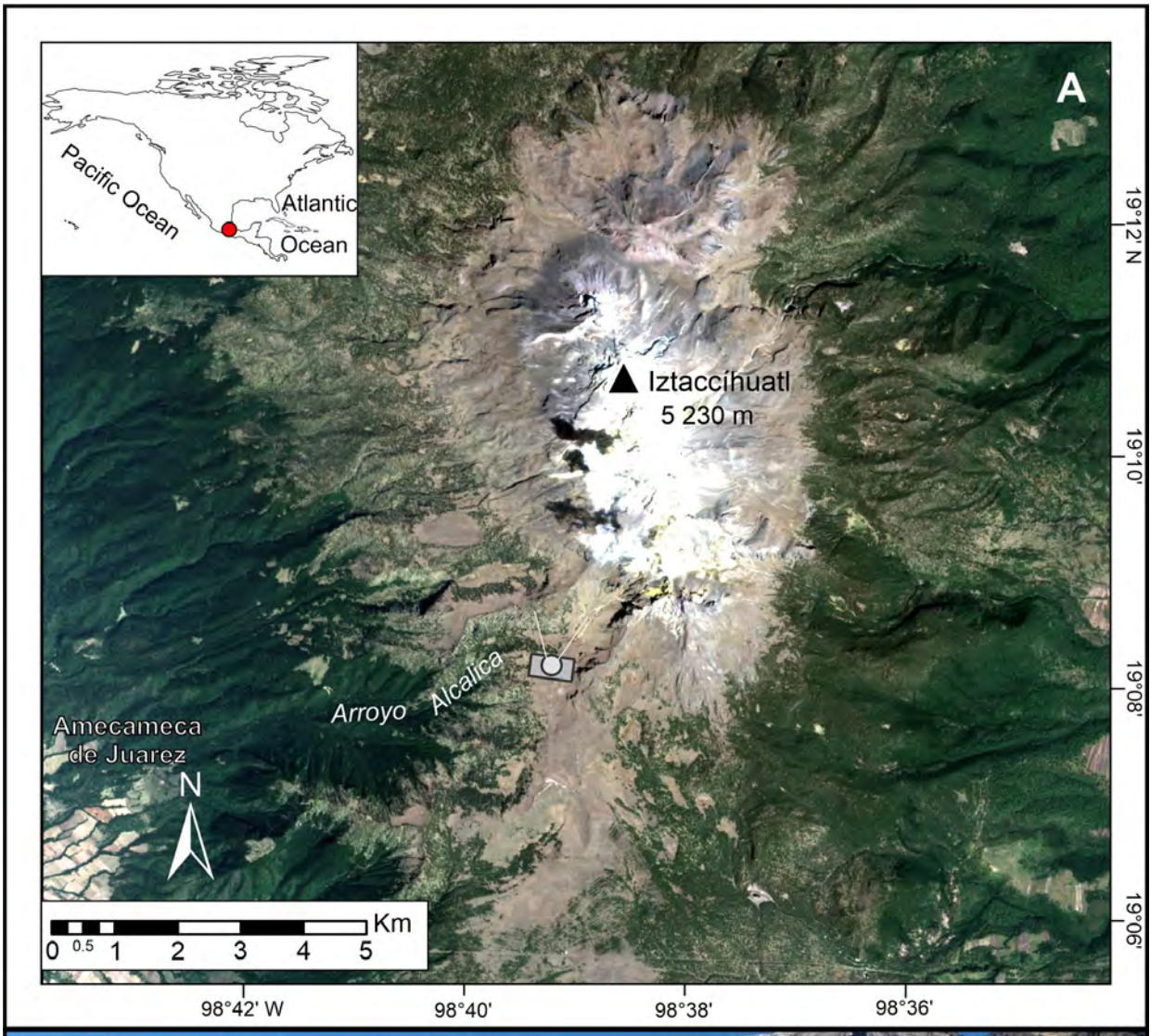
A
Pacific Ocean
Atlantic
Ocean
Iztaccíhuatl
5 230 m
Arroyo
Alcalica
Amecameca
de Juarez
N
Km
0 0.5 1 2 3 4 5
19°12' N
19°10'
19°08'
19°06'
98°42' W
98°40'
98°38'
98°36'

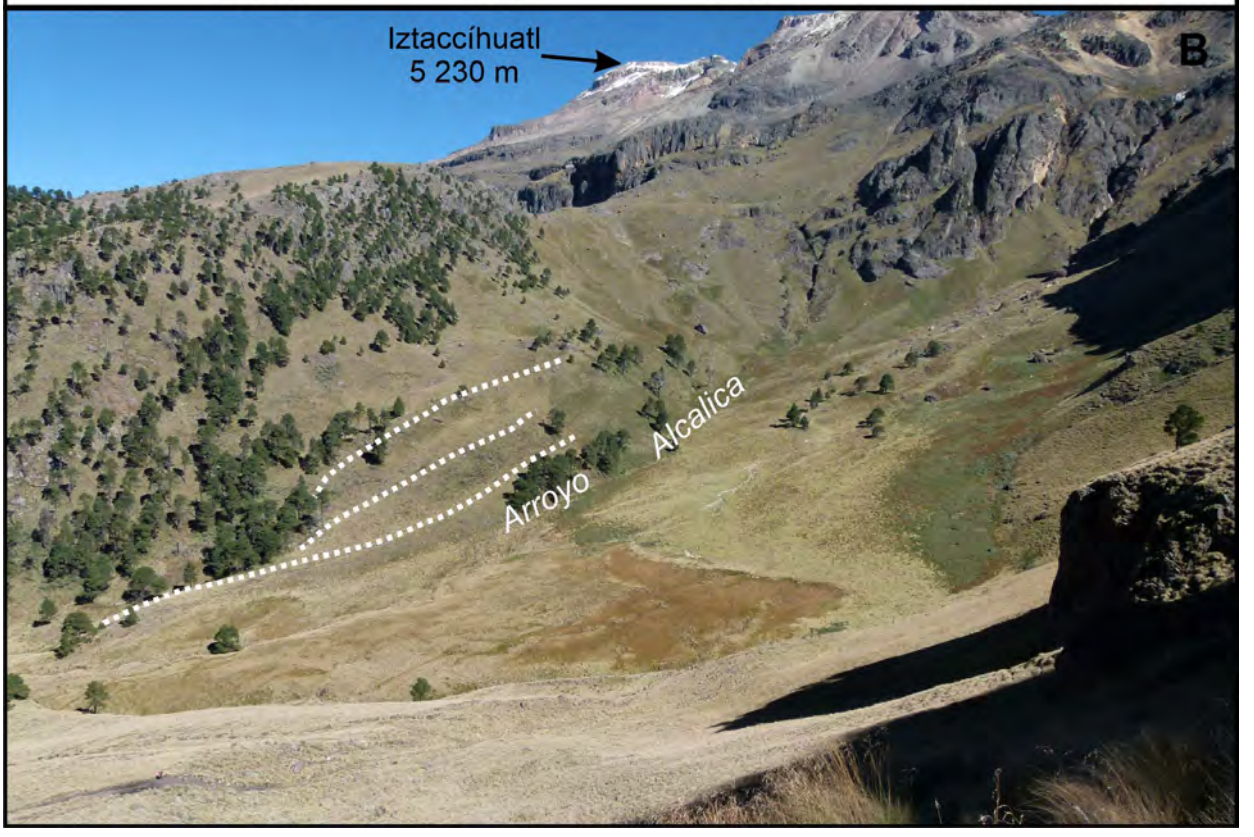
Iztaccíhuatl
5 230 m
B
Arroyo
Alcalica

Table 1. The main climate and glacial evolution features during the Global Last Glacial Maximum (26.5 to 19 ka) in the Americas

REGION	Climate during GLGM in relation to present	ELA depression in LGM in relation to present	Local Last Maximum Ice Extension and its relation to GLGM	Initial deglaciation chronology	Key References
Laurentia	6-7 ˚C colder and great local variability in precipitation		During GLGM Probably from 28 to 20 ka (even 17 ka) with great local variability LIS near-maximum extent for several thousand years	23 to 20 ka, depending on area, but slow prior to 17 ka	Dyke et al., 2002; Ullman et al., 2015b; Robel and Tziperman, 2016; Stokes et al., 2016; Margold et al., 2015; 2018; Stokes, 2017
Alaska	More arid and relatively warm conditions	200-500 m	During GLGM From 24 to 21 ka in the whole region	~20 ka	Kaufman et al., 2003; Tulenko et al., 2018; Pendleton et al., 2015; 2012; Putnam et al., 2013; Briner et al., 2017
Cordillera Ice Sheet and North Cascades	6-7 ºC colder and 40% lower mean annual precipitation	1000–750 m	CIS in the north during GLGM and in the west and south, later up to 16 ka During LGM in North Cascades, from 25 to 21 ka	From 21 to 16 ka	Clague, 2017; Riedel et al. 2010; Bartlein et al. 2011; Riedel, 2017
Yellowstone-Tetons	Around 5.4ºC colder and similar precipitation as at present	900 m	During GLGM From ~22 ka, but in some valleys up to 17-16 ka	~20 to 17 ka, depending of the valleys	Licciardi and Pierce, 2018; Pierce, et al., 2018
Wind River Range, WY	(Est.) > 5.4ºC colder and similar precipitation as at present	~900 m	During GLGM From ~24-22 ka	<22 ka	Dahms 2004; Dahms et al., 2018, 2019; Shakun et al., 2015
Colorado	Around 5.4-8ºC colder and similar precipitation as at present	900 m	During GLGM From ~24 ka, but some valleys up to 17-16 ka	~20 to 17 ka, depending of the valleys	Young et al., 2011; Leonard et al., 2017a, b ; Brugger et al., 2019
Sierra Nevada	5-6ºC lower, 140% higher precipitation	1200 m	During GLGM From 26 to 20 ka	Began at 19 ka and accelerated rapidly after 18 ka	Plummer, 2002; Phillips, 2016, 2017
Mexico	6 - 9°C colder, precipitation lower than modern	1000 m in the interior; 1200-1500 m	During GLGM. Interior part of central Mexico at 21-19 ka, extending to 20-14 ka near the coasts	15 to 14 ka	Vazquez-Selem and Heine, 2011; Vázquez-Selem and Lachniet, 2017

		near the coasts			
Central America	6 - 9°C colder	1100-1400 m	During GLGM and post-LGM Maximum at~25-23 ka in Cordillera Talamanca; subsequent deglaciation and moraines formation ca. 18-16 ka	~17 ka	Roy and Lachniet, 2010; Cunningham, 2019; Potter et al., 2019
Northern Andes	8°C colder and wetter	1420-850 m	Pre-GLGM but during the GLGM, ~21 ka in Sierra Nevada, Venezuela	From ~21 to 16 ka	van der Hammen, T., 1981; Schubert and Rinaldi, 1987; Thouret et al., 1996; Stansell et al., 2007; Brunschön and Behling, 2009; Angel, 2016; Angel et al., 2016; Angel et al., 2017
Peru and Bolivia	~5-8° C colder precipitation was slightly higher	Variability, from 800 to 1200 m	Pre-GLGM; GLGM and post GLGM, with average of 25 ka, from 32 to 17 ka	From ~22 to ~17 ka	Seltzer et al., 2002; Mark et al., 2005; Rodbell et al., 2008; Mark, 2017
Northern Chile	Colder and strong spatial gradients in moisture availability from north to south	900 m	Pre-GLGM 45-35 ka 30-25 ka and GLGM ~22-19 ka, and in some sectors 17-15 ka,	North Arid Diagonal, up to < 15 ka. South 17 ka	Ward et al., 2015; Cesta and Ward, 2016; Ward et al., 2017; Martin et al., 2018
Central Andes of Argentina	Colder and slightly wetter conditions	800 m	Pre-GLGM (~40-50 ka), with LGM minor and variable expansion: between ~26 and ~19 ka	From ~21 ka	Martini et al., 2017; Moreiras et al., 2017; Zech J. et al., 2017; Terrizano et al., 2017; D'Arcy et al., 2019
Patagonia	6-7° C colder and wetter in northern Patagonia	ca. 900 m	Pre-GLGM (~48 and ~30 ka), with LGM minor expansion and variable: between ~26.9 and 18.8 ka	between 19.5-17.5-ka	Moreno et al. 2015; Darvill et al., 2016; Hein et al., 2017; Garcia et al., 2018; Hubbard et al., 2005; Denton et al., 1999
Tierra del Fuego	6-7°C colder	~1000 m?	Pre GLGM? GLGM expansion by ~25 ka, but pre-GLGM moraines may be more extensive	~18 ka	Hall et al., 2013, 2017; Menounos et al., 2013

Table 2. The main climate and glacial evolution features during the Heinrich 1 Stadial (17.5 to 14.6 ka) in the Americas.

REGION	Climate during H-1 in relation to present	ELA depression in H1 in relation to present	Glacial evolution during H-1	Key References
LAURENTIA			No clear evidence for major glacial readvances during or soon after H-1. Important changes in the location of ice dispersal centres, with subsequent effects on ice flow patterns and some lobe advances. In general, ice sheet thinning tendency	Stokes et al., 2005; Koester et al., 2017;
ALASKA	Cold, mild	200-500 m	Identified some standstills or re-advances in glacial fronts at ~17-16.5 ka, but there was significant recession of most of glaciers over all this period	Pendleton et al., 2015; Kopczynski et al., 2017; Briner et al., 2017
Cordillera Ice Sheet and North Cascades	6-7 ºC colder and 40% lower mean annual precipitation influenced by CIS expansion	1000–750 m few hundred meters above the LGM	The ice sheet reached its maximum extent during H-1 Some glaciers left moraines closely nested inside the LGM moraines, that could belong to the H-1 expansion	Cosma et al., 2008; Troost, 2016; Clague, 2017; Kaufman et al., 2004; Porter and Swanson, 2008; Riedel et al., 2010
Yellowstone-Tetons	Colder and similar precipitation	900 m, with great local variability	Some valleys reach their local maximum ice advance at ~17 ka, while others experienced extensive recession.	Licciardi and Pierce, 2018; Pierce et al., 2018
Wind River Range, WY	Est. colder w/ similar precipitation	60-170m (S-to-N)	Stagnant ice remains w/in 13 km of LLGM max in some trunk valleys while riegels become ice-free, suggesting de-coupling of cirque from valley ice ~18-17 ka. 'Temple Lake' moraines form 15-14 ka	Shakun et al., 2015a; Dahms et al., 2018, 2019; Marcott et al., 2019.
Colorado	Colder and similar precipitation	900 m, with great local variability	Some valleys reach their local maximum ice advance at ~17-16 ka, while others experienced extensive recession. Rapid retreat afterwards.	Laabs et al., 2009; Young et al., 2011; Shakun et al., 2015a; Leonard et al., 2017a, b; Brugger et al., 2019
Sierra Nevada	3º colder and 160% of precipitation	900 m	Strong evidence of glacial advance during H1 at 16.2 ka. Extensive retreat afterwards	Plummer, 2002; Phillips, 1996, 2017
Mexico	Cold and dry	900 m in the interior; 1200-1500 m near the coasts	Minor recession in the interior but overall strong evidence of glacial advance or stillstand coeval to H-1 (17-15 ka)	Vázquez-Selem and Lachniet, 2017

Central America	Cold conditions	Unknown	Moraine formation dated at ca. 18-16 ka; glacier recession by 15 ka	Cunningham et al., 2019; Potter et al., 2019
Northern Andes	Cold temperatures but higher than in the LGM	Unknown, but likely with great variability	Local glacial advances from 17.5-15 ka in the context of general deglaciation	Rull, 1998; Brunschön and Behling, 2009; Angel et al., 2016; 2017
Peru and Bolivia	The coldest period since LGM with cooling of ~3°C. Drier in central Peru. In the Altiplano the first part of H1 (~18 to 16.5 ka) was drier, followed by the Lake Tauca highstand from 16.5 to 14.5 ka with an increase of precipitation > 130 %	Large variability, from similar to LGM to few hundred meters	Most of the glaciers retreated just prior to H-1, but multiple glaciers re-advanced during H-1, in Peru and Bolivia, with average moraine age of 16.1 ka with a standard deviation of 1.1 ka	Alcalá-Reygosa, 2017; Mark, 2017; Martin et al., 2018
Northern Chile	~3.5ºC colder and sharp precipitation gradient with decreasing precipitation from Lake Tauca to the south.	900 m of regional difference in relation to precipitation distribution	Moraines dating to the LGM and earlier were overridden during the Tauca highstand wet phase (~17-15 ka) in mountains surrounding Lake Tauca, but to the south the Tauca-phase moraine is either absent or found high in the valleys.	Ward et al., 2017; Martin et al., 2018
Central Andes of Argentina	Glacial advances occurred synchronous with the expansion of Altiplano lakes	620 m	New advances in some sectors between 17 and 15 ka and in other sectors, deglaciation from 17 ka. Moraines of H-1 located up-valley from those of the LGM.	Zech J. et al., 2009 , 2017; Martini et al., 2017;
Patagonia	Warming tendency throughout the period. Average interglacial temperatures by 16.8 ka	Trending toward values similar to the present	Widespread deglaciation along the region, with exception of short stabilization at ~16.9-16.2 ka in a few glaciers. Glaciers in central Patagonia were near to modern ice limits before ~16 ka	Boex et al. 2013; Moreno et al. 2015; Henriquez et al., 2017; Mendelova et al., 2017; Bendle et al., 2017
Tierra de Fuego	Sudden, large-scale warming.	Unknown, but likely within a few hundred meters of present by 16.8 ka	Rapid glacier recession, with no evidence of stillstands. Cordillera Darwin icefield had contracted to within the present-day fjords by 16.8 ka	McCulloch et al., 2005b; Kaplan et al., 2008; Menounos et al., 2013; Hall et al., 2013, 2017

Table 3. The main climate and glacial evolution features during the Bølling-Allerød interstadial and Antarctic Cold Reversal (14.6–12.9 ka) in the Americas.

REGION	Climate during B-A/ACR in relation to present	ELA depression during BA/ACR in relation to present	Glacial evolution during B-A/ACR	Key References
LAURENTIA			General ablation in marginal areas in B-A and marked retreat acceleration along the southern and western margins, with development of proglacial lakes. Some readvances not related to climatic forcing. Northern margin stable.	Carlson et al., 2012; Ullman et al., 2015b; Margold et al., 2015; 2018; Dyke, 2004; Stokes, 2017
ALASKA	Unknown but some data suggest an important climate change		Widespread glacier retreat around the time of the Bølling onset. Glaciers were smaller than their eventual late Holocene extents by 15 ka	Badding et al., 2013; Pendleton et al., 2015
Cordillera Ice Sheet and North Cascades	Positive temperature anomaly of 1–2 ºC early in the BA, and increase in mean annual precipitation of 250 mm. Brief cold periods with -1.5 ºC temperature drop caused the small glacier advances later in the BA	CIS lowered more than 500 m in the early BA. ELAS ~500-700 m	Rapid disintegration of the CIS in the North Cascades and western Canada from 14.5–14.0 ka Glacial tongues transformed into a labyrinth of dead ice in valleys and between CIS and LIS Minor glacial advances between 13.6 and 13.3 ka. Top-down deglaciation of the ice sheet led to exposure of valley heads and cirques before adjacent valley floors	Liu et al. 2009; Peltier et al. 2015; Menounos et al. 2017; Lambeck et al. 2017; Riedel 2017; Clague 2017
Yellowstone-Tetons	warming climate	Increasing to present day	Some valleys continue advancing after 16 ka in the SW, due to their exposure to greater precipitation, the Yellowstone as a whole experienced an intensive deglaciation 15-14 ka	Licciardi and Pierce, 2018; Pierce et al., 2018
Wind River Range, WY	Warming prior to cooling during IACP/ACR	Increasing to near present	Glaciers retreat behind their H-1 moraines by ~15 ka, possibly to cirque headwalls. ^{10}Be ages suggest some begin to re-advance ~13.6-3 ka correlative with the Inter-Ållerød Cold Period (IACP) and the ACR	Dahms et al., 2018, 2019 ; Shakun et al., 2015.
Colorado	temperature and summer insolation increasing	Increasing to present day	Deglaciation was culminated by ~14 ka, and by 13 ka most of the glaciers had disappeared	Laabs et al., 2009; Young et al., 2011; Shakun et al., 2015a; Leonard et al, 2017a,b
Sierra Nevada	summer-warm and high-insolation	Increasing to present day, with a short depression of ~150 m	Glaciers had retreated to cirque headwalls by about 15.5 ka, well before the start of the BA at 14.7 ka.	Bowerman, 2011; Phillips, 2016, 2017

			Glacier advanced following the Bølling-Ållerød transition, for short interval, correlative with both the Inter-Ållerød Cold Period and the ACR, but also the YD	
Mexico	Warming tendency	rose at least 200 m	Initial deglaciation, allowing for the formation of small recessional moraines close to those of the maximum advance from 15 to 14 ka and accelerated from 14 ka.	Vázquez-Selem and Lachniet, 2017
Central America	Warming trend	Unknown	Glacier retreat and standstills 15-10 ka	Potter et al., 2019
Northern Andes	2.9°±0.8°C colder and 10% increase in annual precipitation	Depression of 500 m	Glacier advances have been related to ACR in the Sierra Nevada del Cocuy, Colombia	Jomelli et al., 2014, 2016
Peru and Bolivia	Colder in the beginning and end of the ACR and variability in the precipitation	Great variability, from similar to present to depression of 500 m	Glaciers advancing in multiple regions of Peru of Bolivia around 13.5 ka	Jomelli et al., 2014, 2016, 2017; Stansell et al., 2015; 2017
Northern Chile	Drier than H1 or YD		No glacial advances have been dated with sufficient precision to distinguish between the YD and the ACR, but possible ACR moraines at recessed positions	Ward et al., 2015; 2017
Central Andes of Argentina	Similar to present-day precipitation		No generalized glacial activity in the region, but possible ACR moraines	D'Arcy et al., 2019
Patagonia	1.6-1.8°C colder	Depression of 260 m	Several advances during ACR south of 47°S but no evidence of a glacial advance north of 47°S	Moreno et al., 2009; Glasser et al., 2011; Sagredo et al., 2011; Strelin et al., 2011; García et al., 2012; Nimick et al., 2016; Sagredo et al., 2018
Tierra de Fuego	Colder		Cirque moraines in the Fuegian Andes have been dated to the ACR. Overall, little work has been done on ACR ice extent in this region.	Menounos et al., 2013

Table 4. The main climate and glacial evolution features during Younger Dryas (12.9–11.7 ka) in the Americas.

REGION	Climate during YD in relation to present	ELA depression during YD in relation to present	Glacial evolution during YD	Final stages of deglaciation	Key References
LAURENTIA			Glacial recession slowed and some moraine systems were built because of some marginal re-advances. Several ice streams switched on caused by climatically forced. However, there was rapid retreat along other margins.	Following the YD, deglaciation occurred rapidly. Retreat towards the positions of the major ice dispersal centres with some interruptions, such as the 8.2 ka event, to be completed by 7 ka	Dyke, 2004; Margold et al., 2018; Lakeman et al., 2018;
ALASKA	Cooling is notable only in the South and in the beginning of YD. The rest was warmer than the late Holocene. Increase in precipitation due to transgressive flooding of Bering Strait around the time of the YD.	<0-80 m	Limited evidence for glacier re-advances and most of the glaciers retreated up-valley of their late Holocene extent prior to the YD		Briner et al., 2002; 2017; Kaufman et al., 2010
Cordillera Ice Sheet and North Cascades	The climate was variable at the century time scale, with maximum cooling of ~2–3 ºC	ELA 200-400 m below modern values in the North Cascades, but fluctuated 100-200 m	Many alpine glaciers and at least two remnant lobes of the CIS advanced. They were small advances, only several hundred meters beyond late Holocene maximum positions attained during the Little Ice Age. In North Cascades there are multiple closely nested YD moraines	Ice-free by 11.6 ka in many sites in western Canada. In British Columbia extent was only slightly larger at 11 ka than today.	Osborn et al., 2012; Menounos et al., 2017; Riedel, 2017;
Yellowstone-Tetons			The only glacial advance detected is in the Lake Solitude cirque in the east slope of		Licciardi and Pierce, 2008

			Teton Range, with a moraine that closed a small cirque at 12.9 ± 0.7 ka		
Wind River Range, WY	Cooling; Precip ?	~40-80m (S-to-N)	'Alice Lake' moraines in fifteen cirque valleys 0.1-0.5 km behind H-1/Oldest Dryas moraines. 13.6-11.2 ka in Stough Basin and Cirque of the Towers; 13.3 ka in Titcomb Basin.	Ice-free until Late Holocene. Two re-advances (pre-LIA pro-talus/moraines; LIA moraines).	Dahms, 2002; Dahms et al., 2010, 2018, 2019; Shakun et al., 2015.
Colorado	Cooling evidence		Most of the valleys were largely ice-free by ~15-13 ka with no clear evidence of re-advance during the YD.		Leonard et al., 2017a
Sierra Nevada	Evidence of 1°C cooling and 140 % precipitation increase		Unclear whether Recess Peak advance is YD or pre-YD		Bowerman, 2011
Mexico	~4-5°C colder and relatively dry conditions	650-800 m	In the mountains of central Mexico >4200 m glaciers formed a distinctive group of closely spaced moraines at 3800-3900 m from 13-12 to ~10.5 ka	Mountains <4000 m in central Mexico were ice-free by 11.5 ka; mountains <4200 m ice-free between 10.5 and 10 ka; highest peaks of central Mexico (>4400 m) have evidence of a short but distinctive advance 8.5 to 7.5 ka	Vázquez-Selem and Lachniet, 2017
Central America			Conflicting evidence: full deglaciation prior to YD, ca. 15.2 ka (Cunningham et al., 2018); glaciation coeval to YD and full deglaciation before 9.7 ka (Orvis and Horn, 2000; Potter et al., 2019)	Ice-free before 9.7 ka or probably as early as 15.2 ka, depending on the authors	Orvis and Horn, 2000; Cunningham et al., 2019; Potter et al., 2019-
Northern Andes	2.2-3.8°C colder than today, and drier climate in the Venezuelan Andes		Evidence of glacier advance is limited and mainly located at elevations higher than 3800 m a.s.l.		Salgado-Labouriau and Schubert, 1977; Carrillo et al., 2008; Rull et al., 2010; Stansell et al., 2010; Angel et al. 2017
Peru and Bolivia	More precipitation in the South indicated by high level of Coipasa paleolake	Scarce records and great variability	The ice was in a general retreating phase during the YD. Only local evidence of advances at the start of YD, mainly in southwestern Peru.	Multiple glaciers advanced or experienced stillstands in the Central Andes during the early Holocene. Glaciers then seem	Mark et al., 2017; Bromley et al., 2011; Alcalá-Reygosa et al., 2017

				to have rapidly retreated through the remaining early Holocene	
Northern Chile	100-150% wetter than modern		There are no glacial landforms in the immediate vicinity of the Arid Diagonal dated with sufficient precision to distinguish between the YD and the ACR; possible YD moraines in recessed positions at a few locations.		Ward et al., 2015
Central Andes of Argentina	Cooler and wetter conditions. Synchronous with the expansion of Altiplano lakes	480 m	Evidence of local advances during YD	After the YD or H-1 there is no widespread glacial activity	Martini et al., 2017; D'Arcy et al., 2019
Patagonia	No clear cooling and great variability in precipitation		After reaching their maximum late-glacial extent during the ACR, Patagonian glaciers underwent net recession and thinning during the YD. This general trend was interrupted by stillstands or minor readvances that deposited small moraines south of 47ºS	A widespread warm/dry interval is evident between 11-8 ka and the glaciers continued decreasing through the early Holocene, when most glaciers approached their present-day configuration	Moreno et al., 2010; Strelin et al., 2011; Kaplan et al., 2016; Glasser et al., 2012; Sagredo et al., 2018; Moreno et al., 2018a,b
Tierra de Fuego	No clear cooling		A glacier in the Fuegian Andes had reached positions comparable to the Little Ice Age by 12.5-11.2 ka. Probably glaciers were in recession throughout Tierra del Fuego.	Recession may have been rapid in the early Holocene	Menounos et al., 2013; Hall et al., 2013; 2017

Declaration of interests

 The authors declare that they have no known competing financial interests or personal relationships that could have appeared to influence the work reported in this paper.

☐The authors declare the following financial interests/personal relationships which may be considered as potential competing interests: